

**An examination of current methods to prescribe exercise intensity: validity of different approaches and effects on cell signalling events associated with mitochondrial biogenesis**

**Nicholas Alan Jamnick**

Institute for Health and Sport (IHES)

College of Sport & Exercise Science

Victoria University

Melbourne, Australia

Principal Supervisor: Professor David Bishop

Associate Supervisor: Professor David Pyne

Associate Supervisor: Dr. Cesare Granata

## Abstract

While seemingly simple, the underlying exercise prescription to bring about the desired adaptations to exercise training is as complicated as that of any drug. Prescribing the frequency, duration, or volume of training is relatively simple as these factors can be altered by manipulating the number of exercise sessions per week, the duration of each session, or the total work performed in a given time frame (e.g., per week). However, prescribing exercise intensity is more complex and there is controversy regarding the reliability and validity of the many methods used to determine and prescribe intensity. Despite their common use, it is apparent  $\dot{V}O_2$  and HR based exercise prescription has no merit to elicit a homogeneous and explicit homeostatic response. Alternatively, the use of submaximal anchors has been employed and perceived to represent shifts in the metabolic state of the working muscle and represent a demarcating point to define training zones. Whereas, the domains of exercise are independent of these anchors and defined by their distinct homeostatic responses, and offer a valid concept for normalising exercise intensity (*Chapter 1; Review 1*). Furthermore, the relationship between graded exercise test (GXT) derived anchors and constant work load derived anchors is at this point *non sequitur* and we discourage using submaximal anchors interchangeably (*Chapter 2; Study 1*).

Mitochondria are organelles found inside skeletal muscle cells and their main role is the production of adenosine triphosphate (ATP) which is necessary for skeletal muscle contractions. The bioenergetics demands associated with aerobic exercise lead to a homeostatic perturbation, activating sensor proteins that initiates gene expression through transcriptional and translational processes leading to the development of mitochondrial proteins. The source of ATP production modulates the homeostatic perturbations that activate the sensor proteins which include: an increase in the redox state of the cell ( $NAD^+/NADH$ ), an increase in ATP

turnover (measured via AMP/ATP), increased calcium flux and mechanical stress and these are largely influenced by the source of ATP production. These perturbations act as signals to activate sensor proteins that ultimately modulate transcriptional coactivators associated with mitochondrial biogenesis (*Chapter 3; Review 2*). Despite the relationship between exercise intensity and mitochondrial biogenesis, submaximal exercise intensity is almost exclusively prescribed relative to maximal oxygen uptake or maximal work rate. The well-established limitation of these methods is the inability to normalise exercise intensity; specifically, to elicit a homogenous homeostatic perturbations. Thus, employing methodology that normalises exercise intensity based on homeostatic perturbations may modulate the activation of signalling kinases and the extent of gene expression (*Chapter 4; Study 2*).

# OFFICE FOR RESEARCH TRAINING, QUALITY AND INTEGRITY

## DECLARATION OF CO-AUTHORSHIP AND CO-CONTRIBUTION: PAPERS INCORPORATED IN THESIS

*This declaration is to be completed for each conjointly authored publication and placed at the beginning of the thesis chapter in which the publication appears.*

### 1. PUBLICATION DETAILS (to be completed by the candidate)

Title of Paper/Journal/Book:

Surname:  First name:

Institute:  Candidate's Contribution (%):

Status:

Accepted and in press:

Date:

Published:

Date:

### 2. CANDIDATE DECLARATION

I declare that the publication above meets the requirements to be included in the thesis as outlined in the HDR Policy and related Procedures – [policy.vu.edu.au](http://policy.vu.edu.au).

Date

### 3. CO-AUTHOR(S) DECLARATION

In the case of the above publication, the following authors contributed to the work as follows:

The undersigned certify that:

1. They meet criteria for authorship in that they have participated in the conception, execution or interpretation of at least that part of the publication in their field of expertise;
2. They take public responsibility for their part of the publication, except for the responsible author who accepts overall responsibility for the publication;



- 3. There are no other authors of the publication according to these criteria;
- 4. Potential conflicts of interest have been disclosed to a) granting bodies, b) the editor or publisher of journals or other publications, and c) the head of the responsible academic unit; and
- 5. The original data will be held for at least five years from the date indicated below and is stored at the following **location(s)**:

R Drive

Name(s) of Co-Author(s)	Contribution (%)	Nature of Contribution	Signature	Date
Javier Botella	5	Data Collection, Manuscript Preparation		18/10/2019
David Pyne	5	Study Design, Data Analysis, Manuscript Preparation		15-Oct-19
David Bishop	10	Ethics Application, Data Analysis, Manuscript Preparation		15Oct-19
Nicholas Jamnick	80	Study Design, Data Collection, Ethics Application, Data Analysis, Manuscript		18/10/19

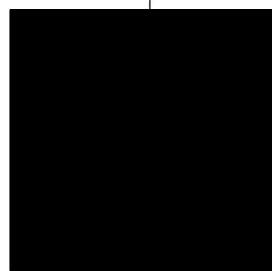
Updated: September 2019

**PART A:**

**DETAILS OF INCLUDED PAPERS: THESIS BY PUBLICATION**

Please list details of each Paper included in the thesis submission. Copies of published Papers and submitted and/or final draft Paper manuscripts should also be included in the thesis submission

Item/ Chapter No.	Paper Title	Publication Status (e.g. published, accepted for publication, to be revised and resubmitted, currently under review, unsubmitted but proposed to be submitted)	Publication Title and Details (e.g. date published, impact factor etc.)
2	Manipulating graded exercise test variables affects the validity of the lactate threshold and VO2peak	Published	Plos One (30/07/2018)



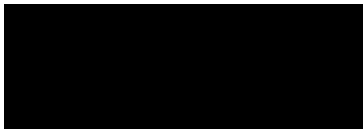
Declaration by [candidate name]:  
**Nicholas Jamnick**

Date: *18/10/2019*

**Student Declaration**

“I, Nicholas Alan Jammick, declare that the PhD thesis entitled “An examination of current methods to prescribe exercise intensity: validity of different approaches and effects on cell signalling events associated with mitochondrial biogenesis” is no more than 100,000 words in length including quotes and exclusive of tables, figures, appendices, bibliography, references and footnotes. This thesis contains no material that has been submitted previously, in whole or in part, for the award of any other academic degree or diploma. Except where otherwise indicated, this thesis is my own work”.

Signature



Date: 18/09/2019

## Table of Contents

<b>ACKNOWLEDGEMENTS .....</b>	<b>8</b>
<b>LIST OF PUBLICATIONS, CONFERENCES, AND AWARDS .....</b>	<b>9</b>
PUBLICATIONS (INCLUDED IN APPENDICES).....	9
CONFERENCES .....	10
BOOK CHAPTERS' .....	11
<b>AWARDS .....</b>	<b>12</b>
<b>LIST OF FIGURES.....</b>	<b>13</b>
CHAPTER 1 .....	13
CHAPTER 2.....	16
CHAPTER 3.....	18
CHAPTER 4.....	20
<b>LIST OF TABLES.....</b>	<b>25</b>
CHAPTER 1 .....	25
CHAPTER 2.....	26
CHAPTER 4.....	27
<b>CHAPTER 1: AN EXAMINATION AND CRITIQUE OF CURRENT METHODS TO PRESCRIBE EXERCISE INTENSITY .....</b>	<b>29</b>
1.1 INTRODUCTION.....	30
1.2 PRESCRIBING EXERCISE INTENSITY RELATIVE TO MAXIMAL ANCHORS .....	40
1.2.1 Maximal Oxygen Uptake.....	40
1.2.2 Maximal Work Rate and Peak Treadmill Speed .....	44
1.2.3 Maximum Heart Rate.....	45
1.2.4 Conclusion: Prescribing Exercise Intensity Relative to Maximal Anchors .....	46
1.3 PRESCRIBING EXERCISE INTENSITY RELATIVE TO SUBMAXIMAL ANCHORS .....	46
1.3.1 Blood Lactate.....	48
1.3.1.1 Lactate Thresholds .....	50
1.3.1.1.1 LT1 .....	50
1.3.1.1.2 LT2 .....	51
1.3.1.2 Maximal Lactate Steady State .....	52
1.3.2 Gas Exchange .....	54
1.3.2.1 Ventilatory/Gas Exchange Threshold.....	54
1.3.3.2 Respiratory Compensation Point .....	57
1.3.3 Critical Power/Speed.....	59
1.3.4 Conclusion: Prescribing Exercise Relative to Submaximal Anchors.....	64
1.4 PRESCRIBING EXERCISE INTENSITY RELATIVE TO A MAXIMAL AND SUBMAXIMAL/RESTING VALUES .....	64
1.4.1. Average Work Rate of Maximal and Submaximal Anchor “Delta”.....	65
1.4.2 Oxygen Uptake and Heart Rate Reserve.....	66
1.4.3 Conclusion: Prescribing Exercise Intensity Relative to a Maximal and Submaximal/Resting Value. 66	66
1.5 CONCLUSIONS .....	67
<b>CHAPTER 2: MANIPULATING GRADED EXERCISE TEST VARIABLES AFFECTS THE VALIDITY OF THE LACTATE THRESHOLD AND <math>\dot{V}O_{2PEAK}</math>.....</b>	<b>68</b>
2.1 INTRODUCTION.....	69
2.2 MATERIALS AND METHODS .....	71
2.2.1 Participants/Experimental Design.....	71
2.2.2 Equipment/Instruments .....	72
2.2.3 GXTs with Verification Exhaustive Bout.....	72
2.2.4 Constant Power Exercise Bouts to Establish the Maximal Lactate Steady State.....	73
2.2.5 LT and Respiratory Compensation Point Calculations .....	74
2.2.6 Data Analysis.....	77

2.2.7 Statistical Analysis.....	80
2.3 RESULTS.....	80
2.3.1 MLSS.....	80
2.3.2 Validity of LT Estimates.....	82
2.3.3 $\dot{W}_{max}$ and $\dot{V}O_{2max}$ .....	91
2.4 DISCUSSION.....	94
2.5 CONCLUSION.....	98

**CHAPTER 3: REVIEW OF LITERATURE: INFLUENCE OF EXERCISE INTENSITY ON BIOENERGETICS, HOMEOSTATIC PERTURBATIONS, SIGNALING KINASES, AND GENES ASSOCIATED WITH EXERCISE INDUCED MITOCHONDRIAL BIOGENESIS. .... 99**

3.1 INTRODUCTION.....	100
3.2 EXERCISE INTENSITY INFLUENCING THE “PRIMARY MESSENGERS” ASSOCIATED WITH EXERCISE-INDUCED MITOCHONDRIAL BIOGENESIS: BIOENERGETICS AND HOMEOSTATIC PERTURBATIONS.....	105
3.2.1 Fatty Acids.....	105
3.2.2 Fatty Acid Metabolism and Exercise Intensity.....	107
3.2.3 Glycolysis/Lactate.....	110
3.2.4 Lactate and Exercise Intensity.....	111
3.2.5 Reduction-Oxidation Reaction (Redox State).....	113
3.2.6 Redox State & Exercise Intensity.....	113
3.2.7 ATP Turnover.....	114
3.2.8 AMP:ATP Ratio & Exercise Intensity.....	114
3.2.9 Calcium Flux.....	116
3.2.10 Calcium Flux & Exercise Intensity.....	116
3.2.11 Reactive Oxygen Species (ROS).....	117
3.2.12 Reactive Oxygen Species & Exercise Intensity.....	118
3.2.13 Mechanical Stress.....	118
3.2.14 Mechanical Stress & Exercise Intensity.....	119
3.2.15 Summary of the Influence of Exercise Intensity on the Primary Messengers.....	119
3.3 EXERCISE INTENSITY INFLUENCING THE “SECONDARY MESSENGERS” ASSOCIATED WITH EXERCISE-INDUCED MITOCHONDRIAL BIOGENESIS.....	121
3.3.1 Exercise Intensity Modulating AMPK.....	121
3.3.2 Exercise Intensity Modulating CaMKII.....	124
3.3.3 Exercise Intensity Modulating p38.....	125
3.3.4 Exercise Intensity Modulating SIRT1 Activity.....	126
3.4 INFLUENCE OF EXERCISE INTENSITY ON TRANSCRIPTION FACTORS.....	127
3.4.1 Fatty Acid Binding Protein.....	127
3.4.2 PGC-1 $\alpha$ Protein, The “Master Regulator” of Mitochondrial Biogenesis.....	127
3.4.3 p53 Protein - “Guardian of the Genome” and Metabolic Regulator.....	128
3.4.5 Histone Deacetylase (HDAC).....	129
3.4.6 cAMP Response Element-Binding Protein (CREB).....	129
3.4.7 Conclusion.....	130
3.5 INFLUENCE OF EXERCISE INTENSITY ON GENE ASSOCIATED WITH MITOCHONDRIAL BIOGENESIS.....	130
3.5.1 PPAR mRNA.....	130
3.5.2 PGC-1 $\alpha$ mRNA.....	131
3.5.3 p53 mRNA.....	131
3.5.4 Nuclear Respiratory Factors (NRF-1/2).....	133
3.5.5 TFAM, Mitochondrial Transcription Factor.....	134
3.5.6 Conclusion.....	134
3.6 PRESCRIBING EXERCISE TO MODULATE THE “PRIMARY MESSENGERS”.....	135
3.7 CONCLUSION.....	137

<b>CHAPTER 4: THE INFLUENCE OF EXERCISE INTENSITY PRESCRIBED RELATIVE TO THE MAXIMAL LACTATE STEADY STATE ON SIGNALING PATHWAYS ASSOCIATED WITH MITOCHONDRIAL BIOGENESIS IN HUMAN SKELETAL MUSCLE.....</b>	<b>138</b>
4.1 INTRODUCTION.....	139
4.2 MATERIALS AND METHODS .....	141
4.2.1 <i>Ethical approval</i> .....	141
4.2.2 <i>Participants</i> .....	141
4.2.3 <i>Experimental Design</i> .....	142
4.2.4 <i>Equipment/Instruments</i> .....	143
4.2.5 <i>Exercise Protocols</i> .....	143
4.3 STATISTICAL ANALYSIS .....	155
4.4 RESULTS.....	156
4.4.1 <i>Metabolic and Power Data</i> .....	156
4.4.2 <i>Cytosolic Signalling Kinases</i> .....	159
4.4.3 <i>Transcriptome Response</i> .....	161
4.4.4 <i>Whole Muscle mRNA</i> .....	165
4.5 DISCUSSION.....	175
4.6 CONCLUSIONS .....	182
<b>CHAPTER 5: FINDINGS, LIMITATIONS, AND PRACTICAL APPLICATIONS .....</b>	<b>183</b>
5.1 KEY FINDINGS.....	184
5.2 LIMITATIONS OF THE PRESENT WORK.....	189
5.3 RECOMMENDATIONS FOR FUTURE RESEARCH.....	191
5.4 PRACTICAL APPLICATIONS .....	192
<b>REFERENCES .....</b>	<b>194</b>
<b>APPENDICES.....</b>	<b>230</b>

## **Acknowledgements**

The Office. Season 7, Episode 19. Minute 14:45

~Michael Scott

## List of Publications, Conferences, and Awards

### Publications (Included in Appendices)

Pettitt, R. W., **Jamnick, N. A.**, Kramer, M., & Dicks, N. D. (2019). A Different Perspective of the 3-Minute All-Out Exercise Test. **The Journal of Strength & Conditioning Research**, 33(8), e223-e224.

**Jamnick, N. A.**, Botella, J., Pyne, D. B., & Bishop, D. J. (2018). Manipulating graded exercise test variables affects the validity of the lactate threshold and  $\dot{V}O_{2peak}$ . **PloS ONE**, 13(7), e0199794.

Strom, C. J., Pettitt, R. W., Krynski, L. M., **Jamnick, N. A.**, Hein, C. J., & Pettitt, C. D. (2018). Validity of a customized submaximal treadmill protocol for determining  $\dot{V}O_{2max}$ . **European Journal of Applied Physiology**, 1-7.

Granata, C., **Jamnick, N. A.**, & Bishop, D. J. (2018). Training-induced changes in mitochondrial content and respiratory function in human skeletal muscle. **Sports Medicine**, 48(8), 1809-1828.

Granata, C., **Jamnick, N. A.**, & Bishop, D. J. (2018). Principles of exercise prescription, and how they influence exercise-induced changes of transcription factors and other regulators of mitochondrial biogenesis. **Sports Medicine**, 48(7), 1541-1559.

Kramer, M., Clark, I. E., **Jamnick, N. A.**, Strom, C., & Pettitt, R. W. (2018). Normative Data for Critical Speed and  $D'$  for High-Level Male Rugby Players. **The Journal of Strength & Conditioning Research**, 32(3), 783-789.

Pettitt, R. W., & **Jamnick, N. A.** (2017). Commentary on "Measurement of the maximum oxygen uptake  $\dot{V}O_{2max}$ :  $\dot{V}O_{2peak}$  is no longer acceptable". **Journal of Applied Physiology**, 123(3), 696-696.

Dicks, N. D., **Jamnick, N. A.**, Murray, S. R., & Pettitt, R. W. (2016). Load determination for the 3-minute all-out exercise test for cycle ergometry. **International Journal of Sports Physiology and Performance**, 11(2), 197-203.

**Jamnick, N. A.**, By S., Pettitt C. D., & Pettitt R. W. (2016). Comparison of the YMCA and a Custom Submaximal Exercise Test for Determining  $\dot{V}O_{2max}$ . **Medicine & Science in Sport & Exercise**, 48(2): 254-259

## Conferences

Bishop, D. J Granata, C., Relijic, B., Botella J., **Jamnack, N. A.**, Kuang, J., Janssen, H., Thorburn, D. R., Frazier, A. E., & Stroud, D. A., (2018). Analysis of the mitochondrial proteome from human skeletal muscle in response to endurance training reveals volume-dependent remodelling. AussieMit. Melbourne, Victoria.

**Jamnack, N. A.**, Botella J., Pyne D. B., & Bishop, D. J. (2018). Manipulating graded exercise test variables affects the validity of the lactate threshold and  $\dot{V}O_{2peak}$ . American College of Sports Medicine. Minneapolis, Minnesota

**Jamnack, N. A.**, Botella J., Pyne D. B., & Bishop, D. J. (2018). Manipulating graded exercise test variables affects the validity of the lactate threshold and  $\dot{V}O_{2peak}$ . Exercise Sport Science of Australia. Brisbane, Queensland

Bishop D. J., Kuang J., Granata C., Botella J., **Jamnack N, A.**, Janssen H. A. Increased respiratory chain supercomplex formation & mitochondrial respiration in response to exercise training in human skeletal muscle. Cell Symposia; Exercise Metabolism. May 21-23, 2017. Gothenburg, Sweden.

**Book Chapters'**

Bishop, D. J., & **Jamnick, N. A.** (2018). Anaerobic Lactacid Energy System. *Kinanthropometry and Exercise Physiology* (293-317)

Bishop, D.J., Skinner, T. & **Jamnick, N. A.** (2018). Lactate Threshold. In: "ESSA student manual for Health, Exercise and Sport Assessment". Ed Coombes and Skinner. Elsevier.

## **Awards**

International PhD Research Scholarship (Victoria University)

## List of Figures

### Chapter 1

**Figure 1.1.** The five aerobic training zones (L1-L5) based on the first and second lactate threshold ( $LT_1$  and  $LT_2$ ) derived from a GXT. The  $LT_1$  (i.e., lactate transition 1) represents the rise in blood lactate above baseline. The  $LT_2$  (i.e., lactate transition 2) represents an acceleration of blood lactate accumulation.

**Figure 1.2.** The training intensity distribution model divides intensity into 3 zones, where zones 1 and zone 2 are demarcated by  $LT_1$  and GET/VT and zones 2 and 3 by  $LT_2$ , RCP, and MLSS. Each zone is characterised by  $\%HR_{max}$ ,  $\%\dot{V}O_{2max}$ , absolute blood lactate value, and relationship with a submaximal anchor.

**Figure 1.3.** Prescribing exercise intensity based on physiological domains<sup>2</sup>. Each domain can be characterised by a specific oxygen uptake ( $\dot{V}O_2$ ) kinetic and blood lactate response. The moderate domain can be characterised by a plateau of  $\dot{V}O_2$  and blood lactate concentrations near baseline levels, the heavy domain by an observed ‘slow component’ of  $\dot{V}O_2$  with a delayed steady state, and a rise in blood lactate above baseline with subsequent plateau, and the severe by a ‘slow component’ without a steady state of  $\dot{V}O_2$  and a continual increase in blood lactate.

**Figure 1.4 (A & B).** A)  $\dot{V}O_2$ , and B) blood lactate responses during moderate, heavy and severe exercise. Moderate (green line), heavy (yellow line), and severe exercise (red line). A)  $\dot{V}O_2$  kinetics during moderate exercise is depicted by mono-exponential uptake response with an attained steady state. During heavy and severe exercise there is a delayed steady state (i.e., a slow component) due to the curvilinear increase in the  $\dot{V}O_2$ -work rate relationship (grey shaded area). During heavy exercise there is a delayed steady state following the slow component. During severe exercise there is an observed  $\dot{V}O_2$  slow component absent of a steady state and continuous exercise results in the attainment of  $\dot{V}O_{2max}$ . B) The blood lactate response during moderate exercise remains at baseline due to the predominant source of energy being derived via oxidative phosphorylation. The blood lactate response during heavy exercise is an increase above baseline with a steady state. The blood lactate during severe exercise is a rise above baseline with an absence of a steady state.

**Figure 1.5.** Schematic illustrating the domain-specific muscle recruitment pattern contributing to the slow component of oxygen uptake, absence of an oxygen uptake plateau, and the blood lactate response. During continuous, moderate exercise, type I muscle fibres are predominantly

recruited, ATP is produced solely via mitochondrial ATP turnover (i.e., Krebs Cycle),  $O_2$  demand is equal to  $O_2$  availability, and muscle and blood lactate levels remain at baseline. During continuous, heavy exercise, type I and IIa muscle fibres are recruited, ATP is produced via mitochondrial and cytosolic ATP turnover, the recruitment of less efficient type IIa muscle fibres and the increase in ventilation due to increased non-metabolic  $CO_2$  production results in the delayed steady state of oxygen uptake (i.e., a slow component), and the reliance on non-mitochondrial ATP turnover results in an increase in blood lactate above baseline with an achieved steady state mirroring the oxygen uptake pattern. During continuous, severe exercise, type I, IIa and IIx muscle fibres are recruited, ATP is produced via mitochondrial, cytosolic ATP turnover and via a continual depletion of the phosphocreatine stores (PCr), which results in the continual increase in  $O_2$  uptake until the cessation of exercise. The recruitment of less efficient type IIa and IIx muscle fibres increase the amplitude of the slow component, further increase ventilation (i.e., hyperventilation) due to increased non-metabolic  $CO_2$  production. Lastly, intramuscular lactate production exceeds lactate oxidation, which results in lactate appearance exceeding disappearance. MCT = monocarboxy transporter

**Figure 1.6.** Expected and observed  $VO_2$  response relative to power. During low exercise intensities there is a linear  $VO_2$ -work rate relationship. As exercise intensity increases the relationship between  $VO_2$  and work rate becomes curvilinear and the observed work rate associated with 70% of  $VO_{2max}$  is lower than that expected for a linear relationship (282 vs. 332 W). Figure redrawn from Zoldaz et. al. [2] .

**Figure 1.7. (A-C).** (A) Plasma lactate, (B) ammonia, and (C) hypoxanthine values comparing trained (solid line) and untrained (dashed line) when exercising at 70% of  $\dot{V}O_{2peak}$  (dark circles) and 95% of the work rate associated with a  $1 \text{ mmol L}^{-1}$  increase in blood lactate above baseline (B+1) (dark triangles). When exercising at 70% of  $VO_{2peak}$  the plasma lactate (i.e., at 20 and 40 minutes) and ammonia values (i.e., after 40 and 60 minutes) were significantly different for the untrained participants compared to all other groups; furthermore, there were no significant differences for hypoxanthine. Figure redrawn from Baldwin et. al. [3].

**Figure 1.8.** Data demonstrating the relationship between maximum work rate ( $W_{max}$ ) and graded exercise test (GXT) duration.  $W_{max}$  derived from a GXT is a function of the slope (increase in work rate relative to time) ( $W s^{-1}$ ). Dark circles represent mean and the whiskers

the standard deviation. Call outs are the average slope of the graded exercise test. Redrawn from Adami et al. [4].

**Figure 1.9. (A - C).** A.) Representative blood lactate response to exercise performed at 97, 100 and 103% of the MLSS (Traditional Criteria). Blood lactate increased 0.7, 0.8 and 1.3 mmol·L<sup>-1</sup> from 10 to 30 minutes at 97, 100 and 103% of the MLSS, respectively. B.) Representative blood lactate response using criteria developed by Hering et al. [5]. Threshold criteria 2 was achieved were blood lactate increased  $\geq 0.5$  mmol·L<sup>-1</sup> and was  $\geq 4$  mmol·L<sup>-1</sup> without a change in speed. Therefore, speed was decreased by 0.1 m·s<sup>-1</sup> to confirm the MLSS. C.) Representative lactate threshold (LT) curve with 14 different LTs. Log-log = power at the intersection of two linear lines with the lowest residual sum of squares; log = using the log-log method as the point of the initial data point when calculating the D<sub>max</sub> or Modified D<sub>max</sub>; poly = Modified D<sub>max</sub> method calculated using a third order polynomial regression equation; exp = Modified D<sub>max</sub> method calculated using a constant plus exponential regression equation; OBLA = onset of blood lactate accumulation; B + absolute values the intensity where blood lactate increases above baseline.

**Figure 1.10. (A-E).** Representative gas exchange and blood lactate data from an incremental/graded exercise test illustrating the method(s) to determine the: ventilatory threshold (VT), gas exchange threshold (GET) and first lactate threshold (LT<sub>1</sub>). (A) VT: the first break point in ventilation (V<sub>E</sub>), (B) GET: disproportionate increase in nonmetabolic CO<sub>2</sub> production relative to O<sub>2</sub> consumption (VO<sub>2</sub>) (i.e., excess CO<sub>2</sub>), (C) VT: systemic increase in V<sub>E</sub>/VO<sub>2</sub>, (D) VT: systemic increase in pressure of end tidal oxygen consumption (P<sub>ET</sub>O<sub>2</sub>), and (E) VT: plateau in pressure of end tidal carbon dioxide expiration (P<sub>ET</sub>CO<sub>2</sub>) following in increase.

**Figure 1.11. (A-C).** Representative gas exchange and blood lactate data from an incremental/graded exercise test illustrating the method(s) to determine the: respiratory compensation point (RCP) and second lactate threshold (LT<sub>2</sub>). (A) RCP: the second break point in ventilation (V<sub>E</sub>), (B) RCP: a breakpoint in V<sub>E</sub> relative to CO<sub>2</sub> expiration (V<sub>E</sub>/VCO<sub>2</sub>) following a plateau), and (C) RCP: second breakpoint in pressure of end tidal carbon dioxide expiration (P<sub>ET</sub>CO<sub>2</sub>) following plateau.

**Figure 1.12. (A & B).** A) Linear distance-time model from race performances (800 M, 1500 M, mile, 3000 M and 5000 M) calculating critical speed (slope; 5.51 m·s<sup>-1</sup>) and curvature

constant (intercept;  $D' = 177$  M). Times retrieved from iaaf.com; athlete code: 14564446. B) Work rate profile from 3 min-all-out-test (3MT). The dashed line represents CP and CS, the average work rate from the last 30 seconds of the 3MT.  $W'/D'$  represents the work performed above CP and CS,  $W'/D' = 150$  seconds \* (Average Work rate of 150 seconds – CP and CS)

**Figure 1.13. (A-E).** Blood lactate and muscle metabolic responses 5% above and below CP. Mean SD blood lactate concentrations (A), intramuscular lactate concentrations (B), phosphocreatine concentration (C), intramuscular pH (D), and intramuscular glycogen concentrations (E). Data redrawn from Vanhatalo et al. [6].

## Chapter 2

**Figure 2.1.** Representative blood lactate curve with 14 LTs calculated from GXT<sub>4</sub> (participant #9). The power of the MLSS was 302 W and the blood lactate concentration was 2.85 mmol·L<sup>-1</sup>. Log-log = power at the intersection of two linear lines with the lowest residual sum of squares; log = using the log-log method as the point of the initial data point when calculating the  $D_{\max}$  or Modified  $D_{\max}$ ; poly = Modified  $D_{\max}$  method calculated using a third order polynomial regression equation; exp = Modified  $D_{\max}$  method calculated using a constant plus exponential regression equation; OBLA = onset of blood lactate accumulation; B + absolute value = the intensity where blood lactate increases above baseline.

**Figure 2.2 (A-D).** Forrest Plots of the difference ( $ES \pm 95\%$  CI) between the MLSS and the power calculated from the 13 lactate thresholds derived from (A) GXT<sub>3</sub>, (B) GXT<sub>4</sub>, (C) GXT<sub>7</sub> and (D) GXT<sub>10</sub> (52 in total and excluding log-log). The solid vertical bar represents no difference from the MLSS and the dashed vertical bars represents the threshold between a trivial and small difference ( $ES = 0.2$ ) established by Cohen [7] and Hopkins [8]. log = using the log-log method as the initial data point when calculating the  $D_{\max}$  or Modified  $D_{\max}$ ; poly = Modified  $D_{\max}$  method calculated using a third order polynomial regression equation; exp = Modified  $D_{\max}$  method calculated using a constant plus exponential regression equation; OBLA = onset of blood lactate accumulation

**Figure 2.3.** Bland-Altman plots displaying agreement between measures of the power associated with the RCP regression equation (RCPMLSS) calculated from GXT1 and the MLSS. The differences between measures (y-axis) are plotted as a function of the mean of the two measures (x-axis) in power (Watts). The horizontal solid line represents the mean difference between the two measures (i.e., bias). The two horizontal dashed lines represent the

limits of agreement (1.96 x standard deviation of the mean difference between the estimated lactate threshold via the RCPMLSS and the maximal lactate steady state). The dotted diagonal lines represent the boundaries of the 95% CI for MLSS reliability (CV = 3.0%; 95%; CI = 3.8%) calculated from Hauser et al., [9] (RCP = respiratory compensation point).

**Figure 2.4.** Bland-Altman plots displaying agreement between measures of the power associated with the baseline plus 1.5 mmol·L<sup>-1</sup> calculated from GXT3 and the MLSS. The differences between measures (y-axis) are plotted as a function of the mean of the two measures (x-axis) in power (Watts). The horizontal solid line represents the mean difference between the two measures (i.e., bias). The two horizontal dashed lines represent the limits of agreement (1.96 x standard deviation of the mean difference between the lactate threshold and the maximal lactate steady state). The dotted diagonal lines represent the boundaries of the 95% CI for MLSS reliability (CV = 3.0%; 95%; CI = 3.8%) calculated from Hauser et al. [9].

**Figure 2.5 (A-D).** Bland-Altman plots displaying agreement between measures of the power associated with the (A) OBLA 2.5 mmol·L<sup>-1</sup>, (B) Modified D<sub>max</sub>, (C) Log-Poly-Modified D<sub>max</sub>, (D) Log-Exp-Modified D<sub>max</sub> calculated from **GXT4** and the MLSS. The differences between measures (y-axis) are plotted as a function of the mean of the two measures (x-axis) in power (Watts). The horizontal solid line represents the mean difference between the two measures (i.e., bias). The two horizontal dashed lines represent the limits of agreement (1.96 x standard deviation of the mean difference between the lactate threshold and the maximal lactate steady state). The dotted diagonal lines represent the boundaries of the 95% CI for MLSS reliability (CV = 3.0%; 95%; CI = 3.8%) calculated from Hauser et al., [9] (log = Modified D<sub>max</sub> method using the log-log method as the point of the initial lactate point; poly = Modified D<sub>max</sub> method calculated using a third order polynomial regression equation; exp = Modified D<sub>max</sub> method calculated using a constant plus exponential regression equation; OBLA = onset of blood lactate accumulation.).

**Figure 2.6.** Bland-Altman plots displaying agreement between measures of the power associated with the (A) OBLA 2.5 mmol·L<sup>-1</sup> (GXT<sub>7</sub>), (B) OBLA 3.0 mmol·L<sup>-1</sup> (GXT<sub>7</sub>), (C) Log-Exp-Modified D<sub>max</sub> calculated from **GXT<sub>7</sub>** and the MLSS. The differences between measures (y-axis) are plotted as a function of the mean of the two measures (x-axis) in power (Watts). The horizontal solid line represents the mean difference between the two measures (i.e., bias). The two horizontal dashed lines represent the limits of agreement (1.96 x standard

deviation of the mean difference between the lactate threshold and the maximal lactate steady state). The dotted diagonal lines represent the boundaries of the 95% CI for MLSS reliability (CV = 3.0%; 95%; CI = 3.8%) calculated from Hauser et al., [9] (log = Modified  $D_{\max}$  method using the log-log method as the point of the initial lactate point; exp = Modified  $D_{\max}$  method calculated using a constant plus exponential regression equation; OBLA = onset of blood lactate accumulation.).

**Figure 2.7 (A & B).** Bland-Altman plots displaying agreement between measures of the power associated with the (A) OBLA 3.0 mmol·L<sup>-1</sup>, (B) OBLA 3.5 mmol·L<sup>-1</sup> calculated from **GXT<sub>10</sub>** and the MLSS. The differences between measures (y-axis) are plotted as a function of the mean of the two measures (x-axis) in power (Watts). The horizontal solid line represents the mean difference between the two measures (i.e., bias).

### Chapter 3

**Figure 3.1.** Energy Schematic for Skeletal Muscle During Exercise. ATP hydrolysis, catalyzed by myosin ATPase, powers skeletal muscle contraction. From Egan et al. [10].

**Figure 3.2.** Schematic illustrating the influence of the biogenetics and homeostatic perturbations associated with exercise intensity influencing the signalling kinases activating exercise induced mitochondrial biogenesis.

**Figure 3.3 (A & B).** Transmission electron microscopy (TEM) of (A) oxidative (type I) and (B) glycolytic (type II) muscle fibres. Black arrows pointing at intramuscular triglycerides (IMTG). Dashed arrows pointing at mitochondria (M). TEM figures from unpublished data.

**Figure 3.4.** (A-C) (A) Epinephrine and norepinephrine concentrations at different intensities prescribed relative to percentages of  $VO_{2\max}$  following 30 min of exercise. Data redrawn from Romijn et al. [11]. (B) Mean (SD) of fat (FAT) and carbohydrate (CHO) oxidation rates (g·min<sup>-1</sup>) as a function of percentage of maximal oxygen uptake ( $VO_{2\max}$ ). (C) Mean (SD) of fat (FAT) oxidation rates (g·min<sup>-1</sup>) and blood lactate concentrations as a function of percentage of maximal oxygen uptake ( $VO_{2\max}$ ). Data retrieved from 17 trained participants Jamnick et al. [1]. from a graded exercise test that used 4-minute stages from 17 trained cyclists.

**Figure 3.5.** Contributions of energy expenditure during sustained exercise derived from plasma glucose, plasma free fatty acids (FFA), intramuscular triglycerides (IMTG), other fat sources and muscle glycogen stores. Data redrawn from Romijn et al. [11] (i.e., 25%, 65%, and 85%

of  $\dot{V}O_{2\max}$ ), and from van Loon et. al. [12] (i.e., rest, 44%, 57%, and 72% of  $\dot{V}O_{2\max}$ ) where exercise was prescribed as a percentage of maximal oxygen uptake ( $\dot{V}O_{2\max}$ ). Romijn et al. [11] recruited 5 endurance trained cyclists ( $\dot{V}O_{2\max} = \sim 67 \text{ mL}\cdot\text{kg}^{-1}\cdot\text{min}^{-1}$ ) van Loon et. al. [12] recruited 8 trained male cyclists ( $\dot{V}O_{2\max} = \sim 73.5 \text{ mL}\cdot\text{kg}^{-1}\cdot\text{min}^{-1}$ )

**Figure 3.6 (A-C).** Figures illustrating the relationship between exercise intensity and intramuscular lactate production (A), (B) reduction-oxidation state of muscle measured ratio between reduced and oxidised form of Nicotinamide adenine dinucleotide ( $\text{NAD}^+/\text{NADH}$ ) (solid line) and intramuscular lactate concentrations (dashed line) Sahlin et al. [13] (C), NADH production concentrations in whole muscle, type 1 and type II (D). Exercise intensity was prescribed relative to percentage of maximal oxygen uptake ( $\dot{V}O_{2\max}$ ).

**Figure 3.7. (A & B).** (A) Schematic illustrating the three-step process by which adenosine monophosphate (AMP) is produced via adenosine diphosphate (ADP) production via adenosine triphosphate (ATP) hydrolysis and the Adenylate kinase reaction. AMP is deaminated into inosine monophosphate (IMP), and during high ATP production IMP is converted back into AMP via adenylo succinate and produces an adenosine. (B) Figure illustrating the relationship between exercise intensity prescribed as a percentage of  $\dot{V}O_{2\max}$  and ATP turnover measured via the ratio between AMP and ATP (AMP:ATP).

**Figure 3.8 (A & B).** Figures illustrating the relationship between exercise intensity prescribed as a percentage maximal oxygen uptake ( $\dot{V}O_{2\max}$ ) and (A) muscle fibre recruitment, (B) indirect measure of  $\text{Ca}^{2+}$  flux via glycogen phosphorylase  $V_{\max}$ . Redrawn from Howlett et al. [14] and Egan et al [15].

**Figure 3.9.** Figure illustrating the relationship between exercise intensity and reactive oxygen species production. There was a significant increase above baseline following exercise quantified at 90-100% of maximal oxygen uptake. Redrawn from Sureda et. al. [16].

**Figure 3.10.** Figures illustrating the relationship between in vivo (rat plantaris) muscle tension (Mean  $\pm$  SD) and concentric, isometric and eccentric muscle contractions. Redrawn from Martineau et al. [17].

**Figure 3.11.** Figure illustrating the relationship between exercise intensity prescribed as a percentage of  $\dot{V}O_{2\max}$  and the redox state of the cell, blood and intramuscular lactate, carbohydrate and fat oxidation, the AMP/ATP ratio, and adrenaline (i.e., epinephrine and

norepinephrine). Mathematical models (e.g., exponential plus constant or quadratic regression) were derived from *in vivo* studies using data from Figures 3.3 - 3.5. Data was scaled to yield homogenous y-axis values.

**Figure 3.12 (A & B).** Figures illustrating the relationship between exercise intensity prescribed as a percentage of maximal oxygen uptake ( $VO_{2max}$ ) and (A)  $\alpha 2$  AMP-activated protein kinase (AMPK) activity, and (B) the phosphorylation of AMPK.

**Figure 3.13 (A & B).** Figures illustrating the relationship between exercise intensity prescribed as a percentage of maximal oxygen uptake ( $VO_{2max}$ ) and (A) phosphorylation of phospholamban, and (B) calcium-calmodulin-dependent kinase II (CaMKII). Data redrawn from Rose et al. [18] and Egan et al. [15].

**Figure 3.14 (A-D).** Figures illustrating the relationship between exercise intensity and PGC-1 $\alpha$  mRNA. Panel A depicts the relationship between maximal power ( $W_{max}$ ) and mean fold change in PGC-1 $\alpha$  mRNA (3.2-6 hours from the onset of exercise). Panel B depicts the relationship between  $W_{max}$  and fold change in PGC-1 $\alpha$  mRNA relative to the exercise session length. Dashed curved lines represent 95% confidence intervals. Panel C is a rolling average (5 data points) of % of  $W_{max}$  and the fold change in PGC-1 $\alpha$  mRNA. Panel D is a rolling average (5 data points) of % of  $W_{max}$  and the fold change in PGC-1 $\alpha$  mRNA relative to exercise session length. The  $W_{max}$  were organised low to high, this and the (C) fold changes in PGC-1 $\alpha$  mRNA and (D) fold changes in PGC-1 $\alpha$  mRNA relative to exercise session length were averaged via rolling average (5 data points). (D) There was a disproportionate change in PGC-1 $\alpha$  mRNA relative to exercise session length above 65%  $W_{max}$ .

## Chapter 4

**Figure 4.1.** The exercise intensity and biopsy order of the research project. The pre biopsy was taken prior to each exercise bout (8:00), the post biopsy was taken immediately after each exercise bout (~08:45), the +4 h biopsy was taken four hours from the onset of exercise (12:15), and the +24 h biopsy was taken 24 hours from the onset of exercise (+1 Day; 8:15). The exercise bouts were performed in a randomised order and the mean (SD) times for the exercise bouts were 43.8 (12.1), 38.1 (10.5) and 33.8 (9.2) minutes for MLSS-18%, MLSS-6%, and MLSS+6%, respectively.

**Figure 4.2. Figure 4.2.** Schematic of the fractionation protocol. The protocol yields three subcellular fractions from frozen human skeletal muscle (i.e., nuclear, cytosol and mitochondria). Adapted from Dimauro et al. [19] (<sup>#</sup> Excess NaCl was removed via acetone precipitation). The homogenate was suspended in ice-cold acetone (1:6), stored at -80°C for 1 hour, and centrifuged at 13,000g for 20 minutes. Pellet was washed with ice-cold acetone, spun at 13,000g for 1 minute, and pellet was resuspended in 50 mM Tris (pH = 6.8), 100 mM dithiothreitol and 2% sodium dodecyl sulfate), and sonicated (2 x 3 s). Bottom figure illustrates the subcellular fractionation purity using histone 3 (H3), lactate dehydrogenase (LDH), and cytochrome c oxidase subunit 4 isoform 1 (COX-IV-1). PMSF: phenylmethylsulfonyl fluoride

**Figure 4.3.** Schematic of mRNA library construction flow chart.

**Figure 4.4 (A-C).** The influence of exercise intensity on metabolic responses during the exercise biopsy trials. (A) Mean  $\pm$  SD of blood lactate concentrations ( $\text{mmol}\cdot\text{L}^{-1}$ ) during the first 30 minutes of the exercise biopsy trials. -18% of the MSS (black boxes), -6% of the MLSS (grey shaded boxes), and +6% of the MLSS (open boxes). (B) Mean  $\pm$  SD of fat and carbohydrate (carb) oxidation ( $\text{kcal}\cdot\text{min}^{-1}$ ) rates measured via stoichiometric equations as described by Frayn, during the last minute of the exercise biopsy trials. (C) Mean  $\pm$  SD of intramuscular lactate concentrations at rest and immediate post exercise. \$ = significantly different from previous time point. \* = significantly different from Pre; # = significantly different from -18%; ¶ = significantly different from -6%.

**Figure 4.5 (A-D).** The influence of exercise intensity on signalling kinases measured in the cytosolic fraction immediately post, +4, and +24 hours from the onset of exercise performed at -18% of the maximal lactate steady state (MLSS) (black bars), -6% of the MLSS (grey shaded bars), and +6% of the MLSS (open bars). Mean fold changes  $\pm$  SD in arbitrary units (AU) for the protein content of phosphorylated (A) rapamycin (mTOR), (B)  $\text{Ca}^{2+}$  calmodulin dependent protein kinase II (CaMKII), (C) acetyl-CoA carboxylase (ACC), (D) AMP-activated protein kinase alpha (AMPK), (E) p38 mitogen-activated protein kinase (p38 MAPK). Expression of each signalling kinase was normalised to their total protein content. \* = significantly different from Pre

**Figure 4.6.** Primary component analysis of samples.

**Figure 4.7 (A & B).** Venn diagram illustrating the influence of exercise intensity on the large scale transcriptional response (i.e., number of differentially expressed genes) in whole skeletal muscle biopsy samples +4 (A) and +24 hours (C) from the onset of exercise. ( $\log_2\text{FC} = 1$ ; Q-

value = 0.001). KEGG classification of genes unique to each intensity in whole skeletal muscle biopsy samples +4 (B) and +24 hours (D) from the onset of exercise. -18% of the maximal lactate steady state (MLSS) (black bars), -6% of the MLSS (grey shaded bars), and +6% of the MLSS (open bars).

**Figure 4.8 (A-C).** Bar graphs illustrating the influenced of exercise intensity on total number of differentially expressed genes (A), and the number of upregulated (B) and down-regulated (C) genes immediately post, +4, and +24 hours from the onset of exercise performed at -18% of the maximal lactate steady state (MLSS) (black bars), -6% of the MLSS (grey shaded bars), and +6% of the MLSS (open bars).

**Figure 4.9 (A-D).** Bar graphs illustrating the influenced of exercise intensity on the number of upregulated genes +4 h (A), and +24 h (B), and downregulated genes +4 h (C), and +24 h (D), from the onset of exercise specific to endocrine/metabolic diseases, immune system function, endocrine system function, signalling molecules and interactions, signal transduction and energy metabolism. -18% of the maximal lactate steady state (MLSS) (black bars), -6% of the MLSS (grey shaded bars), and +6% of the MLSS (open bars).

**Figure 4.10 (A-F).** The influence of exercise intensity on whole skeletal muscle mRNA immediately post, +4, and +24 hours from the onset of exercise performed at -18% of the maximal lactate steady state (MLSS) (black bars), -6% of the MLSS (grey shaded bars), and +6% of the MLSS (open bars). Mean fold changes  $\pm$  SD in arbitrary units (AU) for (A) Peroxisome proliferator-activated receptor gamma coactivator 1-alpha isoform 1 (PGC-1 $\alpha$ -1), (B) Peroxisome proliferator-activated receptor gamma coactivator 1-alpha isoform 4 (PGC-1 $\alpha$ -4), (C) peroxisome proliferator-activated receptor gamma coactivator 1-alpha (PGC-1 $\alpha$ ) total, (D) tumour suppressor protein 53 (p53), (E) Superoxide dismutase 2 (SOD2) and (F) cyclin-dependent kinase inhibitor 1 (p21). Expression of each target gene was normalised to the geometric mean of expression of the three most stable genes (i.e., TBP, B2M and GAPDH). \* = significantly different from Pre; # = significantly different from -18%.

**Figure 4.11 (A-F).** The influence of exercise intensity on whole skeletal muscle mRNA immediately post, +4, and +24 hours from the onset of exercise performed at -18% of the maximal lactate steady state (MLSS) (black bars), -6% of the MLSS (grey shaded bars), and +6% of the MLSS (open bars). Mean fold changes  $\pm$  SD in arbitrary units (AU) for (A) Succinate dehydrogenase complex iron sulfur subunit B (SDHB), (B) peroxisome proliferator-activated receptor delta (PPAR $\delta$ ), (C) peroxisome proliferator-activated receptor gamma

(PPAR $\gamma$ ), (D) Pyruvate dehydrogenase lipoamide kinase isozyme 4 (PDK4), (E) Fatty acid translocase/CD36 (FAT/CD36), (F) Cytochrome b-c1 complex subunit 2 (UQRC2). Expression of each target gene was normalised to the geometric mean of expression of the three most stable genes (i.e., TBP, B2M and GAPDH). \* = significantly different from Pre.

**Figure 4.12 (A-F).** The influence of exercise intensity on whole skeletal muscle mRNA immediately post, +4, and +24 hours from the onset of exercise performed at -18% of the maximal lactate steady state (MLSS) (black bars), -6% of the MLSS (grey shaded bars), and +6% of the MLSS (open bars). Mean fold changes  $\pm$  SD in arbitrary units (AU) for (A) Monocarboxylate transporter 1 (MCT1), (B) Monocarboxylate transporter 4 (MCT4), (C) Sodium-hydrogen antiporter 1 (NHE1), (D) Vascular endothelial growth factor (VEGF), (E) Mitochondrial Fission Factor (MFF) and (F) Mitofusin 2 (MFN2). Expression of each target gene was normalised to the geometric mean of expression of the three most stable genes (i.e., TBP, B2M and GAPDH).

**Figure 4.13 (A-F).** The influence of exercise intensity on whole skeletal muscle mRNA immediately post, +4, and +24 hours from the onset of exercise performed at -18% of the maximal lactate steady state (MLSS) (black bars), -6% of the MLSS (grey shaded bars), and +6% of the MLSS (open bars). Mean fold changes  $\pm$  SD in arbitrary units (AU) for (A) Superoxide dismutase 1 (SOD1), (B) Activating transcription factor 2 (ATF2), (C) Nuclear respiratory factor 1 (NRF1), (D) Transcription factor EB (TFEB), (E) NAD-dependent deacetylase sirtuin-1 (SIRT1) and (F) CAMP responsive element binding protein 1 (CREB1). Expression of each target gene was normalised to the geometric mean of expression of the three most stable genes (i.e., TBP, B2M and GAPDH).

**Figure 4.14 (A-F).** The influence of exercise intensity on whole skeletal muscle mRNA immediately post, +4, and +24 hours from the onset of exercise performed at -18% of the maximal lactate steady state (MLSS) (black bars), -6% of the MLSS (grey shaded bars), and +6% of the MLSS (open bars). Mean fold changes  $\pm$  SD in arbitrary units (AU) for (A) Mitochondrial intermembrane space import and assembly protein 40 (CHCDH4), (B) cytochrome c oxidase subunit 4 isoform 1 (COX4-1), (C) Citrate Synthase (CS), (D) Cytochrome (Cyt C), (E) Cytochrome b-c1 complex subunit 2 (DRP1), and (F) Mitochondrial transcription factor A (TFAM). Expression of each target gene was normalised to the geometric mean of expression of the three most stable genes (i.e., TBP, B2M and GAPDH).

**Figure 4.15 (A-F).** The influence of exercise intensity on whole skeletal muscle mRNA measured via RNA-Sequencing immediately post, +4, and +24 hours from the onset of exercise performed at -18% of the maximal lactate steady state (MLSS) (black bars), -6% of the MLSS (grey shaded bars), and +6% of the MLSS (open bars). Mean fold changes  $\pm$  SD in arbitrary units (AU) for (A) Peroxisome proliferator-activated receptor gamma coactivator 1-alpha total (PGC-1 $\alpha$ -total), (B) tumour suppressor protein 53 (p53), (C) Superoxide dismutase 2 (SOD2), (D) cyclin-dependent kinase inhibitor 1 (p21), (E) peroxisome proliferator-activated receptor delta (PPAR $\delta$ ), and (F) Pyruvate dehydrogenase lipoamide kinase isozyme 4 (PDK4).

**Figure 4.16.** Representative western blots for the phosphorylation and total of mammalian target of rapamycin (mTOR), Ca<sup>2+</sup>/calmodulindependent protein kinase II (CaMKII), acetyl-CoA carboxylase (ACC), AMP-activated protein kinase alpha (AMPK) protein, acetyl-CoA carboxylase (ACC) protein, p38 mitogen-activated protein kinase (p38 MAPK) protein.

## List of Tables

### Chapter 1

**Table 1.1 (Moderate).** Evidence of the oxygen uptake kinetic response ( $\dot{V}O_2$ ), blood and intramuscular lactate response, muscle fibre recruitment (based on glycogen utilisation), phosphocreatine (PCr) utilisation, intramuscular nicotinamide adenine dinucleotide (NADH) concentration and substrate utilisation determined via indirect calorimetry and infusion tracer during **moderate** exercise.  $\dot{V}O_2$  plateau = a plateau in oxygen uptake kinetics without a slow component; baseline lactate = lactate values were not different from baseline values during continuous exercise; PCr plateau = a plateau in PCr utilisation during continuous exercise following the non-steady state primary component of moderate exercise; NADH below baseline = low/no cytosolic ATP turnover and free fatty acid (FFA), intramuscular triglycerides (IMTG), and plasma glucose as a source of ATP production.  $\dot{V}O_{2max}$  = maximal oxygen uptake; GET = gas exchange threshold; VT = ventilatory threshold; - = not measured. Studies included prescribed exercise below the gas exchange/ventilatory threshold or below ~45%  $\dot{V}O_{2max}$ .

**Table 1.2. (Heavy).** Evidence of the oxygen uptake kinetic response ( $\dot{V}O_2$ ), blood and intramuscular lactate response, muscle fibre recruitment (based on glycogen utilisation), phosphocreatine (PCr) utilisation, intramuscular nicotinamide adenine dinucleotide (NADH) concentration, and substrate utilisation determined via indirect calorimetry and infusion tracer during **heavy** exercise.  $\dot{V}O_2$  slow component & plateau = a plateau in oxygen uptake kinetics with an observed slow component, characterised by statistical analysis or via on-transient modelling techniques; plateau above baseline lactate = lactate values were higher compared to baseline values and stabilised during continuous exercise; PCr plateau = a plateau in PCr utilisation during continuous exercise following the non-steady state primary and slow component associated with heavy exercise; NADH above baseline = NADH values above baseline, which is indicative of cytosolic ATP turnover, and free fatty acid (FFA), intramuscular triglycerides (IMTG), plasma glucose and muscle glycogen stores as a source of ATP production.  $\dot{V}O_{2max}$  = maximal oxygen uptake; GET = gas exchange threshold;  $\Delta$  = average work rate of GET and  $\dot{V}O_{2max}$ ; CP = critical power; - = not measured. Studies included prescribed exercise below the critical power or between 46 and 84% of  $\dot{V}O_{2max}$ .

**Table 1.3.** Evidence of the oxygen uptake kinetic response ( $\dot{V}O_2$ ), blood and intramuscular lactate response, muscle fibres recruitment (based on glycogen utilisation), phosphocreatine (PCr) utilisation for ATP turnover, intramuscular nicotinamide adenine dinucleotide (NADH),

and substrate utilisation determined via indirect calorimetry and infusion tracer during **severe** exercise.  $\dot{V}O_2$  slow component & no plateau = absence of a plateau in oxygen uptake kinetics with an observed slow component, characterised by statistical analysis or via on-transient modelling techniques; no plateau above baseline lactate = lactate values were higher compared to baseline values and continued to rise until the cessation of exercise; PCr no plateau = no plateau in PCr utilisation during continuous exercise following the non-steady state primary and slow component associated with severe exercise; NADH above baseline = NADH values above baseline, which is indicative of cytosolic ATP turnover and free fatty acid (FFA), intramuscular triglycerides (IMTG), plasma glucose, and muscle glycogen stores as a source of ATP production.  $\dot{V}O_{2max}$  = maximal oxygen uptake; CP = critical power; - = not measured. Studies included prescribed exercise above the critical power or above 85% of  $\dot{V}O_{2max}$  and below 100% of  $\dot{V}O_{2max}$ .

**Table 1.4.** The five aerobic training zone system based on the first and second lactate threshold (LT<sub>1</sub> and LT<sub>2</sub>) derived from a GXT. Each zone is characterised by a % of HR<sub>max</sub>, an absolute blood lactate value, a rating of perceived exertion, and the relationship with a submaximal anchor [20, 21].

**Table 1.5.** The training intensity distribution model divides intensity into 3 zones, where zones 1 and zone 2 are demarcated by LT<sub>1</sub>, GET/VT and zones 2 and 3 are demarcated by LT<sub>2</sub>, RCP and MLSS. Each zone is characterised by a % of HR<sub>max</sub>, %  $\dot{V}O_{2max}$ , absolute blood lactate value, and the relationship with submaximal anchor [22-25].

**Table 1.6.** Prescribing exercise intensity based on physiological domains<sup>2</sup>. Each domain can be characterised by their specific oxygen uptake ( $\dot{V}O_2$ ) kinetic and blood lactate response. The components of  $\dot{V}O_2$  kinetics refers to the  $\dot{V}O_2$  on-transient exponential modelling [26].

## Chapter 2

**Table 2.1.** The mean  $\pm$  standard deviation (SD) of the 14 lactate thresholds calculated from the 4 prolonged graded exercise tests (i.e., GXT<sub>3</sub>, GXT<sub>4</sub>, GXT<sub>7</sub> and GXT<sub>10</sub>), and the respiratory compensation point (RCP) and the maximal lactate steady state (MLSS) estimated from the RCP (RCP<sub>MLSS</sub>) calculated from GXT<sub>1</sub>.

**Table 2.2.** Mean, standard deviation, and range of the  $\dot{V}O_2$  and power associated with the maximal lactate steady state (MLSS) expressed as a percentage of the maximal power ( $\dot{W}_{max}$ ) and  $\dot{V}O_{2peak}$  measured during each GXT.

**Table 2.3.** Mean  $\pm$  standard deviation, mean difference (MD), intraclass correlation coefficient (ICC), Lin's concordance correlation coefficient ( $\rho_c$ ), standard error of the measurement (SEM), effect size (ES) with 95% confidence limits, and coefficient of the variation (%CV) between the maximal lactate steady state (MLSS) and the eleven thresholds included in our analysis.

**Table 2.4.** Mean difference (MD), effect size (ES), and p-value comparing the influence of graded exercise test stage length on all 14 lactate threshold methods.

**Table 2.5.** Mean and standard deviation of  $\dot{V}O_{2max}$  - highest measured  $\dot{V}O_2$  during any graded exercise test (GXT); GXT  $\dot{V}O_2$  -highest measured  $\dot{V}O_2$  during each GXT; VEB  $\dot{V}O_2$  highest measured  $\dot{V}O_2$  during each verification exhaustive bout (VEB);  $\dot{V}O_{2peak}$ , highest measured  $\dot{V}O_2$  during either the GXT or corresponding VEB.

**Table 2.6.** Mean difference (MD) and standard deviation, effect size (ES), coefficient of the variation (CV) and p-value (p) for the measured  $\dot{V}O_{2peak}$  values from GXT<sub>1</sub> compared with the  $\dot{V}O_{2peak}$  values from GXT<sub>3</sub>, GXT<sub>4</sub>, GXT<sub>7</sub>, and GXT<sub>10</sub> and for the  $\dot{V}O_{2peak}$  values from GXT<sub>1</sub> compared with the  $\dot{V}O_{2peak}$  values from the VEB following GXT<sub>3</sub>, GXT<sub>4</sub>, GXT<sub>7</sub>, and GXT<sub>10</sub>.

## Chapter 4

**Table 4.1.** Details of primer sequences used for RT-qPCR.

**Table 4.2** Mean  $\pm$  SD values from the constant power exercise biopsy trials [-18%, -6, and +6% of the maximal lactate steady state (MLSS), and at the MLSS for power (Watts), percentage of maximal work rate from 8-12 minute GXT (% of  $\dot{W}_{max}$ ), end exercise absolute blood lactate, change ( $\Delta$ )” in blood lactate from to 10 to 30 minutes during the constant power exercise bout, end exercise oxygen uptake ( $\dot{V}O_2$ ), end exercise oxygen uptake expressed as a percentage of maximal oxygen uptake from 8-12 minute GXT (%  $\dot{V}O_{2max}$ ), and end exercise oxygen uptake expressed as a percentage of oxygen uptake associated with the MLSS (%  $\dot{V}O_2$  of MLSS).

**Table 4.3** Effect Sizes [Low and High, 90% confidence intervals] for changes in whole skeletal muscle mRNA, immediately post, 4 and 24 hours from the onset of exercise at -18%, -6% and +6% of the maximal lactate steady state (MLSS). **Trivial** < 0.3; **Small** < 0.6; **Moderate** < 1.2; **Large** < 2.0, **Very Large** < 4.0.



**Chapter 1: An Examination and Critique of Current Methods to Prescribe  
Exercise Intensity**

## 1.1 Introduction

Exercise training is commonly employed to improve both athletic performance and health [27]. However, while seemingly simple, the underlying exercise prescription to bring about the desired adaptations is as complicated as that of any drug [28]. Many studies report that training-induced changes in factors such as maximal aerobic power ( $\dot{V}O_{2\max}$ ) [29-31], cardiac function [32], respiratory function [33], cognitive function [34], insulin sensitivity [35], mitochondrial function and content [36], and bone mineral density [37], are influenced by the frequency, duration, volume, and intensity of the exercise stimulus. Prescribing the frequency, duration, or volume of training is relatively simple as these factors can be altered by manipulating the number of exercise sessions per week, the duration of each session, or the total work performed in a given time frame (e.g., per week). However, exercise intensity is more complex and there is controversy regarding the reliability and validity of the many methods used to determine and prescribe exercise intensity.

Methods for prescribing exercise intensity include a percentage of various anchor measurements, such as  $\dot{V}O_{2\max}$  and  $\dot{V}O_{2\text{peak}}^1$ , maximum heart rate ( $\% \text{HR}_{\max}$ ), and maximum work rate (i.e., power or velocity) (i.e.,  $\dot{W}_{\max}$  or  $\dot{V}_{\max}$ , respectively), derived from a graded exercise test (GXT). Submaximal anchors are purported to represent shifts in the metabolic state of the working muscle and are derived from a GXT can also be used to prescribe exercise intensity, including the ventilatory threshold (VT), the gas exchange threshold (GET), the respiratory compensation point (RCP), and the <sup>\$</sup>first and second lactate threshold ( $\text{LT}_1$  and  $\text{LT}_2$ ) [38, 39]. Other anchor measurements, such as the maximal lactate steady state (MLSS) and critical power/speed (CP and CS) [38, 40, 41], can also be derived from a series of constant

<sup>1</sup> $\dot{V}O_{2\max}$ : refers to the maximal oxygen uptake value from an 8- to 12-minute GXT confirmed via a verification exhaustive bout (VEB);  $\dot{V}O_{2\text{peak}}$ : refers to the peak oxygen uptake value from a <8- or >12-minute GXT or a  $\dot{V}O_2$  value not confirmed via a VEB [1]. <sup>\$</sup> $\text{LT}_1$  and  $\text{LT}_2$  refers to the purported methods that demarcate the moderate-heavy and heavy-severe domains of exercise, respectively.

work rate bouts. CP and CS are metrics can also be derived using a 3-min all-out exercise test (3MT) [42, 43]. There are methods that prescribe intensity based on the differences between resting and maximal values (i.e., reserve), these methods are called the HR reserve ( $\%HR_R$ ) and  $\dot{V}O_2$  reserve ( $\%\dot{V}O_2$ ). Lastly, the delta (i.e.,  $\Delta$ ) method uses the percent difference between a maximal anchor and submaximal anchors (e.g.,  $\dot{W}_{max}$  and GET) [44]. Although these common methods to prescribe exercise intensity, are often and used interchangeably, there is research challenging this practice [45-49].

An alternative approach for prescribing exercise intensity is based on training distributions or zones [21, 23, 50]. For example, one model creates five exercise intensity zones or levels based upon  $LT_1$  and  $LT_2$  derived from a GXT (**Figure 1.1**) [21]. Another model, which uses anchors paired with the retrospective analyses of athlete training distributions, has been used to yield three different training zones (**Figure 1.2**) [22, 23, 25, 28, 51, 52]. These models rely on maximal and submaximal anchors to demarcate the different training zones; however, there is little evidence to confirm the validity of the applied anchors to identify the various training zones. There is also a training model based on the domains of exercise, which are independent of submaximal anchors and defined by homeostatic perturbations (i.e., oxygen uptake kinetics and the blood lactate response) [6, 26, 40, 41, 53-63] (**Figure 1.3**)<sup>2</sup>. Nonetheless, submaximal anchors are often used to define the domains of exercise and are used interchangeably, despite little evidence to support the validity of this approach.

<sup>2</sup>The extreme domain is a supramaximal domain and defined as an intensity above  $\dot{V}O_{2max}$ . Methods to appropriately demarcate the extreme domain are beyond the scope of this review and will not be discussed.

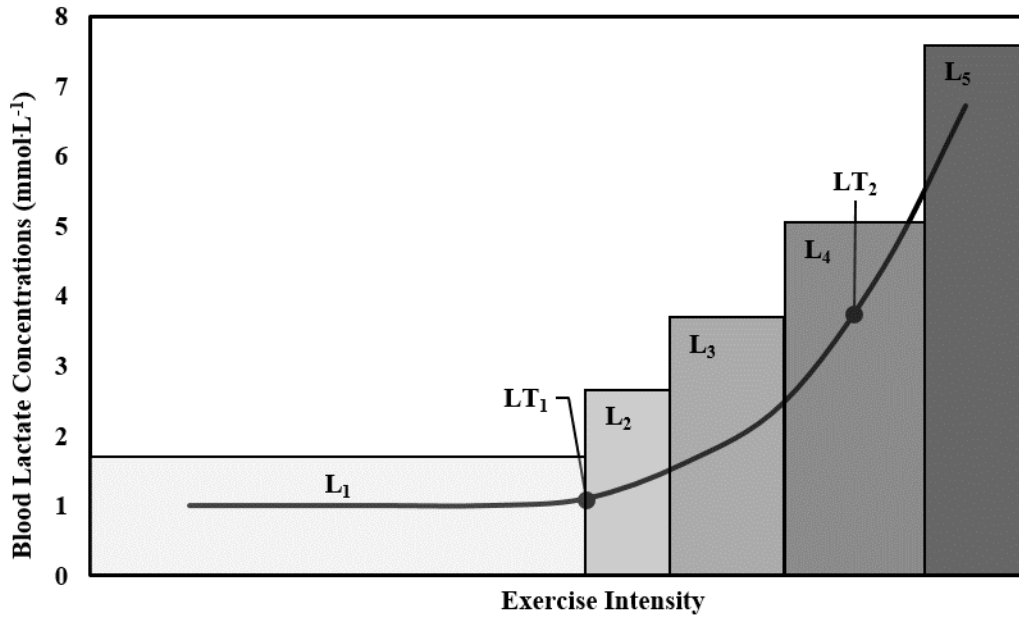


**Figure 1.1.** The five aerobic training zones (L1-L5) based on the first and second lactate threshold ( $LT_1$  and  $LT_2$ ) derived from a GXT. The  $LT_1$  (i.e., lactate transition 1) represents the rise in blood lactate above baseline. The  $LT_2$  (i.e., lactate transition 2) represents an acceleration of blood lactate accumulation.

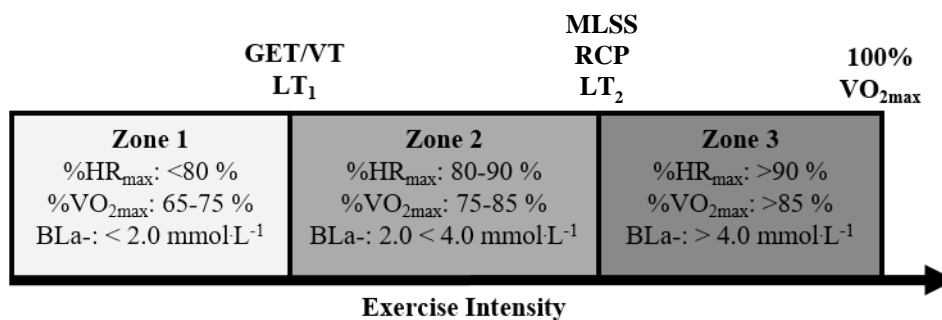


**Figure 1.2.** The training intensity distribution model divides intensity into 3 zones, where zones 1 and zone 2 are demarcated by  $LT_1$ /GET/VT and zones 2 and 3 by  $LT_2$ /RCP/MLSS. Each zone is characterised by % $HR_{max}$ , % $\dot{V}O_{2max}$ , absolute blood lactate value, and relationship with a submaximal anchor.

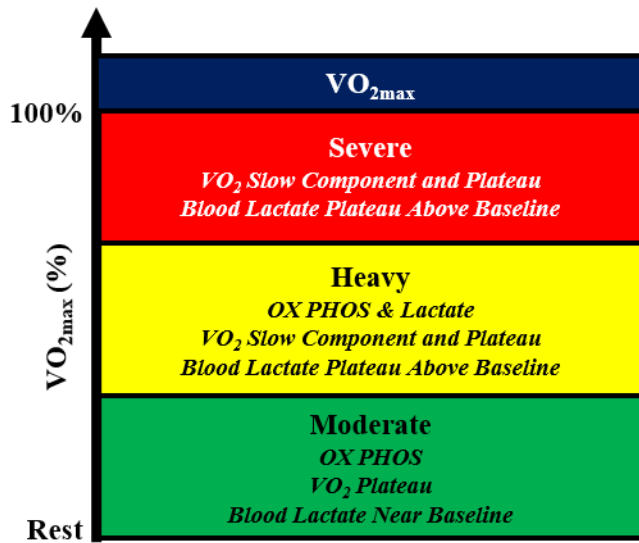


**Figure 1.3.** Prescribing exercise intensity based on physiological domains<sup>2</sup>. Each domain can be characterised by a specific oxygen uptake ( $\dot{V}O_2$ ) kinetic and blood lactate response. The moderate domain can be characterised by a plateau of  $\dot{V}O_2$  and blood lactate concentrations near baseline levels, the heavy domain by an observed ‘slow component’ of  $\dot{V}O_2$  with a delayed steady state, and a rise in blood lactate above baseline with subsequent plateau, and the severe by a ‘slow component’ without a steady state of  $\dot{V}O_2$  and a continual increase in blood lactate.

An implicit assumption is that different methods of prescribing an apparently equivalent exercise intensity will result in similar homeostatic disturbances in all participants and provide a similar training stimulus [64]. Although there has been limited research directly assessing this assumption, it is clear that ostensibly similar exercise intensities can result in very different homeostatic perturbations [44, 65-68]. For example, exercise prescribed between 60 and 80% of  $\dot{V}O_{2max}$  is often referred to as moderate intensity [69, 70]; however, large differences in homeostatic perturbations (e.g.,  $\dot{V}O_2$  kinetics) have been reported across multiple studies for exercise performed within those percentages of  $\dot{V}O_{2max}$  [44, 65-68] – discussed in sections 1.2.1 - 1.2.3. Some investigators have proposed that exercise prescribed relative to submaximal anchor points (e.g., GET/VT and CP) will result in a more homogenous homeostatic perturbations [38, 68]. However, the proposed validity of these anchors has also been called into question [26, 41-43, 71-86] discussed in section 1.3.

There is a clear relationship between increasing exercise intensity and the magnitude of homeostatic perturbations in response to exercise [6, 14, 53, 57, 62, 63, 87-94] and these include systemic responses (e.g., increased  $\dot{V}O_2$  and blood lactate concentration), changes in intramuscular substrates and metabolites (e.g., intramuscular PCr, lactate, and ATP), and

mechanical stress [10, 87, 88]. Although all of these perturbations are influenced by exercise intensity [95, 96], many are of limited value to routinely quantify exercise intensity given the lack of research, or the invasive nature of the techniques required to obtain some measures (e.g., muscle biopsies). For this reason, less-invasive, systemic responses, such as  $\dot{V}O_2$  and blood lactate concentration, which are associated with intramuscular changes [6, 87, 88, 97-99], are typically used as indicators of homeostatic perturbations in response to different exercise intensities (**Figure 1.4**).

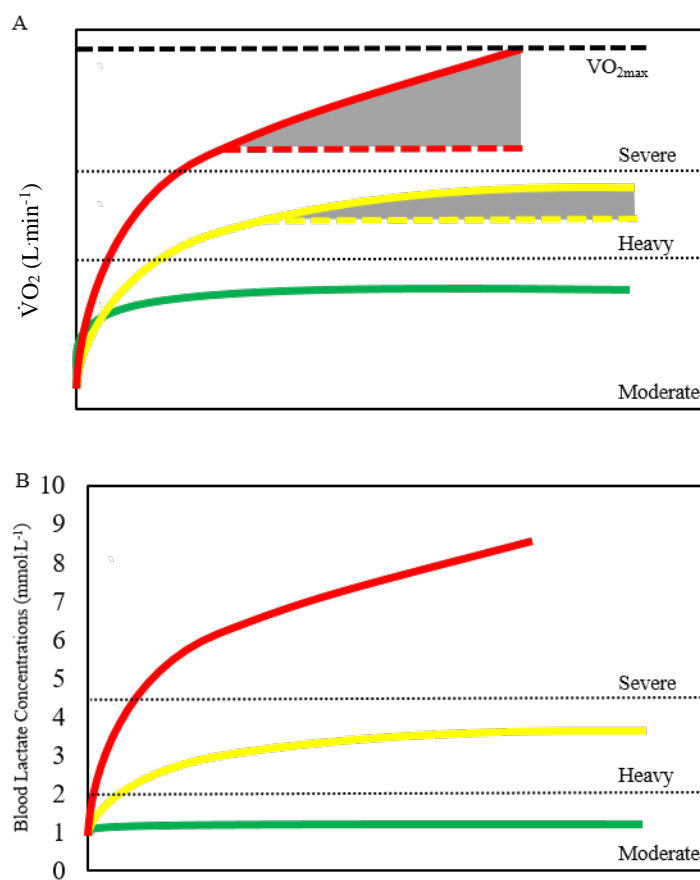


**Figure 1.4 (A & B)** A)  $\dot{V}O_2$ , and B) blood lactate responses during moderate, heavy and severe exercise. Moderate (green line), heavy (yellow line), and severe exercise (red line). A)  $\dot{V}O_2$  kinetics during moderate exercise is depicted by mono-exponential uptake response with an attained steady state. During heavy and severe exercise there is a delayed steady state (i.e., a slow component) due to the curvilinear increase in the  $\dot{V}O_2$ -work rate relationship (grey shaded area). During heavy exercise there is a delayed steady state following the slow component. During severe exercise there is an observed  $\dot{V}O_2$  slow component absent of a steady state and continuous exercise results in the attainment of  $\dot{V}O_{2max}$ . B) The blood lactate response during moderate exercise remains at baseline due to the predominant source of energy being derived via oxidative phosphorylation. The blood lactate response during heavy exercise is an increase above baseline with a steady state. The blood lactate during severe exercise is a rise above baseline with an absence of a steady state.

Oxygen uptake kinetics and blood lactate responses are reflective of intramuscular perturbations and can be monitored with relative ease [38, 90]. A plateau of  $\dot{V}O_2$  and blood lactate concentrations near baseline level indicates that ATP production is being met predominantly via oxidative phosphorylation [57, 59, 100, 101], type I muscle fibre recruitment [102], a low rate of muscle glycogen depletion [103], low calcium flux [14], and that muscle lactate and  $H^+$  concentrations will be similar to baseline values [87, 88] (**Table 1.1; Figure 1.4 and 1.5**). An observed 'slow component' of  $\dot{V}O_2$ , with a delayed steady state, and a rise in blood lactate above baseline with a subsequent plateau, represents a plateau of intramuscular lactate concentration [57], and a decrease in contractile efficiency attributable to increased cytosolic ATP turnover [104]. This effect is a consequence of the recruitment of type II muscle fibres [55, 59, 105-107], a moderate rate of glycogen depletion [103] and calcium flux [14], and a decrease and subsequent plateau in muscle pH [6] (**Table 1.2; Figure 1.4 and 1.5**). A 'slow component' without a steady state of  $\dot{V}O_2$  and a continual increase in blood lactate [62] is indicative of increased cytosolic ATP turnover (with a continual increase in intramuscular lactate concentrations) [13, 57, 59, 106, 107], contribution of phosphocreatine stores to ATP turnover [6, 63], added recruitment of highly fatigable type II muscle fibres [55, 105], rapid rates of muscle glycogen depletion [92, 103], high calcium flux [14], and a continual decrease in muscle pH [6] (**Table 1.3; Figure 1.4 and 1.5**). Although training status influences exercise tolerance at a given intensity [108], overall muscle glycogen content [109], discrete  $\dot{V}O_2$  patterns (e.g., the phase II time constant) [110, 111], and intramuscular lactate oxidation (i.e., lactate shuttle) [93, 112], these factors have little influence on the  $\dot{V}O_2$  and blood lactate kinetic responses during exercise in healthy individuals [3, 113-115]. Therefore, prescribing exercise intensity based on homeostatic perturbations (i.e., systemic responses) could be an effective method to normalise exercise intensity (i.e., to elicit an explicit and/or homogenous homeostatic perturbation) between individuals.

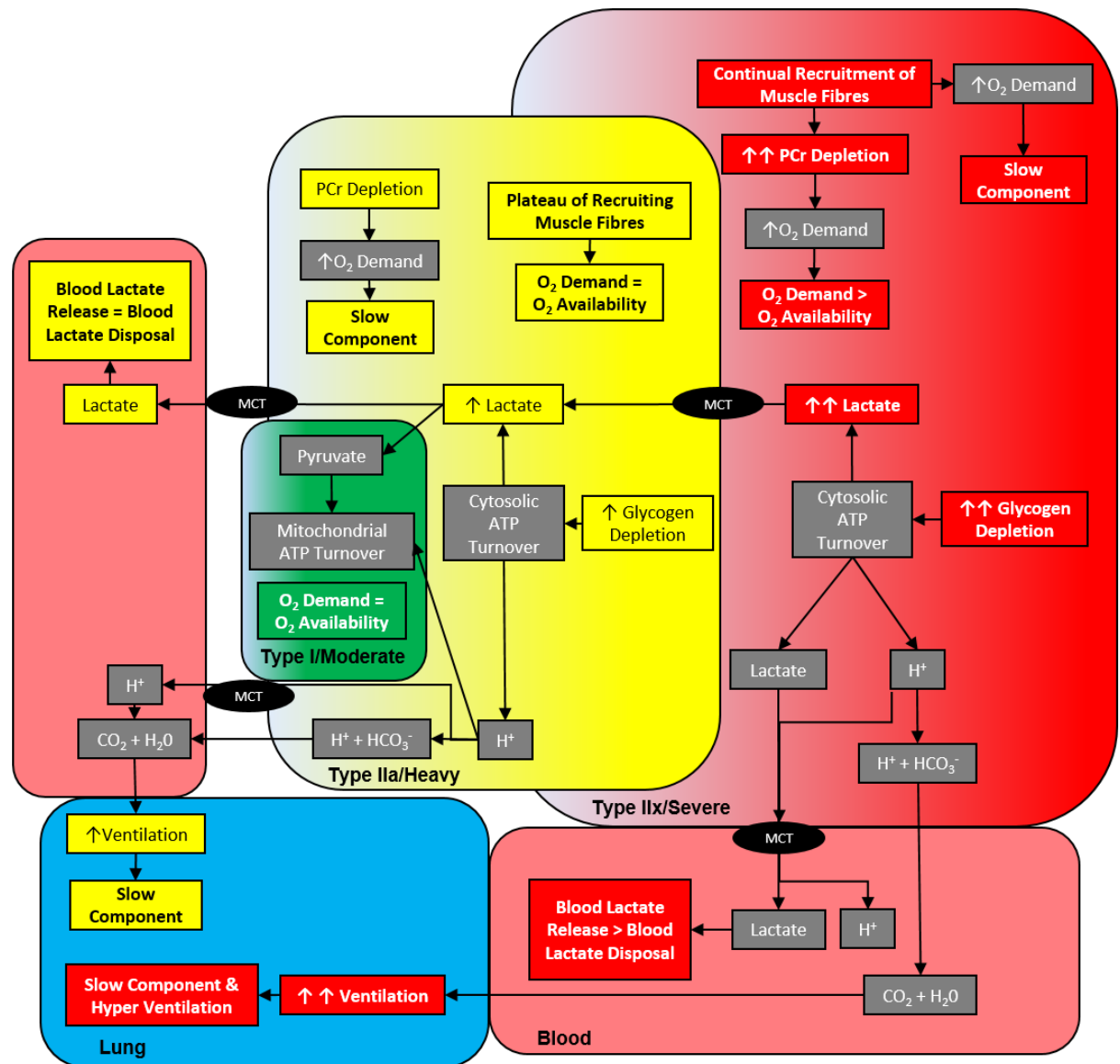


**Figure 1.5.** Schematic illustrating the domain-specific muscle recruitment pattern contributing to the slow component of oxygen uptake, absence of an oxygen uptake plateau, and the blood lactate response. During continuous, moderate exercise, type I muscle fibres are predominantly recruited, ATP is produced solely via mitochondrial ATP turnover (i.e., Krebs Cycle),  $O_2$  demand is equal to  $O_2$  availability, and muscle and blood lactate levels remain at baseline. During continuous, heavy exercise, type I and IIa muscle fibres are recruited, ATP is produced via mitochondrial and cytosolic ATP turnover, the recruitment of less efficient type IIa muscle fibres and the increase in ventilation due to increased non-metabolic  $CO_2$  production results in the delayed steady state of oxygen uptake (i.e., a slow component), and the reliance on non-mitochondrial ATP turnover results in an increase in blood lactate above baseline with an achieved steady state mirroring the oxygen uptake pattern. During continuous, severe exercise, type I, IIa and IIx muscle fibres are recruited, ATP is produced via mitochondrial, cytosolic ATP turnover and via a continual depletion of the phosphocreatine stores (PCr), which results in the continual increase in  $O_2$  uptake until the cessation of exercise. The recruitment of less efficient type IIa and IIx muscle fibres increase the amplitude of the slow component, further increase ventilation (i.e., hyperventilation) due to increased non-metabolic  $CO_2$  production. Lastly, intramuscular lactate production exceeds lactate oxidation, which results in lactate appearance exceeding disappearance. MCT = monocarboxy transporter

**Table 1.1 (Moderate).** Evidence of the oxygen uptake kinetic response ( $\dot{V}O_2$ ), blood and intramuscular lactate response, muscle fibre recruitment (based on glycogen utilisation), phosphocreatine (PCr) utilisation, intramuscular nicotinamide adenine dinucleotide (NADH) concentration and substrate utilisation determined via indirect calorimetry and infusion tracer during **moderate** exercise.  $\dot{V}O_2$  plateau = a plateau in oxygen uptake kinetics without a slow component; baseline lactate = lactate values were not different from baseline values during continuous exercise; PCr plateau = a plateau in PCr utilisation during continuous exercise following the non-steady state primary component of moderate exercise; NADH below baseline = low/no cytosolic ATP turnover and free fatty acid (FFA), intramuscular triglycerides (IMTG), and plasma glucose as a source of ATP production.  $\dot{V}O_{2max}$  = maximal oxygen uptake; GET = gas exchange threshold; VT = ventilatory threshold; - = not measured. Studies included prescribed exercise below the gas exchange/ventilatory threshold or below ~45%  $\dot{V}O_{2max}$ .

Reference	Exercise Intensity % $\dot{V}O_{2max}$	Oxygen Uptake Kinetics	Blood Lactate	Intramuscular Lactate	Muscle Fibres Recruited	PCr Utilisation	NADH	Substrate Utilisation
Gollnick et al., [103]	31% of $\dot{V}O_{2max}$	-	Baseline	-	Type I	-	-	-
Jorfeldt et al., [57]	29% of $\dot{V}O_{2max}$	-	Baseline	Baseline	-	-	-	-
Vøllestad & Blom, [116]	43% of $\dot{V}O_{2max}$	-	Baseline	-	Type I	-	-	-
Sahlin et al., [13]	40% of $\dot{V}O_{2max}$	-	-	Baseline	-	-	Below Baseline	-
Spriet et al., [117]	40%	-	-	Baseline	-	-	Type I and II Below Baseline	-
Barstow & Moe, [118]	35% of $\dot{V}O_{2max}$	$\dot{V}O_2$ Plateau	-	-	-	-	-	-
Romijn et al., [11]	25% of $\dot{V}O_{2max}$	-	-	-	-	-	-	FFA, IMTG, Glucose
Barstow et al., [101]	80% of GET	$\dot{V}O_2$ Plateau	-	-	-	Plateau	-	-
Rossiter et al., [100]	80% of VT	$\dot{V}O_2$ Plateau	-	-	-	Plateau	-	-
Bell et al., [119]	80% of VT	$\dot{V}O_2$ Plateau	-	-	-	-	-	-
Simmonds et al., 2013	80% of GET	$\dot{V}O_2$ Plateau	Baseline	-	-	-	-	-
Black et al., [94]	90% of GET	$\dot{V}O_2$ Plateau	Baseline	Baseline	-	Plateau	-	-

**Table 1.2 (Heavy).** Evidence of the oxygen uptake kinetic response ( $\dot{V}O_2$ ), blood and intramuscular lactate response, muscle fibre recruitment (based on glycogen utilisation), phosphocreatine (PCr) utilisation, intramuscular nicotinamide adenine dinucleotide (NADH) concentration, and substrate utilisation determined via indirect calorimetry and infusion tracer during **heavy** exercise.  $\dot{V}O_2$  slow component & plateau = a plateau in oxygen uptake kinetics with an observed slow component, characterised by statistical analysis or via on-transient modelling techniques; plateau above baseline lactate = lactate values were higher compared to baseline values and stabilised during continuous exercise; PCr plateau = a plateau in PCr utilisation during continuous exercise following the non-steady state primary and slow component associated with heavy exercise; NADH above baseline = NADH values above baseline, which is indicative of cytosolic ATP turnover, and free fatty acid (FFA), intramuscular triglycerides (IMTG), plasma glucose and muscle glycogen stores as a source of ATP production.  $\dot{V}O_{2max}$  = maximal oxygen uptake; GET = gas exchange threshold;  $\Delta$  = average work rate of GET and  $\dot{V}O_{2max}$ ; CP = critical power; - = not measured. Studies included prescribed exercise below the critical power or between 46 and 84% of  $\dot{V}O_{2max}$ .

Reference	Exercise Intensity	Oxygen Uptake Kinetics	Blood Lactate	Intramuscular Lactate	Muscle Fibres Recruited	PCr Utilisation	NADH	Substrate Utilisation
Gollnick et al., [103]	64% of $\dot{V}O_{2max}$	-	Plateau Above Baseline	-	Type I and II	-	-	-
Jorfeldt et al., [57]	51% & 71% of $\dot{V}O_{2max}$	-	Plateau Above Baseline	Plateau Above Baseline	-	-	-	-
Vøllestad & Blom, [116]	61% of $\dot{V}O_{2max}$	-	Plateau Above Baseline	-	Type I & IIa	-	-	-
Sahlin et al., [13]	75% of $\dot{V}O_{2max}$	-	-	Above Baseline	-	-	Above Baseline	-
Spriet et al., [117]	75% of $\dot{V}O_{2max}$	-	-	Above Baseline	-	-	Type I and II Above Baseline	-
Romijn et al., [11]	65% of $\dot{V}O_{2max}$	-	-	-	-	-	-	FFA, IMTG, Glucose, Glycogen
Jones et al., [120]	90% of CP	-	-	-	-	Plateau	-	-
Simmonds et al., 2013	$\Delta$ 40% of GET & $\dot{V}O_{2peak}$	$\dot{V}O_2$ Slow Component & Plateau	Plateau Above Baseline	-	-	-	-	-
Vanhatalo et al., [6]	95% of CP	$\dot{V}O_2$ Slow Component & Plateau	Plateau Above Baseline	Plateau Above Baseline	-	Plateau	-	-
Black et al., [94]	~92% of CP	$\dot{V}O_2$ Slow Component & Plateau	Plateau Above Baseline	Above Baseline	-	Below Baseline	-	-

**Table 1.3 (Severe).** Evidence of the oxygen uptake kinetic response ( $\dot{V}O_2$ ), blood and intramuscular lactate response, muscle fibres recruitment (based on glycogen utilisation), phosphocreatine (PCr) utilisation for ATP turnover, intramuscular nicotinamide adenine dinucleotide (NADH), and substrate utilisation determined via indirect calorimetry and infusion tracer during **severe** exercise.  $\dot{V}O_2$  slow component & no plateau = absence of a plateau in oxygen uptake kinetics with an observed slow component, characterised by statistical analysis or via on-transient modelling techniques; no plateau above baseline lactate = lactate values were higher compared to baseline values and continued to rise until the cessation of exercise; PCr no plateau = no plateau in PCr utilisation during continuous exercise following the non-steady state primary and slow component associated with severe exercise; NADH above baseline = NADH values above baseline, which is indicative of cytosolic ATP turnover and free fatty acid (FFA), intramuscular triglycerides (IMTG), plasma glucose, and muscle glycogen stores as a source of ATP production.  $\dot{V}O_{2max}$  = maximal oxygen uptake; CP = critical power; - = not measured. Studies included prescribed exercise above the critical power or above 85% of  $\dot{V}O_{2max}$  and below 85% of  $\dot{V}O_{2max}$ .

Reference	Exercise Intensity	Oxygen Uptake Kinetics	Blood Lactate	Intramuscular Lactate	Muscle Fibres Recruited	PCr Utilisation	NADH	Substrate Utilisation	$\dot{V}O_{2max}$ Attained
Jorfeldt et al., [57]	87% of $\dot{V}O_{2max}$	NA	Above Baseline & No Plateau	No Plateau Above Baseline	NA	NA	NA	NA	NA
Vøllestad & Blom, [116]	91% of $\dot{V}O_{2max}$	NA	Above Baseline & No Plateau	No Plateau Above Baseline	Type I, IIa, IIax & IIx	NA	NA	NA	NA
Sahlin et al., [13]	100% of $\dot{V}O_{2max}$	NA	NA	Above Baseline	NA	NA	Above Baseline	NA	NA
Spriet et al., [117]	100% of $\dot{V}O_{2max}$	NA	NA	Above Baseline	NA	NA	Type I and II Above Baseline	NA	NA
Poole et al., [62]	105% of CP	$\dot{V}O_2$ Slow Component & No Plateau	Above Baseline & No Plateau	NA	NA	NA	NA	NA	Yes
Romijn et al., [11]	85% of $\dot{V}O_{2max}$	NA	NA	NA	NA	NA	NA	FFA, IMTG, Glucose, Glycogen	NA
Jones et al., [120]	110% of CP	NA	NA	NA	NA	Continual Depletion & No Plateau	NA	NA	NA
Vanhatalo et al., [6]	105% of CP	$\dot{V}O_2$ Slow Component & No Plateau	Above Baseline & No Plateau	NA	NA	No Plateau	NA	NA	Yes
Black et al., [94]	105% of CP	$\dot{V}O_2$ Slow Component & No Plateau	Above Baseline & No Plateau	Above Baseline	NA	NA	NA	NA	Yes

The aim of this review is to evaluate the most common methods used to prescribe exercise intensity, and discuss their reliability and validity based on the ability to yield distinct and/or homogeneous homeostatic perturbations. We address protocol designs, criteria for establishing anchors, and the limitations of each method. Discrepancies in the assumed validity and concurrent validity (i.e., agreement between anchors) of the methods used to normalise and prescribe exercise intensity are also discussed. Lastly, recommendations for prescribing exercise intensity and future research directions are provided [38].

## 1.2 Prescribing Exercise Intensity Relative to Maximal Anchors

In both applied and laboratory settings, exercise intensity is often prescribed based on a percentage of an individual's  $\dot{V}O_{2\max}$ ,  $HR_{\max}$ ,  $\dot{W}_{\max}$ , or  $\dot{V}_{\max}$  [27, 95, 121]. Percent maximum prescriptions presume that all participants within a cohort will experience similar homeostatic perturbations to the same relative intensity. While research has shown this assumption has shortcomings in normalising exercise intensity [3, 65-67, 122, 123], these methods continue to be used to prescribe exercise intensity.

### 1.2.1 Maximal Oxygen Uptake

The optimal protocol for establishing  $\dot{V}O_{2\max}$  is an 8- to 12-minute GXT followed by a subsequent verification exhaustive bout (VEB) [124-126]. The  $\dot{V}O_{2\max}$  value is deemed valid when the difference between the observed  $\dot{V}O_2$  values from the GXT and VEB are within the variability of the measurement (i.e.,  $CV = 3\%$ ) [1, 42, 125, 127-132]. There is a high test-retest reliability for establishing  $\dot{V}O_{2\max}$  ( $CV < 3\%$ ) [38, 131]; however, decreasing the GXT slope (i.e.,  $W \cdot s^{-1}$ ) (which increases GXT duration) reduces the reliability [133-136]. Furthermore, decreasing the GXT slope lowers the  $\dot{V}O_{2\max}$  [1, 137-140] and can cause the agreement between observed  $\dot{V}O_2$  values from the GXT and VEB to exceed the variability of the measurement [1, 128]. Thus, the validity of the  $\dot{V}O_{2\max}$  is protocol-dependent, and the calculated  $\dot{V}O_{2\max}$  value is lower and less reliable if the GXT duration exceeds 12 minutes.

Prescribing intensity as a fixed percentage of  $\dot{V}O_{2\max}$  requires constant monitoring to verify the desired  $\dot{V}O_2$  response is maintained during prolonged exercise [15, 141, 142]. Furthermore, to maintain a constant percentage of  $\dot{V}O_{2\max}$  when exercise is performed at intensities above moderate requires frequent/regular adjustments to the work rate to compensate for the continual increase in  $\dot{V}O_2$  (i.e., the slow component) [55, 67]. In lieu of constant monitoring of  $\dot{V}O_2$ , some researchers extrapolate a work rate from the  $\dot{V}O_2$ -work rate

relationship derived from a GXT. However, this relies on the assumption of a linear relationship between  $\dot{V}O_2$  and work rate [44, 70, 143], whereas this relationship shifts from linear to curvilinear during the latter stages portion of a GXT [2, 144, 145] (**Figure 1.6**). The mean response time (MRT) or time for the pulmonary  $\dot{V}O_2$  to reflect the metabolic demand of the working muscle increases curvilinearly and becomes more variable [146], increasing the departure of the observed  $\dot{V}O_2$  response from the assumed linearity. For example, when researchers extrapolated a work rate evoking 70% of  $\dot{V}O_{2max}$  based on the results of a GXT, four of the nine participants achieved their  $\dot{V}O_{2max}$  in under 20 min of exercise [44]. Assuming a linear relationship or using a standardised extrapolation technique does not accommodate for the observed curvilinear relationship in the  $\dot{V}O_2$ -work rate relationship, and it is difficult to achieve a fixed percentage of  $\dot{V}O_{2max}$  without constant monitoring/verification.

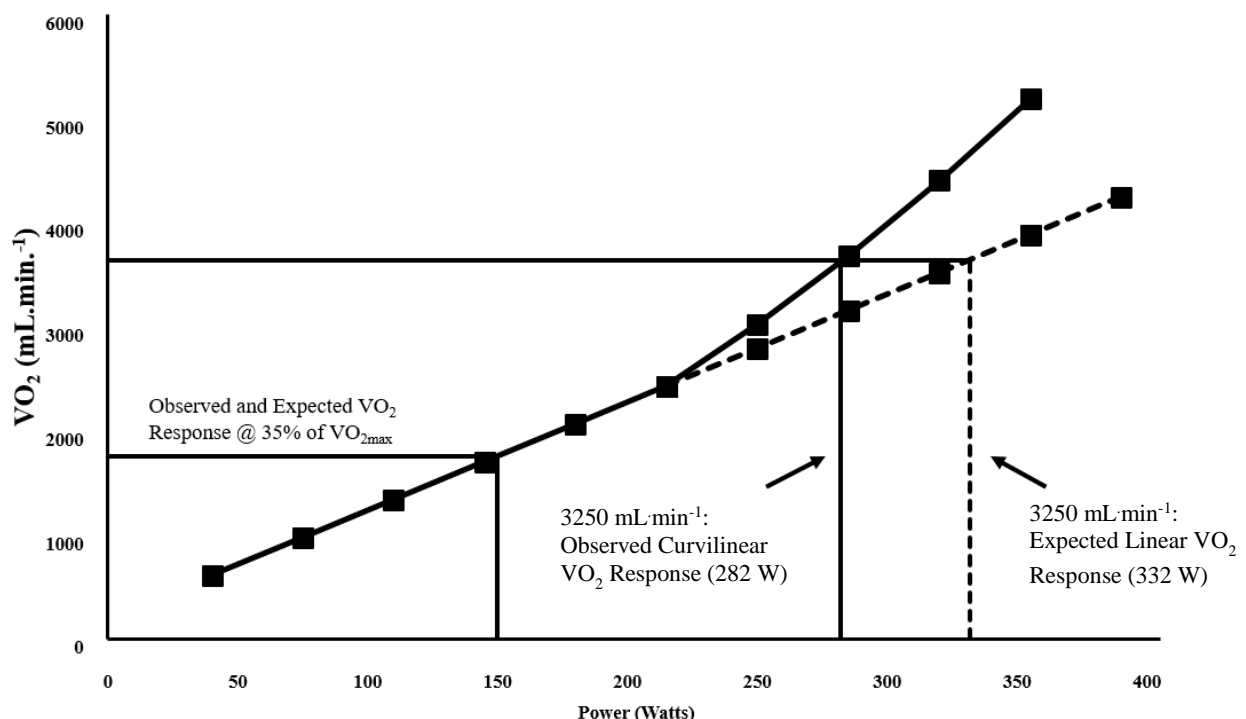


**Figure 1.6.** Expected and observed  $\dot{V}O_2$  response relative to power. During low exercise intensities there is a linear  $\dot{V}O_2$ -work rate relationship. As exercise intensity increases the relationship between  $\dot{V}O_2$  and work rate becomes curvilinear and the observed work rate associated with 70% of  $\dot{V}O_{2max}$  is lower than that expected for a linear relationship (282 vs. 332 W). Figure redrawn from Zoldaz et. al. [2].

It is not surprising that studies have demonstrated that prescribing exercise intensity as a percentage of  $\dot{V}O_{2\max}$  (i.e., 60 to 75%  $\dot{V}O_{2\max}$ ) is not a valid method to elicit similar physiological responses in different individuals. For example, exercise prescribed at 70% of  $\dot{V}O_{2\max}$  (i.e., a work rate corresponding to ~70% of  $\dot{V}O_{2\max}$ ) resulted in significantly higher concentrations of plasma markers (i.e., plasma ammonia and hypoxanthine) associated with metabolic stress in untrained compared with trained individuals (**Figure 1.7**) [3]. Another study examined the blood lactate response at fixed percentages of  $\dot{V}O_{2\max}$  (i.e., 60 and 75% of  $\dot{V}O_{2\max}$ ) determined via  $\dot{V}O_2$ -work rate extrapolation, and a large variability (CV = 52 and 41%, respectively) was observed for the blood lactate responses [67]. Furthermore, modest decreases in work rate were required to maintain  $\dot{V}O_2$  at 75% of  $\dot{V}O_{2\max}$ , which was attributed to the  $\dot{V}O_2$  slow component. Moreover, higher inter-subject physiological responses and perceptual effort variability were evident when prescribing exercise relative to  $\dot{V}O_{2\max}$  was compared with prescribing exercise relative to the average work rate of the work rate associated with the GET and  $\dot{W}_{\max}$  [44]. A high variability was also observed among highly trained cyclists for muscle glycogen utilisation (17 to 83 mmol·kg<sup>-1</sup>) and respiratory exchange ratios (0.81 to 0.97) when cycling at ~79% of  $\dot{V}O_{2\max}$  [141]. Therefore, the evidence does not support the validity of using a fixed percentage of  $\dot{V}O_{2\max}$  to prescribe exercise intensity in order to obtain similar homeostatic perturbations in all participants. There is an apparent difference between trained and untrained individuals when exercising at the same percentage of  $\dot{V}O_{2\max}$ ; moreover it is interesting to note that the same phenomena can be observed in homogenous population.

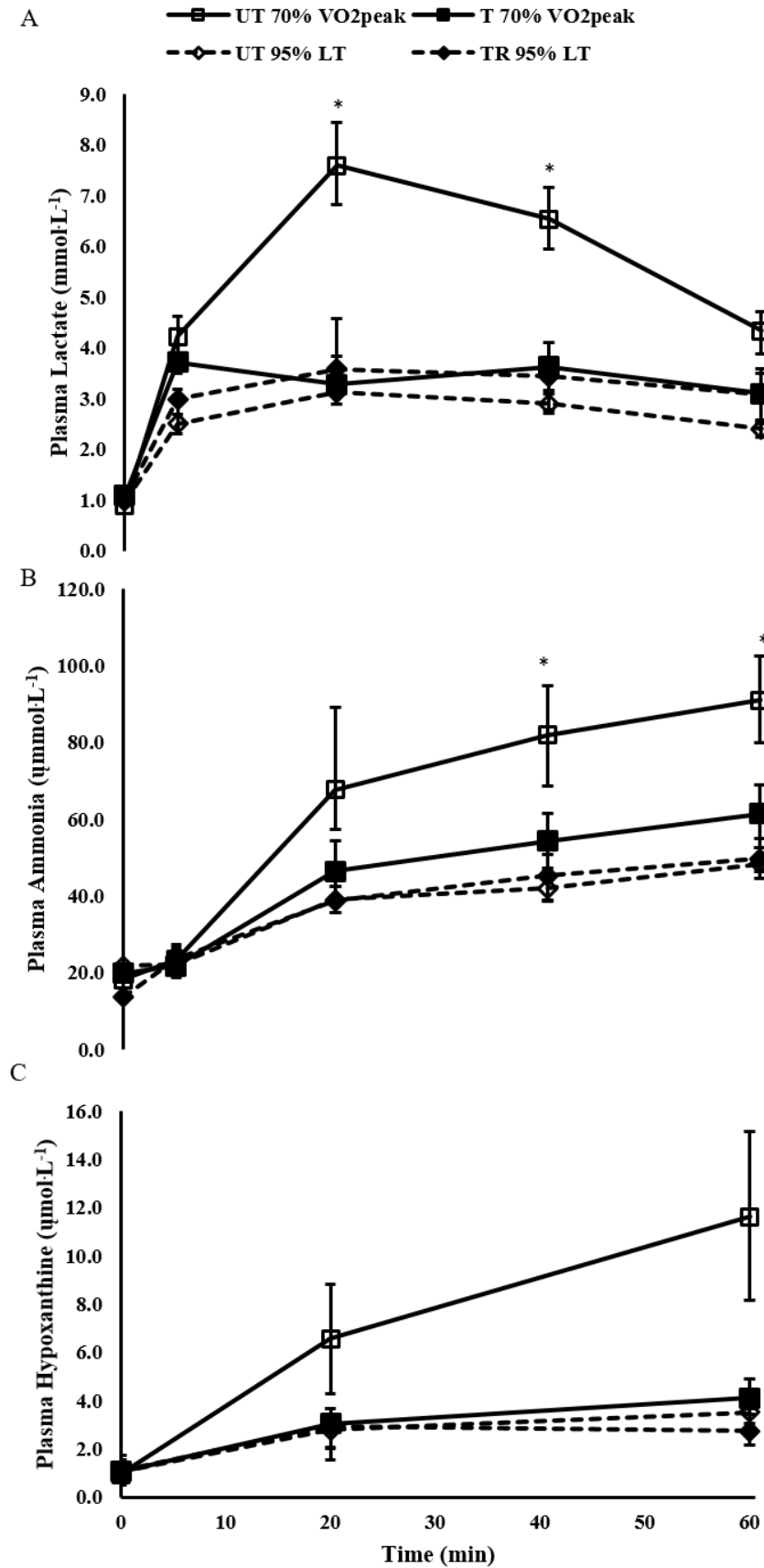


**Figure 1.7 (A-C).** (A) Plasma lactate, (B) ammonia, and (C) hypoxanthine values comparing trained (solid line) and untrained (dashed line) when exercising at 70% of  $\dot{V}O_{2peak}$  (dark circles) and 95% of the work rate associated with a  $1 \text{ mmolL}^{-1}$  increase in blood lactate above baseline (B+1) (dark triangles). When exercising at 70% of  $\dot{V}O_{2peak}$  the plasma lactate (i.e., at 20 and 40 minutes) and ammonia values (i.e., after 40 and 60 minutes) were significantly different for the untrained participants compared to all other groups; furthermore, there were no significant differences for hypoxanthine. Figure redrawn from Baldwin et. al. [3].

### 1.2.2 Maximal Work Rate and Peak Treadmill Speed

There is a high test-retest reliability for establishing both  $\dot{W}_{\max}$  and  $\dot{V}_{\max}$  (CV <3.0%) [147]; however, this is constrained to identical GXT protocols. Unfortunately, there is no recommended protocol design for determining  $\dot{W}_{\max}$  and  $\dot{V}_{\max}$  and these values are often reported and compared as though they are independent of protocol design;  $\dot{W}_{\max}$  and  $\dot{V}_{\max}$  are in fact a function of GXT slope [148, 149], and decreasing GXT slope results in lower  $\dot{W}_{\max}$  and  $\dot{V}_{\max}$  values [1, 4, 138, 150, 151]. For example, increasing mean GXT duration from 7 to 30 minutes (i.e., a slope of 0.83 and 0.14  $\text{W}\cdot\text{s}^{-1}$ , respectively) resulted in an  $\sim 108$  W decrease in mean  $\dot{W}_{\max}$  (**Figure 1.6**) [4]. As  $\dot{W}_{\max}$  and  $\dot{V}_{\max}$  are functions of slope, to reasonably compare  $\dot{W}_{\max}$  and  $\dot{V}_{\max}$  between studies and within a study cohort or population the GXT slope must be considered [152].

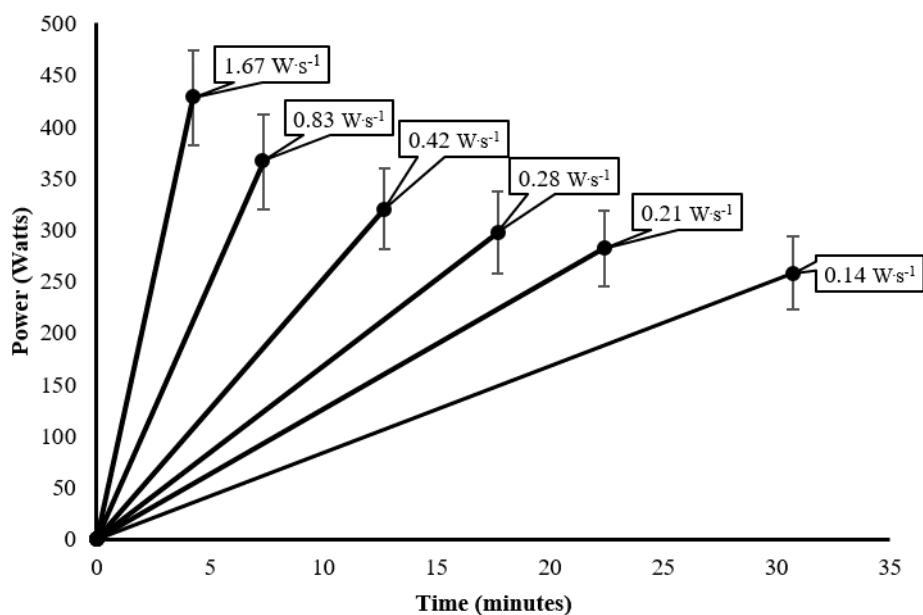


**Figure 1.8.** Data demonstrating the relationship between maximum work rate ( $\dot{W}_{\max}$ ) and graded exercise test (GXT) duration.  $\dot{W}_{\max}$  derived from a GXT is a function of the slope (increase in work rate relative to time) ( $\text{W}\cdot\text{s}^{-1}$ ). Dark circles represent mean and the whiskers the standard deviation. Call outs are the average slope of the graded exercise test. Redrawn from Adami et al. [4].

Prescribing exercise as a percentage of  $\dot{W}_{\max}$  and  $\dot{V}_{\max}$  requires only a simple percentage calculation and is often used to assign the same relative exercise intensity to participants in research studies [3]. However, to my knowledge, no study has compared the individual

physiological responses to exercise prescribed as a fixed percentage of  $\dot{W}_{\max}$  or  $\dot{V}_{\max}$ , determined from the same or different GXT protocol. It is worth noting that the physiological significance of  $\dot{W}_{\max}$  and  $\dot{V}_{\max}$  has been called into question [4, 40, 148]. By simply manipulating slope a positive or negative training effect can be concluded in the absence of an intervention, and controlling for slope in lieu of GXT duration may underestimate the post-intervention value as the GXT duration would likely be extended. There is currently no evidence supporting the prescription of exercise relative to  $\dot{W}_{\max}$  and  $\dot{V}_{\max}$  as a valid method to normalise exercise intensity between individuals.

### *1.2.3 Maximum Heart Rate*

The  $HR_{\max}$  is typically determined during a laboratory GXT, which occurs in conjunction with the measurement of  $\dot{V}O_{2\max}$ , and has a high test-retest reliability (CV = 0.9 to 3.2%) [38, 133-136, 153-155]. The  $HR_{\max}$  does not appear to be influenced by the GXT protocol [156, 157]; however, higher values are observed during field testing (e.g., 20 m shuttle-run) ( $>4 \text{ beats} \cdot \text{min}^{-1}$ ) [158-160]. As with  $\dot{V}O_{2\max}$ , prescribing exercise as a percentage of  $HR_{\max}$  requires constant monitoring of HR or extrapolation of the HR-work rate relationship. Similar to  $\dot{V}O_2$  during heavy and severe exercise, there is an observed HR slow component [161]; thus, the extrapolation of a HR is subject to similar limitations as the extrapolation of  $\dot{V}O_2$ . Notwithstanding the known limitations of prescribing exercise as a percentage of  $HR_{\max}$ , given its simplicity it remains a staple for prescribing exercise intensity.

Despite its common usage, only one study has investigated the validity of using a percentage of  $HR_{\max}$  to normalise exercise intensity [68]. When participants exercised at 60, 70 and 80% of  $HR_{\max}$ , one of the thirty-one participants was above their VT (as defined by Wasserman et. al. [162]) when exercising at 70% of  $HR_{\max}$ , whereas 17 of the 31 participants

were above the VT while exercising at 80% of  $HR_{max}$ . Thus, exercise performed at fixed percentages of  $HR_{max}$  can yield large differences in homeostatic perturbations between individuals, and does not appear to be a valid method to normalise exercise intensity.

#### *1.2.4 Conclusion: Prescribing Exercise Intensity Relative to Maximal Anchors*

Although there is high test-retest reliability for  $\dot{V}O_{2max}$ ,  $W_{max}$ ,  $\dot{V}_{max}$ , and  $HR_{max}$ , based on the laboratory and field evidence, prescribing exercise intensity as a fixed percentage of these maximal anchors has substantial shortcomings as a means for normalising exercise intensity between individuals. There is a large variability for the physiological responses at a fixed percentage of  $\dot{V}O_{2max}$  and this response becomes even more variable as the percentage of  $\dot{V}O_{2max}$  increases [67, 141].  $W_{max}$  and  $\dot{V}_{max}$  are not constant parameters and are dependent on GXT slope and the duration of the GXT; there is no evidence supporting exercise prescribed relative to  $W_{max}$  and  $\dot{V}_{max}$  as a valid method to normalise exercise intensity. The GXT protocol influences the determination of  $\dot{V}O_{2max}$ ,  $\dot{W}_{max}$ , and  $\dot{V}_{max}$ ; furthermore, the GXT slope modulates the  $\dot{V}O_2$  and HR-work rate relationship. Thus, extrapolating a work rate from a GXT fails to account for the curvilinear relationship between  $\dot{V}O_2/HR$  and work rate (**Figure 1.6**). Exercise intensity prescribed relative to the maximal anchors results in a heterogeneous homeostatic perturbation, and (a) fixed percentage(s) cannot be used as a valid proxy for submaximal anchors. Given these limitations, it is not recommended to prescribe exercise intensity relative to the maximal anchors as a means to normalise exercise intensity.

### **1.3 Prescribing Exercise Relative to Submaximal Anchors**

An alternative approach to prescribing exercise based on maximal anchors is to use submaximal anchors, which include  $LT_1$ ,  $LT_2$ , GET, VT, RCP, MLSS, CP and CS. These methods rely on gas exchange, blood lactate responses, and the depletion of anaerobic capacity to be established. These anchors can also be used to establish training zones, whereby each method

is used as a reference point for demarcating different training zones. For example,  $LT_1$  and  $LT_2$  and  $\dot{V}O_{2max}$  derived from a GXT have been used to establish five aerobic training zones (i.e., L1-L5), which can also be characterised based on  $\%HR_{max}$ , absolute blood lactate concentrations, and ratings of perceived exertion (**Figure 1.1 and Table 1.4**) [20, 21]. The GET, VT,  $LT_1$ ,  $LT_2$ , RCP, and MLSS have been used in the training intensity distribution models to quantify exercise intensity into 3 zones, and each zone can also be characterised by  $\%HR_{max}$ ,  $\%VO_{2max}$ , and absolute blood lactate values (**Figure 1.2 and Table 1.5**) [22-25, 28]. Thus, the validity of using these submaximal anchors to prescribe exercise intensity can be established by determining if exercise relative to these anchors procedures similar in different individuals.

**Table 1.4.** The five aerobic training zone system based on the first and second lactate threshold ( $LT_1$  and  $LT_2$ ) derived from a GXT. Each zone is characterised by a % of  $HR_{max}$ , an absolute blood lactate value, a rating of perceived exertion, and the relationship with a submaximal anchor [20, 21].

Aerobic Training Zone	Heart Rate (% of $HR_{max}$ )	Blood Lactate ( $mmol\cdot L^{-1}$ )	Rating of Perceived Exertion (RPE) (6-20)	Relative to Sub- Maximal Anchor
L1 (Recovery)	65 – 75 %	< 2.0	<11 (Easy)	< $LT_1$
L2 (Extensive Endurance)	75 – 80 %	2.0 – 2.5	11 – 12 (Light)	$LT_1 < LT_2$
L3 (Intensive Endurance)	80 – 85 %	2.5 – 3.5	13 – 14 (Somewhat Hard)	$LT_1 < LT_2$
L4 (Threshold Training)	85 – 92 %	3.5 – 5.0	15 – 16 (Hard)	< $LT_2$
L5 (Interval Training)	> 92 %	>5.0	17 – 19 (Very Hard)	> $LT_2$

**Table 1.5.** The training intensity distribution model divides intensity into 3 zones, where zones 1 and zone 2 are demarcated by  $LT_1$  and GET/VT and zones 2 and 3 are demarcated by  $LT_2$ , RCP, and MLSS. Each zone is characterised by a % of  $HR_{max}$ ,  $\% \dot{V}O_{2max}$ , absolute blood lactate value, and the relationship with submaximal anchor [22-25].

Training Zone	Heart Rate (% of $HR_{max}$ )	$\% \dot{V}O_{2max}$	Blood Lactate ( $mmol\cdot L^{-1}$ )	Relative to Sub-Maximal Anchor
Zone 1 (Low Intensity)	< 80%	65 – 75%	< 2.0	>GET/VT/ $LT_1$
Zone 2 (Moderate Intensity)	80 – 90%	75 – 85%	2.0 – 4.0	GET/VT/ $LT_1 < RCP/MLSS/LT_2$
Zone 3 (High Intensity)	> 90%	> 85 %	>5.0	>RCP/MLSS/ $LT_2$

Another approach is to prescribe exercise intensity relative to the domains of exercise, where each domain is not defined by  $\%HR_{max}$  or  $\dot{V}O_{2max}$ , absolute blood lactate concentrations, nor submaximal anchors, but rather their distinct homeostatic perturbation (i.e.,  $\dot{V}O_2$  kinetic and blood lactate response) (**Tables 1.1-1.3 and 1.6; Figures 1.3-1.5**). The moderate domain can be characterised by a plateau of  $\dot{V}O_2$  and blood lactate concentrations near baseline levels,

the heavy domain by an observed ‘slow component’ of  $\dot{V}O_2$  with a delayed steady state and a rise in blood lactate above baseline with a subsequent plateau, and the severe domain by a ‘slow component’ without a steady state of  $\dot{V}O_2$  and a continual increase in blood lactate [26, 55, 62, 89, 90, 119, 163]. Nonetheless, even if the domains are not defined sub-maximal anchors, these have also been used to demarcate or estimate the boundaries between the different domains of exercise. Thus, the validity of using the submaximal anchors to prescribe exercise intensity can be established by determining if exercise relative to these anchors produces distinct and homogeneous homeostatic perturbations (i.e., domain-specific) regardless of an individual’s fitness level. Therefore, we assess the validity of the submaximal anchors based on their ability to yield domain specific homeostatic perturbations.

**Table 1.6.** Prescribing exercise intensity based on physiological domains<sup>2</sup>. Each domain can be characterised by their specific oxygen uptake ( $\dot{V}O_2$ ) kinetic and blood lactate response. The components of  $\dot{V}O_2$  kinetics refers to the  $\dot{V}O_2$  on-transient exponential modelling [26].

Domains of Exercise	$\dot{V}O_2$ Kinetic Response	Blood Lactate Response
Moderate	Two component (i.e., Fast and Primary Phase) $\dot{V}O_2$ plateau achieved within 3 minutes	Transient increase at the onset with return to baseline
Heavy	Three component (i.e., Fast, Primary and Slow Component Phase) Delayed $\dot{V}O_2$ plateau by 10-20 minutes	Increase above baseline with plateau
Severe	Two/Three Component (i.e., Fast and/or Primary and Slow Component Phase) No $\dot{V}O_2$ plateau and $\dot{V}O_{2max}$ achieved if sustained	No blood plateau achieved

### 1.3.1 Blood Lactate

Exercise intensity is often prescribed based on serial blood lactate measurements [81]. Prescribing exercise based on blood lactate appears to be a favoured method to normalise exercise intensity compared with fixed percentages of  $\dot{V}O_{2max}$  [3]. The blood lactate values measured during a GXT are used to calculate  $LT_1$  and  $LT_2$  [164] (**Figure 1.1**). The  $LT_1$ , derived from a GXT represents the rise in blood lactate above baseline, and is assumed to demarcate the moderate and heavy domains of exercise. Whereas,  $LT_2$  represents an acceleration of blood lactate purportedly to demarcate the heavy and severe domains of exercise [164]. Alternatively, blood lactate values measured during a series of constant work rate bouts [41] or single exercise

bouts with real-time work rate adjustments [5] are used to establish the MLSS. The MLSS represents the highest intensity where blood lactate appearance and disappearance is in equilibrium and is assumed to demarcate the heavy and severe domains of exercise [165] (Figure 1.9 A and B).

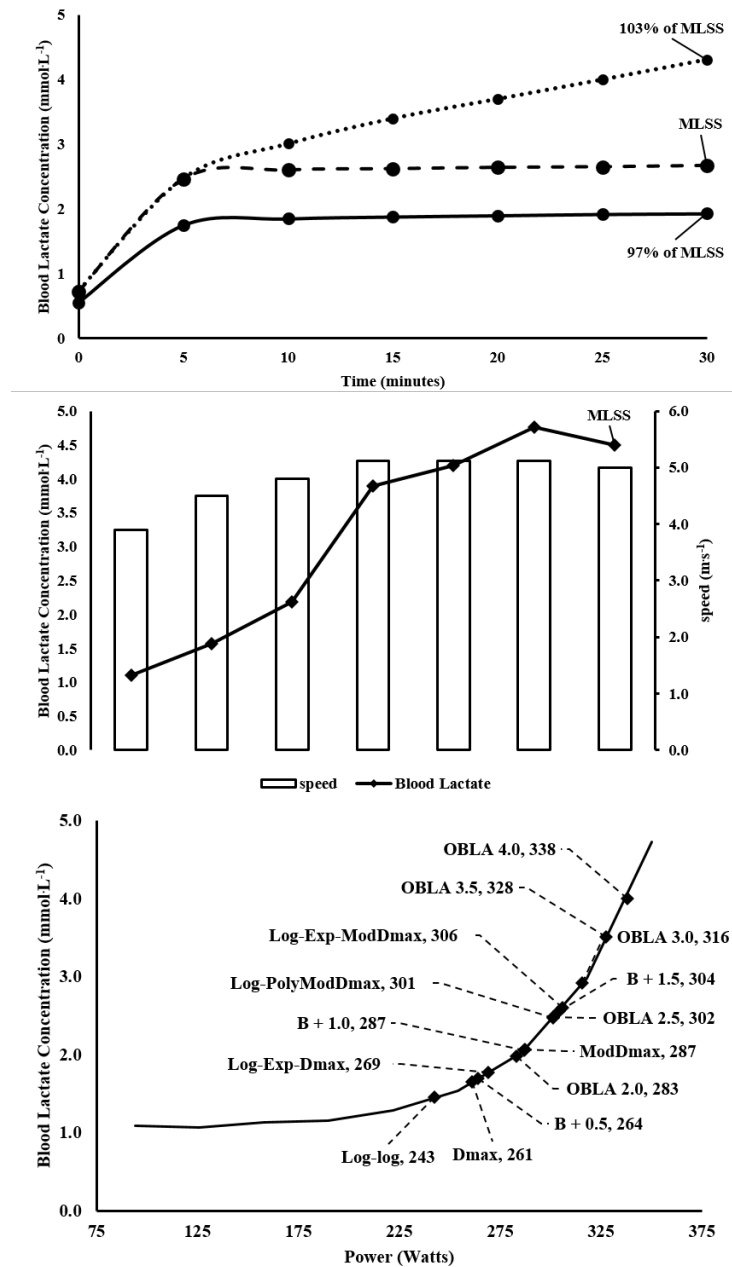


**Figure 1.9 (A - C).** A.) Representative blood lactate response to exercise performed at 97, 100 and 103% of the MLSS (Traditional Criteria). Blood lactate increased 0.7, 0.8 and 1.3 mmol.L<sup>-1</sup> from 10 to 30 minutes at 97, 100 and 103% of the MLSS, respectively. B.) Representative blood lactate response using criteria developed by Hering et al. [5]. Threshold criteria 2 was achieved were blood lactate increased  $\geq 0.5$  mmol.L<sup>-1</sup> and was  $\geq 4$  mmol.L<sup>-1</sup> without a change in speed. Therefore, speed was decreased by 0.1 ms<sup>-1</sup> to confirm the MLSS. C.) Representative lactate threshold (LT) curve with 14 different LTs. Log-log = power at the intersection of two linear lines with the lowest residual sum of squares; log = using the log-log method as the point of the initial data point when calculating the D<sub>max</sub> or Modified D<sub>max</sub>; poly = Modified D<sub>max</sub> method calculated using a third order polynomial regression equation; exp = Modified D<sub>max</sub> method calculated using a constant plus exponential regression equation; OBLA = onset of blood lactate accumulation; B + absolute values the intensity where blood lactate increases above baseline.

### 1.3.1.1 Lactate Thresholds

There is no overall consensus regarding the GXT protocol design to establish the LT – the LT refers to any LT method derived from a GXT. A stage length of at least 3 minutes has been recommended [140] but stage lengths from 1 to 10 minutes have been used [1, 166]. A customised approach for individualised GXT design has been proposed to ensure a homogenous GXT duration [1, 39]. There are at least 30 different methods to calculate the LT, and the calculated work rate at each LT can vary ~30% depending on the method [164] (**Figure 1.9C**). Furthermore, the work rate associated with a specific LT method is influenced by GXT protocol [1, 150]. Given the variability of LT testing between studies it is difficult to compare and reproduce results.

The test-retest reliability for select LT methods has been investigated including a visual inspection point (CV = 51.6%), the  $D_{\max}$  (CV = 3.8 – 10.3%), the onset of blood lactate accumulation (OBLA) of  $4.0 \text{ mmol}\cdot\text{L}^{-1}$  (CV = 3.1-8.2%), and baseline plus 0.5, 1.0 and  $1.5 \text{ mmol}\cdot\text{L}^{-1}$  (CV = 1.2–3.7; 3.4–12.6 and 3.1– 3.4%, respectively) [166-168]. The reliability of many accepted LT methods has yet to be confirmed, even though these methods are often accepted as valid for delineating the domains of exercise and for prescribing exercise intensity.

#### 1.3.1.1.1 $LT_1$

There is no research directly investigating the validity of  $LT_1$  to delineate different domains of exercise in different individuals. To achieve a moderate or heavy domain response exercise is typically prescribed relative to the GET/VT under certain circumstances,  $LT_1$  is similar to GET/VT as their mechanistic basis is closely tied [72, 166, 169-174]. Exercise prescribed relative to an LT method appears to yield a more homogeneous homeostatic perturbation relative to exercise prescribed relative to a percentage of  $\dot{V}O_{2\max}$  [3]. Exercise

prescribed at 95% of the work rate associated with an increase of  $1 \text{ mmol}\cdot\text{L}^{-1}$  above baseline (baseline +  $1.0 \text{ mmol}\cdot\text{L}^{-1}$ ) yielded more homogenous homeostatic perturbations than exercise at 70% of  $\dot{V}O_{2\text{max}}$  [3] (Figure 1.7). This study demonstrates that normalising exercising intensity via blood lactate is superior compared to fixed percentages of  $\dot{V}O_{2\text{max}}$ ; however, there is no evidence supporting the efficacy of baseline +  $1 \text{ mmol}\cdot\text{L}^{-1}$  as a valid LT method to delineate any of the domains exercise [1].

The LT methods associated with  $LT_1$  are the visual inspection point, log-log LT, and an increase in blood lactate of  $0.5 \text{ mmol}\cdot\text{L}^{-1}$  above baseline, these methods are all highly correlated (ICC  $\sim 0.98$ ) [175]. Although highly correlated, the visual inspection point is unreliable, whereas the baseline +  $0.5 \text{ mmol}\cdot\text{L}^{-1}$  has favourable reliability, and the reliability of the log-log LT is uncertain. The log-log LT and baseline +  $0.5 \text{ mmol}\cdot\text{L}^{-1}$  method are least influenced by GXT protocol design and should be assessed for their validity delineate the moderate and heavy domains of exercise.

#### *1.3.1.1.2 LT2*

The  $LT_2$  is often accepted as a valid threshold to demarcate training zones and the heavy and severe exercise domains. Although, there is no research directly investigating the validity of  $LT_2$  to delineate the heavy and severe domains of exercise, its legitimacy has been tested via concurrent validity with the MLSS (discussed in more detail in section 1.3.1.2). There are at least 30 methods to calculate the  $LT_2$  and only select methods can be used to estimate the MLSS [1, 48, 76, 166, 168, 176-179]. However, these outcomes either: were specific to the testing procedures, have not been reproduced, lacked comprehensive statistical analysis, or concluded the  $LT_2$  could not validly estimate the MLSS. Of the more than 30+  $LT_2$  methods, one (i.e., baseline +  $1.5 \text{ mmol}\cdot\text{L}^{-1}$ ) elicits a valid estimation of the MLSS, as reported in two studies that recruited trained cyclists and employed a GXT with 3-min stages [1, 178]. However, the

validity is dependent on GXT stage length as the validity of the method could not be confirmed with any other stage length [1, 166, 180].

The  $D_{\max}$  [74] and Modified  $D_{\max}$  [75] methods are curve-fitting LT models that, despite no evidence to support their validity to identify the MLSS, or to delineate the heavy and severe domains, remains a staple LT method. These methods are influenced by stage length [1], starting intensity [78], regression model employed [77], and the final lactate value [181]. Fixed blood lactate concentrations are also commonly-accepted methods that have been proposed to delineate the domains of exercise (e.g., 2.0 and 4.0  $\text{mmol}\cdot\text{L}^{-1}$ , for the moderate/heavy and heavy/severe domains, respectively) [81, 182]. It is worth noting, however, the original authors cautioned the use of fixed blood lactate concentrations [76] and there is often a broad range of blood lactate concentrations when exercise is performed at the domain boundaries [62]. The validity of  $LT_2$  is often accepted via a single statistical value (e.g.,  $r$  or  $p$  value) or in comparison to other select methods. Where a high correlation ( $r > 0.90$ ) is often deemed valid it is not sufficient to establish validity [183] and agreements compared to other select LTs should be avoided. Instead concurrent validity should be based on *a priori* criteria (i.e., bias  $\pm$  precision vs. standard error) [184]. The validity of the  $LT_2$  relies on agreement with, and the validity, of the MLSS (i.e., concurrent validity) - the validity of one method has been reproduced (baseline + 0.5  $\text{mmol}\cdot\text{L}^{-1}$ ) although the results were specific to testing population (i.e., trained) and GXT protocol design (i.e., 3-min stages).

#### 1.3.1.2 Maximal Lactate Steady State

The original protocol to establish the MLSS requires a series of 30-minute constant work rate bouts, where the rise in blood lactate is  $<1.0 \text{ mmol}\cdot\text{L}^{-1}$  from the 10<sup>th</sup> to the 30<sup>th</sup> minute (**Figure 1.9A**) or a single visit exercise bout requiring a rise in blood lactate above steady state

with modest work rate adjustments (ref. [5] Figure 1) (**Figure 1.9B**). The 30-minute exercise bouts and single visit protocol have a reliability of CV of 3.0 and 1.9%, respectively [5, 9]. The criterion of the MLSS during the 30-minute exercise bouts relies on blood lactate kinetics and a time limit [1, 41, 49]. In contrast, the single visit protocol relies on a rapid accumulation of lactate resulting from modest changes in workload. The MLSS is reliable and can be established with two criteria; however, it is uncertain if these criteria are equivalent and are valid anchors to delineate the heavy and severe domains of exercise.

The MLSS derived from the series of 30-minute bouts purportedly corresponds to the maximal metabolic steady state [46], and it is assumed exercise performed above the MLSS yields a homeostatic perturbation consistent with the severe exercise domain (i.e., no  $\dot{V}O_2$  or blood lactate plateau). Although exercise performed above the MLSS yields blood lactate values above the steady-state criterion, there can be an observed  $\dot{V}O_2$  steady state [79, 185] that occasionally precludes attainment of  $\dot{V}O_{2max}$  [46, 47]. These responses are consistent with the heavy domain of exercise which has led to criticism of this criterion [186]; specifically, the arbitrary nature of defining a blood lactate steady state and a 30-minute time limit [49]. An arbitrary time limit to determine any submaximal anchor or index should be avoided as the time to fatigue at the maximal metabolic steady state varies considerably (i.e., 15 to 60 minutes) [49, 185, 187-189]. Furthermore, a steady state for blood lactate can be achieved beyond 30 minutes, which otherwise would be concluded to be above the MLSS [190]. Although an accepted submaximal anchor for determining a physiological steady state, the 30-minute MLSS typically underestimates the boundary between heavy and severe exercise (see ref [49], for further critique).

The recent publication of a single visit MLSS protocol [5], which requires real-time work rate adjustments based upon blood lactate responses, appears to be a promising alternative to the accepted MLSS test. Establishing the single visit MLSS requires a stage above the MLSS; the purpose of this stage is to verify the MLSS by eliciting a rapid accumulation of lactate relative to a modest increase in work rate [5]. This response is indicative of enhanced motor unit activity and the inability to solely meet ATP demands via oxidative phosphorylation [5, 191, 192]. Although the verification stage provides evidence of non-steady state exercise, the validity of the single visit MLSS to delineate the heavy and severe domains of exercise needs to be confirmed.

### *1.3.2 Gas Exchange*

Gas exchange submaximal anchors (i.e., GET/VT and RCP) detect disproportionate changes in ventilation and non-metabolic CO<sub>2</sub> production relative to VO<sub>2</sub> or work rate [72, 73, 162]. These anchors are assumed to be indicative of the shift in metabolic rate and substrate utilisation within the working muscle, and demarcate the domains of exercise [193, 194]. Prescribing exercise relative to the VT and RCP is more favourable compared to HR-based exercise prescription [195, 196], two studies compared the VT and RCP and HR-based exercise prescription on aerobic adaptations over a 12-week period. Exercise prescribed relative to the VT and RCP attenuated individual variation in training responses compared to HR-based exercise prescription [195, 196]. The likely explanation is the ability of the VT to normalise exercise intensity compared to HR [68]. However, there is no conclusive evidence that these anchors are valid methods to delineate the domains of exercise.

#### *1.3.2.1 Ventilatory/Gas Exchange Threshold*

A high test-retest reliability of the GET/VT has been established (CV = 2.0 -3.5%) [166, 168]. The GET/VT is a non-invasive method that indirectly measures a disproportionate

increase in non-metabolic CO<sub>2</sub> production, a consequence of H<sup>+</sup> accumulation and cytosolic ATP turnover [59, 71-73, 197, 198]. The GET is determined as the inflection point of  $\dot{V}CO_2 - \dot{V}O_2$  (**Figure 1.10A**) and an intensity that elicits an increase from steady state to an excess production of CO<sub>2</sub> (**Figure 1.10B**) [39, 72]. The VT is determined as a systematic increase in  $V_E/\dot{V}O_2$  (**Figure 1.10C**) [198] and partial pressure of end total O<sub>2</sub> (P<sub>ET</sub>O<sub>2</sub>)(**Figure 1.10D**), and the point where partial pressure of end total CO<sub>2</sub> (P<sub>ET</sub>CO<sub>2</sub>) begins to plateau (**Figure 1.10E**) [199]. As these anchors are influenced by slope [151, 173, 200], the optimum GXT duration to determine the GET/VT is 8-12 minutes [39, 201]. Furthermore, identifying these anchors is dependent on the method chosen and whether it is determined via computer or manual technique [170, 202]. There is evidence to support the validity of the GET/VT to normalise exercise intensity and delineate the moderate and heavy domains of exercise.

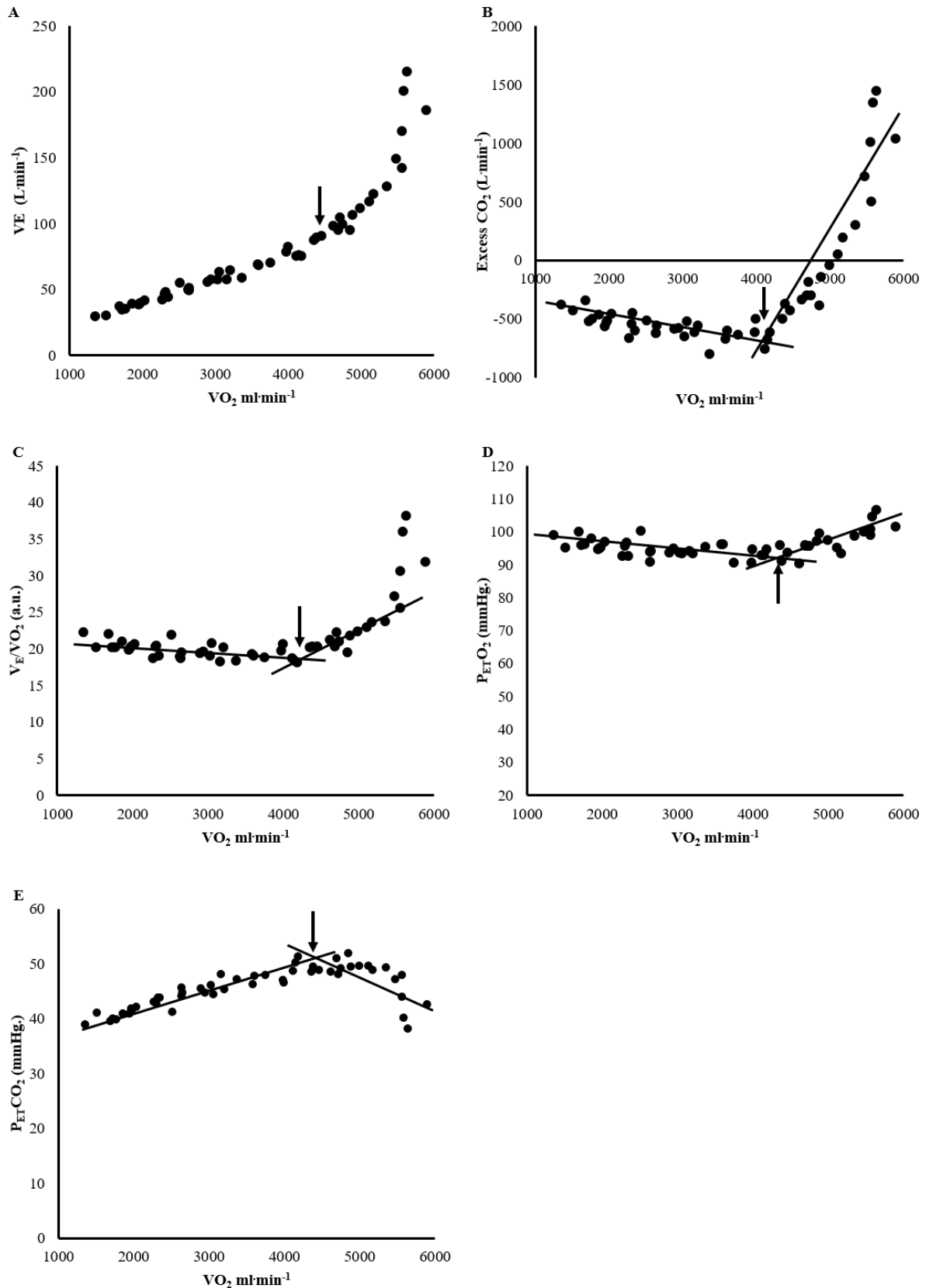


**Figure 1.10 (A-E).** Representative gas exchange and blood lactate data from an incremental/graded exercise test illustrating the method(s) to determine the: ventilatory threshold (VT), gas exchange threshold (GET) and first lactate threshold ( $\text{LT}_1$ ). (A) VT: the first break point in ventilation ( $\text{V}_E$ ), (B) GET: disproportionate increase in nonmetabolic  $\text{CO}_2$  production relative to  $\text{O}_2$  consumption ( $\text{VO}_2$ ) (i.e., excess  $\text{CO}_2$ ), (C) VT: systemic increase in  $\text{V}_E/\text{VO}_2$ , (D) VT: systemic increase in pressure of end tidal oxygen consumption ( $\text{P}_{\text{ET}}\text{O}_2$ ), and (E) VT: plateau in pressure of end tidal carbon dioxide expiration ( $\text{P}_{\text{ET}}\text{CO}_2$ ) following in increase.

Exercise performed below the GET/VT yields a  $\dot{V}O_2$  plateau, and blood and intramuscular lactate accumulation that remains at baseline. In contrast, exercise above the GET/VT results in a  $\dot{V}O_2$  'slow component', a plateau of blood lactate above baseline, and an increase in intramuscular lactate above resting levels/values [90, 94, 119]. However, these homeostatic responses were measured distant from the GET/VT (i.e., 80, 90 and 120% of GET/VT) and the resulting anchors are influenced by GXT and are dependent on a standardised technique to extrapolate the corresponding  $\dot{V}O_2$  or work rate. Specifically, longer duration GXTs yield a lower  $\dot{V}O_2$  (discussed in section 1.2.1 and data Table 2.6) and a work rate associated with the GET/VT and a homogeneous MRT of 60 seconds is typically employed [145, 151, 173]. Although a reliable and established criteria, the ability of the GET/VT to delineate the moderate and heavy domains of exercise [90, 119] has not been shown conclusively. It is likely the GET/VT will establish the boundary between the moderate and heavy domains of exercise. To achieve this future research should employ a customised GXT protocol, incorporate multiple GET/VT criteria (**Figure 1.10**), and measured the on-transient oxygen uptake kinetics of constant work load tests performed at the limits of agreement of the established GET/VT.

#### *1.3.3.2 Respiratory Compensation Point*

A high test-retest reliability of the RCP has been established (CV = 1.9-2.1%) [166, 168]. The RCP, also referred to as the second ventilatory threshold (VT<sub>2</sub>), is a non-invasive marker caused by hyperventilation consequent to an increase in H<sup>+</sup> accumulation that indicates a concomitant increase in blood lactate and H<sup>+</sup> that is greater than the rate of disposal [73, 197, 203]. The optimum GXT duration to establish the RCP is 8- 12 minutes [39], and it can be characterised by a second breakpoint in  $\dot{V}_E$  (**Figure 1.11A**), a clear break point in  $\dot{V}_E/\dot{V}CO_2$  (**Figure 1.11B**), and where P<sub>ET</sub>CO<sub>2</sub> begins to fall after an apparent steady state (**Figure 1.11C**)

[71-73]. As with GET/VT, this anchor is also influenced by GXT slope [173, 204, 205] and is dependent on the extrapolation technique [145, 146], resulting in a discrepancy between the work rate and  $\dot{V}O_2$  associated with the RCP.

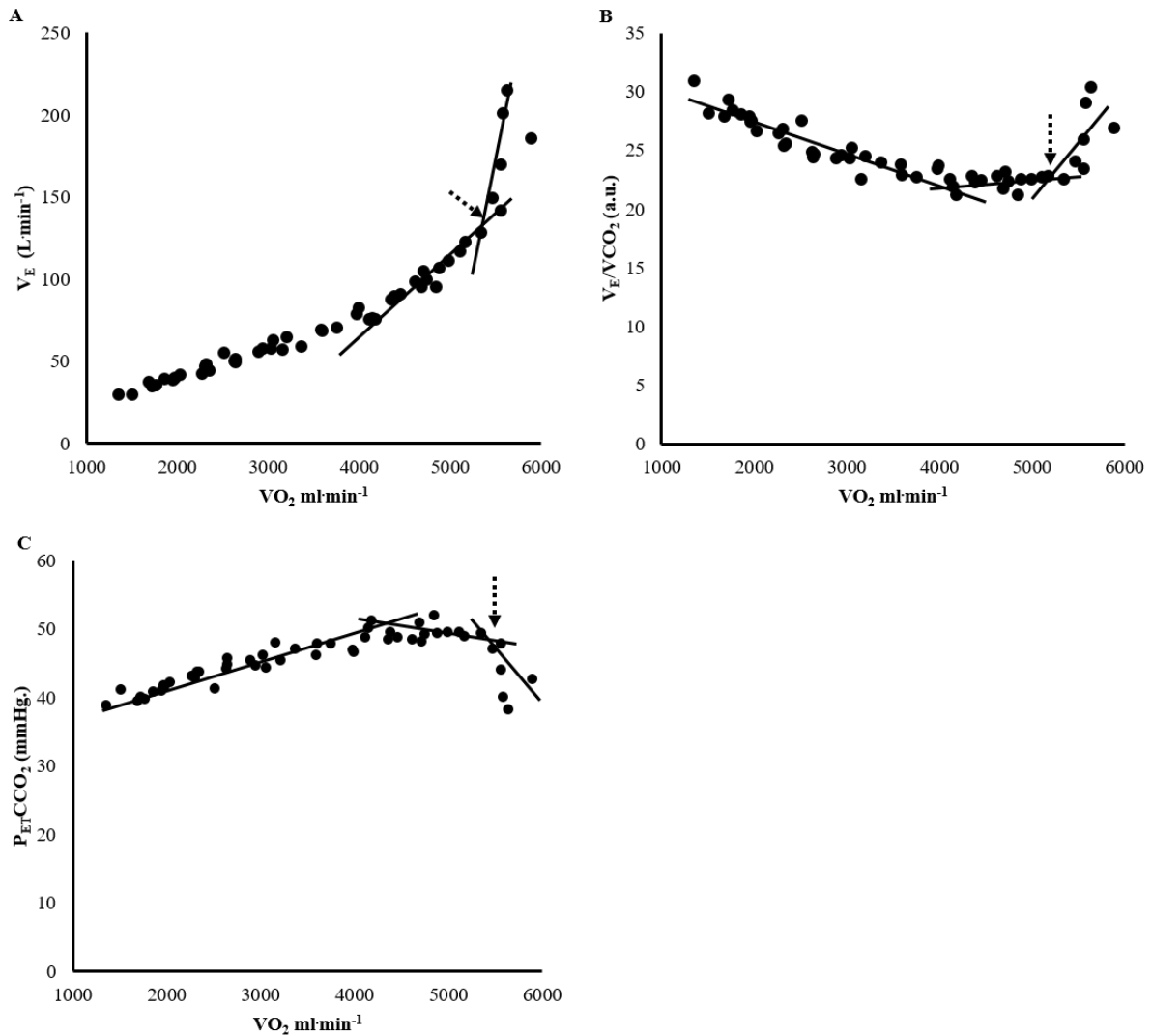


**Figure 1.11 (A-C).** Representative gas exchange and blood lactate data from an incremental/graded exercise test illustrating the method(s) to determine the: respiratory compensation point (RCP) and second lactate threshold ( $LT_2$ ). (A) RCP: the second break point in ventilation ( $\dot{V}_E$ ), (B) RCP: a breakpoint in  $\dot{V}_E$  relative to  $\dot{V}CO_2$  expiration ( $\dot{V}_E/\dot{V}CO_2$ ) following a plateau), and (C) RCP: second breakpoint in pressure of end tidal carbon dioxide expiration ( $P_{ET}CO_2$ ) following plateau.

As the GXT slope decreases, so does the RCP work rate. This relationship is attributed to the slow component during heavy/severe exercise, conflating the gain in  $\dot{V}O_2$  relative to work rate [89, 193, 200, 205] even after adjusting for the MRT of  $\dot{V}O_2$  [145, 200]. Despite the

associated  $\dot{V}O_2$  being independent of GXT slope, assigning a work rate from a GXT should be avoided due to these limitations. To my knowledge, no research has directly confirmed the validity of the RCP to delineate the heavy and severe domains of exercise. However, the validity has been implied based on the concurrent validity with CP [193, 194], where the agreement between  $\dot{V}O_2$  associated with each exercise intensity was based on null hypothesis testing, despite evidence to the contrary [200, 206, 207]. It is recommended that the statistical rigour of confirming equivalence should go beyond null hypothesis testing (e.g., *a priori* criteria) [184, 206]. Thus, the RCP does not appear to be a valid method to delineate the heavy and severe domains of exercise this is based on the influence of the curvilinear  $\dot{V}O_2$ -work rate relationship, and the evidence indicates it should be avoided as a surrogate for the MLSS and CP.

### 1.3.3 Critical Power/Speed

The CP and CS represents the highest intensity without a progressive loss of homeostasis [40] and is widely regarded as a valid determinant of the boundary between heavy and severe exercise [6, 26, 40, 49, 62, 208]. Establishing CP and CS requires either a series of exercise bouts (traditional method) above the expected CP and CS, or a single-effort, all-out, three-minute test (i.e., 3MT) to calculate CP and CS and the curvature constant ( $W/D'$ ) [42, 43, 62, 82-86] (**Figure 12**).

Establishing CP/CS using the traditional method is subject to restrictions, where CP and CS is influenced by the duration of the bouts [209-212], mathematical model employed [213], and type of bout (i.e., time trial vs. exhaustive constant work rate bout) [214, 215] (see [216] for further review). At least two bouts are required to establish CP and CS via the traditional method, and three are recommended to establish the standard error of estimate and

goodness of fit ( $r^2$ ) of the CP and CS and  $W'/D'$  (**Figure 1.12A**). The recommended duration of the exhaustive exercise bouts is 2-15 minutes [40, 62, 209, 217], with at least a five minute difference between the shortest and longest trials [218-220]. The number of trials chosen does not appear to influence CP [221, 222]. By manipulating the duration of running time trials (i.e., 2, 5, and 10 min. vs. 3, 7, and 12 min) there were marked differences in CS and  $D'$  (i.e.,  $\sim 0.12 \text{ m}\cdot\text{s}^{-1}$  and  $\sim 20.3 \text{ M}$ , respectively) [223]. The mathematical model chosen may also influence CP and CS, where the linear and nonlinear models yield higher and lower estimations of CP and CS, respectively [130, 213, 216, 219, 224-229]. Despite recommendations for multiple mathematical models [213], there is not a consensus on best practice to establish the CP and CS. Time-trials may yield higher CP and CS values compared to exhaustive constant work rate bouts [220, 230, 231], as well as lower test-retest variability [215]. There is a high reliability ( $\text{CV} = 2.4 - 6.5\%$ ) [223, 232, 233], but it is recommended that familiarisation trials be implemented to increase reliability [216]. The traditional method is subject to many restrictions that influence the establishment of the CP and CS and the  $W'/D'$ ; furthermore, there is no current established protocol to confirm the identified parameters.

The 3MT requires a single-visit, all-out effort test, where the average work rate computed from the last 30 seconds is the CP and CS [42, 43] (**Figure 1.12B**). There is a high test-retest reliability of the 3MT ( $\text{CV} = 1.2- 6.7\%$ ) [82, 234, 235]. The overarching methodological variable of concern pertaining to the cycling 3MT is the prescribed resistance. While the original 3MT protocol required a GXT to determine the prescribed resistance [43, 82], researchers have since optimised the procedure by prescribing the resistance without a GXT (i.e., a single-visit test) [236], individualised resistance based on fitness level, body mass index, sex, and age [132], and added an exhaustive bout at 10% above CP to verify the observed CP by eliciting  $\dot{V}O_{2\text{max}}$  [130]. Recently, the 3MT has been criticised [216, 237] for

overestimating CP derived via the traditional method - particularly in elite athletes. The validity of the CP and CS derived from a 3MT is typically confirmed by its agreement with the traditional method. In lieu of agreement, validity should be established if exercise performed above and below the derived CP and CS yields systemic responses (e.g.,  $\dot{V}O_2$  kinetics and blood lactate responses) consistent with the heavy and severe domains of exercise.

There is evidence to support the validity of either method to delineate the heavy and severe domains of exercise. In the late 1980's, the first study assessed the homeostatic responses at and above CP (+ 5% of CP) derived via the traditional method [62] and confirmed the validity of CP to establish the boundary between heavy and severe exercise. These results have since been confirmed or reproduced several times [6, 47, 63, 94, 188, 218, 238, 239]. A recent study has strengthened the case for CP as the delineator between heavy and severe exercise. Exercise was performed at an intensity <CP [-7.6% of CP (26 W)], which resulted in the stabilisation of intramuscular lactate, PCr, glycogen, and pH, blood lactate concentrations above baseline, and a  $\dot{V}O_2$  slow 'component' with a plateau (**Figure 1.13**) [6]. In contrast, exercise performed at an intensity >CP [+7.6% of CP (26 W)] disturbed homeostatic control, and evoked a  $\dot{V}O_2$  slow 'component.' Although these data support the validity of the CP to delineate the heavy and severe domains of exercise, the on-transient  $\dot{V}O_2$  responses were not modelled. Moreover, a similar pattern would likely be observed when prescribing exercise intensity ~26 W above and below other submaximal anchors. Future research should address the inconsistencies in the methodology required to determine CP and CS, and validate the derived CP and CS with exercise bouts above and below while monitoring systemic responses.

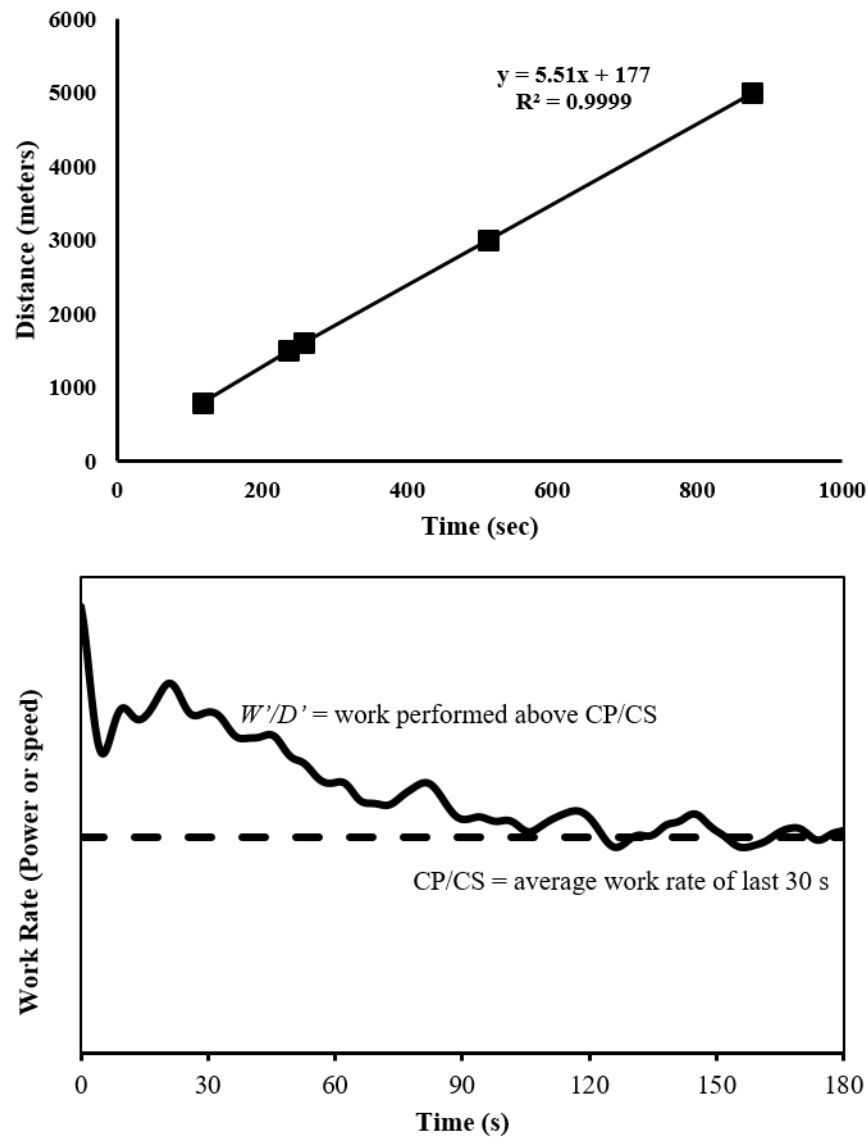


**Figure 1.12 (A & B).** A) Linear distance-time model from race performances (800 M, 1500 M, mile, 3000 M and 5000 M) calculating critical speed (slope;  $5.51 \text{ m s}^{-1}$ ) and curvature constant (intercept;  $D' = 177 \text{ M}$ ). Times retrieved from iaaf.com; athlete code: 14564446. B) Work rate profile from 3 min-all-out-test (3MT). The dashed line represents CP/CS, the average work rate from the last 30 seconds of the 3MT.  $W'/D'$  represents the work performed above CP/CS,  $W'/D' = 150 \text{ seconds} * (\text{Average Work rate of 150 seconds} - \text{CP/CS})$

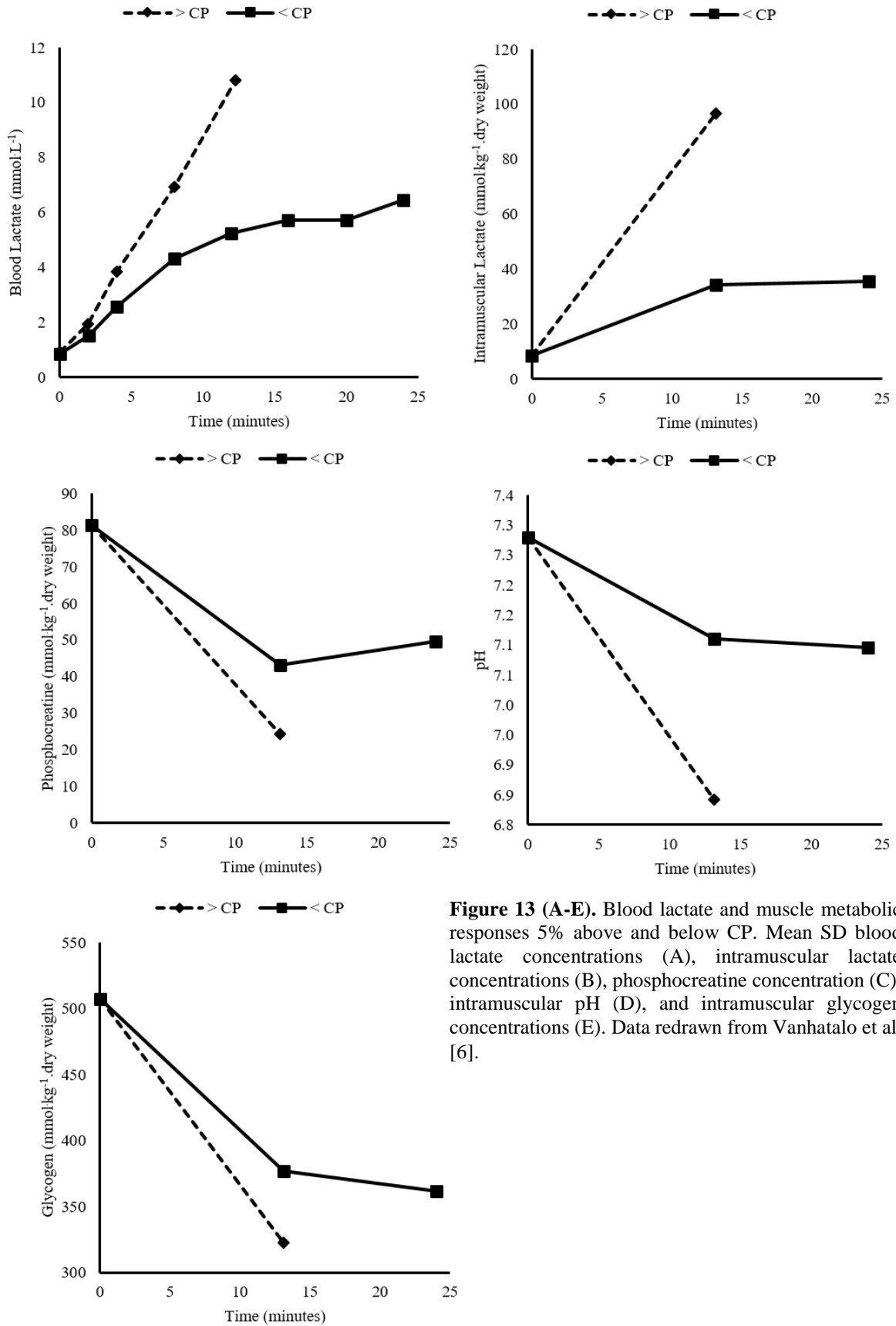


**Figure 13 (A-E).** Blood lactate and muscle metabolic responses 5% above and below CP. Mean SD blood lactate concentrations (A), intramuscular lactate concentrations (B), phosphocreatine concentration (C), intramuscular pH (D), and intramuscular glycogen concentrations (E). Data redrawn from Vanhatalo et al. [6].

#### *1.3.4 Conclusion: Prescribing Exercise Relative to Submaximal Anchors*

Submaximal anchors are commonly used by scientists and researchers to prescribe exercise intensity, and differentiate training zones or domains of exercise. The homeostatic response to exercise performed in proximity to a submaximal anchor should be used to establish the validity of the various submaximal anchors to normalise exercise intensity. However, it appears there is little evidence to support the validity of most commonly used methods. More research is needed to validate  $LT_1$  or GET/VT for delineating the moderate and heavy domains of exercise. The  $LT_2$  is based on the agreement with the MLSS, influenced by GXT protocol design [93], and should be used with caution as a method to prescribe exercise intensity. In some instances exercise above the 30-minute MLSS results in an apparent steady state; therefore, it appears to underestimate the boundary between heavy and severe domains. Future research should address the validity of the single visit MLSS to yield domain-specific homeostatic perturbations. The CP and CS yields the strongest evidence to demarcate the heavy and severe domains of exercise (i.e., to normalise exercise intensity); however, these resulted need to be confirmed via on-transient  $\dot{V}O_2$  kinetics. Lastly, we recommend that the systemic responses of any submaximal anchor be assessed against domain-specific homeostatic perturbations.

#### **1.4 Prescribing Exercise Intensity Relative to a Maximal and Submaximal/Resting Values**

Alternative methods have been recommended to elicit a homogeneous response based on the average work rates between a maximal and submaximal anchor, or the reserve or difference between the maximal anchor and its corresponding resting value [69, 90, 240-242]. Although these methods have been proposed based on the notion they normalise exercise intensity, there has been little research assessing this hypothesis.

#### *1.4.1. Average Work Rate of Maximal and Submaximal Anchor “Delta”*

There is no established protocol for establishing a delta ( $\Delta$ ) or percent difference between a maximal (e.g.,  $\dot{W}_{\max}$  or  $\dot{V}_{\max}$ ) and a submaximal anchor (i.e., GET, VT or LT) from a GXT. To my knowledge, there is also no research directly investigating the reliability of the physiological responses when exercising at intensities established using the  $\Delta$  method. Despite this shortcoming, the  $\Delta$  method has been used [69, 90, 240] and recommended for normalising [44] exercise intensity.

The ability of the “ $\Delta$ ” method to normalise exercise intensity has been compared to fixed percentages of  $\dot{V}O_{2\max}$  [44]. Exercise sessions were performed at 50, 70, and 90% of  $\dot{V}O_{2\max}$ , at 60% of the GET, and  $\Delta 40\%$  and  $\Delta 80\%$  between the GET and  $\dot{V}O_{2\max}$ . The “ $\Delta$ ” method resulted in less inter-subject variability for  $\dot{V}O_2$ ,  $\dot{V}CO_2$ ,  $\dot{V}_E$ , end exercise heart rate, and changes in blood lactate from baseline, when compared to exercise at fixed percentages of  $\dot{V}O_{2\max}$ . A limitation of this study was basing validity on variables with little physiological relevance. For example, the end-exercise heart rate (CV 16-18%) or the difference between rest and end exercise blood lactate are unreliable measures (CV 11- 52%) [9, 243, 244], and there is no evidence supporting these variables as a suitable means to characterise exercise intensity. Although the  $\dot{V}O_2$  response expressed as a percentage of  $\dot{V}O_{2\max}$  was less variable across the “ $\Delta$ ” intensities when compared with fixed percentages of  $\dot{V}O_{2\max}$ , % $\dot{V}O_{2\max}$  has limited utility in normalising exercise intensity and is not able to differentiate between the domains of exercise at intensities above the GET (i.e., heavy and severe) - a concern raised by the authors [44]. The “ $\Delta$ ” method has emerged as a commonly used method to prescribe exercise intensity [44, 69, 89, 119, 245-249], despite the validity being confirmed using unreliable parameters and variables with little physiological merit. Lastly,  $\Delta$  does not normalise exercise intensity to obtain systemic responses consistent with the domains of exercise.

#### *1.4.2 Oxygen Uptake and Heart Rate Reserve*

$\dot{V}O_{2R}$  and  $HR_R$  are methods used to prescribe exercise intensity based on the difference between maximum (i.e.,  $HR_{max}$ ,  $\dot{V}O_{2max}$ ) and resting values (i.e.,  $\dot{V}O_{2rest}$  and  $HR_{rest}$ ) [241, 242]. To date, however, no research has directly investigated the reliability of prescribing exercise via  $HR_R$  or  $\dot{V}O_{2R}$ ; nonetheless, the reliability of these parameters is likely to be related to the reliability of  $\dot{V}O_{2max}$  [1, 42, 125, 127-132],  $\dot{V}O_{2rest}$  [250],  $HR_{max}$  [38, 133-136, 153-155] and  $HR_{rest}$  [38, 251]. Furthermore, it appears that GXT protocol design compromises the efficacy of using either  $\dot{V}O_{2R}$  or  $HR_R$  to prescribe exercise intensity [156, 252]. This shortcoming is likely a consequence of the assumed linearity of the  $\dot{V}O_2/HR_R$ -work rate relationship. The gain in  $\dot{V}O_2$  relative to work rate increases in a curvilinear manner resulting in greater observed  $\dot{V}O_2$  and HR values than predicted [253].

To test the validity of the  $HR_R$  method to normalise exercise intensity, one study investigated the relationship between the  $LT_1$  (i.e., initial rise in blood lactate above baseline  $> 0.2 \text{ mmol}\cdot\text{L}^{-1}$ ) and percent of  $HR_R$  [254]. Extrapolation of the HR-work rate relationship from the GXT indicated that at 85% of  $HR_R$ , 20 of the 31 participants would be exercising above the  $LT_1$ . Similar to % $\dot{V}O_{2max}$  and % $HR_{max}$ , this suggests that HRR cannot be used to identify the submaximal anchor or to delineate the domains of exercise. These results further highlight the inability of  $\dot{V}O_2$  and HR values derived from percentages of  $\dot{V}O_{2max}$ ,  $HR_{max}$ ,  $\dot{V}O_{2R}$  and  $HR_R$  to normalise exercise intensity.

#### *1.4.3 Conclusion: Prescribing Exercise Intensity Relative to a Maximal and Submaximal/Resting Value*

The “ $\Delta$ ” method yields a more homogenous physiological responses than fixed percentages of  $\dot{V}O_{2max}$  [44]. However, the use of unreliable physiological variables raises concern on the efficacy of this method to normalise exercise intensity. Exercise prescribed as

a fixed percentage of  $HR_R$  yields a heterogeneous homeostatic perturbation relative to  $LT_1$ . The reserve methods cannot be recommended as a viable option to normalise exercise intensity.

## 1.5 Conclusions

Exercise intensity is a critical principle of exercise prescription, where the methods described have been employed with the perceived and at times successful ability to normalise exercise intensity. Despite common use, it is apparent  $\dot{V}O_2$ - and HR-based exercise prescription have little merit in eliciting a homogeneous homeostatic disturbance. The use of submaximal anchors has been used to represent shifts in the metabolic state of the working muscle and for demarcation of discrete training zones. In contrast, the domains of exercise are independent of these anchors and defined by their distinct homeostatic responses, and have potential as a more valid means for normalising exercise intensity. Future research should address the validity of submaximal methods to delineate the moderate and heavy domains of exercise. The MLSS is often deemed the gold standard method for identifying the maximal metabolic steady state; however, there is empirical evidence to the contrary [49]. There is however, strong evidence to support the validity of CP and CS to demarcate the heavy and severe domains of exercise. Caution is needed when prescribing exercise intensity solely based on blood lactate concentrations, given there is no conclusive evidence of their ability to act as a proxy for the metabolic state of the working muscle. The relationship between GXT- and constant work load-derived anchors is unclear and the use of submaximal anchors interchangeably is discouraged. Finally, the validity of submaximal anchor-based exercise prescription should be contingent on the systemic responses above and below each discrete anchor specific to the domains of exercise.

## **Chapter 2: Manipulating graded exercise test variables affects the validity of the lactate threshold and $\dot{V}O_{2\text{peak}}$**

This chapter has been published:

Jamnick, N. A., Botella, J., Pyne, D. B., & Bishop, D. J. (2018). Manipulating graded exercise test variables affects the validity of the lactate threshold and  $\dot{V}O_{2\text{peak}}$ . *PLoS ONE*, 13(7), e0199794.

Published version available from: <https://doi.org/10.1371/journal.pone.0199794>

**Note: Since publication the 30 minute MLSS has been called into question as an appropriate delineator of the heavy and severe domains of exercise. Although chapter 4 employs this method as the study design occurred in early 2017, the conclusions in chapter 1 do not follow these results as the latest draft of chapter 1 occurred in 2019.**

## 2.1 Introduction

Sampling of expired gas and blood data during a graded exercise test (GXT) to exhaustion permits identification of the gas exchange threshold (GET), the ventilatory threshold, the lactate threshold (LT), and maximal oxygen uptake ( $\dot{V}O_{2\max}$ ). These indices can distinguish cardiorespiratory fitness, and demarcate the domains of exercise [81, 255] that can be used to prescribe exercise and to optimize training stimuli [31, 38, 121, 256]. However, despite the popularity of these indices, the methods used to determine them can differ substantially and there has been little systematic investigation of their validity [150, 257, 258].

The recommended duration of a GXT to assess  $\dot{V}O_{2\max}$  is 8 to 12 minutes [126, 137, 140, 259]. However, there is little consensus on an appropriate GXT protocol design, including duration, stage length, or number of stages, needed to establish the LT. A stage length of at least 3 minutes has been recommended [140], although an 8-minute stage length has also been suggested for blood lactate concentrations to stabilize [190]. The number of stages and GXT duration will depend on the starting intensity and power increments. Power is typically increased identically [260], regardless of sex or fitness, leading to a heterogenous GXT duration and number of stages completed [167]. A customized approach to LT testing has been recommended to ensure a more homogenous GXT duration [39].

More than 25 methods have been proposed to calculate the LT [164]; these include the power preceding a rise in blood lactate concentration of more than 0.5, 1.0 or 1.5 mmol·L<sup>-1</sup> from baseline [261], the onset of a fixed blood lactate accumulation (OBLA) ranging from 2.0 to 4.0 mmol·L<sup>-1</sup> [262, 263], or the use of curve fitting procedures such as the  $D_{\max}$  or modified  $D_{\max}$  methods (Mod $D_{\max}$ ) [74, 75]. However, many of these ‘accepted’ methods are influenced by GXT protocol design [76, 258] and their underlying validity has not been reported.

Assessing the validity of a measurement requires comparison with a criterion measure. The maximal lactate steady state (MLSS) represents the highest intensity where blood lactate appearance and disappearance is in equilibrium and where energy demand is adequately met by oxidative phosphorylation [165]. Exercise performed above the MLSS results in accelerated blood lactate appearance and it has therefore been suggested as an appropriate criterion measure for the LT [41, 165]. The primary advantages of the MLSS test include its independence of participant effort, it's submaximal and is reliable [9]. However, the disadvantage is the necessity of multiple laboratory visits and that it yields only one index of performance<sup>s</sup>.

$\dot{V}O_{2max}$  is considered the “gold standard” for assessing cardiorespiratory fitness [264] and the highest recorded  $\dot{V}O_2$  from a GXT is often accepted as the  $\dot{V}O_{2max}$  [126]. Establishing the LT requires a GXT that typically exceeds 20 minutes [140]; however, in these instances the highest  $\dot{V}O_2$  may underestimate the  $\dot{V}O_{2max}$  [137] and is termed  $\dot{V}O_{2peak}$ . Recently, the use of a verification exhaustive bout (VEB) has been recommended to confirm the  $\dot{V}O_{2max}$ . However, it is unknown if a VEB performed after a longer duration GXT provides a valid estimate of  $\dot{V}O_{2max}$ .

The aim of this study was to determine the validity of the LT and  $\dot{V}O_{2max}$  derived from a single visit GXT. We hypothesized that our results would yield one or more GXT stage length and LT calculation method combination that provides a valid estimation of the criterion measure of the LT (i.e., MLSS). We also hypothesized the highest  $\dot{V}O_2$  measured during longer duration GXTs would underestimate  $\dot{V}O_{2max}$  and that the highest  $\dot{V}O_2$  value measured during each VEB would be similar to the  $\dot{V}O_{2peak}$  measured during the 8- to 12-minute GXT.

## 2.2 Materials and Methods

### 2.2.1 Participants/Experimental Design

Seventeen trained male cyclists ( $\dot{V}O_{2\max}$   $62.1 \pm 5.8$  mL $\cdot$ kg $^{-1}\cdot$ min $^{-1}$ , age  $36.2 \pm 7.4$  years, body mass index (BMI):  $24.1 \pm 2.0$  kg $\cdot$ m $^{-2}$ ) volunteered for this study which required 7 to 10 visits to the laboratory. Informed consent was obtained from all individual participants included in the study.

Visit one included risk stratification using the American College of Sports Medicine Risk Stratification guidelines [265], written informed consent, self-reported physical activity rating (PA-R) [127], measurement of height and body mass, and completion of a cycling GXT with 1-minute stages (GXT<sub>1</sub>) followed by a VEB. The remaining visits consisted of four cycling GXTs with varying stage length (3-, 4-, 7- and 10-min stages) and a series of 30-min constant power bouts to establish the MLSS. The GXTs and constant power bouts were performed in an alternating order and the order of the GXTs was randomised. Prior to each GXT and the constant power bouts a 5-min warm up was administered at a self-selected power followed by 5 min of passive rest. Participants performed each test at their preferred cadence determined during the initial visit. Antecubital venous blood (1.0 mL) was sampled during all visits (excluding GXT<sub>1</sub>) at rest, and at the end of every stage during the GXTs or every 5 min during the constant power exercise bouts. All participants self-reported abstaining from the consumption of alcohol and caffeine or engaging in heavy exercise 24 h prior to each visit. Participants were given at least 48 h between visits and all tests were completed within 6 weeks. The Victoria University Human Research Ethics Committee approved all procedures (HRE 017-035).

### 2.2.2 Equipment/Instruments

All exercise testing was conducted using an electronically-braked cycle ergometer (Lode Excalibur v2.0, The Netherlands). A metabolic analyser (Quark Cardiopulmonary Exercise Testing, Cosmed, Italy) was used to assess oxygen uptake ( $\dot{V}O_2$ ) on a breath-by-breath basis, and heart rate was measured throughout all tests. Antecubital venous blood was analysed using a blood lactate analyser (YSI 2300 STAT Plus, YSI, USA).

### 2.2.3 GXTs with Verification Exhaustive Bout

Demographic data, PA-R, and measurements of height and body mass were used to estimate  $\dot{V}O_{2\max}$  [266] and maximum power output  $\dot{W}_{\max}$  [127, 267].

$$\text{Est. } \dot{V}O_{2\max} = 56.363 + (1.921 \times \text{PA-R}) - (0.381 \times \text{AGE}) - (0.754 \times \text{BMI}) + (10.987 \times \text{SEX}; 1 = \text{MALE}, 0 = \text{FEMALE})$$

$$\text{Est. } \dot{W}_{\max} = \{[(\text{Est. } \dot{V}O_{2\max} - 7) \times \text{BM}]/1.8\}6.12$$

Where  $\dot{V}O_{2\max}$  is expressed in millilitres per kilogram per minute, BMI is in kilograms, and  $\dot{W}_{\max}$  is in Watts.

A custom GXT protocol with a desired time limit of 10 min was then designed for each participant using:  $\dot{W}_{\max}/10 \text{ min} = 1\text{-min intensities } (\text{W} \cdot \text{min}^{-1})$ . Additional customized protocols were designed for each of the remaining GXTs based on a percentage of the measured  $\dot{W}_{\max}$  from GXT<sub>1</sub>. The predicted  $\dot{W}_{\max}$  was 80%, 77%, 72% and 70% for GXT<sub>3</sub>, GXT<sub>4</sub>, GXT<sub>7</sub>, and GXT<sub>10</sub>, respectively. The target number of stages for each participant was nine; the initial stage and subsequent stages of the remaining GXTs were determined using the following equations:

Stage 1 Power + Predicted  $\dot{W}_{\max}$  \*25%

Subsequent power increments = (Predicted  $\dot{W}_{\max}$  – Stage1/8)

where stage 1 power and predicted  $\dot{W}_{\max}$  subsequent power increments are expressed in Watts.

A 5-min recovery was administered after each GXT, followed by a VEB performed at 90% of  $\dot{W}_{\max}$  measured from GXT<sub>1</sub> to measure the highest measured  $\dot{V}O_2$  measure ( $\dot{V}O_{2\text{peak}}$ ) [39].

#### *2.2.4 Constant Power Exercise Bouts to Establish the Maximal Lactate Steady State*

The power associated with the respiratory compensation point (RCP) from GXT<sub>1</sub> was used in a regression equation (Eqn. 5) to estimate the MLSS ( $RCP_{\text{MLSS}}$ ) and the first constant power exercise [268]. The RCP was determined as the average of the power output associated with: 1) the break point in ventilation relative to expired carbon dioxide ( $\dot{V}_E/\dot{V}CO_2$ ), 2) second break point in  $\dot{V}_E$  and 3) the fall in end-tidal carbon dioxide ( $P_{\text{ET}CO_2}$ ) after an apparent steady state [71-73].

$$\text{Estimated MLSS (RCPMLSS)} = 23.329 + (0.79127 * \text{RCP})$$

where the  $RCP_{\text{MLSS}}$  and RCP are expressed in Watts

Participants performed 3 min of baseline cycling at 20 W prior to each constant power bout. The MLSS was established as the highest intensity where blood lactate increased <1.0

mmol·L<sup>-1</sup> from the 10<sup>th</sup> to the 30<sup>th</sup> minute [41]. If the blood lactate concentration increased >1.0 mmol·L<sup>-1</sup> the power was decreased by 3%, otherwise the power was increased by 3% [9]. This process continued until the MLSS was obtained.

### 2.2.5 LT and Respiratory Compensation Point Calculations

The LTs were calculated from GXT<sub>3,4,7 and 10</sub> using 14 methods (4 GXTs \* 14 LTs = 56 LTs in total), and the RCP and the RCP<sub>MLSS</sub> were also calculated from GXT<sub>1</sub> (56 LTs + RCP and RCP<sub>MLSS</sub> = 58 total estimates):

1. Log-log: The lactate curve was divided into two segments and the intersection point of the two lines with the lowest residuals sum of squares was taken as the LT [269].
2. OBLA value of 2.0, 2.5, 3.0, 3.5, or 4.0 mmol·L<sup>-1</sup> [76, 81, 182].
3. Baseline + absolute value(s) (B + mmol·L<sup>-1</sup>) : The intensity at which blood lactate concentration increased 0.5, 1.0 or 1.5 mmol·L<sup>-1</sup> above baseline value(s) [144, 270].
4. D<sub>max</sub>: The point on the third order polynomial regression curve that yielded the maximum perpendicular distance to the straight line formed by the two end points of the curve [74].
5. Modified D<sub>max</sub> (ModD<sub>max</sub>): The intensity at the point on the third order polynomial regression curve that yielded the maximal perpendicular distance to the straight line formed by the point preceding the first rise in blood lactate concentration of >0.4 mmol·L<sup>-1</sup> lactate and the final lactate point [75].
6. Exponential D<sub>max</sub> (Exp-D<sub>max</sub>): The point on the exponential plus-constant regression curve that yielded the maximum perpendicular distance to the straight line formed by the two end points of the curve [77, 271].
7. Log-log Modified D<sub>max</sub> (Log-Poly-ModD<sub>max</sub>): The intensity at the point on the third order polynomial regression curve that yielded the maximal perpendicular distance

to the straight line formed by the intensity associated with the log-log LT and the final lactate point.

8. Log-log Exponential Modified  $D_{\max}$  method (Log-Exp-Mod $D_{\max}$ ): The intensity at the point on the exponential plus-constant regression curve that yielded the maximal perpendicular distance to the straight line formed by the intensity associated with the log-log LT and the final lactate point.
9. RCP: refer to *Constant Power Exercise Bouts to Establish the Maximal Lactate Steady State* method section.
10. The estimated MLSS was based on a regression equation based on the RCP from  $GXT_1$  ( $RCP_{MLSS}$ ) (Eqn. 5).

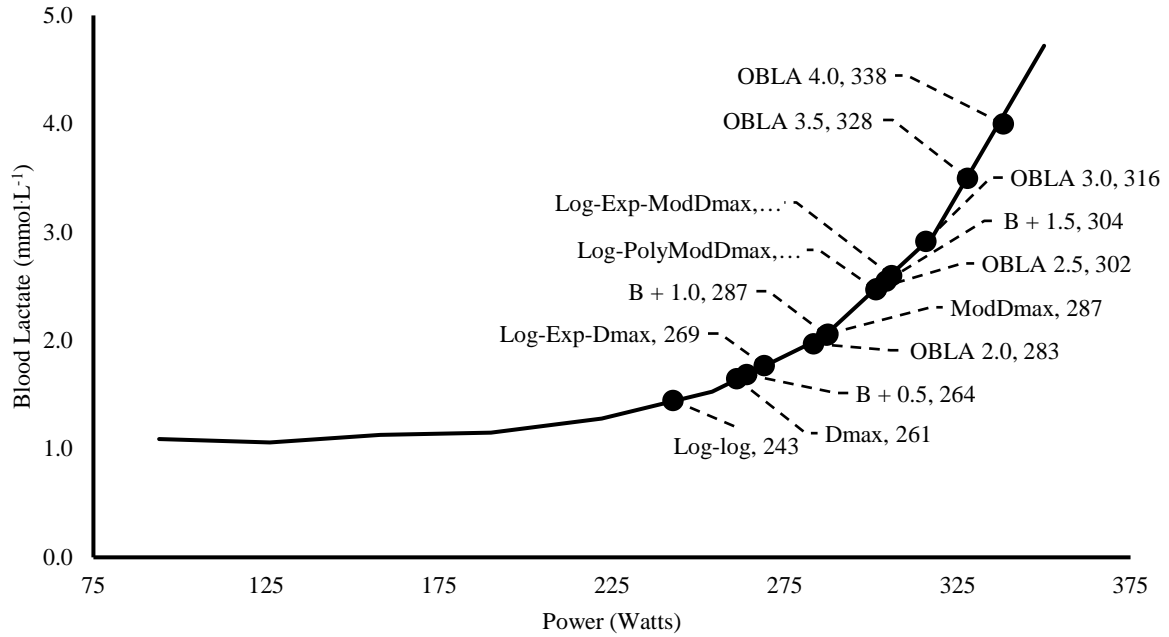


**Figure 2.1 Representative blood lactate curve with 14 LTs calculated from GXT<sub>4</sub> (participant #9).** The power of the MLSS was 302 W and the blood lactate concentration was 2.85 mmol·L<sup>-1</sup>. Log-log = power at the intersection of two linear lines with the lowest residual sum of squares; log = using the log-log method as the point of the initial data point when calculating the D<sub>max</sub> or Modified D<sub>max</sub>; poly = Modified D<sub>max</sub> method calculated using a third order polynomial regression equation; exp = Modified D<sub>max</sub> method calculated using a constant plus exponential regression equation; OBLA = onset of blood lactate accumulation; B + absolute value = the intensity where blood lactate increases above baseline.

### 2.2.6 Data Analysis

Breath-by-breath data were edited individually with values greater than three standard deviations from the mean excluded [272]. The data was interpolated on a second-by-second basis and averaged into 5- and 30-s bins [193, 273]. The highest measured  $\dot{V}O_2$  value from every GXT and VEB was determined as the highest 20-s rolling average. The  $\dot{V}O_{2max}$  was computed as the highest  $\dot{V}O_2$  measured from any GXT or VEB. The  $\dot{V}O_{2peak}$  for each GXT was defined as the highest measured  $\dot{V}O_2$  from either the GXT or the subsequent VEB. The  $\dot{W}_{max}$  for every GXT was determined as the power from the last completed stage plus the time completed in the subsequent stage multiplied by the slope (Eqn. 6). The  $\dot{V}O_2$  response at the MLSS was determined by the average  $\dot{V}O_2$  value during the last two minutes of the 30-minute constant power bout.

$$\dot{W}_{max} = \text{Power of Last Stage (W)} + [\text{slope (W.s}^{-1}) * \text{time (sec.)}] \text{ (Eqn. 6)}$$

Calculated LTs were excluded if the mean difference between the MLSS and calculated LT was greater than the error of the measurement of the MLSS [coefficient of the variation (CV%) = 3%, 7.9 W] [9], the effect size (ES) was greater than 0.2, or the Pearson Product moment correlation coefficient ( $r$ ) was less than 0.90. Using these criteria, 10 of the 56 LTs and the  $RCP_{MLSS}$  (Eqn. 5) were included in the analysis (Table 2.1).

**Table 2.1. The mean  $\pm$  standard deviation (SD) of the 14 lactate thresholds calculated from the 4 prolonged graded exercise tests (i.e., GXT<sub>3</sub>, GXT<sub>4</sub>, GXT<sub>7</sub> and GXT<sub>10</sub>), and the respiratory compensation point (RCP) and the maximal lactate steady state (MLSS) estimated from the RCP (RCP<sub>MLSS</sub>) calculated from GXT<sub>1</sub>. Also shown is the mean difference (MD), the Pearson product moment correlation (r) and effect size (ES) of the difference when compared with the MLSS. (log = using the log-log method as the point of the initial data point when calculating the D<sub>max</sub> or Modified D<sub>max</sub>; poly = Modified D<sub>max</sub> method calculated using a third order polynomial regression equation; exp = Modified D<sub>max</sub> method calculated using a constant plus exponential regression equation; OBLA = onset of blood lactate accumulation, B + = baseline lactate value plus an absolute lactate value). **Bold** represents the LT that met the three criteria for inclusion in our final analysis: mean difference less than 7.9 Watts, Pearson moment product correlation >0.90, and a less than trivial ES difference from the MLSS (ES <0.2)**

		GXT <sub>3</sub>	GXT <sub>4</sub>	GXT <sub>7</sub>	GXT <sub>10</sub>
Log-log LT	Mean SD (W)	211 $\pm$ 43	202 $\pm$ 38	200 $\pm$ 40	196 $\pm$ 41
	MD (W)	53.1	62.8	64.8	68.3
	r	0.84	0.89	0.87	0.78
	ES	1.28	1.63	1.62	1.70
OBLA 2.0	Mean SD (W)	262 $\pm$ 40	249 $\pm$ 39	247 $\pm$ 39	245 $\pm$ 37
	MD (W)	2.1	15.1	17.3	19.6
	r	0.86	0.94	0.94	0.93
	ES	-0.05	-0.38	-0.44	-0.50
OBLA 2.5	Mean SD (W)	276 $\pm$ 42	<b>262 <math>\pm</math> 40</b>	<b>258 <math>\pm</math> 40</b>	255 $\pm$ 38
	MD (W)	-11.9	<b>2.0</b>	<b>6.7</b>	9.2
	r	0.89	<b>0.95</b>	<b>0.94</b>	0.93
	ES	0.30	<b>-0.05</b>	<b>-0.17</b>	-0.23
OBLA 3.0	Mean SD (W)	288 $\pm$ 43	273 $\pm$ 41	<b>267 <math>\pm</math> 41</b>	<b>264 <math>\pm</math> 39</b>
	MD (W)	-23.2	-8.8	<b>-2.2</b>	<b>0.4</b>
	r	0.90	0.96	<b>0.95</b>	<b>0.93</b>
	ES	0.59	0.22	<b>0.06</b>	<b>-0.01</b>
OBLA 3.5	Mean SD (W)	297 $\pm$ 45	282 $\pm$ 41	274 $\pm$ 41	<b>272 <math>\pm</math> 40</b>
	MD (W)	-32.8	-18.1	-10.0	<b>-7.3</b>
	r	0.91	0.96	0.95	<b>0.93</b>
	ES	0.83	0.46	0.25	<b>0.19</b>
OBLA 4.0	Mean SD (W)	306 $\pm$ 46	291 $\pm$ 42	281 $\pm$ 42	279 $\pm$ 41
	MD (W)	-41.3	-26.3	-16.8	-14.2
	r	0.91	0.97	0.95	0.93
	ES	1.05	0.67	0.43	0.36
Baseline + 0.5	Mean SD (W)	235 $\pm$ 38	229 $\pm$ 40	228 $\pm$ 41	225 $\pm$ 37
	MD (W)	29.4	35.6	36.6	39.5
	r	0.74	0.81	0.83	0.82
	ES	-0.75	-0.90	-0.93	-1.00
Baseline + 1.0	Mean SD (W)	255 $\pm$ 39	239 $\pm$ 40	236 $\pm$ 39	235 $\pm$ 39
	MD (W)	9.5	25.3	27.9	29.1
	r	0.88	0.92	0.93	0.91
	ES	-0.24	-0.64	-0.71	-0.74
Baseline + 1.5	Mean SD (W)	<b>270 <math>\pm</math> 41</b>	254 $\pm$ 41	250 $\pm$ 39	248 $\pm$ 39
	MD (W)	<b>-6.0</b>	10.1	14.7	16.8
	r	<b>0.90</b>	0.94	0.94	0.92
	ES	<b>0.15</b>	-0.26	-0.37	-0.43
Dmax	Mean SD (W)	246 $\pm$ 34	232 $\pm$ 36	223 $\pm$ 31	216 $\pm$ 33
	MD (W)	18.6	31.9	41.6	48.8
	r	0.94	0.97	0.96	0.95
	ES	-0.47	-0.81	-1.06	-1.24
Modified Dmax	Mean SD (W)	278 $\pm$ 37	<b>267 <math>\pm</math> 39</b>	255 $\pm$ 40	248 $\pm$ 37
	MD (W)	-13.2	<b>-2.9</b>	9.7	15.9
	r	0.90	<b>0.91</b>	0.93	0.92
	ES	0.33	<b>0.07</b>	-0.25	-0.40
Log-Poly-MDmax	Mean SD (W)	280 $\pm$ 42	<b>265 <math>\pm</math> 42</b>	255 $\pm$ 39	248 $\pm$ 40
	MD (W)	-15.5	<b>-1.1</b>	9.5	16.5
	r	0.94	<b>0.96</b>	0.96	0.92
	ES	0.39	<b>0.03</b>	-0.24	-0.42
Exp-Dmax	Mean SD (W)	256 $\pm$ 35	243 $\pm$ 36	234 $\pm$ 34	228 $\pm$ 35
	MD (W)	8.0	21.8	30.8	36.8
	r	0.92	0.97	0.96	0.94
	ES	-0.20	-0.55	-0.78	-0.93

<b>Log-Exp-MDmax</b>	<b>Mean SD (W)</b>	286 ± 42	<b>271 ± 42</b>	<b>260 ± 39</b>	253 ± 40
	<b>MD (W)</b>	-21.7	<b>-7.0</b>	<b>4.3</b>	11.1
	<b>r</b>	0.94	<b>0.97</b>	<b>0.96</b>	0.93
	<b>ES</b>	0.55	<b>0.18</b>	<b>-0.11</b>	-0.28
<b>GXT<sub>1</sub></b>					
<b>RCP<sub>MLSS</sub></b>	<b>Mean SD (W)</b>	<b>271 ± 39</b>			
	<b>MD (W)</b>	<b>-6.71</b>			
	<b>r</b>	<b>0.92</b>			
	<b>ES</b>	<b>-0.17</b>			
<b>RCP</b>	<b>Mean SD (W)</b>	315 ± 40			
	<b>MD (W)</b>	-50.4			
	<b>r</b>	0.91			
	<b>ES</b>	1.27			

### 2.2.7 Statistical Analysis

A one-way analysis of variance with repeated measures was used to assess significant differences between the MLSS and the calculated LTs. Agreement between the MLSS and the calculated LTs was evaluated using a two-way mixed intraclass calculation coefficient (ICC), standard error of the measurement (SEM), Lin's concordance correlation coefficient ( $p_c$ ) [274], Bland-Altman plots [275], ( $r$ ), CV% [233, 276] and a magnitude-based inference approach involving standardised differences (ED) [7, 8]. Differences between  $\dot{V}O_{2\text{peak}}$  values measured during each GXT were assessed using ES, p-values, and the CV%. Agreement between  $\dot{V}O_2$  measured during each GXT and subsequent VEB was evaluated using intraclass calculation coefficient (ICC), SEM, and CV% [233]. Descriptive statistics are reported as the mean  $\pm$  SD. Alpha was set to  $P \leq 0.05$ .

## 2.3 Results

### 2.3.1 MLSS

The power associated with the MLSS was  $264 \pm 39$  W, and the blood lactate concentrations at the 10<sup>th</sup> and 30<sup>th</sup> min were  $2.8 \pm 0.8$  and  $3.3 \pm 0.8$  mmol·L<sup>-1</sup>, respectively. The blood lactate values at 3% above the MLSS ( $272 \pm 41$  W) at the 10<sup>th</sup> and 30<sup>th</sup> min were  $3.6 \pm 0.8$  and  $5.0 \pm 0.9$  mmol·L<sup>-1</sup>, respectively. The  $\dot{V}O_2$  at the MLSS was  $3892 \pm 441$  mL·min<sup>-1</sup> ( $50.5 \pm 4.0$  mL·kg<sup>-1</sup>·min<sup>-1</sup>). For each GXT the  $\dot{V}O_2$  at the MLSS and the power at the MLSS are shown in Table 2.1.

**Table 2.2** Mean, standard deviation, and range of the  $\dot{V}O_2$  and power associated with the maximal lactate steady state (MLSS) expressed as a percentage of the maximal power ( $\dot{W}_{max}$ ) and  $\dot{V}O_{2peak}$  measured during each GXT. *Note: The  $\dot{V}O_2$  at the MLSS was  $81.4 \pm 4.7$  % of the  $\dot{V}O_{2max}$ . (Defined as the highest measured  $\dot{V}O_2$  during any GXT)*

	<b>GXT<sub>1</sub></b>	<b>GXT<sub>3</sub></b>	<b>GXT<sub>4</sub></b>	<b>GXT<sub>7</sub></b>	<b>GXT<sub>10</sub></b>
<b><math>\dot{V}O_2</math> at MLSS</b>	$83.0 \pm 4.5$	$84.7 \pm 4.7$	$86.1 \pm 5.9$	$88.4 \pm 6.0$	$90.2 \pm 5.3$
<b>(% of <math>\dot{V}O_{2peak}</math>)</b>	[75.5 - 90.7]	[76.6 - 91.9]	[73.9 - 94.2]	[77.4 - 103.2]	[78.7 - 99.9]
<b>Power at MLSS</b>	$62.9 \pm 3.9$	$78.4 \pm 4.3$	$82.4 \pm 3.6$	$87.3 \pm 4.4$	$89.6 \pm 4.7$
<b>(% of <math>\dot{W}_{max}</math>)</b>	[56.8 - 71.7]	[69.8 - 84.4]	[73.7 - 88.8]	[79.8 - 96.0]	[81.6 - 98.1]

### 2.3.2 Validity of LT Estimates

Comparisons of the 58 estimations of the MLSS and the calculated MLSS are detailed in Table 2.1. Figure 2.2 displays the standardized difference of the 13 LTs calculated for each GXT (52 in total) and the MLSS (all log-log methods were excluded given an  $ES > 1.0$ ). Ten of the calculated LTs and the  $RCP_{MLSS}$  met our inclusion criteria for final analysis - detailed comparisons with the MLSS are provided in Table 2.3 and Figure 2.3. Figure 2.3 shows Bland-Altman plots of the 11 estimations included in our analysis; the newly developed  $ModD_{max}$  LT calculations (**Figure 2.3; Panels E, F and I**) had the lowest limits of agreement with the MLSS. The log-log polynomial modified  $D_{max}$  (Log-Poly- $ModD_{max}$ ) method derived from  $GXT_4$  provided the best estimation of the MLSS (Figure 2.3, Panel E). There was an inverse relationship between the power calculated for each of the 14 LTs and stage length (Tables 2.1 and 2.4).

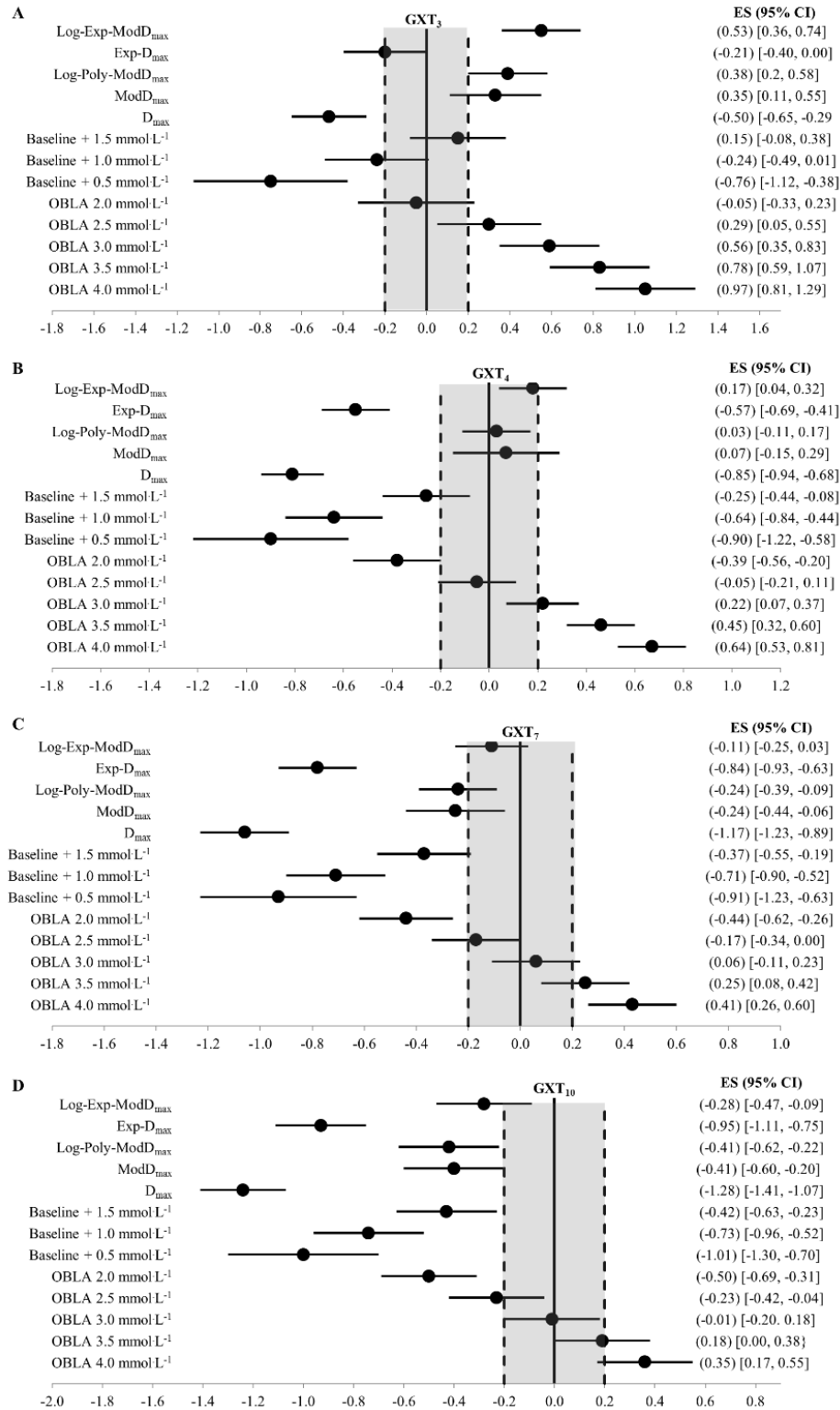


**Figure 2.2 (A-D) Forrest Plots of the difference (ES ± 95% CI) between the MLSS and the power calculated from the 13 lactate thresholds derived from (A) GXT<sub>3</sub>, (B) GXT<sub>4</sub>, (C) GXT<sub>7</sub> and (D) GXT<sub>10</sub> (52 in total and excluding log-log). The solid vertical bar represents no difference from the MLSS and the dashed vertical bars represents the threshold between a trivial and small difference (ES = 0.2) established by Cohen [7] and Hopkins [8]. log = using the log-log method as the initial data point when calculating the D<sub>max</sub> or Modified D<sub>max</sub>; poly = Modified D<sub>max</sub> method calculated using a third order polynomial regression equation; exp = Modified D<sub>max</sub> method calculated using a constant plus exponential regression equation; OBLA = onset of blood lactate accumulation**

**Table 2.3.** Mean  $\pm$  standard deviation, mean difference (MD), intraclass correlation coefficient (ICC), Lin's concordance correlation coefficient ( $\rho_c$ ), standard error of the measurement (SEM), effect size (ES) with 95% confidence limits, and coefficient of the variation (%CV) between the maximal lactate steady state (MLSS) and the eleven thresholds included in our analysis. (RCP<sub>MLSS</sub> = MLSS estimate based on the respiratory compensation point; log = Modified D<sub>max</sub> method using the log-log method as the point of the initial lactate point; poly = Modified D<sub>max</sub> method calculated using a third order polynomial regression equation; exp = Modified D<sub>max</sub> method calculated using a constant plus exponential regression equation; OBLA = onset of blood lactate accumulation)

	Mean $\pm$ SD (W)	MD (W)	ICC [95% CI]	$\rho_c$	SEM [95% CI] (W)	ES [95% CI]	CV [95% CI] (%)
<b>MLSS</b>	<b>264 <math>\pm</math> 39</b>						
<b>RCP<sub>MLSS</sub></b>	271 $\pm$ 39	6.7	0.92 [0.78 – 0.97]	0.90	11.2 [8.3 – 17.0]	0.17 [-0.04 – 0.38]	6.0 [4.4 – 9.4]
<b>Baseline + 1.5 mmolL<sup>-1</sup></b>	270 $\pm$ 41	6.0	0.90 [0.75 – 0.97]	0.90	12.5 [9.3 – 19.0]	0.15 [-0.08 – 0.38]	6.6 [4.9 – 10.4]
<b>OBLA 2.5 mmolL<sup>-1</sup></b>	262 $\pm$ 40	-2.0	0.95 [0.87 – 0.98]	0.95	8.7 [6.5 – 13.2]	-0.05 [-0.21 – 0.11]	5.3 [3.9 – 8.4]
<b>Modified D<sub>max</sub></b>	267 $\pm$ 39	2.9	0.91 [0.76 – 0.98]	0.90	11.7 [8.7 – 17.9]	0.07 [-0.15 – 0.29]	7.0 [5.1 – 11.0]
<b>Log-Poly-MD<sub>max</sub></b>	265 $\pm$ 42	1.1	0.96 [0.90 – 0.99]	0.96	7.9 [5.8 – 12.0]	0.03 [-0.11 – 0.17]	4.4 [3.2 – 6.9]
<b>Log-Exp-MD<sub>max</sub></b>	271 $\pm$ 42	7.0	0.97 [0.91 – 0.99]	0.95	7.5 [5.6 – 11.4]	0.18 [0.04 – 0.32]	4.1 [3.0 – 6.3]
<b>OBLA 2.5 mmolL<sup>-1</sup></b>	258 $\pm$ 41	-6.7	0.94 [0.85 – 0.98]	0.93	9.4 [7.0 – 14.3]	-0.17 [-0.34 – 0.00]	4.9 [3.6 – 7.7]
<b>OBLA 3.0 mmolL<sup>-1</sup></b>	267 $\pm$ 41	2.2	0.95 [0.86 – 0.98]	0.95	9.2 [6.9 – 14.1]	0.06 [-0.11 – 0.23]	5.1 [3.7 – 8.0]
<b>Log-Exp-MD<sub>max</sub></b>	260 $\pm$ 39	-4.3	0.96 [0.89 – 0.99]	0.95	7.8 [5.8 – 11.9]	-0.11 [-0.25 – 0.03]	4.1 [3.0 – 6.4]
<b>OBLA 3.0 mmolL<sup>-1</sup></b>	264 $\pm$ 39	-0.4	0.93 [0.82 – 0.98]	0.93	10.2 [7.6 – 15.5]	-0.01 [-0.20 – 0.18]	5.5 [4.0 – 8.6]
<b>OBLA 3.5 mmolL<sup>-1</sup> (n = 16)</b>	275 $\pm$ 39	6.9	0.93 [0.82 – 0.98]	0.91	10.3 [7.7 – 15.7]	0.19 [0.00 – 0.38]	5.5 [4.0 – 8.7]

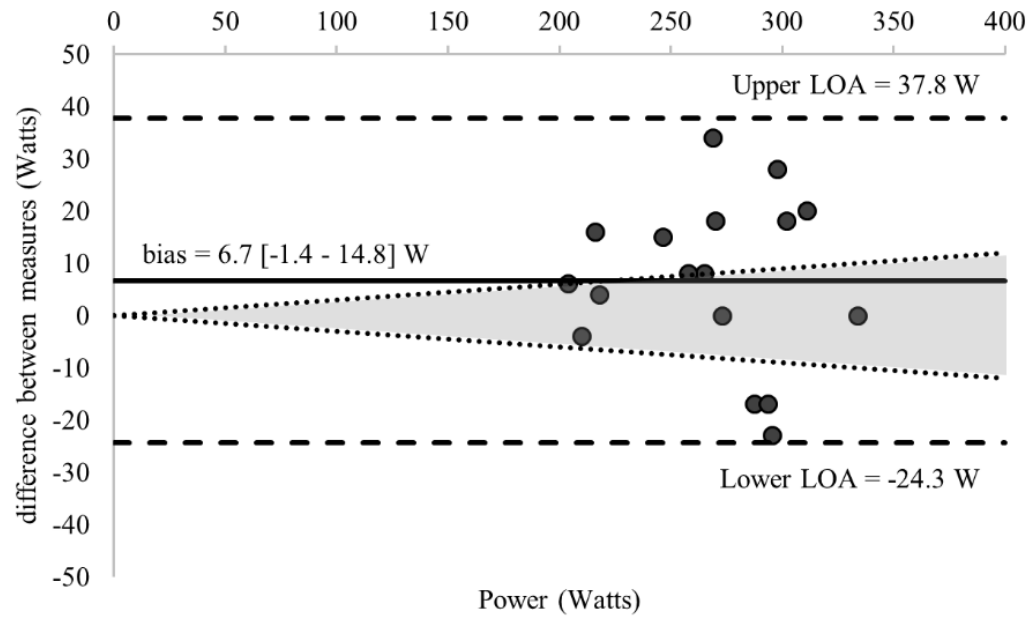


**Figure 2.3. Bland-Altman plots displaying agreement between measures of the power associated with the RCP regression equation (RCPMLSS) calculated from GXT1 and the MLSS.** The differences between measures (y-axis) are plotted as a function of the mean of the two measures (x-axis) in power (Watts). The horizontal solid line represents the mean difference between the two measures (i.e., bias). The two horizontal dashed lines represent the limits of agreement (1.96 x standard deviation of the mean difference between the estimated lactate threshold via the RCPMLSS and the maximal lactate steady state). The dotted diagonal lines represent the boundaries of the 95% CI for MLSS reliability (CV = 3.0%; 95%; CI = 3.8%) calculated from Hauser et al., [9] (RCP = respiratory compensation point).

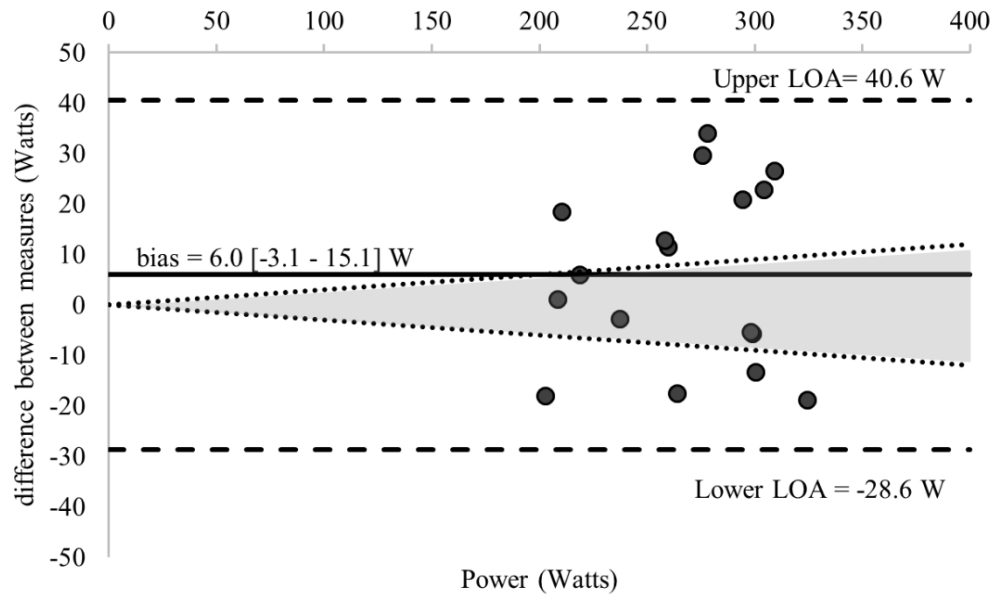


**Figure 2.4. Bland-Altman plots displaying agreement between measures of the power associated with the baseline plus  $1.5 \text{ mmol}\cdot\text{L}^{-1}$  calculated from GXT3 and the MLSS.** The differences between measures (y-axis) are plotted as a function of the mean of the two measures (x-axis) in power (Watts). The horizontal solid line represents the mean difference between the two measures (i.e., bias). The two horizontal dashed lines represent the limits of agreement ( $1.96 \times$  standard deviation of the mean difference between the lactate threshold and the maximal lactate steady state). The dotted diagonal lines represent the boundaries of the 95% CI for MLSS reliability ( $\text{CV} = 3.0\%$ ;  $95\%$ ;  $\text{CI} = 3.8\%$ ) calculated from Hauser et al. [9].

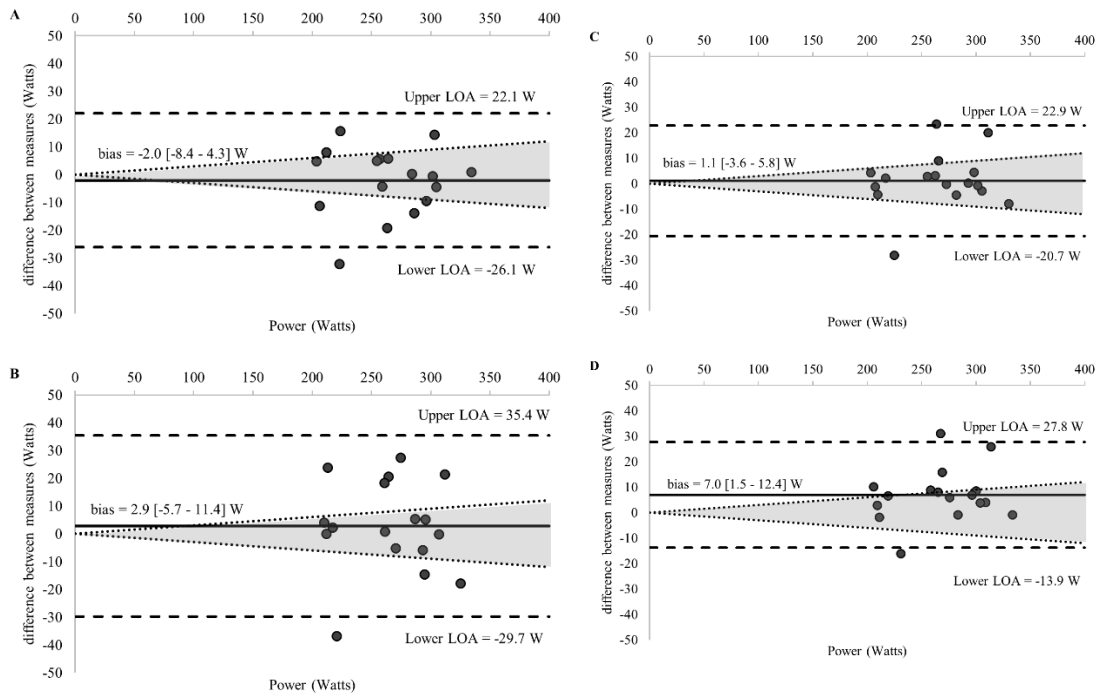


**Figure 2.5.** (A-D) Bland-Altman plots displaying agreement between measures of the power associated with the (A) OBLA  $2.5 \text{ mmol}\cdot\text{L}^{-1}$ , (B) Modified  $D_{\text{max}}$ , (C) Log-Poly-Modified  $D_{\text{max}}$ , (D) Log-Exp-Modified  $D_{\text{max}}$  calculated from **GXT4** and the MLSS. The differences between measures (y-axis) are plotted as a function of the mean of the two measures (x-axis) in power (Watts). The horizontal solid line represents the mean difference between the two measures (i.e., bias). The two horizontal dashed lines represent the limits of agreement ( $1.96 \times$  standard deviation of the mean difference between the lactate threshold and the maximal lactate steady state). The dotted diagonal lines represent the boundaries of the 95% CI for MLSS reliability ( $\text{CV} = 3.0\%$ ;  $95\%$ ;  $\text{CI} = 3.8\%$ ) calculated from Hauser et al. [9] (log = Modified  $D_{\text{max}}$  method using the log-log method as the point of the initial lactate point; poly = Modified  $D_{\text{max}}$  method calculated using a third order polynomial regression equation; exp = Modified  $D_{\text{max}}$  method calculated using a constant plus exponential regression equation; OBLA = onset of blood lactate accumulation.).

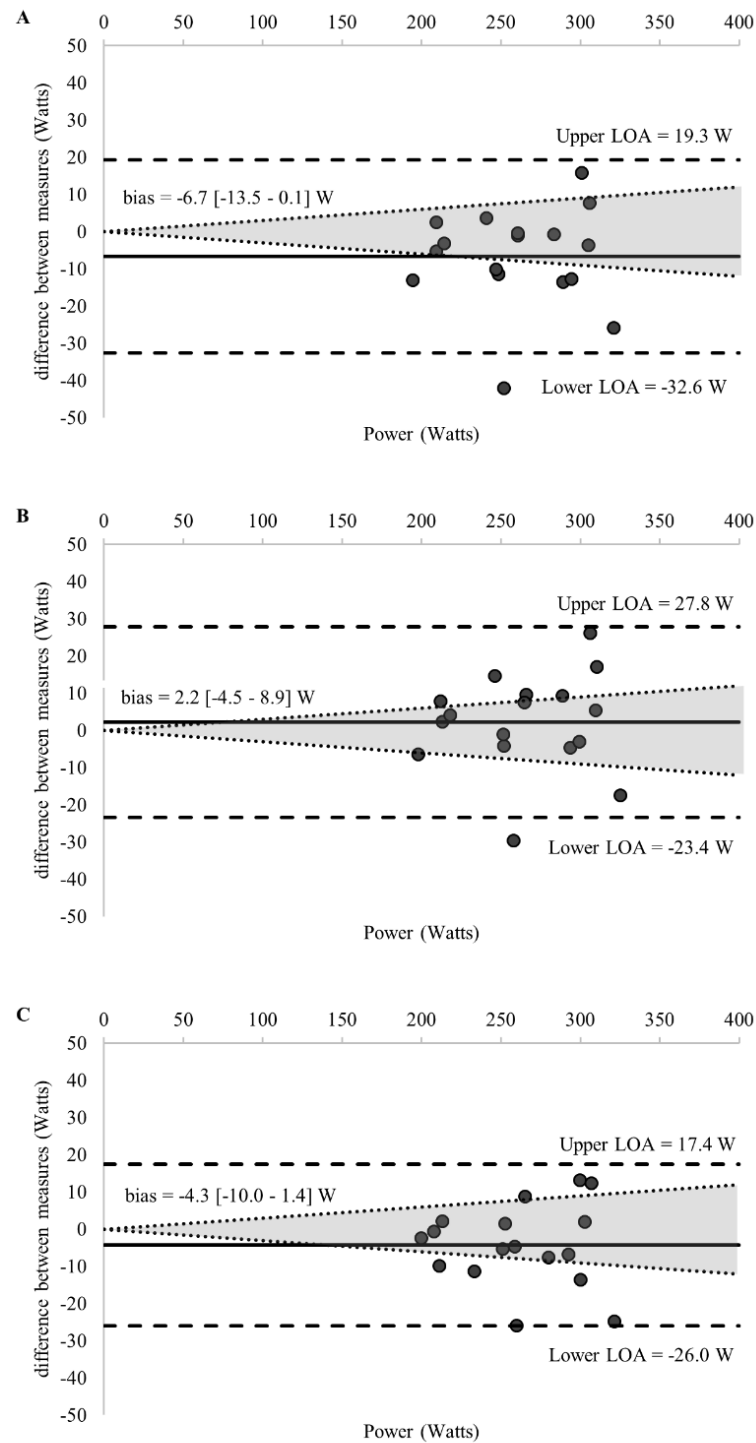


**Figure 2.6.** (A-C) Bland-Altman plots displaying agreement between measures of the power associated with the (A) OBLA 2.5 mmol·L<sup>-1</sup> (GXT<sub>7</sub>), (B) OBLA 3.0 mmol·L<sup>-1</sup> (GXT<sub>7</sub>), (C) Log-Exp-Modified D<sub>max</sub> calculated from GXT<sub>7</sub> and the MLSS. The differences between measures (y-axis) are plotted as a function of the mean of the two measures (x-axis) in power (Watts). The horizontal solid line represents the mean difference between the two measures (i.e., bias). The two horizontal dashed lines represent the limits of agreement (1.96 x standard deviation of the mean difference between the lactate threshold and the maximal lactate steady state). The dotted diagonal lines represent the boundaries of the 95% CI for MLSS reliability (CV = 3.0%; 95%; CI = 3.8%) calculated from Hauser et al. [9] (log = Modified D<sub>max</sub> method using the log-log method as the point of the initial lactate point; exp = Modified D<sub>max</sub> method calculated using a constant plus exponential regression equation; OBLA = onset of blood lactate accumulation).

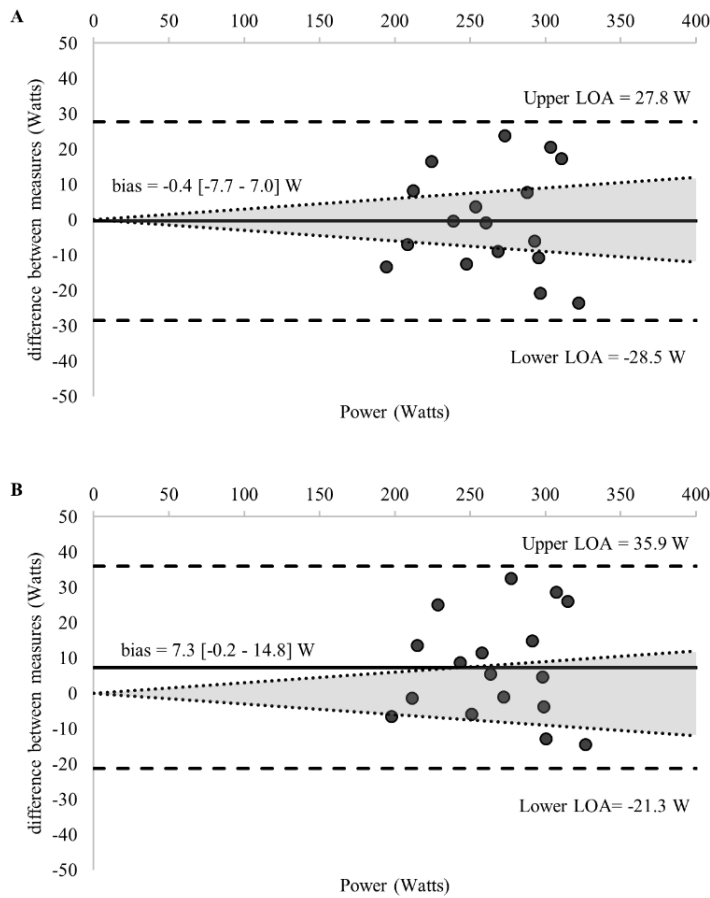


**Figure 2.7.** (A-B) Bland-Altman plots displaying agreement between measures of the power associated with the (A) OBLA 3.0 mmol·L<sup>-1</sup>, (B) OBLA 3.5 mmol·L<sup>-1</sup> calculated from **GXT10** and the MLSS. The differences between measures (yaxis) are plotted as a function of the mean of the two measures (x-axis) in power (Watts). The horizontal solid line represents the mean difference between the two measures (i.e., bias). The two horizontal dashed lines represent the limits of agreement (1.96 x standard deviation of the mean difference between the lactate threshold and the maximal lactate steady state). The dotted diagonal lines represent the boundaries of the 95% CI for MLSS reliability (CV = 3.0%; 95%; CI = 3.8%) calculated from Hauser et al., 2014 (OBLA = onset of blood lactate accumulation.).



### 2.3.3 $\dot{W}_{max}$ and $\dot{V}O_{2max}$

There was an inverse relationship between GXT duration and both  $\dot{W}_{max}$  and  $\dot{V}O_{2peak}$  (Table 2.5). The  $\dot{V}O_{2peak}$  values derived from GXT<sub>3</sub> and GXT<sub>4</sub> were similar to the  $\dot{V}O_{2peak}$  measured during GXT<sub>1</sub> (Table 2.6); however, the values were outside the variability of the measurement (CV > 3%) [9].  $\dot{V}O_{2peak}$  values from GXT<sub>1</sub> and the corresponding VEB had the highest agreement (MD = 0.5 mL·kg<sup>-1</sup>·min<sup>-1</sup>, ICC = 0.96, SEM = 1.1 mL·kg<sup>-1</sup>·min<sup>-1</sup> and CV = 2.0%) compared with any GXT and corresponding VEB. The remaining GXTs and corresponding VEB had a CV of 3.3, 2.0, 3.5 and 5.2%, for GXT<sub>3</sub>, GXT<sub>4</sub>, GXT<sub>7</sub> and GXT<sub>10</sub>, respectively. The VEB performed following the longer duration GXTs (GXT<sub>3-10</sub>) underestimated the  $\dot{V}O_{2peak}$  from GXT<sub>1</sub> (Table 2.6).

**Table 2.5.** Mean and standard deviation of  $\dot{V}O_{2max}$  - highest measured  $\dot{V}O_2$  during any graded exercise test (GXT); GXT  $\dot{V}O_2$  - highest measured  $\dot{V}O_2$  during each GXT; VEB  $\dot{V}O_2$  highest measured  $\dot{V}O_2$  during each verification exhaustive bout (VEB);  $\dot{V}O_{2peak}$ , highest measured  $\dot{V}O_2$  during either the GXT or corresponding VEB. Mean and standard deviation of GXT duration, max power (Watts) from each GXT, percentage of maximum power from the prolonged GXT expressed as a percentage of W maximum power from GXT<sub>1</sub> and power of each VEB (Watts) from the GXTs. Relative power of the verification exhaustive bout expressed as a percentage (%) of the maximal power measured during the GXT. The subscript (i.e., 1, 3, 4, 7 or 10) refers to the stage duration (minutes) for each test

	<b>GXT<sub>1</sub></b>	<b>GXT<sub>3</sub></b>	<b>GXT<sub>4</sub></b>	<b>GXT<sub>7</sub></b>	<b>GXT<sub>10</sub></b>
<b><math>\dot{V}O_{2max}</math> (mL·kg<sup>-1</sup>·min<sup>-1</sup>)</b>			62.1 ± 5.8		
<b>GXT <math>\dot{V}O_2</math> (mL·kg<sup>-1</sup>·min<sup>-1</sup>)</b>	60.6 ± 5.4	58.2 ± 5.3	57.3 ± 5.7	56.4 ± 5.2	54.9 ± 4.9
<b>VEB <math>\dot{V}O_2</math> (mL·kg<sup>-1</sup>·min<sup>-1</sup>)</b>	60.1 ± 5.8	58.9 ± 5.9	58.8 ± 6.1	56.4 ± 5.9	54.7 ± 6.6
<b><math>\dot{V}O_{2peak}</math> (mL·kg<sup>-1</sup>·min<sup>-1</sup>)</b>	61.0 ± 5.3	59.7 ± 5.4	58.9 ± 6.0	57.3 ± 5.4	56.2 ± 5.5
<b>GXT Duration (min)</b>	11.3 ± 0.9	26.8 ± 1.4	34.9 ± 1.9	59.2 ± 3.3	81.6 ± 4.6
<b>Maximum Power (Watts)</b>	420 ± 55	337 ± 46	321 ± 47	303 ± 43	295 ± 43
<b>Percent <math>\dot{W}_{max}</math> of GXT<sub>1</sub> (%)</b>	100	80.3 ± 2.9	76.4 ± 3.1	72.1 ± 3.6	70.3 ± 4.0
<b>VEB (Watts)</b>			378 ± 50		
<b>VEB (% of GXT <math>\dot{W}_{max}</math>)</b>	90	109.7 ± 3.8	118.4 ± 18.7	125.4 ± 19.3	128.8 ± 20.4

**Table 2.6.** Mean difference (MD) and standard deviation, effect size (ES), coefficient of the variation (CV) and p-value (p) for the measured  $\dot{V}O_{2\text{peak}}$  values from GXT<sub>1</sub> compared with the  $\dot{V}O_{2\text{peak}}$  values from GXT<sub>3</sub>, GXT<sub>4</sub>, GXT<sub>7</sub>, and GXT<sub>10</sub> and for the  $\dot{V}O_{2\text{peak}}$  values from GXT<sub>1</sub> compared with the  $\dot{V}O_{2\text{peak}}$  values from the VEB following GXT<sub>3</sub>, GXT<sub>4</sub>, GXT<sub>7</sub>, and GXT<sub>10</sub>

	GXT <sub>1</sub> vs. GXT <sub>3</sub>	GXT <sub>1</sub> vs. GXT <sub>4</sub>	GXT <sub>1</sub> vs. GXT <sub>7</sub>	GXT <sub>1</sub> vs. GXT <sub>10</sub>
<b>MD (mL·kg<sup>-1</sup>·min<sup>-1</sup>)</b>	-1.2 ± 3.3	-2.1 ± 4.2	-3.7 ± 4.7	-4.8 ± 3.7
<b>ES</b>	0.23	0.36	0.69	0.88
<b>CV (%)</b>	3.8	4.9	5.6	4.6
<b>p</b>	0.13	0.06	< 0.01	< 0.01
	GXT <sub>1</sub> vs. VEB GXT <sub>3</sub>	GXT <sub>1</sub> vs. VEB GXT <sub>4</sub>	GXT <sub>1</sub> vs. VEB GXT <sub>7</sub>	GXT <sub>1</sub> vs. VEB GXT <sub>10</sub>
<b>MD (mL·kg<sup>-1</sup>·min<sup>-1</sup>)</b>	-2.1 ± 5.9	-2.1 ± 6.1	-4.6 ± 5.9	-6.2 ± 6.6
<b>ES</b>	0.37	0.37	0.81	1.04
<b>CV (%)</b>	4.2	4.9	6.1	5.9
<b>p</b>	0.02	0.98	0.03	0.03

The subscript (i.e., 1, 3, 4, 7 or 10) refers to the stage duration (minutes) for each test

## 2.4 Discussion

The main findings of the present study are as follows. Only 11 of the 58 threshold values met our inclusion criteria as valid estimates of the MLSS. Of the 11 methods included in our analysis, three of the ModD<sub>max</sub> methods yielded the most favourable estimations of the MLSS, and the Log-Poly-ModD<sub>max</sub> derived from GXT<sub>4</sub> provided the best estimation of the MLSS. There was an inverse relationship between stage length and LT, and this effect was larger in all D<sub>max</sub> methods compared with the OBLA and baseline plus absolute lactate value methods. The  $\dot{V}O_{2peak}$  values measured during the longer duration GXTs (GXT<sub>3-10</sub>) underestimated the  $\dot{V}O_{2max}$  and the  $\dot{V}O_{2peak}$  values obtained from GXT<sub>1</sub> (MD = 1.2 to 4.8 mL·kg<sup>-1</sup>·min<sup>-1</sup>). Finally, contrary to our hypothesis, the VEB after the longer duration GXTs did not yield  $\dot{V}O_{2peak}$  values comparable to the  $\dot{V}O_{2peak}$  derived from GXT<sub>1</sub>.

The use of five GXT protocols, 14 common LT methods, the RCP and RCP<sub>MLSS</sub> resulted in 58 unique thresholds. However, despite their common use, we observed that only 11 of these values met our criteria for inclusion (MD < 7.9 W; ES < 0.2; r > 0.90). Of the four D<sub>max</sub> methods included in our analysis, one consisted of the traditional ModD<sub>max</sub> method [75]. This had the poorest agreement relative to the other ModD<sub>max</sub> methods included in our analysis. The remaining three D<sub>max</sub> methods are new variations of the ModD<sub>max</sub> method, and the Log-Poly-ModD<sub>max</sub> derived from GXT<sub>4</sub> had the highest correlation and lowest mean difference with the MLSS. These variations of the ModD<sub>max</sub> method use the power at the log-log LT as the initial intensity to calculate the ModD<sub>max</sub> and then either the traditional third-order polynomial or exponential plus-constant regression curve to fit the lactate curve [74, 77]. Although the validity of these three methods has not previously been assessed, the favourable estimations of the MLSS may be related to the greater objectivity with which they determine the intensity that corresponds with the initial rise in blood lactate concentration [269].

Although the original  $D_{\max}$  method is a commonly cited method for determining the LT [74], we observed large mean differences (19 to 49 W) between the  $D_{\max}$  and MLSS. Three previous studies have purported to investigate the validity of this method to estimate the MLSS in trained male cyclists [166, 176, 260]. One concluded that the  $D_{\max}$  method derived from  $GXT_3$  was a valid estimation of the MLSS ( $r = 0.97$ ) [177]. We also observed a high correlation between  $D_{\max}$  and the MLSS ( $r = 0.94$  to  $0.97$ ) (Table 2.1), but, as indicated by the MD and other measures, a high correlation is not sufficient to establish validity [183]. Another study examined  $D_{\max}$  derived from two GXTs with similar durations (36 vs. 39 min), but with different stage lengths (30-s vs. 6-min) [260]. The  $D_{\max}$  derived from  $GXT_{30s}$  was not correlated ( $r = 0.51$ ) with the MLSS, even though the MD was 5 W, whilst the  $D_{\max}$  derived from  $GXT_6$  was correlated ( $r = 0.85$ ); however, it underestimated the MLSS (MD = 22 W). The third study concluded the  $D_{\max}$  derived from  $GXT_1$  yielded poor estimates of the MLSS ( $r = 0.56$ ; bias =  $-1.8 \pm 38.1$  W) [166]. Thus, although some studies [177, 260] have used correlation analysis to suggest the  $D_{\max}$  provides a valid estimate of the MLSS, this is not supported by the more comprehensive assessment of validity performed in the present and other studies [166].

There were five fixed blood LT methods and one baseline plus an absolute value that met our inclusion criteria, and, as previously reported [76, 260], these varied with the GXT protocol used. The baseline +  $1.5 \text{ mmol}\cdot\text{L}^{-1}$  was the only LT derived from  $GXT_3$  included in our analysis (bias =  $-6 \pm 35$  W). This is consistent with the results of one previous study (bias =  $0.5 \pm 24$  W), which also recruited trained male cyclists and had a similar GXT protocol design [178]. Consistent with our findings, this study also reported that an OBLA of  $3.5 \text{ mmol}\cdot\text{L}^{-1}$  derived from  $GXT_3$  did not provide a valid estimation of the MLSS. In contrast, another study confirmed the validity of the OBLA of  $3.5 \text{ mmol}\cdot\text{L}^{-1}$  [176], despite recruiting trained cyclists

and using an identical GXT protocol. These conflicting results are likely attributable to the low reproducibility of the OBLA methods [167].

While none of the OBLAs from GXT<sub>3</sub> met our inclusion criteria, the OBLA methods of 2.5 mmol·L<sup>-1</sup> derived from GXT<sub>4</sub> and GXT<sub>7</sub> provided valid estimations of the MLSS, as did the OBLA of 3.0 mmol·L<sup>-1</sup> derived from GXT<sub>7</sub> and GXT<sub>10</sub>. The OBLA of 3.5 mmol·L<sup>-1</sup> from GXT<sub>10</sub> was the highest fixed blood LT that identified the MLSS. There is no previous data investigating the validity of these OBLA methods. However, it is worth noting that these five methods provided superior estimations of the MLSS compared with the original ModD<sub>max</sub>, but were less favourable than the newly-developed ModD<sub>max</sub> methods.

An OBLA of 4.0 mmol·L<sup>-1</sup> is the most commonly-accepted fixed blood lactate value for estimating the LT or MLSS. Three previous studies have attempted to validate use of an OBLA of 4.0 mmol·L<sup>-1</sup> with cycle ergometry [166, 180, 260]. One study found that it overestimated the MLSS (MD = 49 W) when derived from GXT<sub>1</sub> [166]. The other study reported poor agreement (bias 7 ± 49 W) when OBLA of 4.0 mmol·L<sup>-1</sup> was derived from GXT<sub>4</sub> [180]. The final study observed a poor correlation between an OBLA of 4.0 mmol·L<sup>-1</sup> and the MLSS ( $r = 0.71$ ) [260]. Our results indicated the OBLA of 4.0 mmol·L<sup>-1</sup> overestimated the MLSS across all GXTs. Thus, in agreement with previous research, our results indicate; the OBLA of 4.0 mmol·L<sup>-1</sup> does not accurately estimate the MLSS. It is also worth noting that the original authors cautioned the use of this OBLA method, given the lack of a significant correlation when comparing OBLA methods from a GXT and the MLSS [76].

The RCP derived from an 8- to 12-minute GXT consistently overestimates the MLSS [166, 193], and this was confirmed in our study (Table 2.1). Therefore, we used a regression

equation based on the RCP ( $RCP_{MLSS}$ ) (Eqn. 5) to estimate the starting intensity for establishing the MLSS [268]. Our results indicate there was good agreement between the MLSS and  $RCP_{MLSS}$  (Table 2.3). Nonetheless, for many participants the difference between MLSS and  $RCP_{MLSS}$  exceeded the CV% for the MLSS (Figure 2.3A). Therefore, although the  $RCP_{MLSS}$  can be used as a convenient ‘starting point’ when establishing the MLSS, we recommend methods based on blood sampling from the current study and assessing blood lactate kinetics in real time as recommended by Hering et al. [5] for a more accurate estimation of the MLSS.

Although a single GXT can be used to estimate both  $\dot{V}O_{2max}$  and LT, the optimal test duration for each measure is different [140, 259]. To address this challenge, we added a supramaximal VEB after each GXT, equivalent to that performed following GXT<sub>1</sub>, expecting all VEBs would yield similar  $\dot{V}O_2$  values. However, the  $\dot{V}O_{2peak}$  values from the VEB after the longer duration GXTs underestimated the  $\dot{V}O_{2peak}$  from GXT<sub>1</sub>. Although the  $\dot{V}O_{2peak}$  values from GXT<sub>3</sub> and GXT<sub>4</sub> were similar to GXT<sub>1</sub>, the differences were larger than the typical coefficient of variability for  $\dot{V}O_{2peak}$  (CV < 3%) [128]. Our results are consistent with previous recommendations that longer duration GXTs are not optimal for establishing  $\dot{V}O_{2peak}$  [126, 138]. Furthermore, while a VEB can be used to verify that  $\dot{V}O_{2peak}$  was achieved, it appears that a VEB following a prolonged GXT cannot be used to establish  $\dot{V}O_{2max}$ .

Extending the duration of the GXT stages results in a lower  $\dot{W}_{max}$  [4]. This has implications for exercise prescription, as it is common in sport and exercise science research to prescribe exercise intensity as a percentage of  $\dot{W}_{max}$ . For example, in the present study the MLSS ranged from  $63 \pm 4\%$  (range = 52 to 72%) of  $\dot{W}_{max}$  from GXT<sub>1</sub> to  $82 \pm 4\%$  (range = 74 to 88%) of  $\dot{W}_{max}$  from GXT<sub>4</sub>. Prescribing exercise in the current study cohort at a fixed percentage of  $\dot{W}_{max}$  (e.g., 73% of  $\dot{W}_{max}$ ), would result in all participants exercising above or

below the MLSS, GXT<sub>1</sub> and GXT<sub>4</sub>, respectively. This is important as it has previously been reported that prescribing exercise relative to LT results in a more homogenous physiological response than when exercise performed relative to  $\dot{W}_{\max}$  [3]. This also highlights why it is important to consider the GXT protocol and the method used to determine relative exercise intensity when comparing results between studies.

The wide range of  $\dot{W}_{\max}$  for each GXT is also note-worthy, the  $\dot{W}_{\max}$  range for GXT<sub>1</sub> was 320 to 517 W and the duration ranged from 9 to 12 minutes. Had we employed a standardized GXT (e.g., 35 W increments), and assuming  $\dot{W}_{\max}$  stayed constant, the range would have been 9- to 15 min. Applying this to our longer duration GXTs resulted in a homogenous duration (GXT<sub>4</sub>: 32- to 39 min), whereas a standardised approach (e.g., 35 W increments) would have resulted in a range of 27- to 46 min [180]. Thus, individualizing GXT protocol design is a useful approach to ensure homogenous test duration [39].

## 2.5 Conclusion

In conclusion, the traditional  $D_{\max}$  and OBLA of 4.0 mmol·L<sup>-1</sup> did not provide valid estimates of the MLSS. The best estimation of the MLSS was the Log-Poly-Mod $D_{\max}$  derived from GXT<sub>4</sub>. The superior validity of our newly-developed Mod $D_{\max}$  model may relate to the objectivity for determining the initial rise in blood lactate concentration. It is apparent that both  $\dot{V}O_{2\max}$  and LT cannot be determined in a single GXT, even if the GXT is followed by a VEB. Therefore, to appropriately determine  $\dot{V}O_{2\max}$  the optimum duration of a GXT is 8-12 minutes and the  $\dot{V}O_2$  values measured during the GXT and VEB be within 3% = CV [125]. Our data also highlight how differences in GXT protocol design and methods used to calculate the relative exercise intensity may contribute to the conflicting findings reported in the literature.

**Chapter 3: Review of literature: influence of exercise intensity on bioenergetics, homeostatic perturbations, signaling kinases, and genes associated with exercise induced mitochondrial biogenesis.**

### 3.1 Introduction

Mitochondria are organelles found inside almost every cell in the body and their main role is the generation of adenosine triphosphate (ATP), which is necessary for skeletal muscle contractions [36]. Mitochondria are also involved in cell signalling, apoptosis, cellular metabolism, and hormonal signalling [277-280]. Mitochondria play a pivotal role in many diseases associated with ageing, such as degenerative diseases (e.g., vascular disease, mitochondrial dysfunction), as well as insulin resistance and type 2 diabetes mellitus [35]. Associations between mitochondrial characteristics and endurance performance have also been reported [96]. It is therefore important to better understand factors that influence mitochondrial characteristics.

Mitochondrial biogenesis has been defined by our research group as “the making of new components of the mitochondrial reticulum” [36, 121]. Aerobic exercise is a potent stimulator for promoting mitochondrial biogenesis (i.e., exercise-induced mitochondrial biogenesis), and this can lead to increases in mitochondrial respiration and mitochondria content [95]. The bioenergetic and mechanical demands associated with exercise lead to homeostatic perturbations and the activation of sensor proteins that initiate gene transcription, the translation of genes into proteins, and subsequent modifications of the mitochondrial network [96].

The bioenergetics of exercise refers to the pathway of adenosine triphosphate (ATP) resynthesis during skeletal muscle contractions, which is dependent, at least in part, on exercise intensity [59] (**Figure 1.5; Chapter 1**). Fatty acids and glucose are eventually oxidised within the mitochondria via the tricarboxylic cycle (TCA cycle) and are the predominant sources of energy during rest and sustained low- to moderate-intensity exercise [10, 281]. Non-mitochondrial sources of ATP, which include lactate metabolism and the breakdown of

phosphocreatine stores, have a greater contribution during higher intensity exercise [63]. The exercise bioenergetics also influence subsequent homeostatic perturbations (“primary messengers”), which include an increase in free fatty acid entry into the cell, an increase in lactate production, an increase in the redox state of the cell ( $\text{NAD}^+/\text{NADH}$ ), an increase in reactive oxygen species (ROS), an increase in ATP turnover (measured via AMP/ATP), increased calcium flux, and mechanical stress; many of these are influenced by the biochemical pathways of ATP resynthesis [10, 121] (**Figure 3.1**). These perturbations act as signals to the activate sensor proteins (“secondary messengers”), such as calcium/calmodulin-dependent kinases II (CAMKII), 5' AMP-activated protein kinase (AMPK), p38 mitogen-activated protein kinases (p38 MAPK), and sirtuin 1 (SIRT1) [15, 96]. These “secondary” messengers activate nuclear and mitochondrial proteins, which initiate gene transcription via transcriptional coactivators (e.g., PGC-1 $\alpha$ ), transcriptional activators (e.g., p53, NRF-1/2, and mitochondrial transcription factors [e.g., TFAM]) (**Figure 3.2**). The increases in mRNA content following a single session of exercise leads to translation processes that generate proteins that are subsequently incorporated into mitochondria [121].

If exercise-induced homeostatic perturbations are an important determinant of exercise-induced mitochondrial biogenesis, this suggests that higher exercise intensities (provoking greater homeostatic perturbations) will more strongly activate mitochondrial biogenesis. In support of this, an apparent relationship between exercise intensity and the signalling pathways associated with exercise-induced mitochondrial biogenesis has been reported [10, 15, 18, 69, 121, 152, 282-286]. However, this may be attributed to much of the published research is that submaximal exercise intensity is almost exclusively prescribed relative to maximal oxygen uptake ( $\dot{V}\text{O}_{2\text{max}}$ ) or maximal work rate ( $\dot{W}_{\text{max}}$ ) (**Chapter 1; Section 1.2**). A

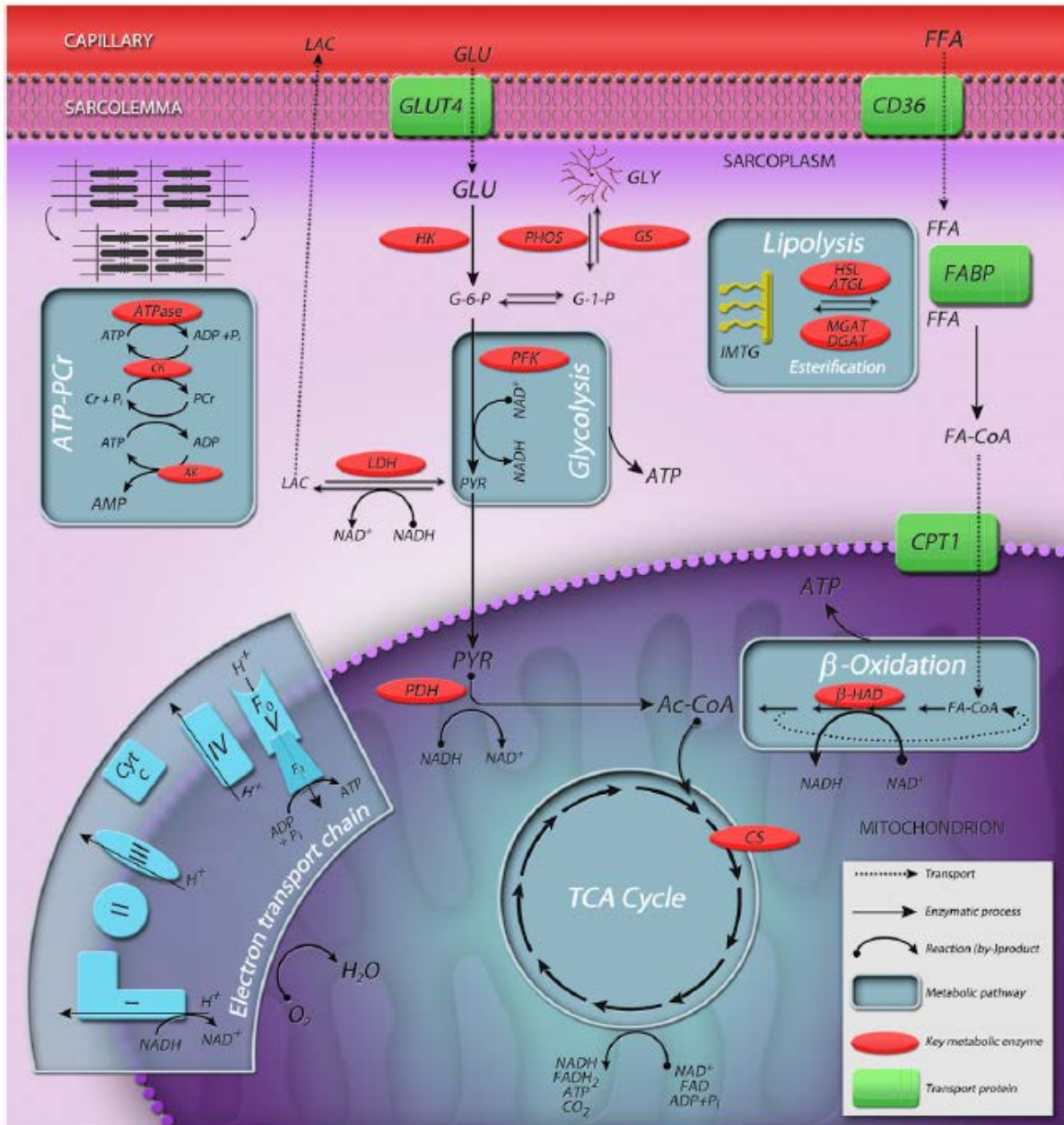


**Figure 3.1.** Energy Schematic for Skeletal Muscle During Exercise. ATP hydrolysis, catalyzed by myosin ATPase, powers skeletal muscle contraction. Metabolic pathways of ATP generation in skeletal muscle include (1) the ATP phosphagen system wherein the degradation of PCr by creatine kinase (CK) produces free Cr and Pi, which is transferred to ADP to re-form ATP; the adenylate kinase (AK) (myokinase) reaction catalyzes the formation of ATP and AMP from two ADP molecules; (2) anaerobic glycolysis, where glucose-6-phosphate derived from muscle glycogen (GLY) (catalyzed by glycogen phosphorylase, PHOS) or circulating blood glucose (GLU) (catalyzed by hexokinase, HK), is catabolized to pyruvate (PYR), which is reduced to lactate (LAC) by lactate dehydrogenase (LDH), and produces ATP by substrate level phosphorylation; (3) processes of carbohydrate (glycolysis) and lipid ( $\beta$ -oxidation) metabolism producing acetyl-CoA (Ac-CoA), which enters the tricarboxylic acid (TCA) cycle in the mitochondria, coupled to oxidative phosphorylation in the electron transport chain (ETC). The two main metabolic pathways, i.e., glycolysis and oxidative phosphorylation, are linked by the enzyme complex pyruvate dehydrogenase (PDH). GLUT4 facilitates glucose uptake to the sarcoplasm, which may undergo glycolysis or during rest/ inactivity, be stored as glycogen via glycogen synthase (GS). Fatty acyl translocase (FAT/CD36) facilitates long-chain fatty acid transport at the sarcolemma, and, in concert with fatty acid binding protein (FABP) and carnitine palmitoyltransferase 1 (CPT1), across the mitochondrial membrane. FFAs entering the cell may be oxidized via  $\beta$ -oxidation or be diverted for storage as IMTG via esterification by monoacylglycerol acyltransferase (MGAT) and diacylglycerol acyltransferase (DGAT). Liberation of FFAs from IMTG stores via lipolysis in skeletal muscle during exercise occurs via the activities of HSL and ATGL. All pathways of ATP generation are active during exercise, but the relative contribution of each is determined by the intensity and duration of contraction, as a function of the relative power (rate of ATP production) and capacity (potential amount of ATP produced). CS, citrate synthase; Cyt c, cytochrome c; PFK, phosphofruktokinase. From Egan et al. [10]



**Figure 3.2.** Schematic illustrating the influence of the biogenetics and homeostatic perturbations associated with exercise intensity influencing the signalling kinases activating exercise induced mitochondrial biogenesis. Plasma free fatty acids (FFA) enter the muscle cell via fatty acid translocase CD36 (FAT/CD36), which is converted into fatty acid CoA (Fa-CoA), as well as intramuscular triglycerides (IMTGs). Fa-CoA enters into the mitochondria via carnitine palmitoyltransferase 1 and 2 (CPT-1 and CPT-2) where it enters into  $\beta$ -oxidation and the tricarboxylic acid cycle (TCA cycle). FFA activates fatty acid binding protein (FABP) which upregulates peroxisome proliferator-activated receptors (PPARs) and retinoid X receptor (RXR). Plasma glucose enters into the muscle cell via glucose transporter type 4 (GLUT4), where it either is converted into lactate or in acetyl-CoA for oxidative phosphorylation (i.e., TCA cycle). Lactate increases cytosolic reactive oxygen species (ROS), that increases the phosphorylation of calcium ( $\text{Ca}^{2+}$ ) calmodulin-dependent protein kinase II (p-CaMKII).  $\text{Ca}^{2+}$  released from the sarcoplasmic reticulum necessary for the cross bridge cycle upregulates calmodulin and *calcineurin*, which activate transcription factor EB (TFEB), and nuclear factor of activated T-cells (NFAT).  $\text{Ca}^{2+}$  phosphorylates CaMKII which targets *myocyte enhancer factor-2 (MEF2)*, the phosphorylation of Histone deacetylases (HDAC), and *cAMP response element-binding protein (CREB)*. Increased free adenosine monophosphate (AMP) produced with increased ATP synthesis results in the increase in 5' AMP-activated protein kinase (AMPK)  $\alpha$  1 and 2 activity (AMPK  $\alpha$  1/2), which phosphorylates AMPK (p-AMPK), targeting the phosphorylation of HDAC, and NAD-dependent deacetylase sirtuin-1 (SIRT1), and mitochondrial-derived peptide (MOTS-c) translocation from the mitochondria to the nucleus. ROS produced within the mitochondria and mechanical stress of muscular contractions up regulates the phosphorylation of mitogen-activated protein kinases (MAPKs) [i.e., p38, c-Jun NH2-terminal kinases (JNKs), and extracellular signal regulated protein kinases (ERKs)]. These phosphorylate peroxisome proliferator-activated receptor gamma *coactivator 1-alpha (PGC-1 $\alpha$ )*. The activation of nuclear proteins results in gene transcription and translation targeting transcription factor A (TFAM), activating the production of mitochondrial DNA (mtDNA).

limitation of this approach can be the inability to adequately normalise exercise intensity so as to elicit homogeneous homeostatic perturbations in individuals of different fitness levels [3, 44, 65-68]. For example, exercise prescribed at 70% of  $\dot{V}\text{O}_{2\text{max}}$  resulted in significantly higher concentrations of plasma markers (i.e., ammonia and hypoxanthine) associated with metabolic stress in untrained compared with trained individuals [3]. Despite the evidence, these methods remain staples for investigating the effects of different exercise interventions on exercise-induced mitochondrial biogenesis. Prescribing exercise intensity relative to submaximal anchors has been proposed to better differentiate between distinct exercise bioenergetics in individuals of different fitness levels, and is also commonly used in applied exercise physiology (**Chapter 1; Section 1.3**). However, despite their popularity, there is a lack of research on how the prescription of exercise relative to these submaximal parameters affects initiation of pathway regulating exercise-induced mitochondrial biogenesis.

The aim of this review is to highlight the influence of submaximal exercise intensity on substrate utilisation, homeostatic perturbations, the activation of signalling kinases and

transcriptional activators/coactivators, and gene transcription associated with exercise-induced mitochondrial biogenesis. The process by which exercise bioenergetics and homeostatic perturbations activate the signalling kinases that eventually modulate markers of exercise-induced mitochondrial biogenesis will also be described. Lastly, recommendations will be made regarding the methods for prescribing exercise intensity that are more valid methods to normalise exercise intensity and which produce distinct changes in cell signalling pathways associated with exercise induced mitochondrial biogenesis.

### **3.2 Exercise Intensity Influencing the “Primary Messengers” Associated with Exercise-Induced Mitochondrial Biogenesis: Bioenergetics and Homeostatic Perturbations**

#### *3.2.1 Fatty Acids*

Triacylglycerol (TAG) is stored in adipose tissue and consists of a glycerol molecule bound by three fatty acid chains linked together [287]. Removing the fatty acids from the glycerol molecule is defined as lipolysis [12, 288, 289]. Lipolysis is modulated by the endocrine system, specifically by the release of adrenaline [290]. The binding of epinephrine to the  $\beta$ -adrenergic receptor in adipose tissue phosphorylates adipose triglyceride lipase (ATGL) [288, 289], which breaks the first fatty acid from the glycerol molecule forming diacylglycerol (DAG) and releases one fatty acid molecule. Hormone sensitive lipase (HSL) removes the second fatty acid and the third fatty acid is disassociated via monoglycerol lipase [288].

Once released from adipose tissue, fatty acids bind to albumin in the plasma; this facilitates the transport of fatty acids across the cell membrane via transport proteins—predominately fatty acid translocase (FAT/CD36) [291-293]. Fatty acids are also stored within skeletal muscle as intramuscular triglycerides (IMTG) and are converted to Fa-CoA, which is highly present in oxidative muscle fibres (type 1), in proximity to the mitochondria (**Figure**

**3.3)** [294, 295]. Fatty acids with IMTGs are disassociated from the glycerol molecule via lipoprotein (LPL) and HSL and along with fatty acids transported into the muscle they are transported into the mitochondria. Long-chain fatty acids are transported into the mitochondria via the

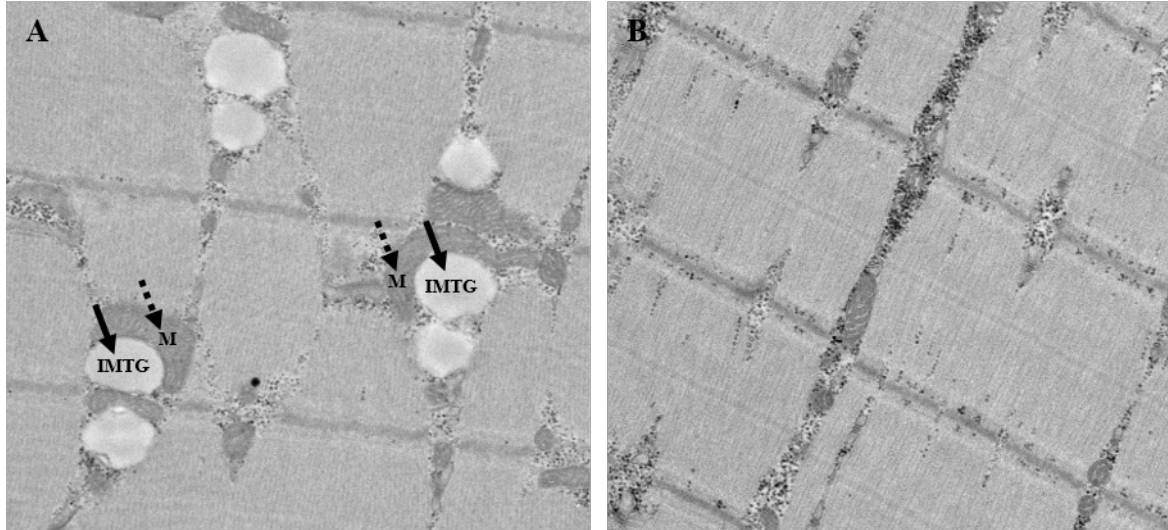


**Figure 3.3 (A & B).** Transmission electron microscopy (TEM) of (A) oxidative (type I) and (B) glycolytic (type II) muscle fibres. Black arrows pointing at intramuscular triglycerides (IMTG). Dashed arrows pointing at mitochondria (M). TEM figures from unpublished data.

carnitine palmitoyltransferase-1 (CPT-1) through the outer mitochondrial membrane [296-298]; short and medium chain fatty acids pass through this membrane without a transport protein [297, 299, 300]. CPT-1 in the intermembrane space catalyses the transfer of a fatty acid acyl group from acyl-CoA and free carnitine forming acyl-carnitine. CPT-II facilitates the transportation of acyl-carnitine across the inner mitochondrial membrane for oxidation. Fatty acid oxidation (beta-oxidation) involves removing hydrogen ion ( $H^+$ ) from fatty acids, which results in the production of acetyl-CoA via the  $\beta$ -Hydoxyl acyl-CoA enzyme [301] and this is further metabolised in the tricarboxylic acid (TCA) cycle. In the TCA, cycle acetyl-CoA combines with oxaloacetate to form citrate resulting in the combustion of acetyl-CoA to  $CO_2$  and  $H_2O$  [302]. The energy released produces 11 ATP molecules per acetyl-CoA molecule oxidised [287, 302].

### 3.2.2 Fatty Acid Metabolism and Exercise Intensity

Lipids are an efficient and rich energy source during submaximal exercise; the body stores >20,000 kcal of potential energy in adipose tissue and IMTGs [287, 303-305]. As previously stated, lipolysis is modulated by the endocrine system and during exercise circulating epinephrine concentrations can increase by >20 times above baseline values (**Figure 3.4A**) [290, 306]; this results in an increase in free fatty acids in the blood of 2- to 3-folds above resting values [307]. During exercise at low intensities (~25% of  $\dot{V}O_{2max}$ ), the oxidation of plasma free fatty acids is the predominant contributor to the overall ATP demand, with a small contribution from IMTG breakdown [11] (**Figure 3.5**). Total fatty acid oxidation increases with increasing exercise intensity to the peak fat oxidation rate - referred to as the maximal fat oxidation rate, which occurs between ~40 and 75% of  $\dot{V}O_{2max}$ . The wide range does not appear to be strongly associated with training status and even amongst a homogeneously trained group there is large variability. [287, 303, 308-311] (**Figure 3.4B**). When exercise intensity exceeds the maximal fat oxidation rate, there is a reduction in fat oxidation, which has been attributed to the large quantities of acetyl-CoA being produced via glycolysis that enter the mitochondria and takes precedent over fatty acid oxidation in the TCA cycle [291, 297]. The acetyl-CoA produced via glycolysis/glycogenolysis for acetyl-carnitine binds with the available carnitine, which would otherwise be used to transport Fa-acyl CoA through CPT-1; thus, decreasing FA-acyl will be available for  $\beta$ -oxidation [291]. The free carnitine buffers excess glycolysis-derived acetyl-CoA by forming acetyl-carnitine; however, by limiting concentrations of free carnitine this results in the inhibition of fatty acid transport across the outer mitochondrial membrane and an eventual reduction in oxidation [12, 287, 309]. Another factor contributing to the reduction in fatty acid oxidation is reduced fatty acid release from adipose tissue, which can be attributed to the decrease in adipotic blood flow [312, 313]. The influence of exercise intensity on fat oxidation is unique compared to other metabolic

pathways and homeostatic perturbations, where there is a rise in fat oxidation until a decrease that is concomitant with the increase in blood lactate above baseline (**Figure 3.4C**) [314].

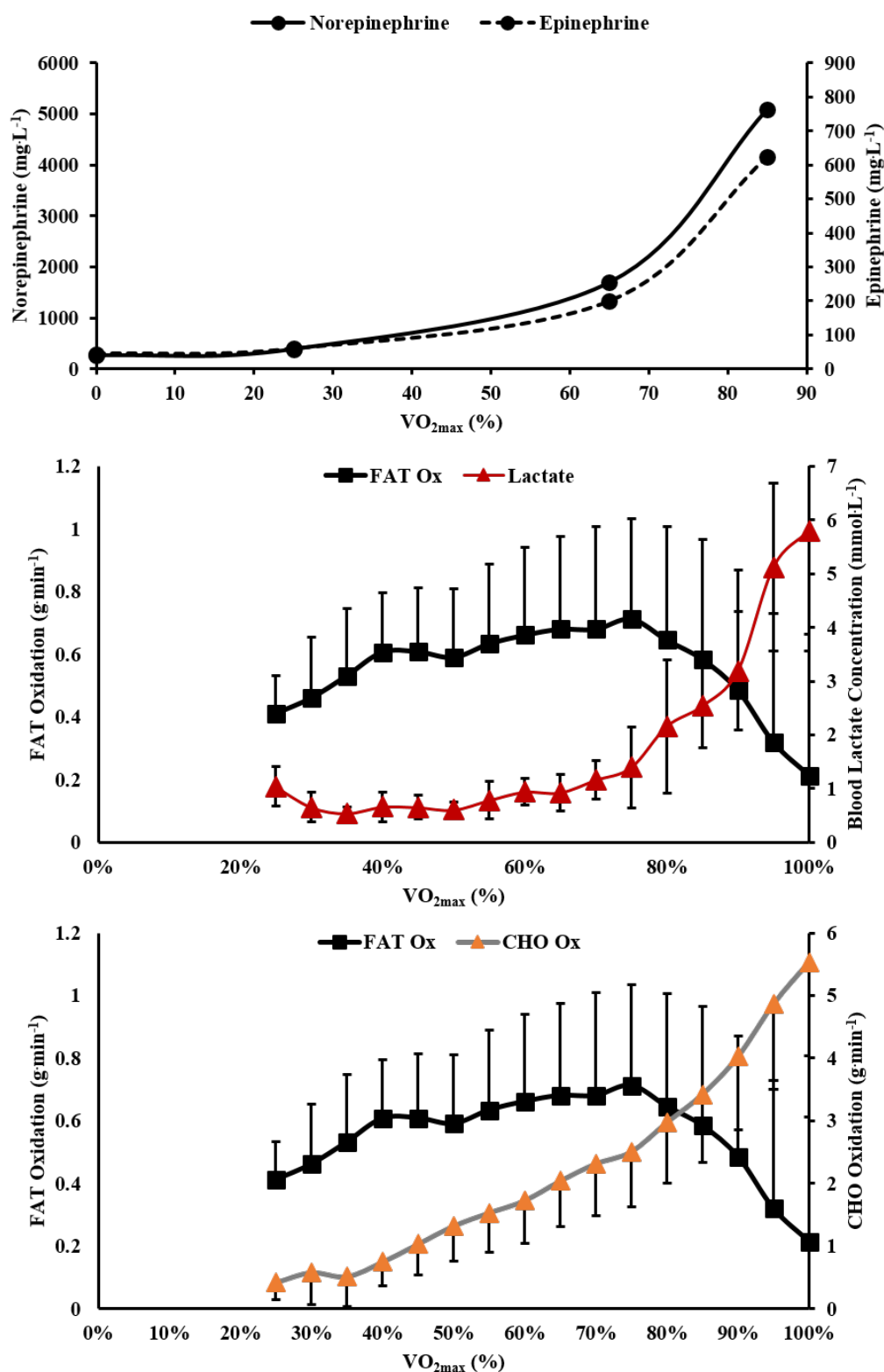


**Figure 3.4 (A - C).** (A) Epinephrine and norepinephrine concentrations at different intensities prescribed relative to percentages of VO<sub>2max</sub> following 30 min of exercise. Data redrawn from Romijn et al. [11] (B) Mean (SD) of fat (FAT) and carbohydrate (CHO) oxidation rates (g·min<sup>-1</sup>) as a function of percentage of maximal oxygen uptake (VO<sub>2max</sub>). (C) Mean (SD) of fat (FAT) oxidation rates (g·min<sup>-1</sup>) and blood lactate concentrations as a function of percentage of maximal oxygen uptake (VO<sub>2max</sub>). Data retrieved from 17 trained participants Jamnick et al. [1] from a graded exercise test that used 4-minute stages from 17 trained cyclists. 0% of VO<sub>2max</sub> = resting values

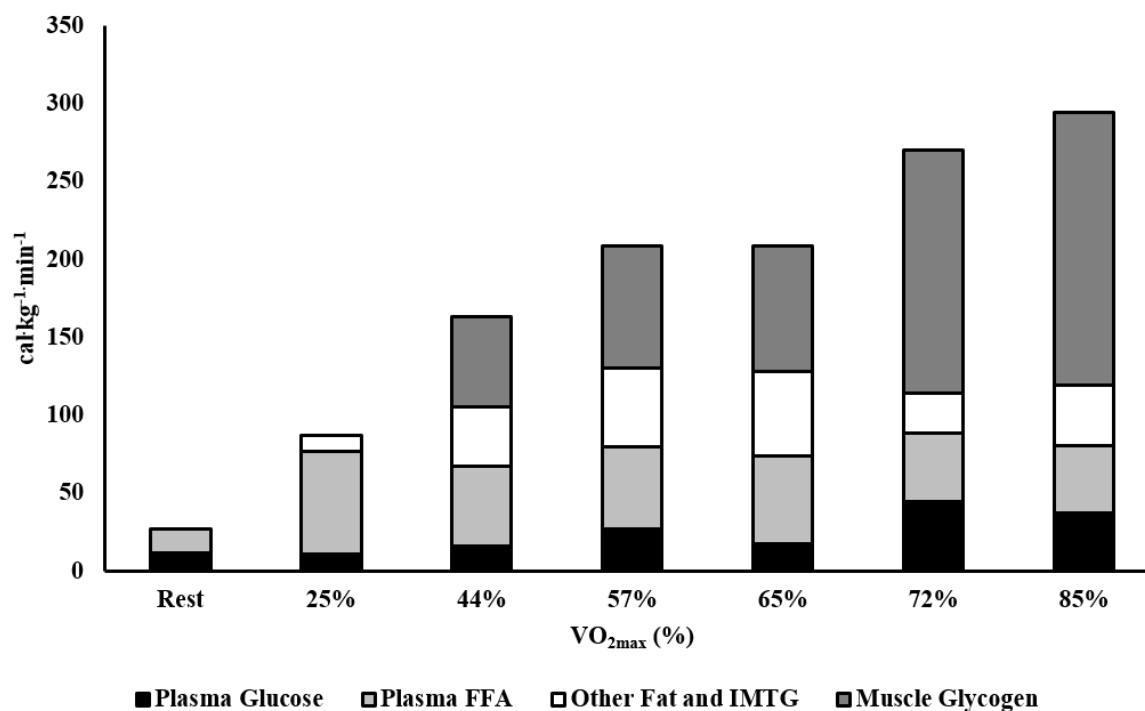


**Figure 3.5.** Contributions of energy expenditure during sustained exercise derived from plasma glucose, plasma free fatty acids (FFA), intramuscular triglycerides (IMTG), other fat sources and muscle glycogen stores. Data redrawn from Romijn et al. [11] (i.e., 25%, 65%, and 85% of  $\dot{V}O_{2max}$ ), and from van Loon et al. [12] (i.e., rest, 44%, 57%, and 72% of  $\dot{V}O_{2max}$ ) where exercise was prescribed as a percentage of maximal oxygen uptake ( $\dot{V}O_{2max}$ ). Romijn et al. [11] recruited 5 endurance trained cyclists ( $\dot{V}O_{2max} = \sim 67 \text{ mL kg}^{-1} \text{ min}^{-1}$ ) van Loon et al. [12] recruited 8 trained male cyclists ( $\dot{V}O_{2max} = \sim 73.5 \text{ mL kg}^{-1} \text{ min}^{-1}$ )

There is a quadratic relationship between fatty acid oxidation and exercise intensity, where there is a low rate of fatty acid oxidation and overall substrate oxidation during low intensities that increases towards to the maximal fat oxidation rate as exercise intensity is increased. This is followed by a continual decrease in fatty acid oxidation due to the decreased carnitine availability caused by accelerated glycolysis (i.e., lactate production) [291, 309]. There appears to be no definitive relationship between  $\dot{V}O_2$  or percentage of  $\dot{V}O_{2max}$  and fat oxidation; however, there appears to be a relationship between rates of fat oxidation and some submaximal anchors. For example, the maximal fat oxidation rate appears to be associated with the ventilatory threshold (VT) ( $r = 0.85$ ) [315] and the lactate threshold (i.e.,  $D_{max}$ ) ( $r = 0.75$ ) [316] and these indices are associated with accelerated glycolysis and increased lactate production [92, 103, 109]. Thus, it appears there is a relationship between lactate production

and fatty acid oxidation during progressive exercise intensity, where there is an exponential increase in blood lactate that occurs in conjunction with a rapid decrease in fat oxidation.

### 3.2.3 Glycolysis/Lactate

Carbohydrates are present in the form of plasma glucose and stored muscle glycogen. The uptake of circulating blood glucose into skeletal muscle occurs by facilitated diffusion via the glucose transporter type 4 (GLUT4) (**Figure 3.1**) [317]. Once glucose has been transported into the cell it is phosphorylated to glucose-6-phosphate (G-6-P) and catalysed by hexokinase-II (HKII) [318]. The breakdown of stored muscle glycogen is regulated by glycogen phosphorylase (GP), which produces glucose-1-phosphate (G-1-P) [319]. Similar to plasma glucose, muscle glycogen is converted to G-6-P from G-1-P via phosphoglucomutase. Phosphofructokinase (PFK) not only catalyses the reaction of G-6-P to the eventual production of pyruvate, it is also the rate limiting enzyme of glycolysis [320]. Pyruvate is formed within the cytosol and during aerobic metabolism it is transported across the outer mitochondria membrane through porins and across the inner membrane through the mitochondrial pyruvate carrier 2 (MPC2) [321]. The oxidation of pyruvate to acetyl-CoA releases CO<sub>2</sub> along with electrons that bind to NAD<sup>+</sup> to form NADH [322]. The energy released from a glucose/glycogen molecule is 30-32 ATP molecules per acetyl-CoA molecule oxidised [318].

Pyruvate can also yield ATP via the lactate dehydrogenase reaction in the cytosol (i.e., pyruvate + NADH + H<sup>+</sup> ↔ lactate + NAD<sup>+</sup>) (**Figure 3.1**) [323]. Through the Law of Mass Action, when cytosolic pyruvate, NADH, or H<sup>+</sup> rises so does the increase in lactate formation [324]. The increase in cytosolic ATP turnover (lactate formation) is a consequence of mitochondrial ATP turnover reaching capacity, which drives increased cytosolic concentrations of pyruvate, NADH, and H<sup>+</sup> [13]. This is attributed to both accelerated

glycolysis and the mitochondria's ability to recycle  $H^+$  reaching capacity, respectively [59, 325]. The primary driver of increased lactate formation is the cytosolic redox state; specifically, cytosolic NADH [13]. NADH produced within the mitochondria via pyruvate dehydrogenase,  $\beta$ -oxidation, and the TCA cycle is consumed during oxidative phosphorylation unless the rate of production exceeds the rate of consumption, which leads to the excess being transported into the cytosol [326, 327]. The ATP yield from lactate is 2 ATP per lactate molecule.

#### *3.2.4 Lactate and Exercise Intensity*

The use of glucose/glycogen for ATP generation yields less potential energy relative to the oxidation of lipids, where ~2,400 kcal of glycogen is stored within the skeletal muscle and liver and ~100 kcal is circulating as blood glucose. As previously stated, acetyl-CoA produced via glycolysis/glycogenolysis inhibits fatty acid oxidation. During low-intensity exercise (~25% of  $\dot{V}O_{2max}$ ) plasma glucose and IMTGs contribute a small portion of the overall energy expenditure, while plasma free fatty acids are the predominant contributor to overall ATP demand (**Figure 3.5**) [11]. As exercise intensity increases, the overall contribution to ATP synthesis from glucose/glycogen breakdown exceeds that from fatty acids (i.e., the cross-over concept) (**Figure 3.4A**) [328]. Maintaining ATP demand with the reduction of fatty acid oxidation results in accelerated glycogenolysis, which is facilitated via catecholamine regulation [117, 329-331]. Epinephrine increases the glycogenolytic rate by interacting with the  $\beta$ -receptor on the cell membrane, which increases adenylate cyclase activity and results in an increase in cAMP and the activation of phosphorylase kinase [332]. Phosphorylase kinase facilitates the transformation from the inactive form of phosphorylase *b* to its active form phosphorylase *a* [117, 333] via calcium release from the sarcoplasmic reticulum [334, 335]; this leads to an increase in glycogen utilisation [330]. Once mitochondrial ATP production is at capacity this drives the formation of lactate in the cytosol, which primarily occurs in the fast-

twitch muscle fibres due to their lower oxidative capacity and propensity for lactate formation [59]. Fast-twitch fibres have a greater expression of lactate dehydrogenase (LDH), which facilitates greater lactate formation [336, 337]; furthermore, these fibres are recruited in a hierarchical fashion (i.e., the size principle), which drives the formation of lactate with increased exercise intensity [102, 338]. Intramuscular lactate formation typically increases exponentially at exercise intensities exceeding  $\sim 45\%$  of  $\dot{V}O_{2\max}$  [12, 57, 80, 87, 88, 97, 98, 323] (**Figure 3.6A**). The increase in intramuscular lactate coincides with the increased rate of carbohydrate oxidation and a decrease in fat oxidation due to the acceleration of acetyl-CoA produced via glycolysis and the recruitment of more glycolytic muscle fibres (**Figure 3.5A**).

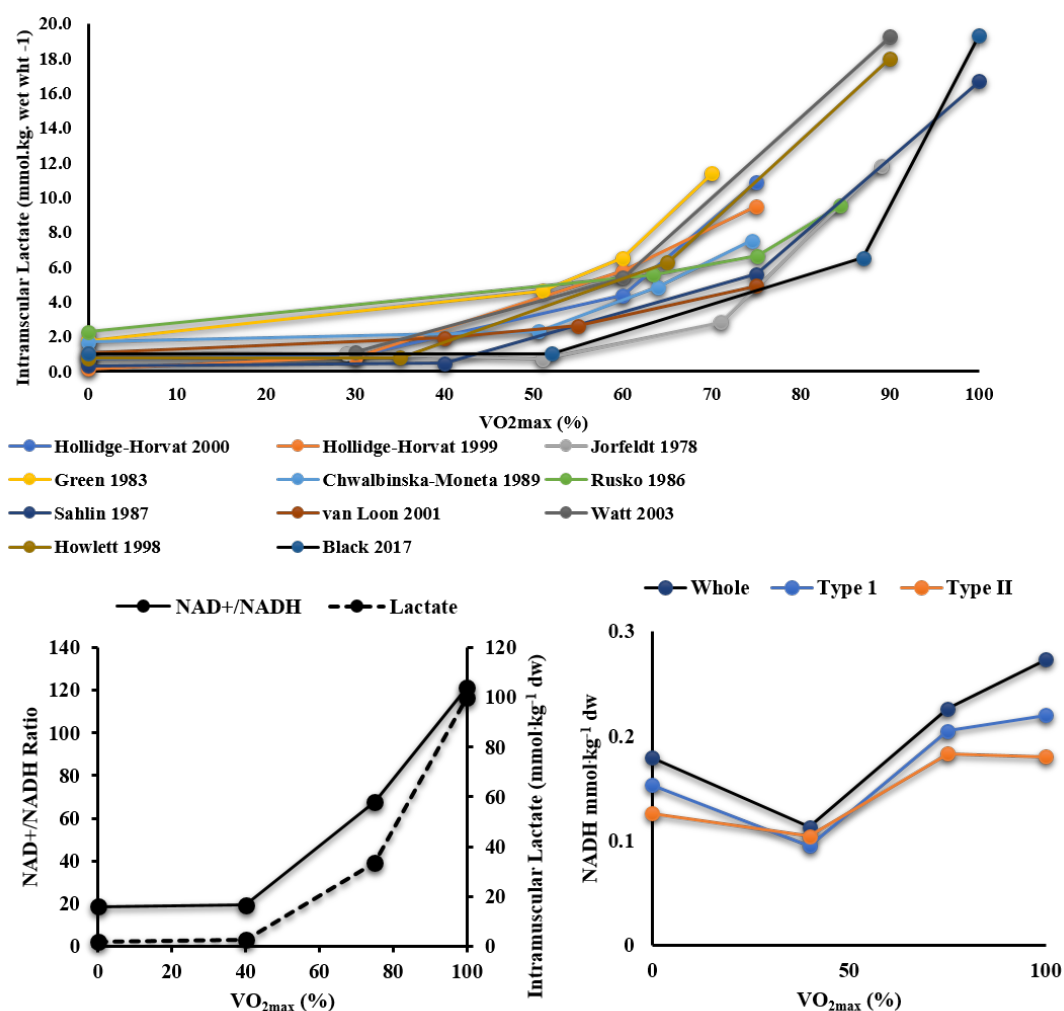


**Figure 3.6 (A-C).** Figures illustrating the relationship between exercise intensity and intramuscular lactate production (A), (B) reduction-oxidation state of muscle measured ratio between reduced and oxidised form of Nicotinamide adenine dinucleotide (NAD<sup>+</sup>/NADH) (solid line) and intramuscular lactate concentrations (dashed line) Sahlin et al. [13] (C), NADH production concentrations in whole muscle, type I and type II (D). Exercise intensity was prescribed relative to percentage of maximal oxygen uptake ( $\dot{V}O_{2\max}$ ). 0% of  $\dot{V}O_{2\max}$  = resting values

### 3.2.5 Reduction-Oxidation Reaction (Redox State)

The redox state of the cell is characterised as the balance between the oxidation (loss of an electron) and reduction (gain of an electron) of molecules, atoms, and ions.  $\text{NAD}^+$  is an important co-enzyme essential for glycolysis, pyruvate formation, the TCA cycle, and oxidative phosphorylation [339]. Enzymes involved in ATP production use  $\text{NAD}^+$  as a hybrid transfer, which catalyses the reduction of  $\text{NAD}^+$  to  $\text{NADH}$  (e.g., pyruvate +  $\text{NAD}^+$   $\leftrightarrow$  Acetyl-CoA +  $\text{NADH}$ ) (**Figure 3.2**) [327]. The  $\text{NAD}^+/\text{NADH}$  ratio regulates cellular redox state, specifically in the mitochondria and nucleus. Mitochondrial  $\text{NAD}^+$  appears to be more abundant and stable compared to cytosolic  $\text{NAD}^+$ , and this maintains oxidative phosphorylation [340]. During increased rates of glycolysis, there is an increased formation of cytosolic  $\text{NADH}$  due to the increased transport of reducing equivalents from the mitochondria to the cytosol [106]. The concomitant increase of cytosolic  $\text{NADH}$  and  $\text{H}^+$  results in increased lactate production and raising  $\text{NAD}^+$ , thus increasing the cytosolic redox state.

### 3.2.6 Redox State & Exercise Intensity

The redox state of muscle increases with exercise intensity; specifically, there is an increase in the  $\text{NAD}^+/\text{NADH}$  ratio above baseline when exercise intensity exceeds  $\sim 40\% \dot{V}\text{O}_{2\text{max}}$  [13] (**Figure 3.6B and 3.6C**). This is attributed to the Law of Mass Action, where  $\text{H}^+$  is raised in the cytosol, which drives the conversion of pyruvate to lactate [59, 106] and the resultant increase in  $\text{NAD}^+$  raises the redox state (**Figure 3.6B**). It is worth noting the redox state in this study was examined in whole muscle and research investigating the redox state of subcellular compartments has only been quantified via *in silico* analysis [326]. Future research should investigate the relationship between cytosolic and mitochondria redox states relative to exercise intensity.

### 3.2.7 ATP Turnover

Changes in cellular energy requirements during muscle contraction are a major contributor to disrupting cellular homeostasis [341]. During contractile activity, energy demand is increased and so is ATP turnover. ATP is synthesised via oxidative phosphorylation (i.e., mitochondrial ATP turnover) and via cytosolic ATP turnover (i.e. lactate oxidation and phosphocreatine breakdown) [59]. ADP is produced via ATP hydrolysis ( $\text{ATP} + \text{H}_2\text{O} \rightarrow \text{ADP} + \text{Pi} + \text{H}^+$ ), which facilitates the production of AMP via the Adenylate kinase reaction ( $2 \text{ADP} \rightarrow \text{ATP} + \text{AMP} + \text{H}^+$ ) (**Figure 3.7A**) [342]. When ATP utilisation exceeds ATP production, deamination of adenosine nucleotides, followed by reamination, causing a rapid increase in AMP resulting in a rise in the AMP:ATP ratio.

### 3.2.8 AMP:ATP Ratio & Exercise Intensity

Similar to intramuscular lactate, the AMP/ATP ratio increases exponentially when exercise intensity exceeds ~45% of  $\dot{V}\text{O}_{2\text{max}}$  [13, 14, 87, 88, 286, 343] (**Figure 3.7B**). This increase is a result of increased cytosolic ATP turnover, and the rate of cytosolic AMP appearance increases when the rate of ATP produced via oxidative phosphorylation exceeds capacity and excess AMP is deaminated into inosine monophosphate (IMP) ( $\text{AMP} + \text{H}^+ \rightarrow \text{IMP} + \text{NH}_4$ ) [344].

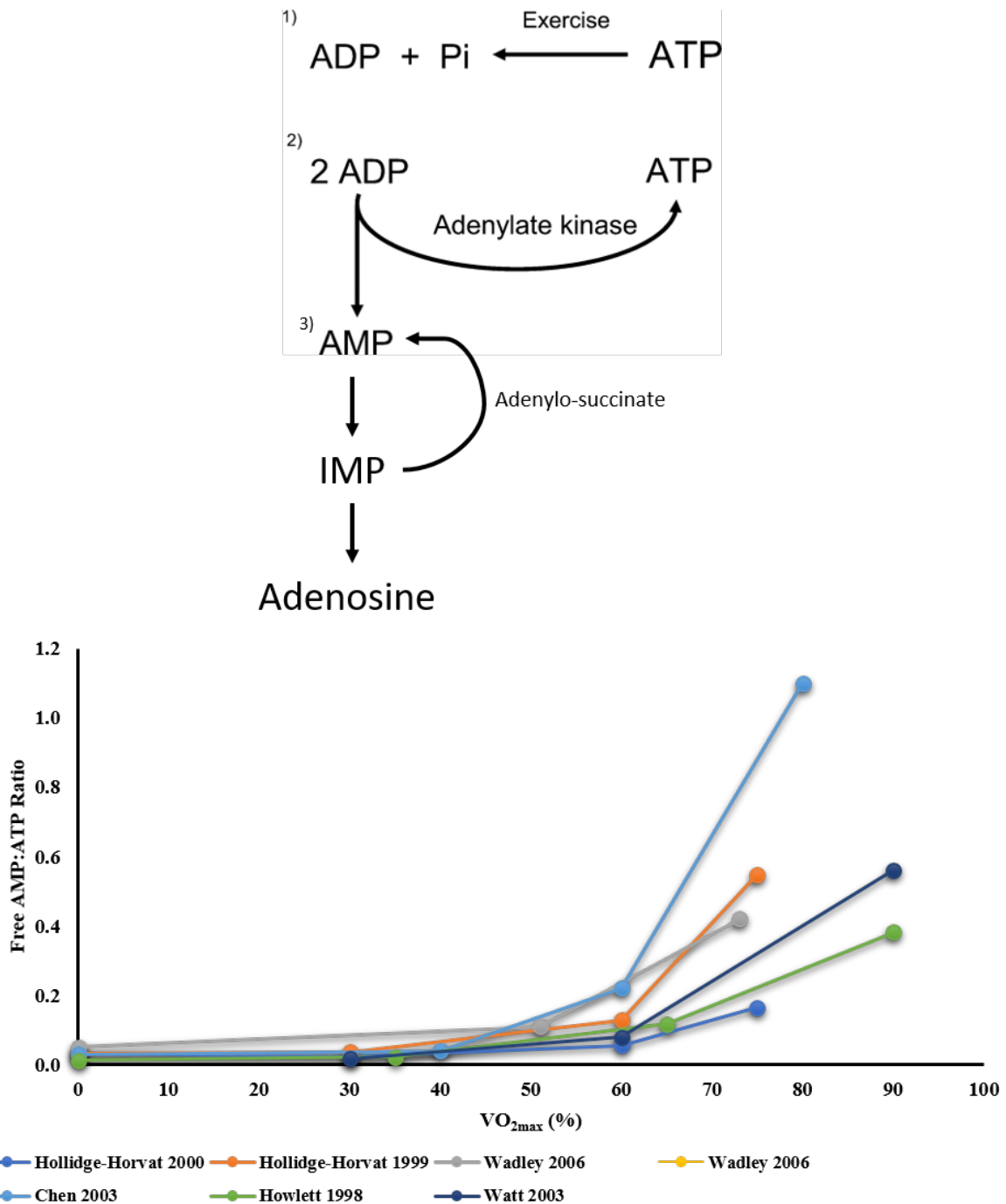


**Figure 3.7 (A & B).** (A) Schematic illustrating the three-step process by which adenosine monophosphate (AMP) is produced via adenosine diphosphate (ADP) production via adenosine triphosphate (ATP) hydrolysis and the Adenylate kinase reaction. AMP is deaminated into inosine monophosphate (IMP), and during high ATP production IMP is converted back into AMP via adenylo succinate and produces an adenosine. (B) Figure illustrating the relationship between exercise intensity prescribed as a percentage of  $\dot{V}\text{O}_{2\text{max}}$  and ATP turnover measured via the ratio between AMP and ATP (AMP:ATP). 0% of  $\dot{V}\text{O}_{2\text{max}}$  = resting values

### 3.2.9 Calcium Flux

The neural activation of a motor unit via the generation of action potential results in the release of  $\text{Ca}^{2+}$  from the sarcoplasmic reticulum.  $\text{Ca}^{2+}$  binds to troponin C and exposes the actin binding site, thus allowing the cross-bridging of striated muscle [345]. It has been postulated that increased  $\text{Ca}^{2+}$  concentration is related to the number of motor units recruited and subsequent greater force [10, 18, 346]. Although difficult to measure *in vivo*, pyruvate dehydrogenase (PDH) activation and glycogen phosphorylase transformation are activated by  $\text{Ca}^{2+}$  and can be used as indirect measure of  $\text{Ca}^{2+}$  flux [14, 347].

### 3.2.10 Calcium Flux & Exercise Intensity

As exercise intensity increases there is greater PDH activation and glycogen phosphorylase transformation [14, 319]. During low-intensity exercise, the muscle fibres with a lower threshold (i.e. slow-twitch fibres) are recruited first, and as exercise intensity increases muscle fibres with larger thresholds (i.e. fast-twitch fibres or type II fibres) are recruited in a hierarchal pattern (**Figure 3.8A**) [102, 338]. This hierarchal recruitment of muscle fibres is the result of the neural activation of more motor units and leads to increased  $\text{Ca}^{2+}$  release from the sarcoplasmic reticulum. An increase in exercise intensity leads to greater  $\text{Ca}^{2+}$  released from the sarcoplasmic reticulum, which increases glycogen phosphorylase activity (**Figure 3.8 B**) [14]. There appears to be a disproportionate transformation/activation of PDH and glycogen phosphorylase as exercise intensity increases. Although free  $\text{Ca}^{2+}$  concentrations were not measured, it is plausible that free  $\text{Ca}^{2+}$  is released disproportionately in response to increases in exercise intensity as muscle fibre recruitment during progressive exercise follows such a pattern [103, 116]. Thus, the decrease in contractile efficiency due to the recruitment of glycolytic muscle fibres likely causes a disproportionate free  $\text{Ca}^{2+}$  release [14].

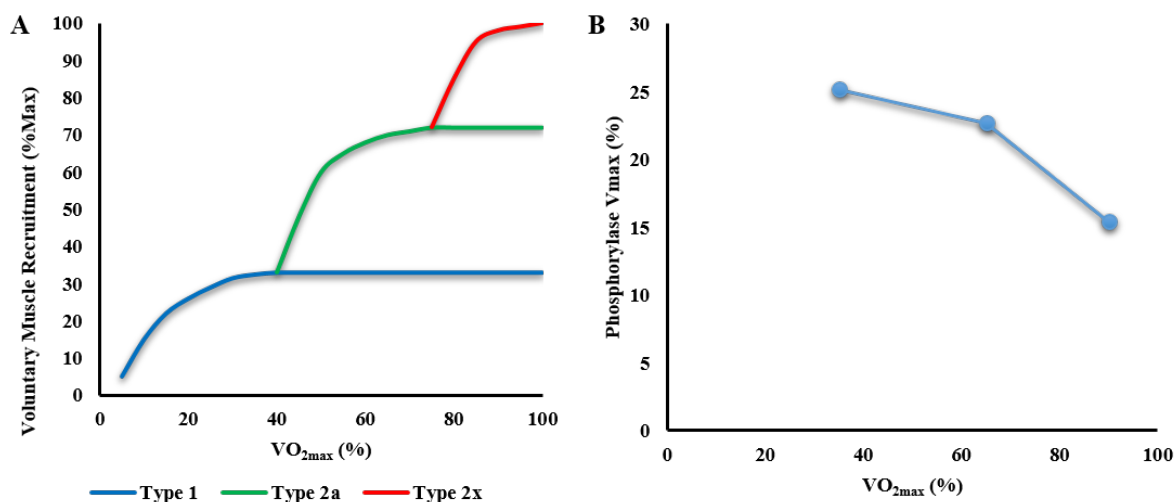


**Figure 3.8 (A & B).** Figures illustrating the relationship between exercise intensity prescribed as a percentage maximal oxygen uptake ( $\dot{V}O_{2max}$ ) and (A) muscle fibre recruitment, (B) indirect measure of  $Ca^{2+}$  flux via glycogen phosphorylase  $V_{max}$ . Redrawn from Howlett et al. [14] and Egan et al [15]. 0% of  $\dot{V}O_{2max}$  = resting values

### 3.2.11 Reactive Oxygen Species (ROS)

Reactive Oxygen Species (ROS) are produced within the mitochondria, when ATP are produced via oxidative phosphorylation, which involves the transportation of  $H^+$  out of the mitochondria via the electron transport chain [348, 349]. As electrons pass through the inner mitochondrial membrane, a series of oxidation-reduction reaction ultimately results in the production of  $H_2O$  or if the oxygen molecule is not reduced, a superoxide radical ( $O_2^-$ ). The  $O_2^-$  is then converted into hydrogen peroxide ( $H_2O_2$ ) via superoxide dismutase (SOD), whilst simultaneously being transported into the cytosol [350]. The other source of ROS produced within the mitochondria, the sarcoplasmic reticulum, the transverse tubules and the plasma membranes are via NADPH oxidase and xanthine oxidase [351]. Moreover, lactate produced via glycolysis also produces ROS [352]. For further review about ROS sources, the reader is referred to Powers and Jackson [353].

### 3.2.12 Reactive Oxygen Species & Exercise Intensity

Low-intensity exercise produces ROS, where a 1- to 3-fold increase in  $O_2^-$  is observed during exercise and during high-intensity exercise the rate of ATP synthesis facilitates increased ROS production [353-356]. Only one study has examined the influence of exercise intensity on markers associated with ROS, where increased exercise intensity resulted in higher lymphocyte ROS production (**Figure 3.9**) [16].

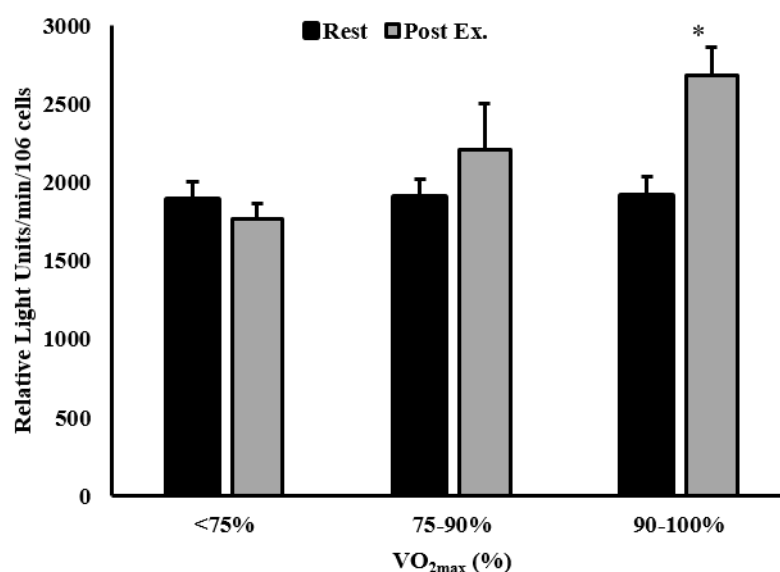


**Figure 3.9.** Figures illustrating the relationship between exercise intensity and reactive oxygen species production. There was a significant increase above baseline following exercise quantified at 90-100% of maximal oxygen uptake. Redrawn from Sureda et. al. [16].

### 3.2.13 Mechanical Stress

Mechanical stress refers to the tension produced via skeletal muscle contractions, which alters both the physical contractile filaments (e.g., myosin and actin) [357, 358] and passive structures of the sarcomere (e.g., titin) [359]. Muscle contractions produce tension at the myosin and actin binding sites and on titin, which connects the thick filament to the z-line. Quantifying muscular tension *in vivo* is difficult; thus, it is often quantified by external force/work produced (e.g., power, total work, etc.). Muscular tension has been measured *in vitro* using rat plantaris and appears to be related to the type of muscular contraction, where eccentric exercise produced the largest amount of tension (**Figure 3.10**) [17].

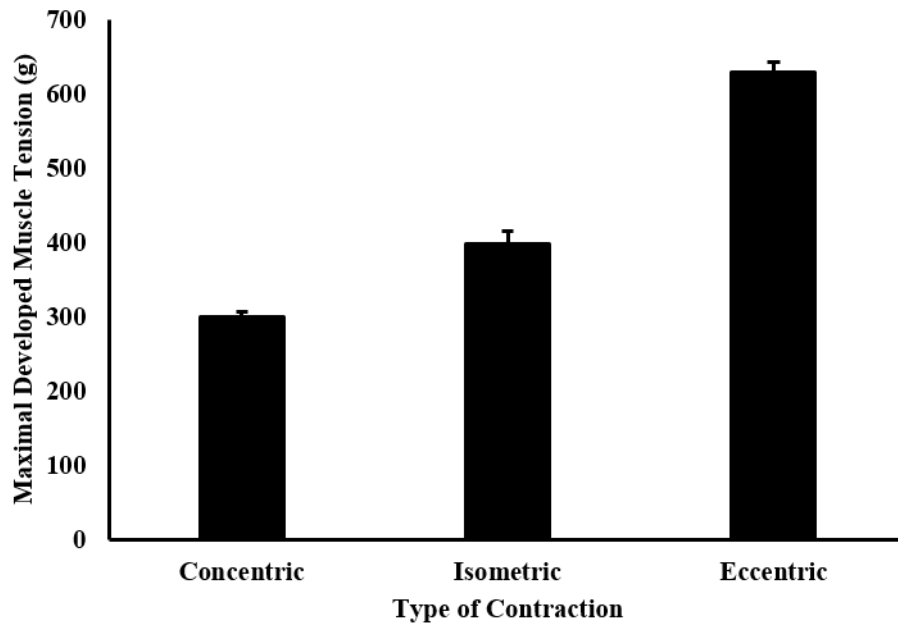


**Figure 3.10.** Figures illustrating the relationship between *in vivo* (rat plantaris) muscle tension (Mean  $\pm$  SD) and concentric, isometric and eccentric muscle contractions. Redrawn from Martineau et al. [17].

#### 3.2.14 Mechanical Stress & Exercise Intensity

As *in vivo* measures of mechanic stress are too challenging to quantify, the level of mechanical stress produced during aerobic exercise is only associated with the amount of external work performed. Thus, increased work rates have been proposed to result in increased mechanical stress [10].

#### 3.2.15 Summary of the Influence of Exercise Intensity on the Primary Messengers

The aim of this section was to discuss and synthesise the current literature of the “primary messengers” that initiate the sequence of exercise-induced mitochondrial biogenesis. While some of these “primary messengers” are well described in the literature and the relationship between exercise intensity is well established, some these messengers remain poorly described and future research should address the relationship with intensity. There is a unique relationship between exercise intensity and the aforementioned primary messengers; specifically, there appears to be disproportionate increase in epinephrine/norepinephrine,

intramuscular and blood lactate, the redox state of the cell, AMP/ATP ratio, ROS, and  $\text{Ca}^{2+}$  flux starting at intensities above  $\sim 45\%$   $\dot{V}\text{O}_{2\text{max}}$  (**Figure 3.11**). Moreover, with this disproportionate increase there is a concomitant decrease in free fatty acid oxidation. The disproportionate increases can be better characterised as a threshold-response relationship, while the relationships between exercise intensity and the fat oxidation rate can be described as a quadratic relationship. The overarching limitation of the discussed research is that exercise intensity is almost exclusively prescribed relative to a maximal anchor and there is little/no research quantifying these primary messengers in relation to exercise-induced mitochondrial biogenesis. Moreover, although it is clear these primary messengers activate the secondary messengers associated with exercise-induced mitochondrial biogenesis, there is little/no research examining the entire exercise-induced mitochondrial biogenesis pathway described in the review. Lastly, it can be expected there will likely be a disproportionate activation of secondary messengers - discussed in the next section.

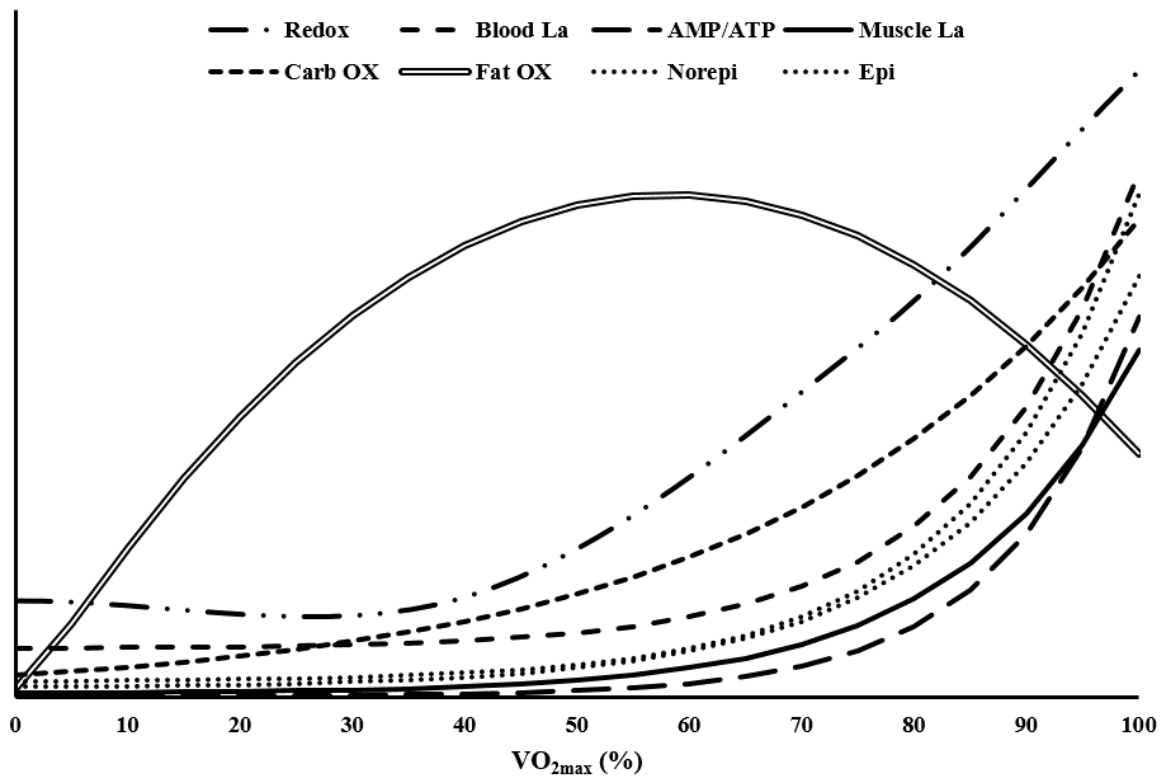


**Figure 3.11.** Figure illustrating the relationship between exercise intensity prescribed as a percentage of  $\dot{V}\text{O}_{2\text{max}}$  and the redox state of the cell, blood and intramuscular lactate, carbohydrate and fat oxidation, the AMP/ATP ratio, and adrenaline (i.e., epinephrine and norepinephrine). Mathematical models (e.g., exponential plus constant or quadratic regression) were derived from *in vivo* studies using data from Figures 3.3 - 3.5. Data was scaled to yield homogenous y-axis values. 0% of  $\dot{V}\text{O}_{2\text{max}}$  = resting values

### 3.3 Exercise Intensity Influencing the “Secondary Messengers” Associated with Exercise-Induced Mitochondrial Biogenesis

The “primary messengers” act as signals that activate the sensor proteins or “secondary messengers,” these messengers such as AMPK, CAMKII, p38 MAPK, and SIRT1 have been well established. The aim of this section to synthesise the known literature of these “secondary messengers” and their relationship with exercise intensity. As with the disproportionate relationship observed with the primary messengers and exercise intensity it is anticipated that a similar relationship will be observed with the secondary messengers.

#### 3.3.1 Exercise Intensity Modulating AMPK

Changes in cellular energy balance activate the signalling protein AMPK, which has been implicated in the regulation of metabolic processes, energy levels, and mitochondrial biogenesis [10]. Activation of AMPK plays an important role in the regulation of metabolism and mitochondrial biogenesis [360]. An increase in the AMP:ATP ratio activates AMPK by the allosteric binding of the AMP molecule to cystathionine  $\beta$ -synthase (CBS) [361]; AMPK can also be activated via phosphorylation at the 172 tyrosine site (Thr<sup>172</sup>) [362], by the tumour suppressor liver kinase B1 (LKB1) [363], and by Ca<sup>2+</sup>/CaM-dependent protein kinase kinase  $\beta$  (CAMKK $\beta$ ) [364, 365]. Moreover, ROS also activates AMPK subunit  $\alpha$ 1/2 [366] and AMPK location and translocation between cellular compartments plays a key role in its activity [367]. These mechanisms illustrate the complex nature of signals subsequent to contractile activity that ultimately activate AMPK.

Similar to the AMP/ATP ratio, AMPK activity (i.e., of subunits  $\alpha$ 1/2) increases when exercise intensity increases [286, 343, 368] (**Figure 3.12 A**). Moreover, increased ROS also modulates AMPK activity and p-AMPK content by modulating the increase in the AMP:ATP ratio [350]. The phosphorylation of AMPK (p-AMPK) is influenced by exercise intensity, where exercise at 40% of  $\dot{V}O_{2\max}$  does not increase p-AMPK [15], and exercise performed at

51 and 55% of  $\dot{V}O_{2\max}$  results in a minimal increase in p-AMPK (1.3, and 1.1 fold-change, respectively) [286, 369]. Exercise performed at higher intensities (70, 73 and 80% of  $\dot{V}O_{2\max}$ ) results in a larger increase in p-AMPK (1.7, 2.2 and 2.8 fold-change, respectively) [15, 286, 369]. This, research suggests that there is greater activation of AMPK at higher exercise intensities, with a possible threshold-response for activation of an intensity 40 to 50%  $\dot{V}O_{2\max}$  (**Figure 3.12 B**).

During muscular contractions greater AMPK activity mediates increases in fatty acid transport to the mitochondria via phosphorylation of acetyl-CoA carboxylase (ACC) [370] and modulates increases in glucose uptake and fatty acid oxidation [371]. Following exercise, AMPK controls mitochondrial biogenesis by modulating gene expression and transcriptional regulation, which leads to a more oxidative phenotype [10]. AMPK activates PGC-1 $\alpha$  via phosphorylation, and the level of activation is modulated by exercise intensity [15, 343]. There are other mechanisms where AMPK indirectly controls PGC-1 $\alpha$ . AMPK enhances

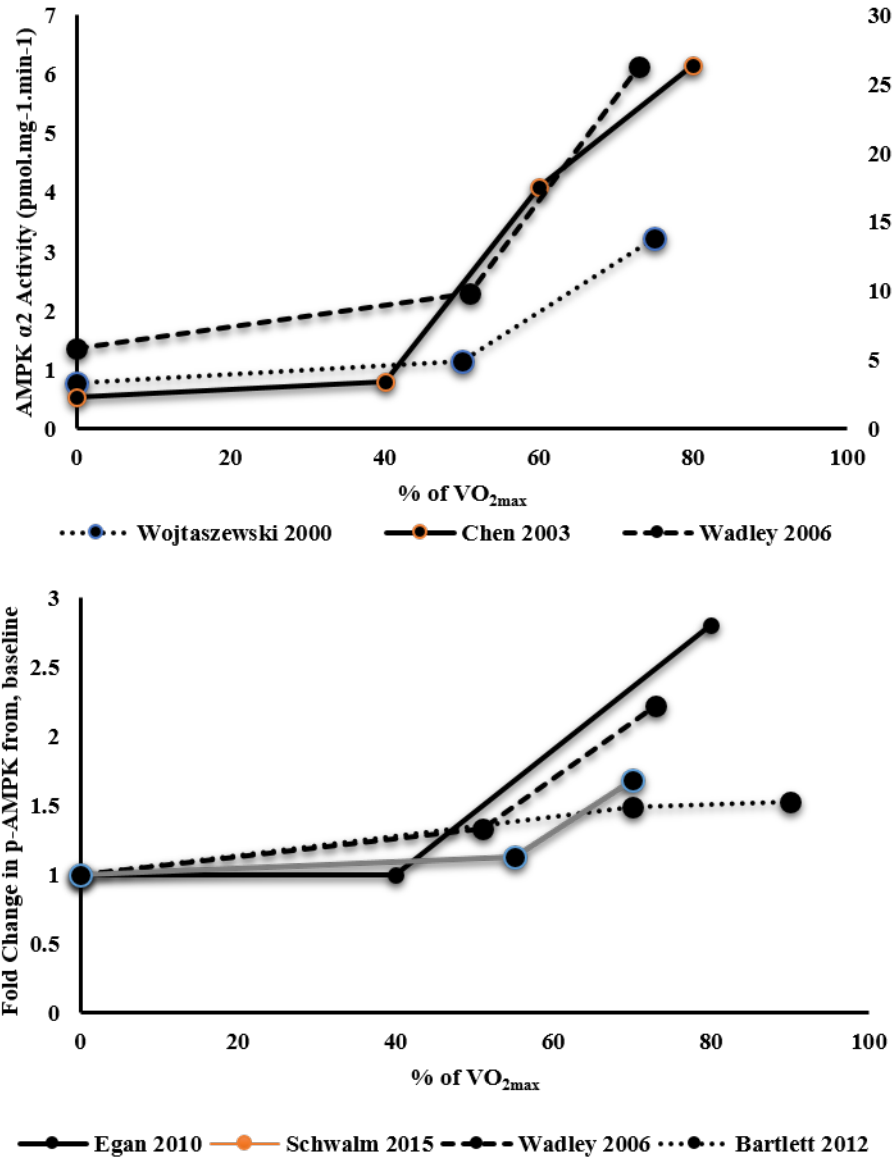


**Figure 3.12 (A & B).** Figures illustrating the relationship between exercise intensity prescribed as a percentage of maximal oxygen uptake ( $\dot{V}O_{2max}$ ) and (A)  $\alpha 2$  AMP-activated protein kinase (AMPK) activity, and (B) the phosphorylation of AMPK. 0% of  $\dot{V}O_{2max}$  = resting values

SIRT1 activity by increasing cellular  $NAD^+$  levels by promoting  $NAD^+$  via  $\beta$ -oxidation, which then modulates PGC-1 activity and other downstream targets via deacetylation [372] (**Figure 3.2**). Furthermore, AMPK can indirectly control PGC-1 $\alpha$  expression via HDAC phosphorylation at Ser<sup>259</sup> and Ser<sup>498</sup>, which results in the export of HDAC from the nucleus

[373]. AMPK also phosphorylates the tumor suppressor p53 at Ser<sup>15</sup> [374], where a single bout of exercise results increased AMPK and phosphorylation of p53 [285, 375].

A mitochondrial-encoded peptide (MOTS-c) is a novel protein involved with protecting against metabolic stress [376]. Metabolic stress induces an AMPK dependent translocation of MOTs-c to the nucleus. MOTS-c regulates genes associated with glucose deprivation; specifically, nuclear factor erythroid 2-related factors (NFE2L2) and NRF-2 [377, 378] (**Figure 3.2**). To date, there is no research investigating the influence of exercise intensity on MOTS-c translocation in human skeletal muscle.

### 3.3.2 Exercise Intensity Modulating CaMKII

As well as playing a pivotal role in the cross-bridge cycle and accelerated glycogenolysis, Ca<sup>2+</sup> is an important activator of different signalling pathways linked to mitochondrial biogenesis. Once released, Ca<sup>2+</sup> binds to calmodulin (CaM), which binds and regulates calmodulin-dependent protein kinases (CaMKs); specifically, CaMKII, the dominant isoform in human skeletal muscle. CaMKII plays a prominent role in transcriptional activity and the regulation of muscle plasticity [10, 121, 379] (**Figure 3.2**). Furthermore, the increase in p-CaMKII is driven by the increase in ROS due to increased lactate production [352, 380, 381]. Exercise intensity appears to be a modulator of the phosphorylation of CaMKII (p-CaMKII) [15, 18, 70]. The phosphorylation of phospholamban (PLN) at Thr<sup>17</sup> (p-PLN<sup>17</sup>) has been identified as a CaMKII substrate in skeletal muscle and is influenced by exercise intensity (**Figure 3.13A**) [18]. p-PLN<sup>17</sup> was increased above baseline at 35%, 60%, and 85% of  $\dot{V}O_{2max}$  and the increase at 85% of  $\dot{V}O_{2max}$  was significantly greater than that at 35% and 60%  $\dot{V}O_{2max}$ . Similarly, when work matched aerobic exercise at 40% and 80% of  $\dot{V}O_{2max}$  was compared there was an increase in the p-CaMKII immediately post exercise at 80% of  $\dot{V}O_{2max}$  compared to

baseline, with no changes immediately following exercise at 40% of  $\dot{V}O_{2\max}$  (**Figure 3.13B**) [15]. This research suggests there is greater activation of CaMKII at higher exercise intensities, with a possible threshold-response for activation of an intensity 40 to 60%  $\dot{V}O_{2\max}$ .

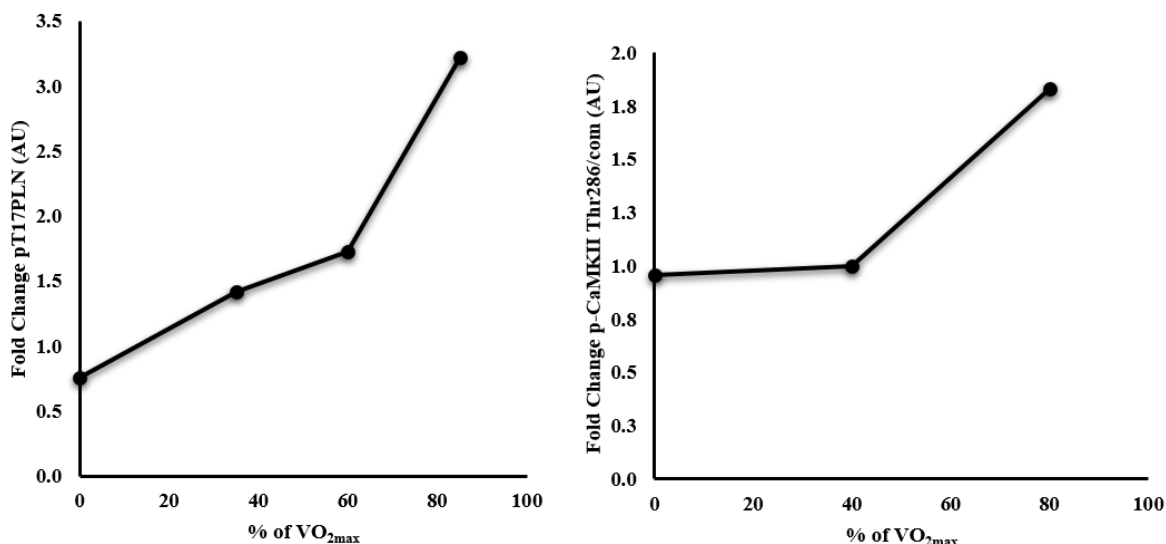


**Figure 3.13 (A & B).** Figures illustrating the relationship between exercise intensity prescribed as a percentage of maximal oxygen uptake ( $\dot{V}O_{2\max}$ ) and (A) phosphorylation of phospholamban, and (B) calcium-calmodulin-dependent kinase II (CaMKII). Data redrawn from Rose et al. [18] and Egan et al. [15]. 0% of  $\dot{V}O_{2\max}$  = resting values

Previous research has demonstrated that raising intracellular  $Ca^{2+}$  in cell culture stimulated signal transduction [382, 383]. Specifically, serum response factor (SRF) myocyte enhancer factor-2 (MEF2), histone deacetylase 4/5 (HDAC), PGC-1 $\alpha$  and nuclear respiratory factor 1 and 2 (NRF-1/2) and cAMP response element binding protein (CREB) [10, 18, 379, 382, 384]; together these transcription factors ultimately induce transcriptional activity.

### 3.3.3 Exercise Intensity Modulating p38

The physical structures of the sarcomere consist of the contractile units (i.e., myosin and actin), responsible for the shortening of the sarcomere and the mechanical stress on the muscle cells. The physical manipulation of the cells leads to transcriptional activity. During muscle contractions, mechanical stress increases mitogen-activated protein kinases (MAPKs)

[10]; specifically, c-Jun NH2-terminal kinases (JNKs) [385], p38 [386], and ERK [387] (**Figure 3.2**).

Mechanical stress and ROS increase the expression of the MAPK family; specifically, increased ROS upregulates p-38 MAPK [388, 389]. The phosphorylation of p38 (p-p38) does not appear to be influenced by submaximal exercise intensity, where there was no observed difference between the p-p38 when comparing exercise performed at 40 and 80% of  $\dot{V}O_{2\max}$  [15]. It is worth noting that a single bout of sprint interval exercise ( $\sim 168\%$  of  $\dot{W}_{\max}$ ) yields a larger increase in p-p38 compared to continuous submaximal exercise ( $\sim 55\%$  of  $\dot{W}_{\max}$ ) [69, 70]. This suggests that submaximal exercise intensities do not provide substantial difference in metabolic stress, unlike sprint interval training, compared to submaximal exercise. Although the activation of p38 appears to be influenced by exercise intensity, there doesn't appear to be a threshold response during submaximal exercise similar with AMPK and CaMKII.

#### *3.3.4 Exercise Intensity Modulating SIRT1 Activity*

The redox state regulates the sirtuin family of enzymes (SIRT1 – 7) [390, 391]; specifically,  $NAD^+$  levels enhance SIRT1 activity. SIRT1 is a  $NAD^+$ -dependent deacetylase that has been described as a “master metabolic sensor” [392, 393]. SIRT1 depends on  $NAD^+$  fluctuations, thus tying its activity to the metabolic state of the cell (**Figure 3.2**). SIRT1 is a downstream regulator of PGC-1 $\alpha$  and p53; SIRT1 activity appears important as an increase in PGC-1 $\alpha$  can be observed, despite a reduction in SIRT1 protein [394, 395]. Although no research has directly investigated the influence of exercise intensity on SIRT1 activity, six weeks of high-intensity interval training resulted in an increase in SIRT1 activity with a decrease in SIRT1 protein. SIRT1 activity may be a better indicator of downstream regulation of coactivators [395, 396]. Furthermore, SIRT1 gene [397, 398] and protein expression [399]

can be elevated after a single bout of exercise. Although no study has directly investigated SIRT1 activity, *in vivo* experiments have demonstrated that SIRT1 activity is increased with cellular stress and modulates PGC-1 $\alpha$  [400, 401]. Therefore, exercise intensity would likely have an effect on SIRT1 activity as cellular stress increases with intensity. The main downstream targets of SIRT1 are PGC-1 $\alpha$  and p53. Activation of PGC-1 $\alpha$  occurs via deacetylation by SIRT1 [327, 402] and requires the activation by AMPK [372]. The deacetylation allows alterations in the cellular redox state for adaptive changes in gene expression and cellular metabolism [372, 400].

### **3.4 Influence of Exercise Intensity on Transcription Factors**

#### *3.4.1 Fatty Acid Binding Protein*

Fatty acids released from adipose tissue act as natural ligands that bind to fatty acid binding protein (FABP), which transports FFAs into the nucleus where they modulate peroxisome proliferator activated receptors (PPARs) PPAR $\alpha$ , PPAR $\delta$  and PPAR $\gamma$  protein [403-406]. This modulation is further influenced by the phosphorylation of AMPK, p38, and extracellular signal regulated protein kinases (ERK) [407]. As previously mentioned exercise intensity influences the modulation of AMPK and p38; however, there is no research investigating the influence of exercise intensity on FABP following an exercise session. Moreover, future research should investigate the localised protein expression of FABP following exercise.

#### *3.4.2 PGC-1 $\alpha$ Protein, The “Master Regulator” of Mitochondrial Biogenesis*

PGC-1 $\alpha$  is an important regulator of exercise-induced mitochondrial biogenesis [96]; specifically, it modulates metabolic control, transcriptional activity, as well as mitochondrial respiratory function and turnover [408, 409]. Increased PGC-1 $\alpha$  protein induces gene expression of PGC-1 $\alpha$ , NRF-1/2, p53, and TFAM [96]; thus, coordinating the gene expression

of mitochondrial-encoded proteins (**Figure 3.2**). An increase in nuclear PGC-1 $\alpha$  protein content has been observed following a single exercise session [410], due to either potential translocation into the nucleus from the cytosol [411, 412] or increased PGC-1 $\alpha$  stability [413]. The increase nuclear PGC-1 $\alpha$  protein is influenced by exercise intensity, as sprint interval training ( $\sim 176 \dot{W}_{\max}$ ) results in larger increases ( $\sim 1.7$  to  $2.3$  fold-change) compared to submaximal ( $\sim 55\%$  of  $\dot{W}_{\max}$ ) exercise intensity ( $\sim 1$  to  $1.5$  fold-change) [69, 410]. Another study observed a significant increase in nuclear PGC-1 $\alpha$  protein following a high intensity interval training session (i.e.,  $10 \times 2$  min @  $79\%$  of  $\dot{W}_{\max}$ ) [414]. Although not explicitly examined, exercise intensity may play a role the increase in nuclear PGC-1 $\alpha$  protein.

#### 3.4.3 p53 Protein - “Guardian of the Genome” and Metabolic Regulator

Increased p-p38 MAPK and p-AMPK are upstream targets [415] of the tumour suppressor protein - p53, which is regarded as the “guardian of the genome” as it regulates processes such as cell cycle arrest, senescence, apoptosis, autophagy, DNA-damage and repair, and tumour suppression [415-417]. p53 also modulates glycolytic and oxidative pathways [418], mitochondrial remodelling, and the transcription of PGC-1 $\alpha$  [419] and TFAM [420]; thus, p53 is an important regulator of mitochondrial biogenesis (**Figure 3.2**). Following a single session of exercise, there is an increase in p53 nuclear protein content [69, 421]; however, the change in nuclear protein does not appear to be influenced by exercise intensity as there was no difference between fold changes when comparing sprint ( $\sim 176 \dot{W}_{\max}$ ) vs submaximal intensity ( $\sim 55\%$  of  $\dot{W}_{\max}$ ) [69]. However, p-p53 in the nucleus does appear to be influenced by exercise intensity, where there was an observed increase following sprint interval training but no increase after 24 minutes of exercise at  $55\%$  of  $\dot{W}_{\max}$  [69]. Another study observed a significant increase in nuclear p53 ( $\sim 1.3$  fold-change) and p-p53 ( $\sim 1.4$  fold-change) following a high-intensity interval training session (i.e.,  $10 \times 2$  min @  $79\%$  of  $\dot{W}_{\max}$ ) [414]. Similar to

PGC-1 $\alpha$ , although not explicitly measured, it appears that exercise intensity may influence the p-p53 following a single exercise session; furthermore, future research should investigate the influence of exercise intensity on the content of p53 in different subcellular fractions.

#### *3.4.5 Histone Deacetylase (HDAC)*

Histone deacetylase (HDAC) is a downstream target of p-AMPK and p-CaMKII and increased levels of HDAC protein are associated with transcriptional activity [422-424]. Furthermore, HDAC subunits 4,5, and 7 are the predominant isoforms in the nucleus of the skeletal muscle [10]. During rest HDAC4/5/7 suppresses myocyte enhancer factor-2 (MEF2), which is responsible for transcriptional activity [425, 426]. However, when activated HDAC leaves the nucleus, HDAC no longer suppresses MEF2 [373], thus allowing MEF2 to act on the binding site of the target gene [424, 426]. p-HDAC4/5/7 is influenced by exercise intensity, as there is a 2.0-fold change immediately following exercise at 80% of  $\dot{V}O_{2max}$  and no observed change following exercise at 40% of  $\dot{V}O_{2max}$  [15]. Thus, it appears that relieved suppression of MEF2 via the HDAC pathway is subject to the magnitude of activation via p-AMPK and p-CaMKII.

#### *3.4.6 cAMP Response Element-Binding Protein (CREB)*

cAMP Response Element-Binding Protein (CREB) is a nuclear transcription factor [427] that modulates the transcription of genes and is a downstream target of p-AMPK and p-CaMKII [428]. Interestingly, there was an exercise intensity-dependent decrease in p-CREB immediately following exercise; specifically, there was a significant decrease following exercise at 80% of  $\dot{V}O_{2max}$ , followed by with significant increases +4.2 h (~1.7 fold-change) and +3.6 h (~1.8 fold change) from the onset of exercise following exercise at 80 and 40% of  $\dot{V}O_{2max}$ , respectively [15]. Furthermore, p-CREB remained elevated (~1.7 fold-change) +19.6 h from the onset of exercise following exercise at 80% of  $\dot{V}O_{2max}$  [15].

### 3.4.7 Conclusion

It appears the aforementioned transcription factors may be influenced by exercise intensity; however, there is little research directly investigating this hypothesis. Moreover, the majority of research has measured mRNA expression or protein content within the whole muscle. The translocation or activation of transcription factors to the nucleus is required to modulate transcriptional activity; therefore, future research should examine the changes in protein content in subcellular fractions. Lastly, future research should employ multiple intensities within the same population to characterise the relationship between exercise intensity and the protein content of transcription factors within subcellular fractions.

## 3.5 Influence of Exercise Intensity on Genes Associated with Mitochondrial Biogenesis

### 3.5.1 PPAR mRNA

The PPARs form heterodimers and bind to cognate DNA response elements along with members of the retinoid X receptor (RXR) family [429], which modulates the expression of PGC-1 $\alpha$ , FAT/CD36, cytochrome *c*, and enzymes involved in fatty acid and  $\beta$ -oxidation [430, 431] (**Figure 3.2**). The subunits of PPARs each have distinct functions. PPAR $\alpha$  is a transcription factor and a major regulator of lipid metabolism in the liver, PPAR $\gamma$  is mainly present in adipose tissue and regulates fatty acid storage and glucose metabolism, and PPAR $\delta$  is associated with an increased oxidative capacity [431]. There is one study that has examined the influence of exercise intensity on PPAR $\delta$  mRNA expression, a significant increase in PPAR $\delta$  mRNA expression following 36 minutes at 80% of  $\dot{V}O_{2\max}$ ; and no increase was observed following exercise at 40%  $\dot{V}O_{2\max}$  [404, 405, 432]. . Another study demonstrated that high-intensity exercise (90% of  $\dot{V}O_{2\text{peak}}$ ) increased PPAR $\gamma$  mRNA [64]; however, there were no increases in PPAR $\alpha$  or PPAR $\delta$  mRNA. Therefore, exercise intensity may influence

PPAR signalling; however, further research needs to elucidate the relationship between mRNA and transcriptional activity.

### 3.5.2 *PGC-1 $\alpha$ mRNA*

A single session of exercise activates the aforementioned signalling kinases ultimately modulating PGC-1 $\alpha$ , where PGC-1 $\alpha$  mRNA can increase ~2 to 15-fold, 3.2 to 6 hours from the onset of exercise [15, 64, 69, 70, 121, 282-285, 410, 434-454] (**Figure 3.14 A**). The fold change in PGC-1 $\alpha$  mRNA appears to be influenced by exercise intensity, where a significant correlation exists with intensity expressed as a percentage of maximal work rate ( $\dot{W}_{\max}$ ). Furthermore, controlling for the length of the training session results in a stronger correlation between PGC-1 $\alpha$  mRNA and maximal work rate (**Figure 3.14B**). By calculating the rolling average of five data points of changes in PGC-1 $\alpha$  mRNA relative to  $W_{\max}$ , there appears to be a disproportionate increase in PGC-1 $\alpha$  mRNA at ~65% of  $W_{\max}$  (**Figure 3.14A and 3.14B**). This may be attributed to the work rates associated with the MLSS and CP occurring at a similar percentage [1, 132].

### 3.5.3 *p53 mRNA*

The tumour suppressor protein p53, is regarded as the “guardian of the genome” as it regulates processes, such as cell cycle arrest, senescence, apoptosis, autophagy, DNA-damage and repair, and tumour suppression [415-417]. p53 also modulates glycolytic and oxidative pathways [418], mitochondrial remodelling, and the transcription of PGC-1 $\alpha$  [419] and TFAM [420]; thus, p53 is an important regulator of mitochondrial biogenesis (**Figure 3.2**). Two studies compared the influence of exercise intensity on p53 mRNA and there was no observed effect [69, 434]. It is worth noting the biopsies were taken within 5 hours from the cessation of exercise, where the transient increases in p53 mRNA have been reported 24 to 48 hours from

exercise [121]. Therefore, the influence of exercise intensity on p53 mRNA +24 hours remains to be investigated.

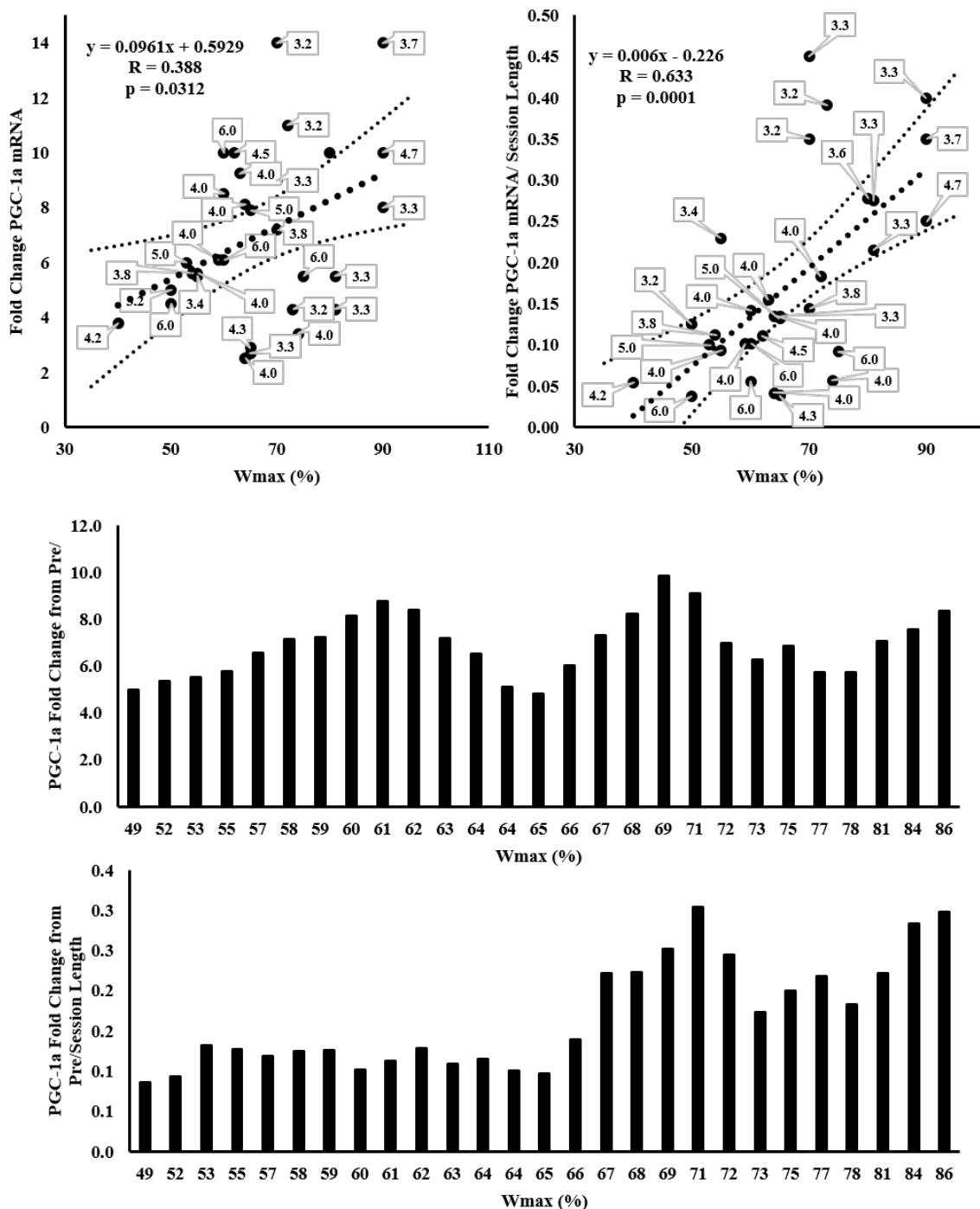


**Figure 3.14 (A-D).** Figures illustrating the relationship between exercise intensity and PGC-1 $\alpha$  mRNA. Panel A depicts the relationship between maximal power ( $W_{max}$ ) and mean fold change in PGC-1 $\alpha$  mRNA (3.2-6 hours from the onset of exercise). Panel B depicts the relationship between  $W_{max}$  and fold change in PGC-1 $\alpha$  mRNA relative to the exercise session length. Dashed curved lines represent 95% confidence intervals. Panel C is a rolling average (5 data points) of % of  $W_{max}$  and the fold change in PGC-1 $\alpha$  mRNA. Panel D is a rolling average (5 data points) of % of  $W_{max}$  and the fold change in PGC-1 $\alpha$  mRNA relative to exercise session length. The  $W_{max}$  were organised low to high, this and the (C) fold changes in PGC-1 $\alpha$  mRNA and (D) fold changes in PGC-1 $\alpha$  mRNA relative to exercise session length were averaged via rolling average (5 data points). (D) There was a disproportionate change in PGC-1 $\alpha$  mRNA relative to exercise session length above 65%  $W_{max}$ .

#### *3.5.4 Nuclear Respiratory Factors (NRF-1/2)*

NRF-1/2 are DNA-binding nuclear transcription factors that modulate mitochondrial biogenesis [455]. NRF-1 is a positive transcriptional regulator activating the expression of metabolic genes associated with the electron transport system and TFAM [456]. NRF-2 is a transcriptional coactivator involved in the expression of cytochrome oxidase and mitochondrial protein import complexes [456]. PGC-1 $\alpha$  coactivates NRF-1/2 increasing transcriptional activity and inducing mitochondrial biogenesis [457]. There is a large body of evidence that supports no change in NRF-1/2 mRNA within 4 hours from a single bout of exercise, the only observed changes were at 4 and 5 hours from exercise [458-460]. This suggests the transient increases in NRF-1/2 could be >4 hours and future research should consider extended biopsy timing to investigate the changes in NRF-1/2 mRNA.

### 3.5.5 TFAM, Mitochondrial Transcription Factor

*TFAM is a nuclear encoded transcription factor regulating mitochondrial DNA and the transcription of 13 mitochondria DNA-encoded subunits of the electron transport system [96]. TFAM is regulated by PGC-1 $\alpha$  [457]. Although increases in whole-muscle TFAM have been observed following exercise training, TFAM protein content does not appear to be influenced by exercise intensity [121, 461]. To date, no research has examined the influence of exercise intensity following a single exercise session of exercise on the subcellular protein content of TFAM. Future research should characterise the influence of exercise intensity on the modulation of TFAM protein. Exercise promotes TFAM binding to mitochondrial DNA [462], and induces the formation of TFAM-PGC-1 $\alpha$  [412] and TFAM-p53 [375] driving mitochondrial transcription activity (**Figure 3.2**). Exercise intensity does appear to influence TFAM mRNA, with sprint interval training yielding a greater increase compared to submaximal exercise [439, 445]; however, the influence of different submaximal intensities remains to be investigated.*

### 3.5.6 Conclusion

Compared to the primary and secondary messengers, the influence of exercise intensity on the transcriptional coactivators is less clear. Most research has examined protein content in whole muscle; thus, making the influence of primary and secondary messengers on the localisation of the protein is unclear. Moreover, I would like to note a concern raised previously, there is large emphasis on mRNA expression. This is potentially problematic due to the ambiguous link between mRNA expression and transcriptional regulation or enzymatic activity; therefore, caution is advised when associating mechanisms with outcomes. Despite this concern, it is still worthwhile to measure the aforementioned targets as these appear to be strongly associated with exercise intensity.

Although the influence of exercise intensity on PGC-1 $\alpha$  mRNA following a single exercise session has been examined, all of the research has employed methods to prescribe intensity that do not normalise exercise intensity. There is a significant correlation between exercise intensity prescribed as a percentage of  $\dot{W}_{\max}$  and fold-change in PGC-1 $\alpha$  mRNA;

however, a linear relationship does not exist between exercise intensity and the “primary” and “secondary” messengers. Therefore, if the messengers are drivers of gene transcription the relationship between intensity and PGC-1 $\alpha$  mRNA a purely linear relationship should not be expected. Similar to protein content, the relationship between p53, NRF-1/2 and TFAM mRNA is less clear, thus future research should address the influence of exercise intensity on less commonly measured transcriptional coactivators associated with exercise-induced mitochondrial biogenesis.

### **3.6 Prescribing Exercise to Modulate the “Primary Messengers”**

The results from the previous sections indicate that exercise-induced mitochondrial biogenesis can be characterised as a downstream process in which the bioenergetics of exercise modulate primary messengers, which modulate the secondary messengers and eventually activate transcriptional coactivators. There appears to be a relationship between the primary messengers and exercise intensity; however, this becomes less evident with the secondary messengers, and transcriptional coactivators. Specifically, it is unclear what type of relationship exists between the secondary messengers, and transcriptional coactivators and exercise intensity (e.g., linear or non-linear, etc.). The uncertainty exists due to limited research, the lack of experiments employing a repeated-measures design, and studies typically prescribing exercise relative to  $\dot{V}O_{2\max}$  or  $W_{\max}$ .

Of the studies employing a repeated-measures design during submaximal exercise, all have employed only two intensities [15, 282, 284, 439]. In one study that investigated the influence of exercise intensity on secondary messengers and PGC-1 $\alpha$  mRNA, exercise was prescribed at 40 and 80% of  $\dot{V}O_{2\max}$  and work matched [15]. The sustainable difference in intensity yielded a discernible activation of the secondary messengers (e.g., p-AMPK<sup>Thr172</sup>, p-

ACC<sup>Ser79</sup>, p-CaMKII<sup>Thr286</sup>, etc.), and PGC-1 $\alpha$  mRNA subsequent 80% of  $\dot{V}O_{2max}$ , whereas a trivial or small upregulation was observed subsequent 40% of  $\dot{V}O_{2max}$ . Due to the considerable difference in intensity it appears that intensity does matter to promote exercise-induced mitochondrial biogenesis. However, by selecting two intensities the relationship cannot be characterised. Therefore, future research should employ 3 or more submaximal intensities separated by an identical power output.

In the aforementioned research, either  $\dot{V}O_{2max}$  or  $W_{max}$  was used to normalise exercise intensity. Prescribing intensity relative to either  $\dot{V}O_{2max}$  or  $W_{max}$  is not a valid means to normalise exercise intensity [44, 65-68] as these methods result in heterogeneous responses (e.g., changes in primary messengers, **Chapter 1; Section 1.2**). Submaximal anchors are also commonly employed methods to prescribe exercise intensity in applied exercise physiology, among sport scientists, and athletes [463] (**Chapter 1; Section 1.3**). The premise of submaximal anchors is they represent transitions between different discernible metabolic states of the muscle [81], and thus yield explicit and homogenous physiological responses [3]. Furthermore, for methods such as the maximal metabolic steady state, exercise performed slightly above these anchors results in the absence of steady state exercise [49, 185]. Thus, exercise performed below and above the metabolic steady state results in a steady state and non-steady state response, respectively, in the primary messengers. Therefore, the disproportionate changes in primary messengers could yield a similar response in the secondary messengers and transcriptional coactivators associated with exercise-induced mitochondrial biogenesis. Future research should characterise the relationship between intensity and markers associated with exercise-induced mitochondrial biogenesis.

### **3.7 Conclusion**

Exercise plays a pivotal role in modulating the pathways and markers associated with exercise-induced mitochondrial biogenesis. Although the relationship between intensity and some of primary/secondary messengers, and transcriptional coactivators, has been researched (e.g., intramuscular lactate, PGC-1 $\alpha$  mRNA), others have limited or no research (e.g., Ca<sup>2+</sup> flux, influence of intensity on MOTS-c translocation, and transcription factor nuclear protein content). Although exercise intensity influences these pathways and markers, the relationship has not been well characterised. Lastly, future research should employ methods that can differentiate between the different metabolic states of the working muscle.

**Chapter 4: The influence of exercise intensity prescribed relative to the maximal lactate steady state on signaling pathways associated with mitochondrial biogenesis in human skeletal muscle.**

## 4.1 Introduction

Mitochondrial biogenesis has been defined by our research group as the making of new components of the mitochondrial reticulum [36, 121]. Aerobic exercise is a potent stimulator of mitochondrial biogenesis (i.e., exercise-induced mitochondrial biogenesis), and this can lead to increases in mitochondrial respiration and mitochondria content [95]. Exercise-induced mitochondrial biogenesis is regulated by homeostatic perturbations that include changes in adenosine triphosphate (ATP) turnover (i.e., AMP:ATP ratio), calcium flux, redox state ( $\text{NAD}^+/\text{NADH}$ ), reactive oxygen species (ROS) production, and lactate concentration [10, 13, 352, 379, 380]. These homeostatic perturbations or “primary messengers” regulate “secondary messengers”, such as  $\text{Ca}^{2+}$ /calmodulin-dependent protein kinase II (CaMKII), mitogen-activated protein kinases (MAPKs), and 5' AMP-activated protein kinase (AMPK). These secondary messengers then regulate the activity and subcellular localisation of transcriptional cofactors and co-regulators (e.g., peroxisome proliferator-activated receptor  $\gamma$  coactivator 1 $\alpha$  [PGC-1 $\alpha$ ]) [10, 15, 62] that coordinate the regulation of genes associated with mitochondrial biogenesis.

There continues to be debate regarding the role of exercise intensity in the regulation of exercise-induced mitochondrial biogenesis [36, 38, 152, 464]. However, few studies have directly compared the effects of different exercise intensities on markers associated with exercise-induced mitochondrial biogenesis [15, 282, 439]. Furthermore, a limitation of most of these studies is that exercise was prescribed as a percentage of maximal oxygen uptake ( $\text{VO}_{2\text{max}}$ ), maximal work rate ( $\dot{W}_{\text{max}}$ ), or maximal heart rate ( $\text{HR}_{\text{max}}$ ). For example, a Google scholar search (04/09/2019) revealed at least 37 studies in humans that examined the effects of a single exercise session on markers of exercise-induced mitochondrial biogenesis (i.e., PGC-1 $\alpha$  mRNA) [15, 64, 69, 70, 121, 282-285, 410, 434-454] and all but one [465] prescribed

exercise as a percentage of  $\dot{V}O_{2\max}$ ,  $\dot{W}_{\max}$  or  $HR_{\max}$ . Research has shown that prescribing exercise relative to the maximal values is not a valid method to normalise exercise intensity and does not elicit homogenous homeostatic perturbations in different individuals (Chapter 1, Section 1.2) [3]. Prescribing exercise relative to sub-maximal anchors is a more valid method to normalise exercise intensity [3] and more research is required to investigate the influence of exercise prescribed relative to submaximal anchors on markers of exercise-induced mitochondrial biogenesis.

It is well known that homeostatic perturbations (e.g., intramuscular lactate accumulation, ROS production, etc.) increase with exercise intensity, with a disproportionate increase when exercise intensity exceeds the maximal steady state (i.e., highest intensity with an observed metabolic steady state) [49]. While this suggests “secondary messengers”, and the subsequent regulation of transcription factors and the transcription of genes, may also change disproportionately when exercise intensity exceeds the maximal steady state there has been little research investigating this hypothesis. Furthermore, despite an apparent relationship between exercise intensity and cell signalling, no studies have investigated more than two intensities within the same population [15, 70, 282]. The use of only two different intensities does not allow researchers to establish if the relationship between exercise intensity and cell signalling is linear or nonlinear. Prescribing exercise relative to the maximal lactate steady state (MLSS) appears to yield more homogenous homeostatic perturbations compared to the use of maximal anchors, and exercise above the MLSS leads to a disproportionate change in homeostatic perturbations [185]. However, it is not known if exercise above the MLSS also results in disproportionate changes in cell signalling.

It has been suggested that prescribing exercise training relative to submaximal anchors is a more effective means to prescribe exercise and will produce greater skeletal muscle adaptations [165]. However, to my knowledge this hypothesis has not been directly assessed. The aim of this study was to investigate the effects of exercise performed relative to the MLSS on exercise-induced cell-signalling, with a focus on commonly measured primary and secondary messengers as well as the differential expression of genes. Three exercise intensities were used, two intensities below (i.e., -18 and -6% MLSS) and one above (+6% MLSS) the MLSS in order to test the hypothesis that there would be a disproportionate change in primary and secondary messengers, and the differential expression of genes, when exercise intensity is increased above the MLSS. The findings of the proposed research will provide researchers, health practitioners, coaches, and sport scientists with a strong rationale for prescribing exercise to induce mitochondrial adaptations to improve endurance performance (and health in non-athlete populations).

## **4.2 Materials and Methods**

### *4.2.1 Ethical approval*

All procedures were performed in accordance with the ethical standards of the institutional research committee, and with the 1964 Helsinki declaration and its later amendments or comparable ethical standards. The Victoria University Human Research Ethics Committee approved all procedures (HRE 017-035) and informed consent was obtained from all participants prior to study participation.

### *4.2.2 Participants*

Ten untrained, moderately trained and highly trained males [ $\dot{V}O_{2\max}$ :  $55.8 \pm 10.0$  mL·kg<sup>-1</sup>·min<sup>-1</sup>; ( $\dot{V}O_{2\max}$  range: 40.7 – 70.3 mL·kg<sup>-1</sup>·min<sup>-1</sup>); age:  $27.5 \pm 7.7$  years; height:  $178.6 \pm 4.3$  cm; body mass:  $71 \pm 4.7$  kg] volunteered for this study.

### 4.2.3 Experimental Design

Participants were required to attend the laboratory 8 to 11 times. There was at least 48 h between the initial visits, with 7 days between the three exercise biopsy trials, and all testing was completed within 8 weeks. Visit one included written informed consent, risk stratification using the American College of Sports Medicine Risk Stratification guidelines [265], a self-reported physical activity rating (PA-R) [127], measurement of height and body mass, and completion of a cycling graded exercise test (GXT) followed by a verification exhaustive bout (VEB). Following visit one, the MLSS was established by a series of 30-min constant-power exercise bouts. Following the establishment of the MLSS, participants completed two constant-power exercise bouts to exhaustion at +6% of the MLSS (+6% of the MLSS was chosen as it is double the coefficient of variation of the MLSS [CV = 3%]) (**Figure 4.1**) [9]. The remaining three visits were performed in a randomised order at -18%, -6% or +6% of the MLSS. Skeletal muscle biopsies were taken from the vastus lateralis prior to, immediately post, +4 hours and +24 hours from the onset of exercise [biopsy timing was based on the findings of Granata et al. [121] to detect the highest changes in PGC-1 $\alpha$  (i.e., +4 h), and pilot data suggesting that +24 h is required to detect significant differences in p53 mRNA)]. Participants performed each test at their preferred cadence, which was established during the initial visit. All participants self-reported abstaining from the consumption of alcohol and caffeine, or engaging in heavy exercise, in the 48 h prior to each visit.

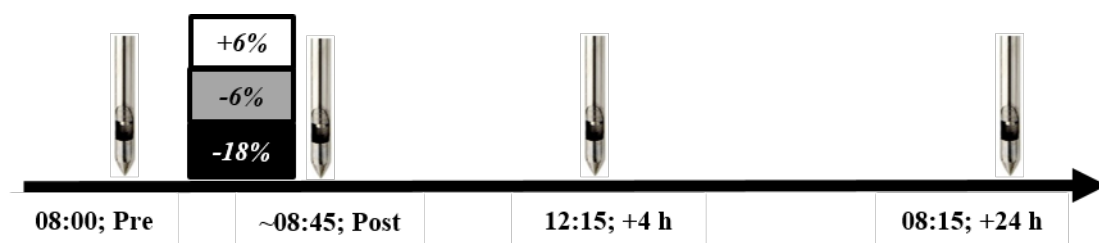


**Figure 4.1.** The exercise intensity and biopsy order of the research project. The pre biopsy was taken prior to each exercise bout (8:00), the post biopsy was taken immediately after each exercise bout (~08:45), the +4 h biopsy was taken four hours from the onset of exercise (12:15), and the +24 h biopsy was taken 24 hours from the onset of exercise (+1 Day; 8:15). The exercise bouts were performed in a randomised order and the mean (SD) times for the exercise bouts were 43.8 (12.1), 38.1 (10.5) and 33.8 (9.2) minutes for MLSS-18%, MLSS-6%, and MLSS+6%, respectively.

#### 4.2.4 Equipment/Instruments

All exercise testing was conducted on an electronically-braked cycle ergometer (Lode Excalibur v2.0, The Netherlands). A metabolic analyser (Quark Cardiopulmonary Exercise Testing, Cosmed, Italy) was used to assess oxygen uptake ( $\dot{V}O_2$ ) on a breath-by-breath basis. Antecubital venous blood was analysed using a blood lactate analyser (YSI 2300 STAT Plus, YSI, USA).

#### 4.2.5 Exercise Protocols

*GXT with Verification Exhaustive Bout.* Demographic data, PA-R, and measurements of height and body mass (BM), were used to estimate  $\dot{V}O_{2\max}$  (Est.  $\dot{V}O_{2\max}$ ) [266] and maximum GXT power (Est.  $\dot{W}_{\max}$ ) [127, 267].

$$\text{Est. } \dot{V}O_{2\max} = 56.363 + (1.921 \times \text{PA-R}) - (0.381 \times \text{AGE}) - (0.754 \times \text{BMI}) + (10.987 \times \text{SEX}; 1 = \text{MALE}, 0 = \text{FEMALE})$$

$$\text{Est. } \dot{W}_{\max} = \{[(\text{Est. } \dot{V}O_{2\max} - 7) \times \text{BM}]/1.8\}6.12$$

Where Est.  $\dot{V}O_{2\max}$  is expressed in millilitres per kilogram per minute, BM is in kilograms, and Est.  $\dot{W}_{\max}$  is in Watts.

A custom GXT protocol with a desired time limit of 10 min was then designed for each participant using: Est.  $\dot{W}_{\max}/10 \text{ min} = 1\text{-min work rate increments (W}\cdot\text{min}^{-1})$ . A 5-min recovery was administered after the GXT, followed by a VEB performed at 90% of  $\dot{W}_{\max}$  obtained from the preceding GXT to confirm  $\dot{V}O_{2\max}$  [39].

*Constant-Power Exercise Bouts to Establish the Maximal Lactate Steady State.* The power associated with the respiratory compensation point (RCP) from the GXT was used in a regression equation (Eqn. 5) to estimate the MLSS ( $Est_{MLSS}$ ) [268]. The RCP was determined as the average of the power associated with: 1) the break point in ventilation relative to expired carbon dioxide ( $\dot{V}_E/\dot{V}CO_2$ ), 2) the second break point in  $\dot{V}_E$ , and 3) the fall in patient end-tidal carbon dioxide ( $P_{ET}CO_2$ ) after an apparent steady state [71-73].

$$Est_{MLSS} = 23.329 + (0.79127 \times RCP)$$

where the  $Est_{MLSS}$  and RCP are expressed in Watts.

Participants then completed a series of 30-min constant-power exercise bouts to establish the MLSS. Participants performed 3 min of baseline cycling at 20 W prior to each 30-min constant-power exercise bout and the first exercise bout was performed at the  $Est_{MLSS}$ . If the blood lactate concentration increased  $>1.0 \text{ mmol}\cdot\text{L}^{-1}$  from the 10<sup>th</sup> to the 30<sup>th</sup> minute the power was decreased by 3%, otherwise the power was increased by 3% [9]. This process continued until the MLSS was obtained. The MLSS was established as the highest intensity where blood lactate increased  $<1.0 \text{ mmol}\cdot\text{L}^{-1}$  from the 10<sup>th</sup> to the 30<sup>th</sup> minute [41]. Antecubital venous blood (1.0 mL) was sampled every 5 min during the 30-min constant-power exercise bouts.

*Constant-Power Exercise Bouts to Exhaustion.* Once the MLSS had been established, participants completed two exhaustive bouts at +6% of the MLSS. The longer time to exhaustion of the two trials was used as the time limit for the subsequent exercise biopsy trial at +6% of the MLSS and was also used to work match the other two exercise biopsy trials. The

total work performed (i.e., Joules) was used to work match the lower-intensity exercise biopsy trials (i.e., -18% and -6% of the MLSS). All participants were able to replicate their time limit performance during the exercise biopsy trial. Antecubital venous blood (1.0 mL) was sampled every 5 min during the three exercise biopsy trials.

*$\dot{V}O_2$  and Power Analysis.* Breath-by-breath data were edited individually, with values greater than three standard deviations from the mean excluded [272]. The data was interpolated on a second-by-second basis and averaged into 5-s bins for the GXT, and 30-s bins for all constant-power exercise bouts and the three exercise biopsy trials [193, 273]. The highest measured  $\dot{V}O_2$  value from the GXT and VEB was determined as the highest 20-s rolling average. The  $\dot{V}O_{2\max}$  was computed as the highest  $\dot{V}O_2$  measured from the GXT or VEB. The end-exercise  $\dot{V}O_2$  response during the exercise at the MLSS and exercise at -18%, -6% and +6% of the MLSS was determined by the average  $\dot{V}O_2$  value during the last two minutes of the constant-power exercise bouts. The  $\dot{W}_{\max}$  for every GXT was determined as the power from the last completed stage plus the time completed in the subsequent stage multiplied by the power increment.

$$\dot{W}_{\max} = \text{Power of Last Stage} + [\text{increment (W}\cdot\text{s}^{-1}) \times \text{time (s)}]$$

### **Fat and Carbohydrate Oxidation Rates**

Measurement of fat and carbohydrate oxidation rates was assessed via stoichiometric equations derived by Frayn [466]:

$$\text{Carbohydrate Utilisation (g}\cdot\text{min}^{-1}) = 4.585 (\dot{V}CO_2) - 3.226 (\dot{V}O_2)$$

$$\text{Fat Utilisation (g}\cdot\text{min}^{-1}) = 1.695 (\dot{V}CO_2) - 1.701 (\dot{V}O_2)$$

Carbohydrate Oxidation ( $\text{kcal}\cdot\text{min}^{-1}$ ) = carbohydrate utilisation ( $\text{g}\cdot\text{min}^{-1}$ ) \* 3.683  
( $\text{kcal}\cdot\text{g}^{-1}$ )

Fat Oxidation ( $\text{kcal}\cdot\text{min}^{-1}$ ) = fat utilisation ( $\text{g}\cdot\text{min}^{-1}$ ) \* 9.746 ( $\text{kcal}\cdot\text{g}^{-1}$ )

### **Skeletal Muscle Exercise Biopsy Trials**

The exercise biopsy trials were performed in a randomised order at a constant power of -18, -6 and +6% of the MLSS. All exercise biopsy trials were performed in the morning following an overnight fast. The average duration of the three exercise biopsy trials was  $43.8 \pm 12.1$ ,  $38.1 \pm 10.5$  and  $33.9 \pm 9.2$  minutes for -18%, -6% and +6% of the MLSS, respectively. Participants were permitted to drink water during exercise and prior to the +4 h biopsy. Participants refrained from any exercise, alcohol, or caffeine between the +4 h and +24 h biopsy. Antecubital venous blood (1.0 mL) was sampled every 5 min during the exercise biopsy trials.

### **Skeletal Muscle Biopsies**

Skeletal muscle biopsies (100 to 175 mg) were taken from the vastus lateralis between the knee and hip joint. A 1-cm incision was made under local anaesthesia (1% Xylocaine), and muscle was extracted using a Bergstrom [467] needle with a modified suction technique [468]. Samples were blotted onto filter paper to remove excess blood prior to being frozen in liquid nitrogen within 15 s of removal. Muscle samples were stored at  $-80^{\circ}\text{C}$  until analysis. Muscle samples were taken from the same leg (i.e., randomised left or right leg) prior to exercise (pre), immediately after (post), 4 hours after the onset of exercise (+4 h) and 24 hours after the onset of exercise (+24 h).

### **Muscle Metabolite Assays (Lactate)**

*Sample Preparation.* Frozen muscle samples (~15 mg) were removed from -80°C storage and transferred on dry ice to a freeze drier for 24 hours (Heto PowerDry LL1500 Freeze Dryer, Thermo Electron Corporation). Freeze-dried muscle samples (2 to 5 mg) collected pre and post the exercise biopsy trials (i.e., -18%, -6% and +6% of the MLSS) were assayed enzymatically for lactate by spectrophotometric analysis using a modification of a previously described protocol [469]. Samples were first homogenised in 0.6 M of perchloric acid (800 µL) using TissueLyser II. Samples were then left on ice for 30 minutes and subsequently centrifuged at 10,000 g for 10 min at 4°C. The supernatant was placed into microcentrifuge tubes, and 150 µL of a KOH (1.2 M)/HEPES (0.125 M) solution was added to the tube for [La<sup>-</sup>] assessment. The pH of the samples was then adjusted using KOH (1.2 M) to increase alkalinity until the pH measured ~9.0. For every 100 µL in each tube, 2 µL of 3.0 M potassium chloride (KCl) was added; the solutions were left on ice for 10 min and then centrifuged at 10,000 g for 10 min at 4°C. The supernatant was extracted and the potassium perchlorate precipitate discarded. Samples were then stored at -80°C until subsequent analysis.

*Muscle Lactate Assay.* Lactate concentrations was measured in triplicate against nine dilutions of a sodium lactate standard (L7022; Sigma Aldrich, St Louis, USA). Each well was filled with 75 µL of standard, sample, and blank into 96-well microtitre plate and 50 µL of assay was added and mixed; the absorbency at 340 nm was measured at 25°C using a microplate spectrophotometer (Spectramax 340, Molecular Devices Corporation, Union City, CA). Once the absorbance was stable ( $< 0.008 \mu\text{m}\cdot\text{L}^{-1}\cdot\text{h}^{-1}$ ), after 5 to 10 min, 10 µL of lactate dehydrogenase (LDH) was added to each well. Following further mixing, the change in absorbency at 340 nm was determined at 15-min intervals. The change in absorbance was calculated once the samples had stabilised ( $< 0.008 \mu\text{m}\cdot\text{L}^{-1}\cdot\text{h}^{-1}$ ). This was approximately 180 min after the addition of LDH. The change in absorbance at 340 nm for the blanks and the

standards increased linearly ( $r > 0.998$ ) across this range to which a standard curve was calculated. The change in absorbance following the addition of LDH reflects intramuscular lactate. The concentration was adjusted to account for the muscle weight of each sample and the dilution of the samples during the above procedure and recorded as  $\text{mmol}\cdot\text{kg}^{-1}\text{ dw}$ .

### **Subcellular Fractionation**

Nuclear, cytosolic, and mitochondrial proteins were extracted from 40 to 90 mg of frozen muscle using modifications of a previously described protocol (**Figure 4.2**) [19]. In brief, muscle samples were thawed on ice in 1.5 mL of SEMH buffer (20 mM Hepes-KOH, pH 7.6; 220 mM Mannitol; 70 mM Sucrose; 1 mM EDTA) containing a protease/phosphatase inhibitor cocktail (1:100) (Cell Signalling Technology, Danvers, USA). The sample was then homogenised using a corded drill with an attached Teflon pestle on ice at 1,000 rpm (2 sets x 20 strokes; 5 min between each set). The homogenate was transferred to a 2-mL microcentrifuge tube, placed on ice for 30 min, vortexed for 15 s, and was then centrifuged at 500 g for 10 min at 4°C. The supernatant ( $S_1$ ) was removed and placed into a 1.5-mL microcentrifuge tube and used to obtain the cytosolic and mitochondrial fractions. Pellet ( $P_1$ ) was re-suspended in 500  $\mu\text{L}$  of SEMH buffer (with a protease/phosphatase inhibitor cocktail; 1:100) and centrifuged at 1,000 g for 15 min at 4°C. The supernatant ( $S_5$ ) was discarded and the pellet ( $P_5$ ) was resuspended in 500  $\mu\text{L}$  of SEMH buffer (w/ protease/phosphatase inhibitor cocktail; 1:100) and centrifuged at 1,000 g for 15 min at 4°C. The supernatant ( $S_6$ ) was discarded and the pellet ( $P_6$ ) was resuspended in 400  $\mu\text{L}$  of NET buffer (20 mM Hepes, pH 7.9; 1.5 mM  $\text{MgCl}_2$ ; 1.5 M NaCl; 0.2 EDTA; 20% Glycerol; 1% Triton-X-100) containing a protease/phosphatase inhibitor cocktail (1:100), kept on ice for 30 min (vortexed every 10 min for 15 s), then passed 10 times through a 3-mL syringe and a 25-gauge needle, followed by 2

freeze thaws and a final centrifugation at 9,000 g for 30 min at 4°C. The supernatant (S<sub>7</sub>) was the resultant nuclear fraction and pellet (P<sub>7</sub>) was discarded.

The supernatant (S<sub>1</sub>) was centrifuged at 2,000 g for 15 min at 4°C, transferred to a 1.5-mL microcentrifuge tube, and the pellet (P<sub>2</sub>) was discarded. The supernatant (S<sub>2</sub>) was centrifuged at 10,000 g for 30 min at 4°C and the supernatant (S<sub>3</sub>) was transferred to a 1.5-mL microcentrifuge tube and was the resultant cytosolic fraction. The pellet (P<sub>3</sub>) was resuspended in 100 uL of SEMH buffer containing protease/phosphatase inhibitor cocktail (1:100) and centrifuged at 12,000 g for 30 min at 4°C. The supernatant (S<sub>4</sub>) was discarded and the pellet (P<sub>4</sub>) was resuspended in 100 uL of Sucrose buffer (10 mM Hepes, pH 7.6; 0.5 M Sucrose) containing protease/phosphatase inhibitor cocktail (1:100) and PMSF (1:200), this was the resultant mitochondrial fraction.

*Protein Assay.* The protein content of muscle-fraction homogenates was measured in duplicate using a commercially available BCA Protein Assay Kit (#23225; Pierce ThermoFisher, USA) against nine serial dilutions. Homogenate (5 µL) and standard (20 µL) was added to a 96-well plate and 5 and 20 µL of 1% of Triton X-100 was added to homogenate and standard, respectively. A 200-µL mixture of BCA (50:1) mixture was added to each well and was incubated for 20 min at 37°C. The plate was shaken for 10 s and protein concentrations were measured via a spectrophotometer (SpectraMax i3 Multi-Mode Platform, San Jose, CA, USA) at an absorbance of 570 nm.

*Immunoblotting.* Equal amounts of protein 12 to 25 µg were loaded into wells on a Criterion 4-12% TGX Stain Free SDS Page gels (Bio-Rad). Gel electrophoresis ran for 80 to

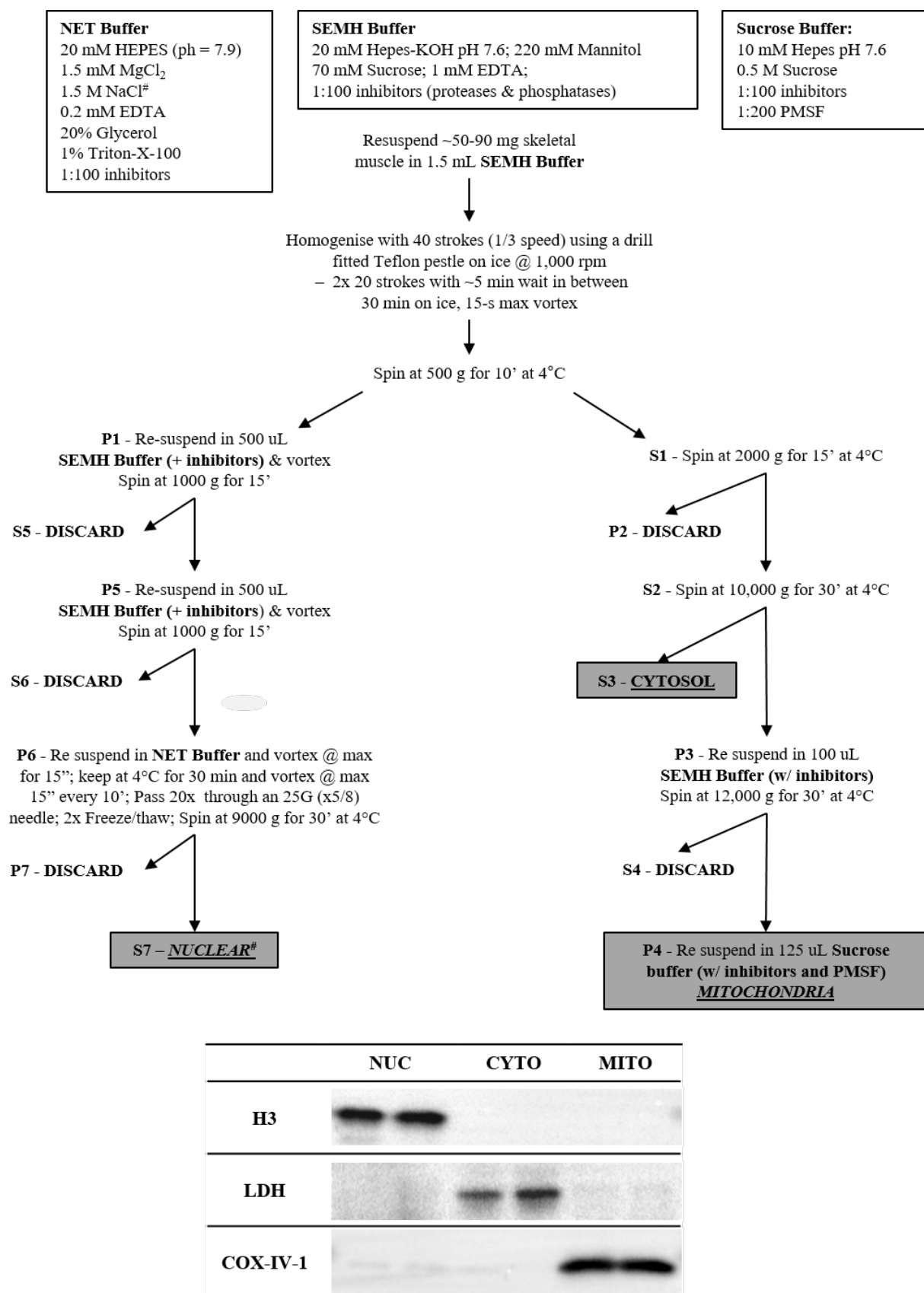


**Figure 4.2.** Schematic of the fractionation protocol. The protocol yields three subcellular fractions from frozen human skeletal muscle (i.e., nuclear, cytosol and mitochondria). Adapted from Dimauro et al. [19] (<sup>#</sup>Excess NaCl was removed via acetone precipitation). The homogenate was suspended in ice-cold acetone (1:6), stored at -80°C for 1 hour, and centrifuged at 13,000g for 20 minutes. Pellet was washed with ice-cold acetone, spun at 13,000g for 1 minute, and pellet was resuspended in 50 mM Tris (pH = 6.8), 100 mM dithiothreitol and 2% sodium dodecyl sulfate), and sonicated (2 x 3 s). Bottom figure illustrates the subcellular fractionation purity using histone 3 (H3), lactate dehydrogenase (LDH), and cytochrome c oxidase subunit 4 isoform 1 (COX-IV-1). PMSF: phenylmethylsulfonyl fluoride

120 min at 80 to 120 V, and proteins were then transferred onto polyvinylidene fluoride (PVDF) membranes (Bio-Rad, Hercules, CA, USA, #1620264) in a commercially available transfer buffer (Bio-Rad, Hercules, CA, USA) using a semi-dry transfer system (Trans-Blot® Turbo™ Transfer System, Bio-Rad, Hercules, CA, USA) for 10 min at 25 V. Stain-free images of the membranes were then taken using a ChemiDoc™ MP imaging system (Bio-Rad, Hercules, CA, USA). The analysis of the nuclear and mitochondrial fractions was not complete in time for thesis submission, and only the results for the cytosolic fraction are included in this thesis.

Membranes were blocked for 60 min in 5% non-fat milk diluted in Tris-buffered saline with 0.1% Tween 20 (TBST) on a rocker at room temperature. Primary antibodies were diluted in 5% BSA and 0.02% NaN<sub>3</sub> in TBST. Primary antibodies for p-ACC<sup>Ser79</sup> (#3661), p-CaMKII<sup>Thr286</sup> (#12716), p-p38 MAPK<sup>Thr180/Tyr182</sup> (#9211), p-AMPK<sup>Thr172</sup> (#2535), p-mTOR<sup>Ser2448</sup> (#5536) were from Cell Signaling Technology (Danvers, MA, USA). The membranes were incubated in primary antibody on a rocker at 4°C overnight, then washed three times in TBST before incubation in a species-specific horseradish peroxidase-conjugated secondary antibody (Donkey Anti-Rabbit IgG, Ab6802, Abcam; or Goat Anti-Rabbit IgG, NEF812001EA, Perkin Elmer, Waltham, MA, USA) for 90 min at room temperature. Membranes were then washed using TBST before being treated with a chemiluminescent solution (Clarity™ Western ECL Substrate, Bio-Rad, Hercules, CA, or SuperSignal™ West Femto Maximum Sensitivity Substrate, ThermoFischer Scientific, Wilmington, DE, depending on the target protein). Images were taken using a ChemiDoc™ MP imaging system (Bio-Rad, Hercules, CA, USA), and proteins were quantified via densitometry (Image Lab 5.0 software, Bio-Rad, Hercules, CA, USA).

## **Quantitative Real-Time Polymerase Chain Reaction**

*RNA Extraction.* Muscle samples (15 to 20 mg) were homogenised in 800 µL of QIAzol lysis reagent using TissueLyser II (Qiagen, Valencia, USA). Total RNA was then isolated using a RNeasy Plus Universal Mini Kit, with the kit instructions modified by replacing ethanol with 2-propanol [470]. The quality of each sample was assessed using Nanodrop spectrophotometer (ThermoFischer Scientific, Wilmington, DE). RNA integrity was measured using the Experion automated electrophoresis system (Bio-Rad). Samples with an RQI score > 8 were deemed to be of sufficient integrity for analysis [470]. Any samples that failed the integrity test required a new sample of muscle tissue to be chipped, homogenised, and RNA extracted. RNA samples were stored at -80°C until further analysis.

*Reverse Transcription.* RNA was reverse transcribed to cDNA using a Thermocycler (s1000; Bio-Rad) and the Bio-Rad iscript RT Supermix (170-8840) in accordance with the manufacturer's instructions. RT system was primed with oligo-dT (15) as per manufactures instruction. Priming was performed at 25°C for 5 min and reverse transcription for 30 min at 42°C. cDNA was stored at -20°C until analysis.

*Quantitative Real-Time PCR.* Relative mRNA expression was measured via qPCR (QuantStudio 7 Flex; Applied Biosystems, Foster City, USA) using Sso Advanced Universal SYBR Green Supermix (Bio-Rad). Primers were either adapted from existing literature or designed using PRIMER-BLAST (<https://www.ncbi.nlm.nih.gov/tools/primer-blast/>) [471] to include all splice variants, and were purchased from Sigma-Aldrich (Table 4.1). The products of each primer was verified. All reactions were performed in duplicate on 384-well plate and prepared using the epMotion 5073 automated pipetting system (Eppendorf AG). The qPCR reaction (5 µL) contained 300 nM of each forward and reverse primer and 2X SsoAdvanced

Universal SYBR Green Supermix (Bio-Rad, Hercules, CA). Assays ran for 10 min at 95°C, followed by 40 cycles of 15 s at 95°C and 60 s at 60°C. Of the six housekeeping genes, TBP, B2M and GAPDH were the most stable. Expression of each target gene was normalised to the geometric mean of the expression of the three most stable genes [470].

**Table 4.1** Details of primer sequences used for RT-qPCR.

Primer Name	Primer Sequence	
	Forward Primer	Backward Primer
<b>PPAR<math>\gamma</math></b>	AAGCGATTCCTTCACTGATA	GTGGAGTAGAAATGCTGGAG
<b>PPAR<math>\delta</math></b>	CATCATTCTGTGTGGAGACCG	AGAGGTAAGGGCATCAGGG
<b>CD36</b>	TTGATTGAAAAATCCTTCTTAGCCA	TGGTTTCTACAAGCTCTGGTTCTT
<b>PGC-1<math>\alpha</math> total</b>	CAGCCTCTTTGCCAGATCTT	TCACTGCACCACTTGAGTCCAC
<b>p53</b>	GTTCCGAGAGCTGAATGAGG	TTATGGCGGGAGGTAGACTG
<b>COX4-1</b>	GAGCAATTTCCACCTCTGC	CAGGAGGCCTTCTCCTTCTC
<b>MFF</b>	CCAAACGCTGACCTGGAAC	TTTCCTGCTACAACAATCCTCTCC
<b>SOD1</b>	GGTCTCACTTTAATCCTCTAT	CATCTTTGTCAGCAGTCACATT
<b>SOD2</b>	CTGGACAAACCTCAGCCCTA	TGATGGCTTCCAGCAACTC
<b>PKD4</b>	GCAGCTACTGGACTTTGGTT	GCGAGTCTCACAGGCAATTC
<b>PGC-1<math>\alpha</math>-4</b>	TCA CAC CAA ACC CAC AGA GA	CTG GAA GAT ATG GCA CAT
<b>ATF2</b>	CACTACAGAAACTCCGGCTT	GAAGCTGCTGCTCTATTTCCG
<b>SIRT1</b>	ACGCTGGAACAGGTTGCGGGA	AAGCGGTTTCATCAGCTGGGCAC
<b>TFEB</b>	CAGATGCCCAACACGCTACC	GCATCTGTGAGCTCTCGCTT
<b>Drp1</b>	CACCCGGAGACCTCTCATTC	CCCATTCTTCTGCTTCCAC
<b>MFN2</b>	CCCCTTGTCTTTATGCTGATGTT	TTTTGGGAGAGGTGTTGCTTATTC
<b>Cytochrome C</b>	GGGCCAAATCTCCATGGTCT	TCTCCCCAGATGATGCCTTT
<b>Tfam</b>	CCGAGGTGGTTTTTCATCTGT	GCATCTGGGTTCTGAGCTTT
<b>CREB1</b>	CAGCACTTCCTACACAGCCT	TCTCGAGCTGCTTCCCTGTT
<b>PGC-1<math>\alpha</math>-1</b>	ATGGAGTGACATCGAGTGTGC T	GAGTCCACCCAGAAAGCTGT
<b>NRF1</b>	CTACTCGTGTGGGACAGCAA	AGCAGACTCCAGGTCTTCCA
<b>MCT1</b>	TGACCATTGTGGAATGCTGT	GAGCCGACCTAAAAGTGGTG
<b>NHE1</b>	TGTGACCTGTTCTCACTGC	CGCTTCGTCTTTGCTTTTT
<b>PPAR<math>\alpha</math></b>	GGCAGAAGAGCCGTCTCTACTTA	TTTGCATGGTTCTGGGTACTGA
<b>CS</b>	TCAGGAAGTGCTTGTCTGGC	ATAGCCTGGAACAACCCGTC
<b>SDHB</b>	AAATGTGGCCCCATGGTATTG	AGAGCCACAGATGCCTTCTCTG
<b>UQCRC2</b>	GCAGTGACCGTGTGTCAGAA	AGGGAATAAAAATCTCGAGAAAGAGC
<b>CHCDH4</b>	GCTTGGCTGTTCTTGTATTTC	GTTTCTCTCTTGCTGCTACTC
<b>Housekeeping</b>		
<b>GAPDH</b>	AATCCCATCACCATCTTCCA	TGGACTCCACGACGTACTCA
<b>B2M</b>	TGCTGTCTCCATGTTTGATGTATCT	TCTCTGCTCCCCACCTCTAAGT
<b>ACTB</b>	GAGCACAGAGCCTCGCCTTT	TCATCATCCATGGTGAGCTGGC
<b>TBP</b>	CAGTGACCCAGCAGCATCACT	AGGCCAAGCCCTGAGCGTAA
<b>Cyclophilin</b>	GTCAACCCACCGTGTCTTCTC	TTTCTGCTGTCTTTGGGACCTTG
<b>18S</b>	CTTAGAGGGACAAGTGCCG	GGACATCTAAGGGCATCACA

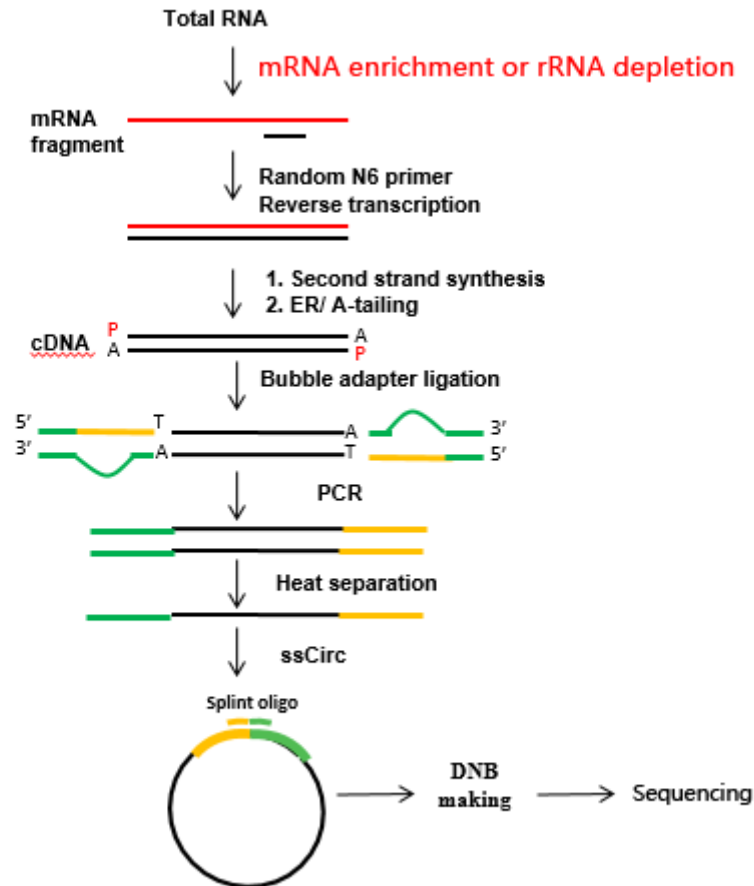


**Figure 4.3.** Schematic of mRNA library construction flow chart.

*cDNA Library Preparation for RNA Sequencing.* A total of 96 total RNA samples from 8 participants were used for RNA sequencing. The total RNA samples were extracted and sent to BGI China for performing library construction and RNA sequencing (Figure 4.3). RNA quality was checked using Agilent 2100 (Agilent Technologies, Santa Clara, USA). The RNA integrity number (RIN) values of the sample were above 8. Approximately 1 $\mu$ g RNA samples were treated as per standard procedure for cDNA library construction by BGI. Briefly, mRNA was selected using Oligo (dT) magnetic beads from total RNA, and fragmented and reverse-transcribed to double-stranded cDNA by N6 random primer. The double-stranded cDNA fragments were first end repaired, then ligated with adapters at 3' end. PCR was then performed to amplify the cDNA fragment with adapters, and the PCR product was heated to denature to

single strand DNA. Finally, single strand DNA was cyclized by the splint oligo sequence to be sequenced by BGISEQ-500 sequencing platform.

*RNA Sequencing.* The average alignment rate of the sample comparison genome was 93.81%, the average alignment rate of the comparison gene set was 86.91%, and the predicted number of new genes was 4,184; the total number of genes detected was 23,239, of which the known gene was 19,186, a total of 33,676 transcripts were detected, of which 27,089 were new alternative splicing isoforms of known protein-coding genes, and 4,184 were transcripts of new protein-coding genes. Treatment of total RNA by mRNA enrichment or rRNA removal, mRNA enrichment: enrichment of mRNA with polyA tail using magnetic beads with OligodT; rRNA removal: hybridization of rRNA with DNA probe, selective digestion of DNA with RNaseH /RNA hybridization strand, and then DNA probe is digested with DNaseI, and purified to obtain the desired RNA. The obtained RNA is fragmented by interrupting the buffer, and the random N6 primer is used for reverse transcription, and then the cDNA double strand is synthesized to form double-stranded DNA. The synthetic double-stranded DNA ends are flattened and phosphorylated at the 5-min end, and the 3-min end forms a sticky end protruding "A", and then a bubbling joint having a convex "T" at the 3-min end is attached. The ligation product is PCR amplified by specific primers. The PCR product is heat-denatured into a single strand, and a single-stranded DNA is cyclised with a bridge primer to obtain a single-stranded circular DNA library (**Figure 4.3**).

### 4.3 Statistical Analysis

Experimental data is presented as means  $\pm$  standard deviations. Signalling and RNA data were evaluated using a two-way (trial x time) ANOVA with repeated measures, with a Bonferroni post-hoc analysis. Comparisons were assessed to identify differences between the

three exercise intensities. The alpha for rejecting the null hypothesis was set at  $p \leq 0.05$ . Effect sizes (ES) were assessed using Cohen's d, with ES thresholds defined as trivial  $< 0.3$ , small  $< 0.6$ , moderate  $< 1.2$ , large  $< 2.0$ , very large  $< 4.0$ , and  $> 4.0$  very very large [8]. Uncertainty of effects is expressed as 90% confidence limits (90% CL). The effect sizes were calculated by assessing the mean difference between values relative to the pooled standard deviations from all three resting samples and the post-exercise time point. Agreement between  $\dot{V}O_2$  observed during the GXTs and VEB was assessed via intraclass correlation (ICC), standard error of the measurement (SEM), and coefficient of the variation (CV%).

$$s_{\text{pooled}} = \sqrt{\frac{(n_1 - 1)s_1^2 + (n_2 - 1)s_2^2 + \dots + (n_k - 1)s_k^2}{n_1 + n_2 + \dots + n_k - k}}$$

## 4.4 Results

### 4.4.1 Metabolic and Power Data

GXT.  $\dot{V}O_2$  values from the GXT and VEB were  $55.2 \pm 10.2$  and  $55.3 \pm 9.6$  mL·kg<sup>-1</sup>·min<sup>-1</sup>, respectively (ICC = 0.99; SEM = 1.1 mL·kg<sup>-1</sup>·min<sup>-1</sup>; CV = 2.0 %), with the highest value from either used as the  $\dot{V}O_{2\text{max}}$  ( $55.8 \pm 10.0$  mL·kg<sup>-1</sup>·min<sup>-1</sup>). The  $\dot{W}_{\text{max}}$  was  $350 \pm 64$  W (range: 271 to 453 W) and the mean GXT duration was  $10.4 \pm 1.1$  minutes (range: 8.7 to 12.1 minutes).

*MLSS and Exercise Biopsy Trials.* The power and metabolic data from the MLSS and the exercise biopsy trials is detailed in **Table 4.2**. The mean power associated with the MLSS was  $220 \pm 48$  W; the mean  $\dot{V}O_2$  of the MLSS expressed as a percentage of  $\dot{V}O_{2\text{max}}$  ranged from 71.4 to 91.1%, and the mean power ranged from 57.5 to 69.6% of  $\dot{W}_{\text{max}}$ . **Figure 4.4, Panel A** illustrates the blood lactate response during the first 30 min of the exercise biopsy trials. Considering the 30-min MLSS criterion, during the -6% MLSS trial participant #5 was above the MLSS ( $\Delta$  Blood Lactate 10 to 30 minutes = 1.9 mmol·L<sup>-1</sup>) and during the +6% MLSS trial participant #8 was below the MLSS ( $\Delta$  Blood Lactate 10 to 30 minutes = 0.6 mmol·L<sup>-1</sup>). **Figure**

**4.4 Panel B** illustrates the total rate of substrate oxidation at each intensity; -18% yielded the greatest amount of fat oxidation ( $\text{kcal}\cdot\text{min}^{-1}$ ). The resting intramuscular lactate values were all similar ( $14.9 \pm 1.9$ ,  $15.8 \pm 2.2$ , and  $13.4 \pm 2.8$   $\text{mmol}\cdot\text{kg}^{-1}$  dw, for -18%, -6%, and +6% MLSS, respectively (**Figure 4.4, Panel C**). While there was a significant increase in intramuscular lactate post exercise for all trials, intramuscular lactate was significantly higher following -6% MLSS compared with -18% MLSS ( $39.3 \pm 11.9$  vs.  $20.8 \pm 4.4$   $\text{mmol}\cdot\text{kg}^{-1}$  dw). Moreover, intramuscular lactate was significantly higher following +6% MLSS compared with -6% MLSS ( $65.1 \pm 12.1$  vs.  $39.3 \pm 11.9$   $\text{mmol}\cdot\text{kg}^{-1}$  dw) (**Figure 4.4, Panel C**). There was a larger gain in post exercise intramuscular lactate relative to power when exercise was performed above the MLSS; intramuscular lactate increased  $0.7$   $\text{mmol}\cdot\text{kg}^{-1}$   $\text{dw}\cdot\text{W}^{-1}$  from -18% to -6% MLSS and  $1.0$   $\text{mmol}\cdot\text{kg}^{-1}$   $\text{dw}\cdot\text{W}^{-1}$  from -6% to +6% MLSS. The mean  $\pm$  SD duration of the three exercise biopsy trials was  $43.8 \pm 12.1$ ,  $38.1 \pm 10.5$  and  $33.9 \pm 9.2$  minutes for -18%, -6% and +6% of the MLSS, respectively. The mean  $\pm$  SD rate of energy expenditure was  $10.8 \pm 2.4$ ,  $12.4 \pm 2.7$ , and  $14.0 \pm 3.1$   $\text{kJ}\cdot\text{min}^{-1}$  for -18%, -6% and +6% of the MLSS, respectively.

**Table 4.2.** Mean  $\pm$  SD and [ranges] of values from the exercise biopsy trials [-18%, -6, and +6% of the maximal lactate steady state (MLSS)], and at the MLSS, for power (Watts), percentage of maximal power derived from the 8-12 minute GXT (% of  $\dot{W}_{\text{max}}$ ), end-exercise blood lactate concentrations, change ( $\Delta$ ) in blood lactate from 10 to 30 minutes during the constant-power exercise bout, end-exercise oxygen uptake ( $\dot{V}\text{O}_2$ ), end-exercise oxygen uptake expressed as a percentage of maximal oxygen uptake derived from 8-12 minute GXT (%  $\dot{V}\text{O}_{2\text{max}}$ ), and end-exercise oxygen uptake expressed as a percentage of the oxygen uptake at the MLSS (% of the MLSS  $\dot{V}\text{O}_2$ ).

	Power (W)	% of $\dot{W}_{\text{max}}$	Blood Lactate ( $\text{mmol}\cdot\text{L}^{-1}$ )	$\Delta$ Blood Lactate ( $\text{mmol}\cdot\text{L}^{-1}$ ) (10 to 30 min)	$\dot{V}\text{O}_2$ ( $\text{mL}\cdot\text{kg}^{-1}\cdot\text{min}^{-1}$ )	% $\dot{V}\text{O}_{2\text{max}}$	% of the MLSS $\dot{V}\text{O}_2$
<b>-18%</b>	$181 \pm 39$ [132 - 257]	$51.4 \pm 3.8$ [47.2 - 57.1]	$1.4 \pm 0.4$ [0.7 - 2.1]	$0.0 \pm 0.1$ [-0.2 - 0.2]	$39.78 \pm 7.71$ [29.4 - 53.4]	$71.4 \pm 5.7$ [58.9 - 78.4]	$86.4 \pm 5.5$ [79.2 - 96.8]
<b>-6%</b>	$207 \pm 45$ [151 - 295]	$59.0 \pm 4.3$ [54.1 - 65.4]	$3.4 \pm 1.5$ [0.6 - 5.7]	$0.6 \pm 0.6$ [-0.4 - 1.9]	$43.54 \pm 7.79$ [33.4 - 54.9]	$78.3 \pm 6.2$ [66.3 - 86.0]	$94.6 \pm 3.7$ [87.2 - 100.5]
<b>MLSS</b>	$220 \pm 48$ [161 - 314]	$62.7 \pm 4.6$ [57.5 - 69.6]	$3.6 \pm 0.8$ [2.2 - 5.8]	$0.7 \pm 0.4$ [0.3 - 0.9]	$46.10 \pm 8.53$ [34.4 - 59.0]	$82.7 \pm 5.7$ [71.4 - 91.1]	100 -
<b>+6%</b>	$234 \pm 51$ [171 - 333]	$66.6 \pm 4.8$ [61.0 - 73.8]	$6.7 \pm 1.9$ [3.4 - 9.9]	$1.9 \pm 0.8$ [0.6 - 3.6]	$48.90 \pm 8.83$ [35.4 - 62.7]	$87.9 \pm 6.8$ [76.3 - 99.2]	$106.4 \pm 6.8$ [97.3 - 121.3]

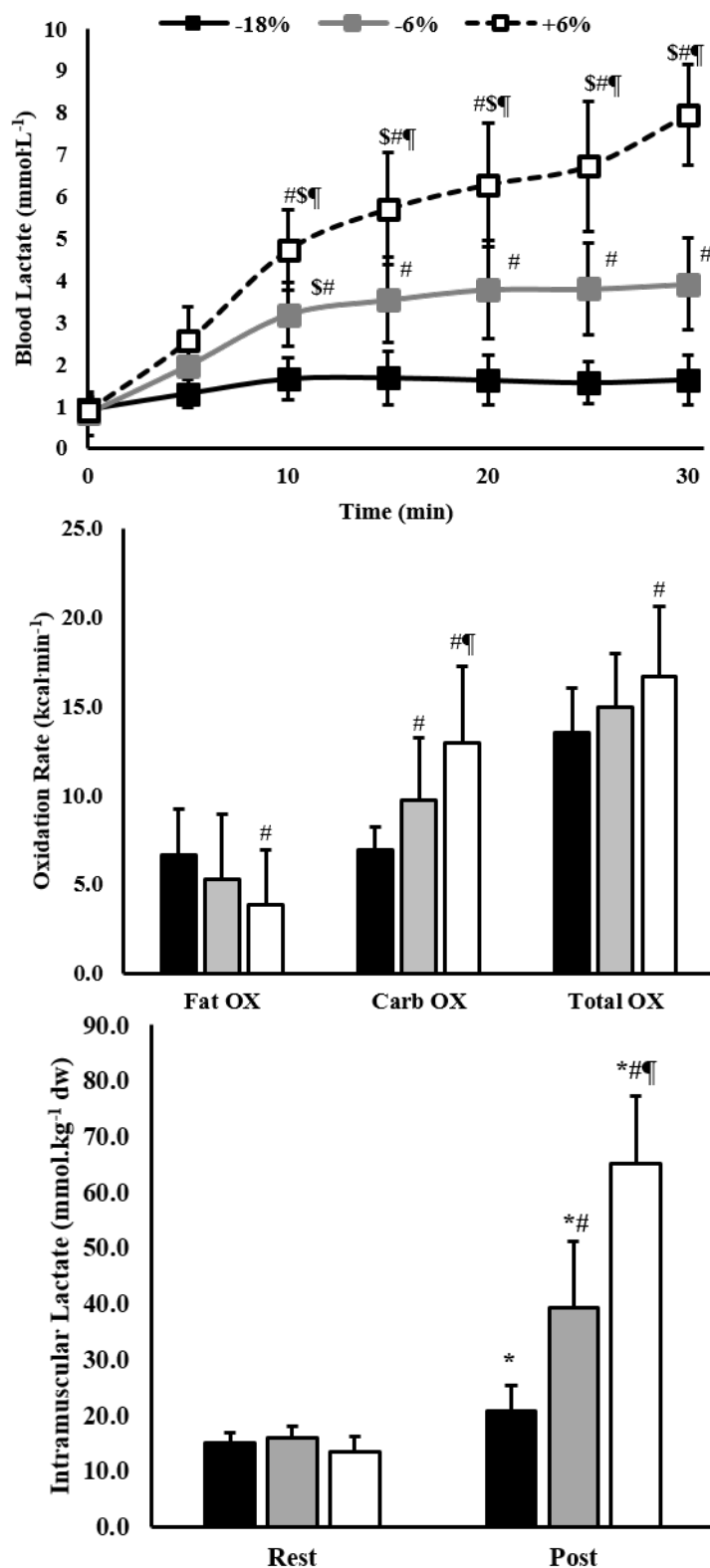


**Figure 4.4 (A-C).** The influence of exercise intensity on metabolic responses during the exercise biopsy trials. (A) Mean  $\pm$  SD of blood lactate concentrations ( $\text{mmol}\cdot\text{L}^{-1}$ ) during the first 30 minutes of the exercise biopsy trials. -18% of the MSS (black boxes), -6% of the MLSS (grey shaded boxes), and +6% of the MLSS (open boxes). (B) Mean  $\pm$  SD of fat and carbohydrate (carb) oxidation ( $\text{kcal}\cdot\text{min}^{-1}$ ) rates measured via stoichiometric equations as described by Frayn, during the last minute of the exercise biopsy trials. (C) Mean  $\pm$  SD of intramuscular lactate concentrations at rest and immediate post exercise. \$ = significantly different from previous time point. \* = significantly different from Pre; # = significantly different from -18%; ¶ = significantly different from -6%.

#### 4.4.2 Cytosolic Signalling Kinases.

**Figure 4.5, Panels A-E**, illustrate the cytosolic signalling kinase response immediately post, as well as +4 and +24 hours from the onset of exercise. There were no significant differences compared to rest, or between conditions, for p-mTOR<sup>Ser2448</sup>, p-CaMKII<sup>Thr286</sup>, p-p38 MAPK<sup>Thr180/Tyr182</sup>, p-ACC<sup>Ser79</sup>, and p-AMPK<sup>Thr172</sup> relative protein abundance. Although not significantly different ( $p = 0.49$ ), immediately post exercise there was a small (ES: 0.39 [CI: 0.22 – 0.56]) and moderate (ES: 0.81 [CI: 0.45 – 1.17]) effect size for the modulation of p-CaMKII<sup>Thr286</sup> following exercise at -6 and +6% of the MLSS, respectively (**Figure 4.5, Panel B**).

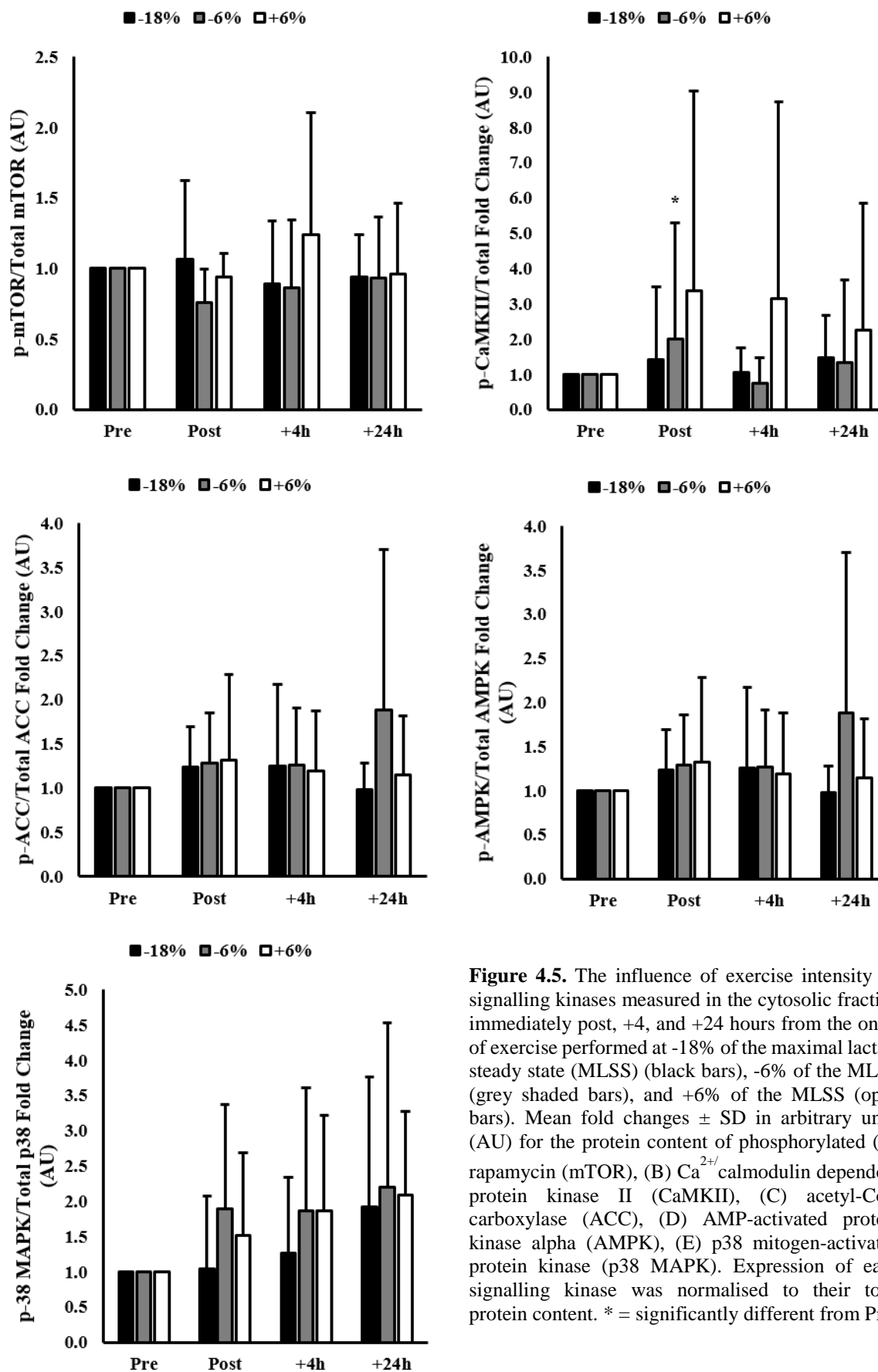


**Figure 4.5.** The influence of exercise intensity on signalling kinases measured in the cytosolic fraction immediately post, +4, and +24 hours from the onset of exercise performed at -18% of the maximal lactate steady state (MLSS) (black bars), -6% of the MLSS (grey shaded bars), and +6% of the MLSS (open bars). Mean fold changes  $\pm$  SD in arbitrary units (AU) for the protein content of phosphorylated (A) rapamycin (mTOR), (B) Ca<sup>2+</sup> calmodulin dependent protein kinase II (CaMKII), (C) acetyl-CoA carboxylase (ACC), (D) AMP-activated protein kinase alpha (AMPK), (E) p38 mitogen-activated protein kinase (p38 MAPK). Expression of each signalling kinase was normalised to their total protein content. \* = significantly different from Pre

#### 4.4.3 Transcriptome Response.

**Figure 4.6** illustrates the principal component analysis. When combining all biopsy times there were 3784, 4977, and 6687 total genes that were differentially expressed following exercise performed at -18%, -6%, and +6% of MLSS, respectively (**Figure 4.7, A & B**). Immediately after exercise, 1047 (up: 432; down: 615), 621 (up: 328; down: 293), and 1635 (up: 509; down: 1126) genes were differently expressed for exercise performed at -18%, -6%, and +6% MLSS, respectively (**Figure 4.8**). Four hours from the onset of exercise, 1502 (up: 852; down: 650), 1530 (up: 1034; down: 496), and 2195 (up: 578; down: 1617) genes were differently expressed for exercise performed at -18%, -6%, and +6% MLSS, respectively (**Figure 4.8**). Twenty-four hours from the onset of exercise, 1235 (up: 688; down: 547), 2826 (up: 2171; down: 655), and 2857 (up: 1058; down: 1799) genes were differently expressed following exercise performed at -18%, -6%, and +6% MLSS, respectively (**Figure 4.8**). A KEGG classification of genes revealed the largest number of upregulated genes was associated with endocrine/metabolic diseases, immune system function, endocrine system function, signalling molecules and interactions, signal transduction, and energy metabolism; whereas the largest number of downregulated genes associated with these functions was subsequent to exercise at +6% MLSS (**Figure 4.9**). Figure 4.15- 4.15 illustrates the fold-change relative to pre exercise values of the six genes of interest as determined via qPCR analysis (i.e., PGC-1 $\alpha$ -total, p53, SOD2, p21, PPAR $\delta$  and PDK4 mRNA).

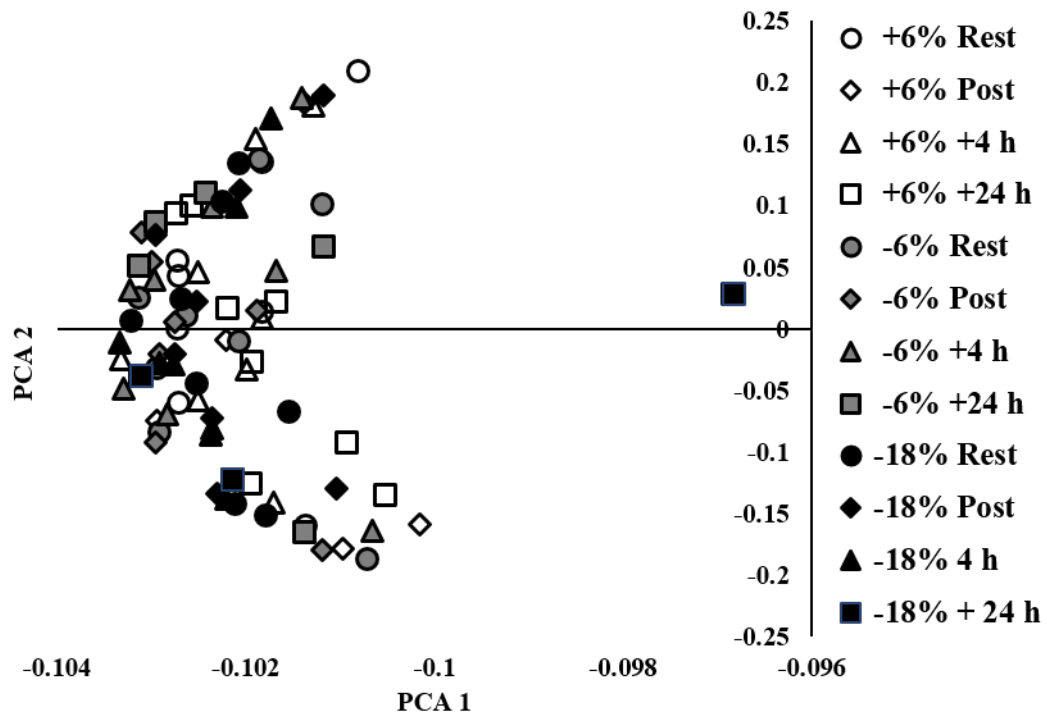
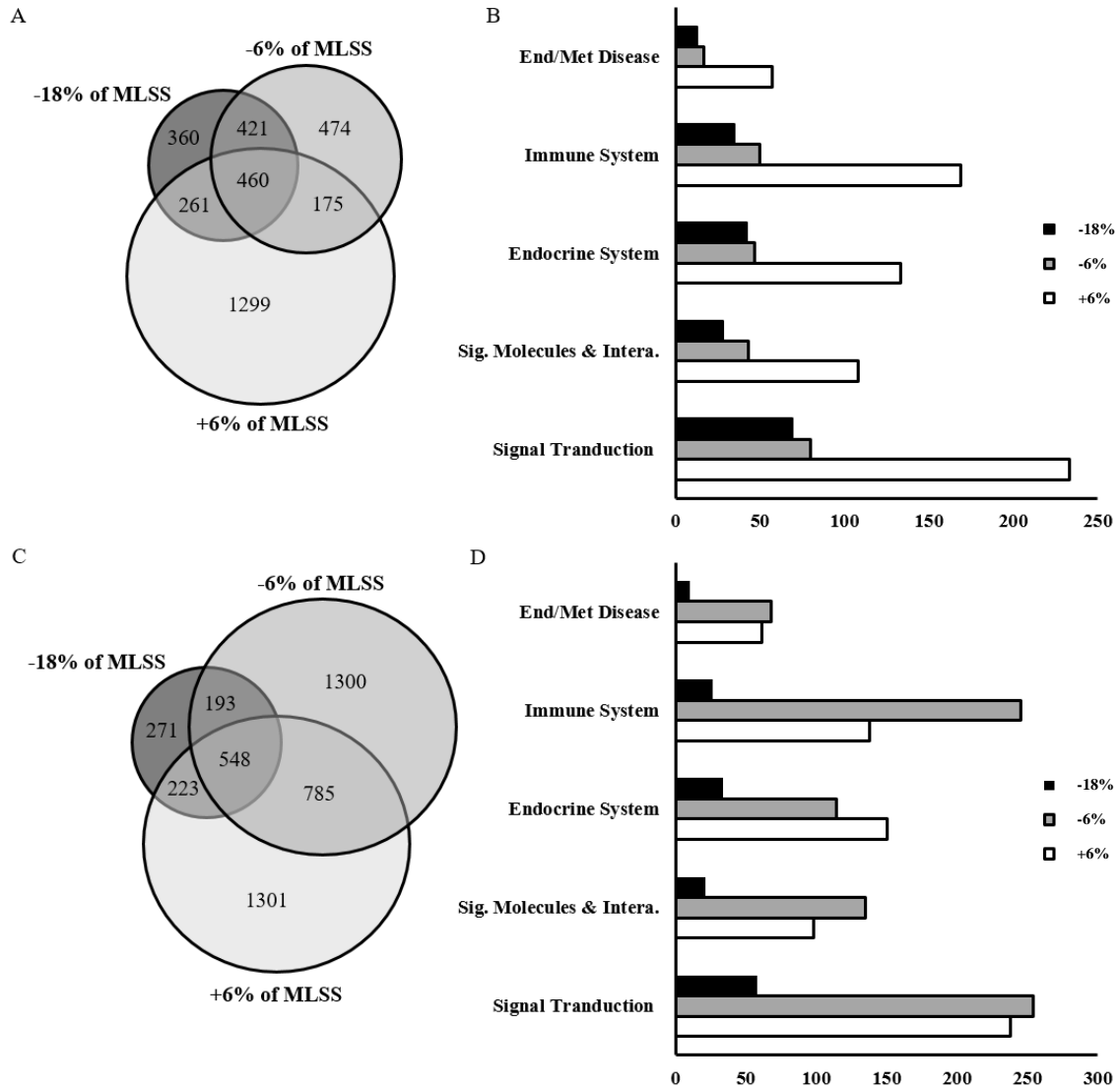
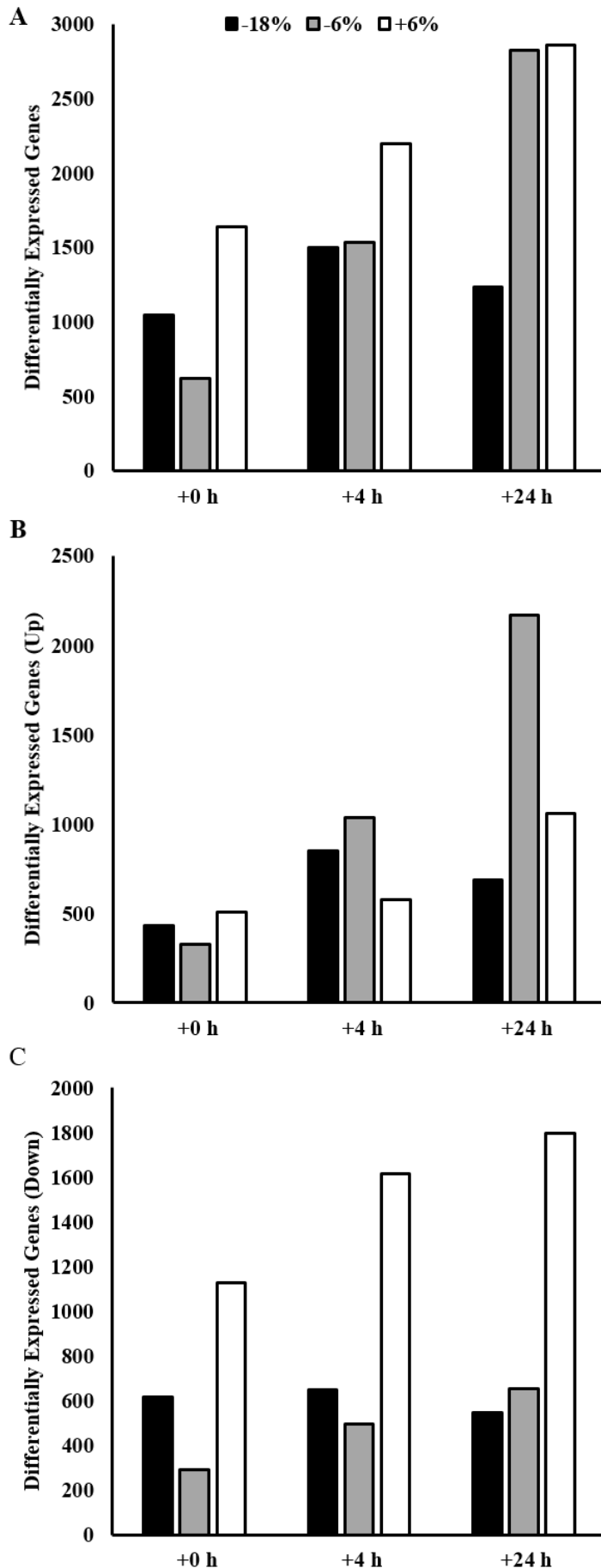


Figure 4.6. Primary component analysis of samples.



**Figure 4.7.** Venn diagram illustrating the influence of exercise intensity on the large scale transcriptional response (i.e., number of differentially expressed genes) in whole skeletal muscle biopsy samples +4 (A) and +24 hours (C) from the onset of exercise. ( $\log_2FC = 1$ ;  $Q\text{-value} = 0.001$ ). KEGG classification of genes unique to each intensity in whole skeletal muscle biopsy samples +4 (B) and +24 hours (D) from the onset of exercise. -18% of the maximal lactate steady state (MLSS) (black bars), -6% of the MLSS (grey shaded bars), and +6% of the MLSS (open bars).



**Figure 4.8.** Bar graphs illustrating the influence of exercise intensity on the total number of differentially expressed genes (A), and the number of upregulated (B) and downregulated (C) genes immediately post, +4, and +24 hours from the onset of exercise performed at -18% of the maximal lactate steady state (MLSS) (black bars), -6% of the MLSS (grey shaded bars), and +6% of the MLSS (open bars).

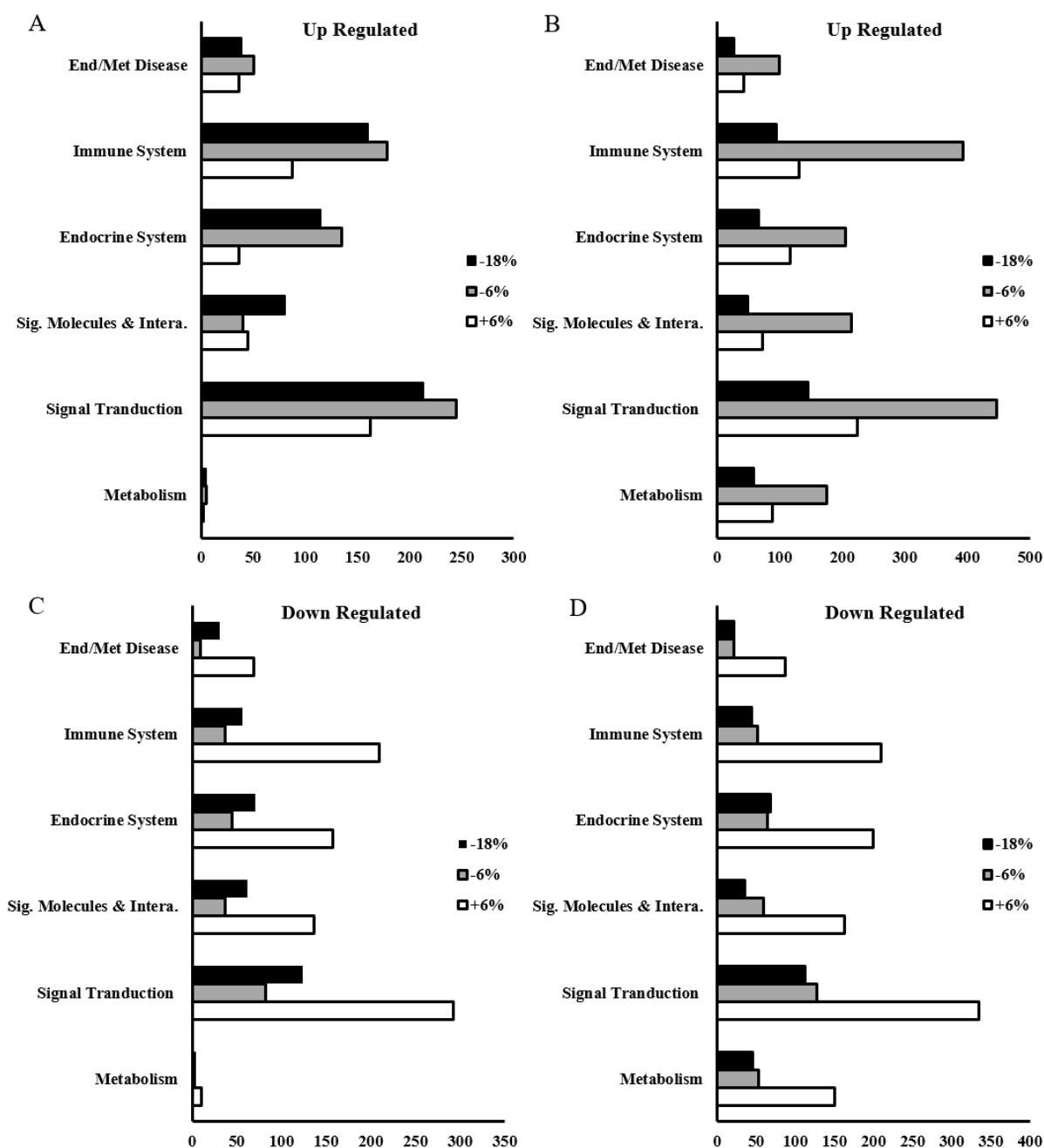


**Figure 4.9.** Bar graphs illustrating the influenced of exercise intensity on the number of upregulated genes +4 h (A), and +24 h (B), and downregulated genes +4 h (C), and +24 h (D), from the onset of exercise specific to endocrine/metabolic diseases, immune system function, endocrine system function, signalling molecules and interactions, signal transduction and energy metabolism. -18% of the maximal lactate steady state (MLSS) (black bars), -6% of the MLSS (grey shaded bars), and +6% of the MLSS (open bars).

#### 4.4.4 Whole Muscle mRNA.

**Figures 4.10 – 4.14** illustrate the mean  $\pm$  SD fold changes compared to the pre-exercise values for the gene targets assessed in the current study. **Table 4.3** details the effect size (90% confidence intervals) and includes a descriptive interpretation of the magnitude of changes in

mRNA content. Significant exercise-induced changes were observed for PGC-1 $\alpha$ -total, p53, SOD2, p21, PPAR $\delta$  and PDK4 mRNA (**Figure 4.10 B - F; Figure 4.11, Panels A, B and D**). Significant increases from pre-exercise values for PGC-1 $\alpha$ -4 was observed +4 h from the onset of exercise at -18% of the MLSS (**Figure 4.10, Panel B; Figure 4.11, Panel A**). Significant increases from pre-exercise values in p21 and p53 mRNA were observed +4 h, and +24 h, respectively, from the onset of exercise at -6%, and +6% MLSS (**Figure 4.10, Panel F; Figure 4.10, Panel D**). PPAR $\delta$  was significantly increased +4 h from pre exercise following exercise at -18 and -6% MLSS (**Figure 4.11, Panel B**). A significant increase was observed in SOD2 mRNA +24 h from rest following exercise at +6% MLSS (**Figure 4.10, Panel E**). A significant increase in PDK4 and PGC-1 $\alpha$ -total mRNA was observed +4 h from the onset of exercise compared to pre following all three exercise intensities (**Figure 4.10, Panel C; Figure 4.11, Panel D**).

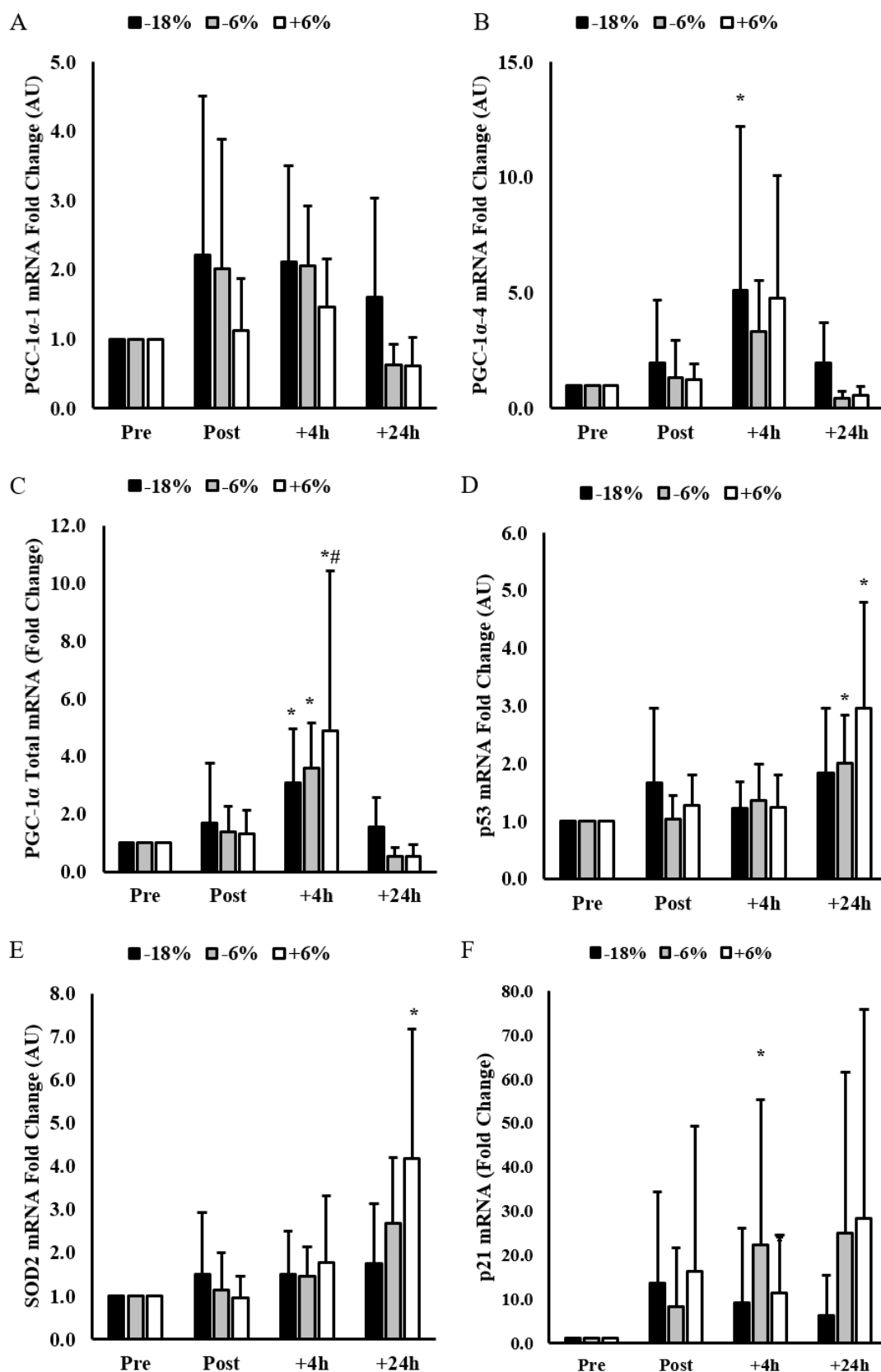


**Figure 4.10 (A-F).** The influence of exercise intensity on whole skeletal muscle mRNA immediately post, +4, and +24 hours from the onset of exercise performed at -18% of the maximal lactate steady state (MLSS) (black bars), -6% of the MLSS (grey shaded bars), and +6% of the MLSS (open bars). Mean fold changes  $\pm$  SD in arbitrary units (AU) for (A) Peroxisome proliferator-activated receptor gamma coactivator 1-alpha isoform 1 (PGC-1 $\alpha$ -1), (B) Peroxisome proliferator-activated receptor gamma coactivator 1-alpha isoform 4 (PGC-1 $\alpha$ -4), (C) peroxisome proliferator-activated receptor gamma coactivator 1-alpha (PGC-1 $\alpha$ ) total, (D) tumour suppressor protein 53 (p53), (E) Superoxide dismutase 2 (SOD2) and (F) cyclin-dependent kinase inhibitor 1 (p21). Expression of each target gene was normalised to the geometric mean of expression of the three most stable genes (i.e., TBP, B2M and GAPDH). \* = significantly different from Pre; # = significantly different from -18%.

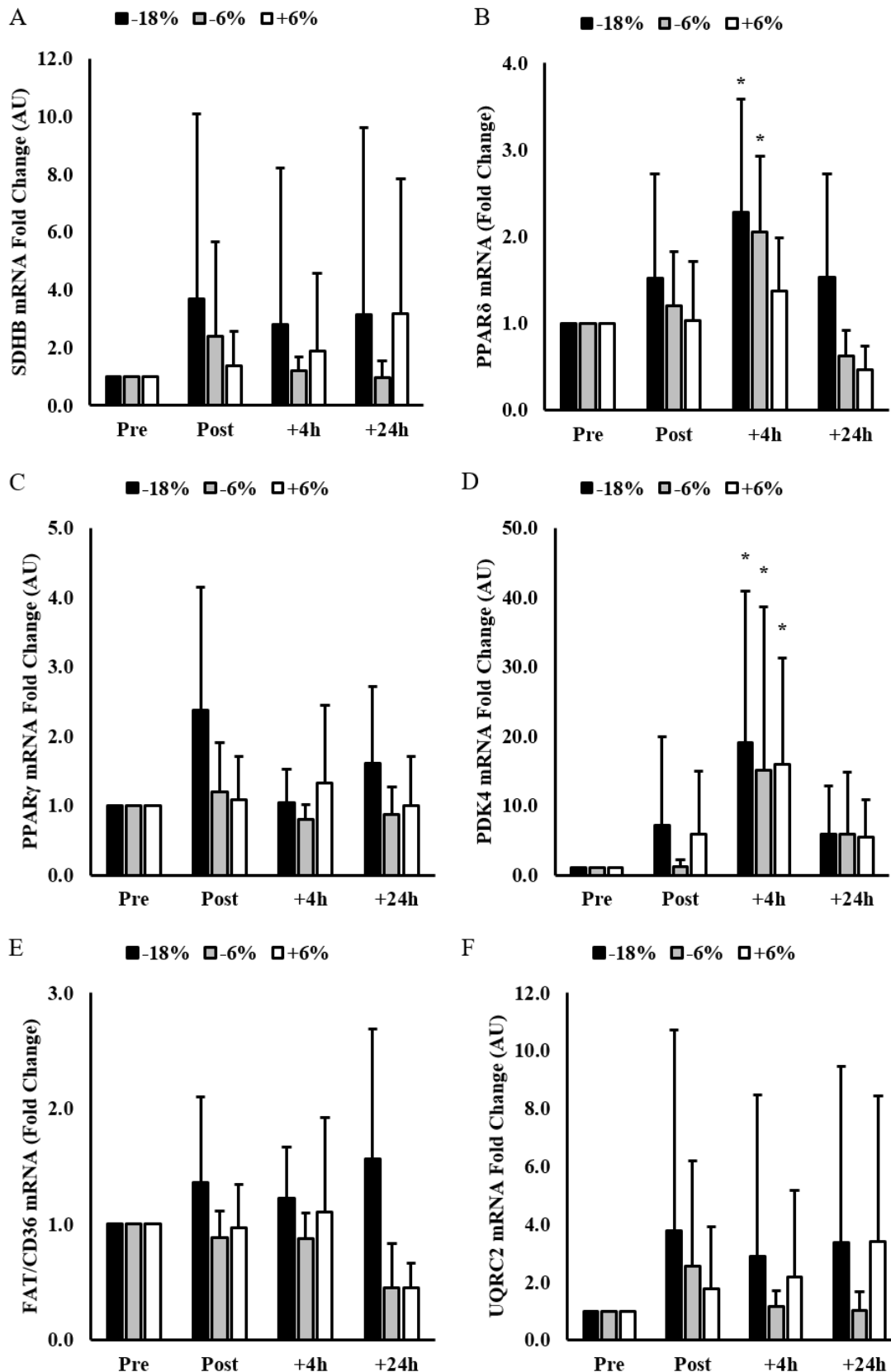


**Figure 4.11 (A-F).** The influence of exercise intensity on whole skeletal muscle mRNA immediately post, +4, and +24 hours from the onset of exercise performed at -18% of the maximal lactate steady state (MLSS) (black bars), -6% of the MLSS (grey shaded bars), and +6% of the MLSS (open bars). Mean fold changes  $\pm$  SD in arbitrary units (AU) for (A) Succinate dehydrogenase complex iron sulfur subunit B (SDHB), (B) peroxisome proliferator-activated receptor delta (PPAR $\delta$ ), (C) peroxisome proliferator-activated receptor gamma (PPAR $\gamma$ ), (D) Pyruvate dehydrogenase lipoamide kinase isozyme 4 (PDK4), (E) Fatty acid translocase/CD36 (FAT/CD36), (F) Cytochrome b-c1 complex subunit 2 (UQRC2). Expression of each target gene was normalised to the geometric mean of expression of the three most stable genes (i.e., TBP, B2M and GAPDH). \* = significantly different from Pre.

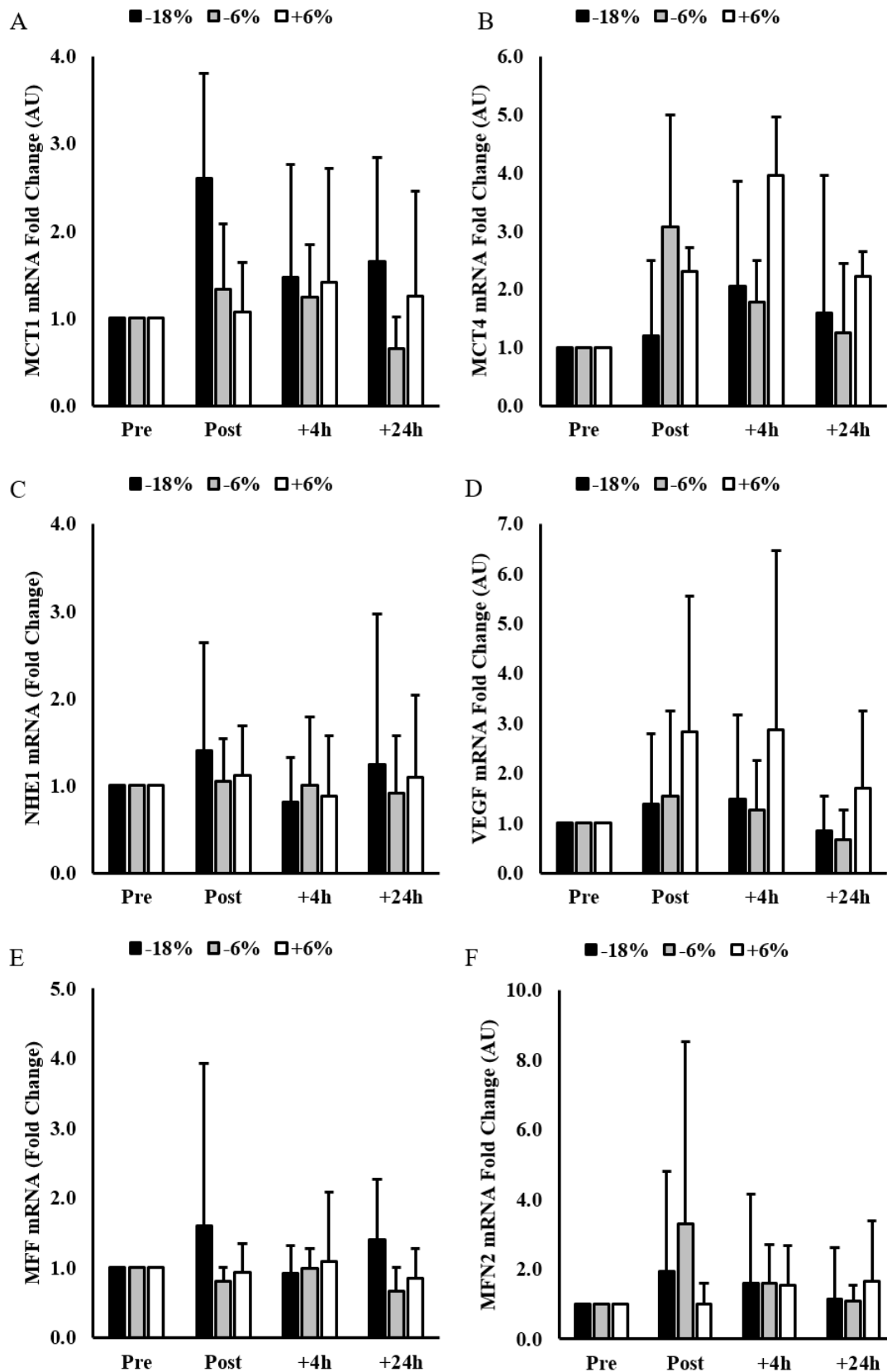


**Figure 4.12 (A-F).** The influence of exercise intensity on whole skeletal muscle mRNA immediately post, +4, and +24 hours from the onset of exercise performed at -18% of the maximal lactate steady state (MLSS) (black bars), -6% of the MLSS (grey shaded bars), and +6% of the MLSS (open bars). Mean fold changes  $\pm$  SD in arbitrary units (AU) for (A) Monocarboxylate transporter 1 (MCT1), (B) Monocarboxylate transporter 4 (MCT4), (C) Sodium-hydrogen antiporter 1 (NHE1), (D) Vascular endothelial growth factor (VEGF), (E) Mitochondrial Fission Factor (MFN2) and (F) Mitofusin 2 (MFN2). Expression of each target gene was normalised to the geometric mean of expression of the three most stable genes (i.e., TBP, B2M and GAPDH).

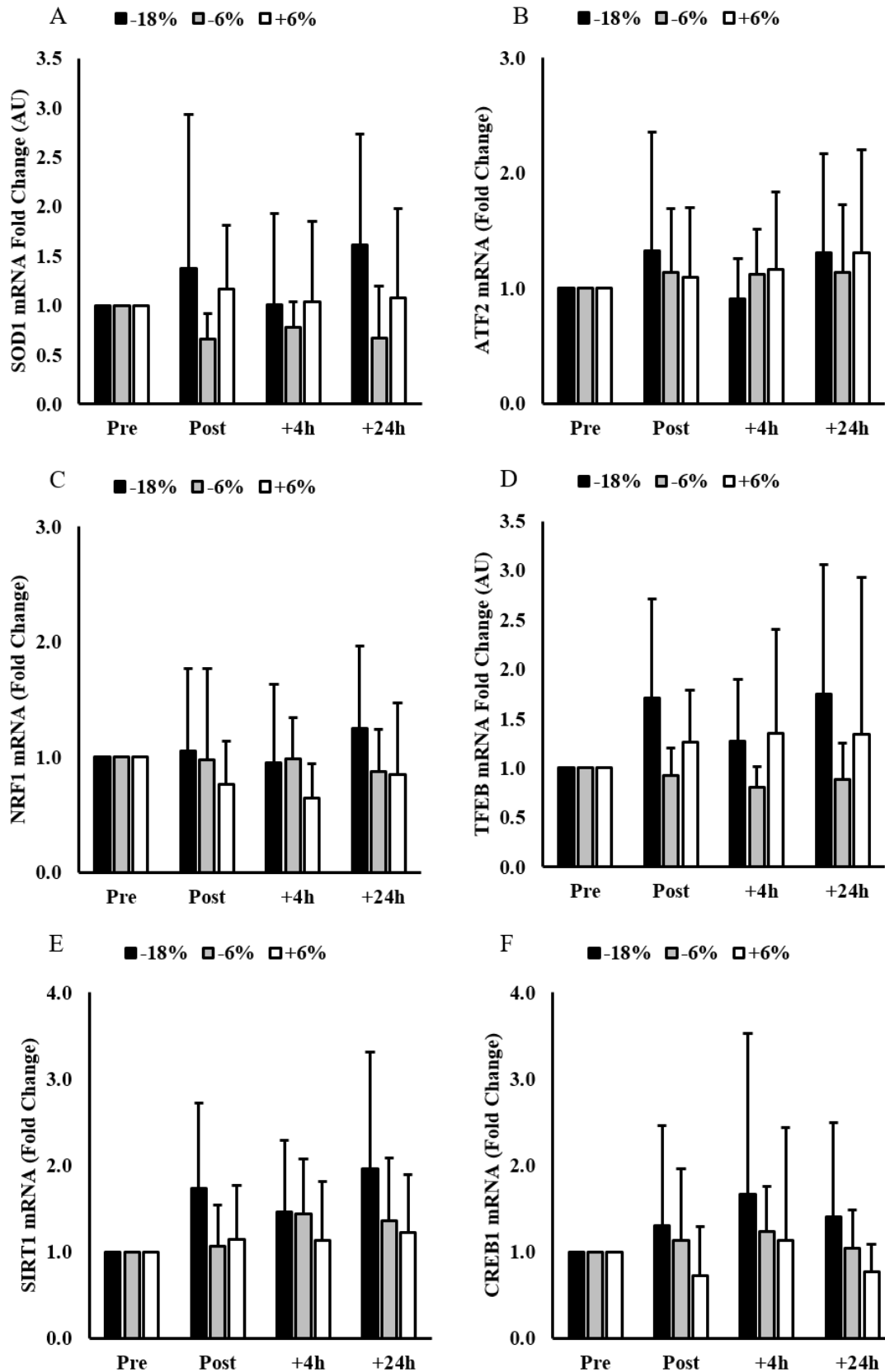


**Figure 4.13 (A-F).** The influence of exercise intensity on whole skeletal muscle mRNA immediately post, +4, and +24 hours from the onset of exercise performed at -18% of the maximal lactate steady state (MLSS) (black bars), -6% of the MLSS (grey shaded bars), and +6% of the MLSS (open bars). Mean fold changes  $\pm$  SD in arbitrary units (AU) for (A) Superoxide dismutase 1 (SOD1), (B) Activating transcription factor 2 (ATF2), (C) Nuclear respiratory factor 1 (NRF1), (D) Transcription factor EB (TFEB), (E) NAD-dependent deacetylase sirtuin-1 (SIRT1) and (F) CAMP responsive element binding protein 1 (CREB1). Expression of each target gene was normalised to the geometric mean of expression of the three most stable genes (i.e., TBP, B2M and GAPDH).

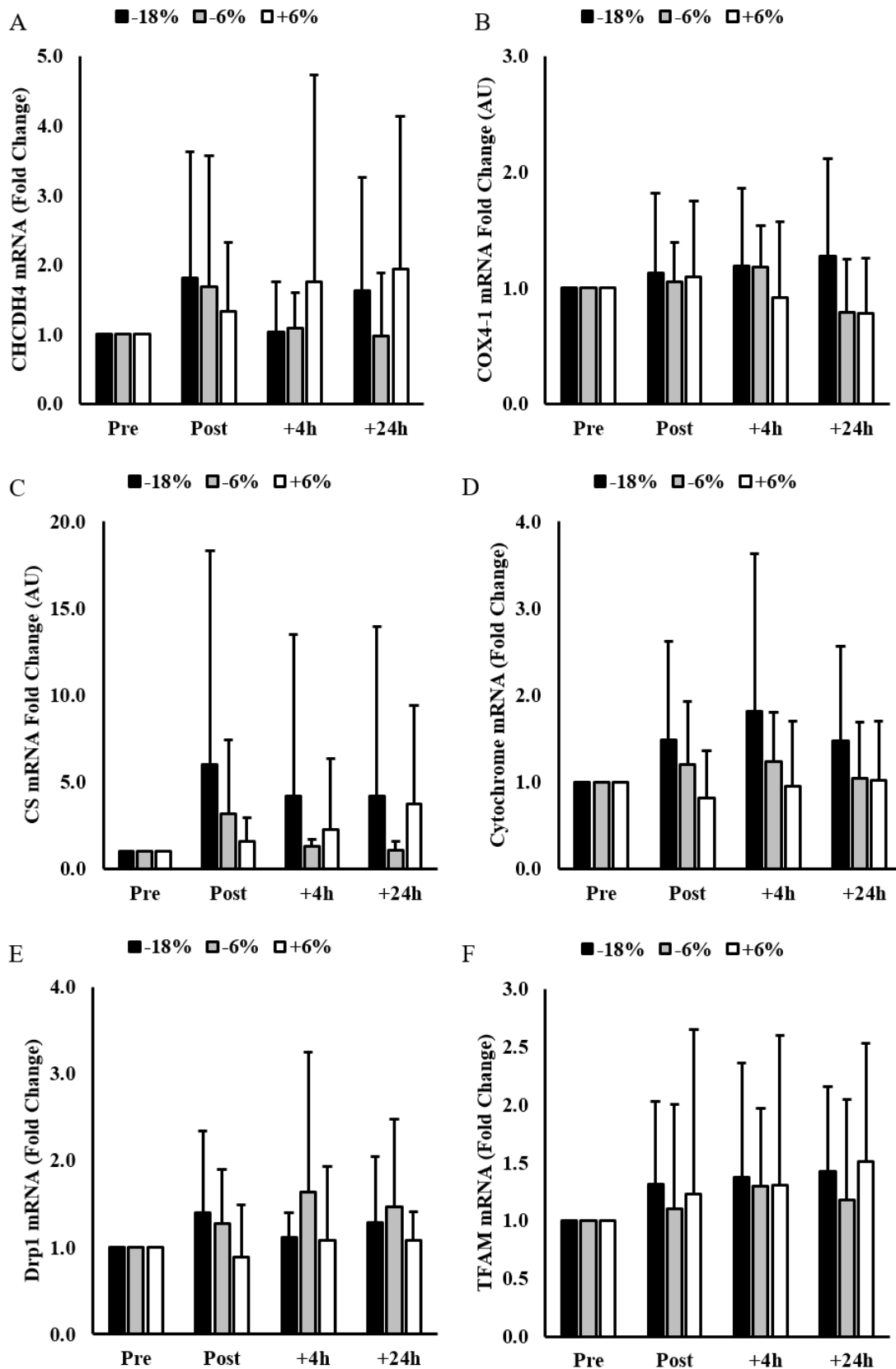


**Figure 4.14 (A-F).** The influence of exercise intensity on whole skeletal muscle mRNA immediately post, +4, and +24 hours from the onset of exercise performed at -18% of the maximal lactate steady state (MLSS) (black bars), -6% of the MLSS (grey shaded bars), and +6% of the MLSS (open bars). Mean fold changes  $\pm$  SD in arbitrary units (AU) for (A) Mitochondrial intermembrane space import and assembly protein 40 (CHCDH4), (B) cytochrome c oxidase subunit 4 isoform 1 (COX4-1), (C) Citrate Synthase (CS), (D) Cytochrome (Cyt C), (E) Cytochrome b-c1 complex subunit 2 (DRP1), and (F) Mitochondrial transcription factor A (TFAM). Expression of each target gene was normalised to the geometric mean of expression of the three most stable genes (i.e., TBP, B2M and GAPDH).

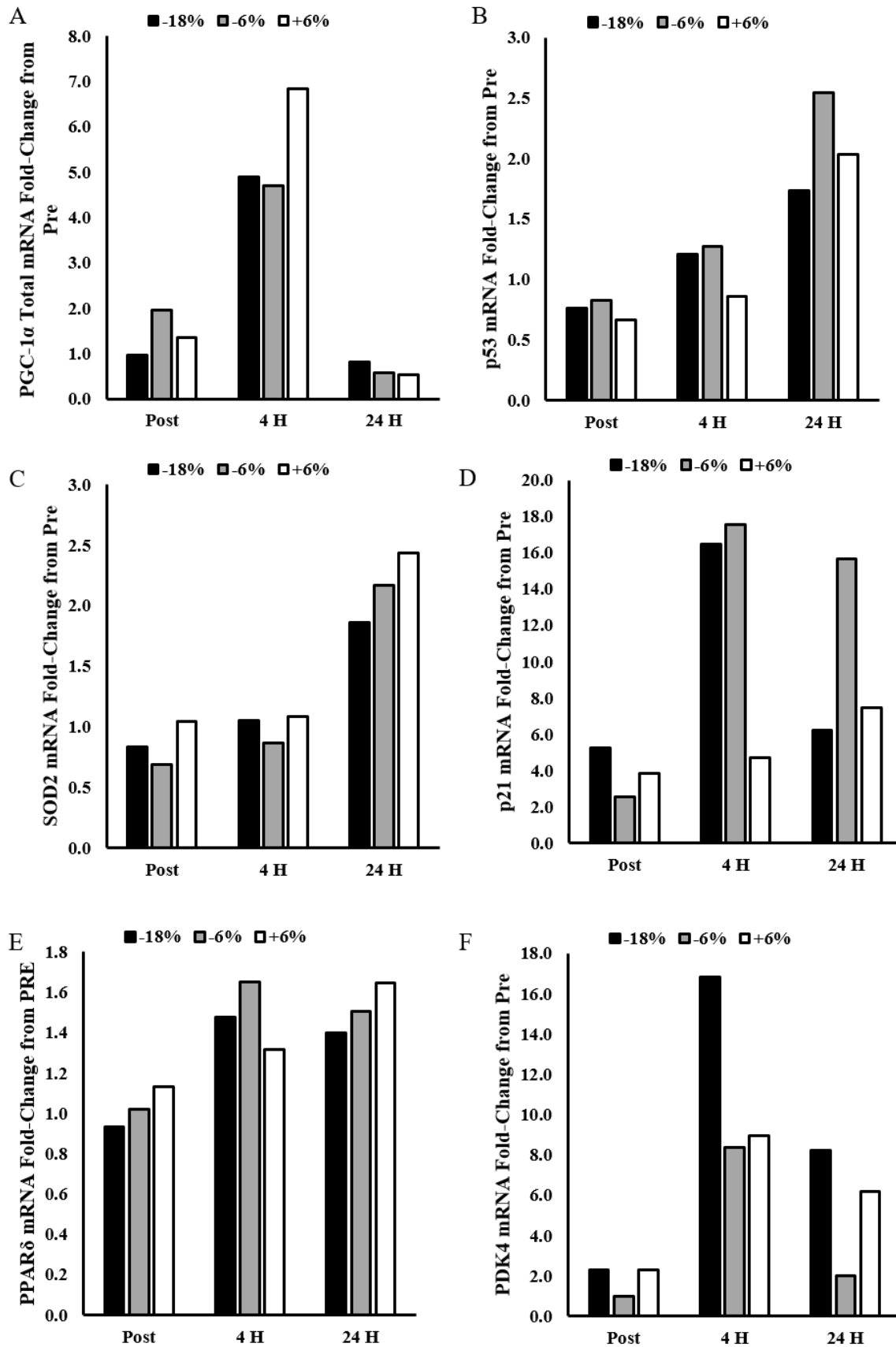


**Figure 4.15 (A-F).** The influence of exercise intensity on whole skeletal muscle mRNA measured via RNA-Sequencing immediately post, +4, and +24 hours from the onset of exercise performed at -18% of the maximal lactate steady state (MLSS) (black bars), -6% of the MLSS (grey shaded bars), and +6% of the MLSS (open bars). Mean fold changes  $\pm$  SD in arbitrary units (AU) for (A) Peroxisome proliferator-activated receptor gamma coactivator 1-alpha total (PGC-1 $\alpha$ -total), (B) tumour suppressor protein 53 (p53), (C) Superoxide dismutase 2 (SOD2), (D) cyclin-dependent kinase inhibitor 1 (p21), (E) peroxisome proliferator-activated receptor delta (PPAR $\delta$ ), and (F) Pyruvate dehydrogenase lipoamide kinase isozyme 4 (PDK4). n = 18

**Table 4.3** Effect Sizes [Low and High, 90% confidence intervals] for changes in whole skeletal muscle mRNA, immediately post, 4 and 24 hours from the onset of exercise at -18%, -6% and +6% of the maximal lactate steady state (MLSS). Trivial < 0.3; Small < 0.6; Moderate < 1.2; Large < 2.0, Very Large < 4.0.

(Effect Size) [Low, High; 90% Confidence Interval] Effect Size: Trivial, Small, Moderate, Large, Very Large and Very Very Large.						
Post Exercise			Post Exercise			
	+4 Hours	+24 Hours	+4 Hours	+24 Hours		
<b>Activating transcription factor 2 (ATF2)</b>			<b>Fatty acid translocase (FAT/CD36)</b>			
-18%	(0.1) [0,0.2] Trivial	(-0.4) [-0.5,-0.3] Small	(0.2) [0.2,0.3] Trivial	(0.3) [0.2,0.4] Trivial	(0.1) [0.1,0.2] Trivial	(0.4) [0.3,0.5] Small
-6%	(0.2) [0.1,0.3] Trivial	(0.2) [0.1,0.3] Trivial	(-0.1) [-0.2,-0.1] Trivial	(-0.3) [-0.4,-0.3] Small	(-0.4) [-0.5,-0.3] Small	(-1.6) [-1.6,-1.5] Large
+6%	(0.1) [0,0.2] Trivial	(0.1) [0,0.2] Trivial	(0.3) [0.2,0.4] Trivial	(-0.2) [-0.3,-0.1] Trivial	(-0.1) [-0.1,0] Trivial	(-1.2) [-1.2,-1.1] Moderate
<b>Mitochondrial intermembrane space import and assembly protein 40 (CHCDH4)</b>			<b>CAMP responsive element binding protein 1 (CREB1)</b>			
-18%	(-0.2) [-0.5,0.1] Trivial	(-0.2) [-0.6,0.1] Trivial	(-0.3) [-0.6,0.1] Trivial	(0) [-3.3,3.3] Trivial	(0.2) [-3.8,4.3] Trivial	(0) [-3.4,3.5] Trivial
-6%	(0.2) [-0.2,0.5] Trivial	(-0.1) [-0.4,0.2] Trivial	(-0.4) [-0.7,-0.1] Small	(0) [-3.2,3.3] Trivial	(0.2) [-3.1,3.4] Trivial	(0.1) [-3.2,3.4] Trivial
+6%	(0.2) [-0.1,0.6] Trivial	(0.1) [-0.3,0.4] Trivial	(0.2) [-0.1,0.5] Trivial	(-0.4) [-3.8,3.1] Small	(-0.4) [-3.7,2.9] Small	(-0.4) [-3.7,2.8] Small
<b>Cytochrome c oxidase subunit 4 isoform 1 (COX4-1)</b>			<b>Citrate Synthase (CS)</b>			
-18%	(0) [-0.7,0.7] Trivial	(0) [-0.6,0.7] Trivial	(0.1) [-0.6,0.8] Trivial	(0.5) [0.4,0.7] Small	(0.2) [0.1,0.3] Trivial	(0) [-0.1,0.1] Trivial
-6%	(0) [-0.8,0.7] Trivial	(0.1) [-0.7,1] Trivial	(-0.5) [-1.2,0.3] Small	(0.8) [0.6,1.1] Moderate	(0.2) [0.2,0.3] Trivial	(0.2) [0.1,0.3] Trivial
+6%	(0.2) [-0.5,0.9] Trivial	(0) [-0.7,0.6] Trivial	(-0.2) [-0.8,0.5] Trivial	(0.2) [0.1,0.3] Trivial	(0.4) [0.3,0.5] Small	(0.8) [0.7,0.9] Moderate
<b>Cytochrome (Cyt C)</b>			<b>Cytochrome b-c1 complex subunit 2 (DRP1)</b>			
-18%	(0.1) [-3.3,1] Trivial	(0.2) [-3.5,3.9] Trivial	(0.2) [-3.3,4] Trivial	(0.3) [0.3,0.3] Trivial	(0.1) [0.1,0.1] Trivial	(0.2) [0.2,0.3] Trivial
-6%	(0) [-3.4,3.3] Trivial	(-0.1) [-3.2,3] Trivial	(-0.4) [-3.5,2.7] Small	(0.1) [0.1,0.1] Trivial	(0.3) [0.3,0.4] Small	(0.3) [0.2,0.3] Trivial
+6%	(-0.4) [-3.8,2.9] Small	(-0.5) [-3.6,2.7] Small	(-0.4) [-3.5,2.6] Small	(-0.4) [-0.5,-0.4] Small	(-0.4) [-0.4,-0.3] Small	(-0.1) [-0.1,-0.1] Trivial
<b>Monocarboxylate transporter 1 (MCT1)</b>			<b>Monocarboxylate transporter 4 (MCT4)</b>			
-18%	(0.3) [-0.6,1.2] Small	(0) [-0.9,0.8] Trivial	(0.1) [-0.8,1] Trivial	(0.8) [0.7,0.9] Moderate	(0.6) [0.6,0.7] Small	(0.2) [0.1,0.3] Trivial
-6%	(0.2) [-0.7,1.2] Trivial	(0) [-0.8,0.8] Trivial	(-0.5) [-1.3,0.3] Small	(0.9) [0.8,1] Moderate	(0.3) [0.3,0.4] Small	(0.1) [0,0.2] Trivial
+6%	(-0.4) [-1.2,0.4] Small	(-0.2) [-1,0.7] Trivial	(-0.3) [-1.2,0.5] Small	(0.5) [0.5,0.6] Small	(0.5) [0.4,0.6] Small	(-0.1) [-0.1,0] Trivial
<b>Mitochondrial Fission Factor (MFF)</b>			<b>Mitofusin 2 (MFN2)</b>			
-18%	(0.2) [0.2,0.2] Trivial	(-0.3) [-0.3,-0.2] Trivial	(0.2) [0.2,0.3] Trivial	(0.1) [0,0.1] Trivial	(0.2) [0.1,0.2] Trivial	(-0.4) [-0.5,-0.4] Small
-6%	(-0.3) [-0.3,-0.3] Trivial	(0) [0,0.1] Trivial	(-0.9) [-0.9,-0.9] Moderate	(0.7) [0.7,0.8] Moderate	(0.2) [0.1,0.2] Trivial	(0) [-0.1,0] Trivial
+6%	(-0.1) [-0.2,-0.1] Trivial	(-0.2) [-0.2,-0.1] Trivial	(-0.4) [-0.4,-0.3] Small	(0) [-0.1,0] Trivial	(0.5) [0.4,0.5] Small	(0.5) [0.5,0.6] Small
<b>Sodium-hydrogen antiporter 1 (NHE1)</b>			<b>Nuclear Respiratory Factor 1 (NRF1)</b>			
-18%	(0) [0,0] Trivial	(-0.7) [-0.7,-0.6] Small	(-0.2) [-0.2,-0.1] Trivial	(-0.2) [-0.2,-0.2] Trivial	(-0.4) [-0.4,-0.4] Small	(0.2) [0.2,0.2] Trivial
-6%	(0) [-0.1,0] Trivial	(-0.3) [-0.3,-0.3] Trivial	(-0.5) [-0.6,-0.5] Small	(-0.1) [-0.2,-0.1] Trivial	(-0.2) [-0.2,-0.2] Trivial	(-0.7) [-0.7,-0.6] Small
+6%	(0.1) [0,0.1] Trivial	(-0.4) [-0.5,-0.4] Small	(-0.2) [-0.2,-0.2] Trivial	(-0.7) [-0.7,-0.7] Moderate	(-1.1) [-1.1,-1.1] Moderate	(-0.6) [-0.6,-0.6] Small

<b>Cyclin-dependent kinase inhibitor 1 (p21)</b>			<b>Tumor protein 53 (p53)</b>			
-18%	(1.1) [1.1,1.2] Moderate	(0.8) [0.7,0.8] Moderate	(1.2) [1.2,1.2] Moderate	(0.4) [0.4,0.4] Small	(0.5) [0.5,0.5] Small	(0.5) [0.5,0.5] Small
-6%	(1.2) [1.2,1.2] Moderate	(1.8) [1.8,1.8] Large	(1.4) [1.4,1.4] Moderate	(-0.1) [-0.1,-0.1] Trivial	(0.5) [0.5,0.5] Small	(1.3) [1.3,1.4] Moderate
+6%	(1.2) [1.2,1.2] Moderate	(1.5) [1.5,1.6] Large	(1.5) [1.4,1.5] Large	(-0.3) [-0.3,-0.2] Trivial	(0.2) [0.2,0.2] Trivial	(1.5) [1.5,1.6] Large
<b>Pyruvate dehydrogenase lipoamide kinase isozyme 4 (PDK4)</b>			<b>Peroxisome proliferator-activated receptor gamma coactivator 1-alpha isoform 1 (PGC-1<math>\alpha</math>-1)</b>			
-18%	(0.7) [0.5,0.9] Moderate	(1.5) [1.4,1.7] Large	(1) [0.9,1.2] Moderate	(0.5) [0.5,0.6] Small	(0.6) [0.5,0.6] Small	(-0.3) [-0.4,-0.3] Small
-6%	(-0.4) [-0.5,-0.4] Small	(1.7) [1.4,1.9] Large	(0.7) [0.6,0.8] Small	(0.9) [0.8,0.9] Moderate	(1.2) [1.1,1.2] Moderate	(-0.6) [-0.7,-0.6] Small
+6%	(0.7) [0.6,0.8] Moderate	(1.1) [0.6,1.7] Moderate	(1.4) [1.3,1.5] Large	(0.1) [0,0.1] Trivial	(0.6) [0.6,0.7] Small	(-0.6) [-0.6,-0.5] Small
<b>Peroxisome proliferator-activated receptor gamma coactivator 1-alpha isoform 4 (PGC-1<math>\alpha</math>-4)</b>			<b>Peroxisome proliferator-activated receptor gamma coactivator 1-alpha (PGC1a-Total)</b>			
-18%	(0.2) [0.1,0.3] Trivial	(1.4) [1.3,1.5] Moderate	(0.4) [0.3,0.5] Small	(0.6) [0.2,1] Small	(1.7) [1.3,2.1] Large	(0.6) [0.3,0.9] Small
-6%	(0.4) [0.1,0.7] Small	(1.1) [0.9,1.3] Moderate	(-1) [-1.1,-0.9] Moderate	(0.5) [-0.1,1.2] Small	(3.1) [2.8,3.4] Very Large	(-1.1) [-1.4,-0.9] Moderate
+6%	(0.1) [0,0.2] Trivial	(1.5) [1.3,1.7] Large	(-0.6) [-0.7,-0.5] Small	(0.4) [0,0.7] Small	(1.8) [1.3,2.3] Large	(-1.1) [-1.3,-0.9] Moderate
<b>Peroxisome proliferator-activated receptor alpha (PPAR<math>\alpha</math>)</b>			<b>Peroxisome proliferator-activated receptor delta (PPAR<math>\delta</math>)</b>			
-18%	(0.1) [-0.4,0.6] Trivial	(1.2) [0.5,1.8] Moderate	(0.4) [-0.2,0.9] Small	(0.4) [0.4,0.4] Small	(1) [1,1] Moderate	(0.2) [0.1,0.2] Trivial
-6%	(0.4) [-0.8,1.5] Small	(0.7) [-0.1,1.5] Moderate	(-0.6) [-1,-0.1] Small	(0.1) [0.1,0.1] Trivial	(1.5) [1.4,1.5] Large	(-0.8) [-0.9,-0.8] Moderate
+6%	(-0.5) [-0.9,0] Small	(0.9) [-0.2,1.9] Moderate	(-0.7) [-1.2,-0.2] Moderate	(0) [-0.1,0] Trivial	(0.5) [0.5,0.6] Small	(-1.3) [-1.4,-1.3] Moderate
<b>Peroxisome proliferator-activated receptor gamma (PPAR<math>\gamma</math>)</b>			<b>Succinate dehydrogenase complex iron sulfur subunit B (SDHB)</b>			
-18%	(0.7) [0.7,0.7] Moderate	(-0.2) [-0.2,-0.2] Trivial	(0.2) [0.1,0.2] Trivial	(0.4) [-0.1,1] Small	(0.1) [-0.4,0.6] Trivial	(0) [-0.5,0.6] Trivial
-6%	(-0.2) [-0.2,-0.2] Trivial	(-0.4) [-0.5,-0.4] Small	(-0.5) [-0.5,-0.5] Small	(0.6) [-1.1,2.4] Small	(0.1) [-0.4,0.6] Trivial	(0.2) [-0.5,0.9] Trivial
+6%	(-0.1) [-0.1,-0.1] Trivial	(0.1) [0.1,0.1] Trivial	(-0.3) [-0.4,-0.3] Small	(0) [-0.5,0.4] Trivial	(0.2) [-0.3,0.7] Trivial	(0.5) [0.1,1] Small
<b>NAD-dependent deacetylase sirtuin-1 (SIRT1)</b>			<b>Superoxide dismutase 1 (SOD1)</b>			
-18%	(0.5) [0.5,0.6] Small	(0.2) [0.2,0.3] Trivial	(0.6) [0.6,0.7] Small	(-0.2) [-0.5,0.1] Trivial	(-0.3) [-0.6,0] Small	(0.2) [-0.2,0.5] Trivial
-6%	(-0.1) [-0.1,0] Trivial	(0.4) [0.4,0.4] Small	(0.2) [0.2,0.2] Trivial	(-0.5) [-0.9,-0.2] Small	(-0.6) [-0.9,-0.2] Small	(-0.9) [-1.2,-0.6] Moderate
+6%	(0.2) [0.2,0.3] Trivial	(0.3) [0.2,0.3] Trivial	(0.3) [0.3,0.3] Small	(0) [-0.3,0.3] Trivial	(-0.1) [-0.4,0.2] Trivial	(-0.2) [-0.5,0.1] Trivial
<b>Superoxide dismutase 2 (SOD2)</b>			<b>Mitochondrial transcription factor A (TFAM)</b>			
-18%	(0.3) [0.3,0.4] Small	(0.1) [0.1,0.2] Trivial	(0.6) [0.6,0.7] Small	(0.2) [0.1,0.3] Trivial	(0.1) [0,0.2] Trivial	(0.4) [0.3,0.5] Small
-6%	(-0.5) [-0.5,-0.5] Small	(-0.2) [-0.2,-0.2] Trivial	(0.6) [0.6,0.7] Small	(-0.1) [-0.2,0] Trivial	(0.2) [0.1,0.3] Trivial	(-0.1) [-0.1,0] Trivial
+6%	(0.2) [0.2,0.2] Trivial	(0.2) [0.2,0.2] Trivial	(1.3) [1.3,1.3] Moderate	(-0.1) [-0.1,0] Trivial	(-0.2) [-0.3,-0.1] Trivial	(0.1) [0,0.2] Trivial
<b>Transcription factor EB (TFEB)</b>			<b>Cytochrome b-c1 complex subunit 2 (UQR2)</b>			
-18%	(0.6) [0.6,0.6] Small	(0.6) [0.6,0.6] Small	(0.1) [0.1,0.1] Trivial	(0.1) [-0.3,0.5] Trivial	(-0.1) [-0.5,0.3] Trivial	(-0.1) [-0.5,0.3] Trivial
-6%	(-0.3) [-0.3,-0.3] Trivial	(-0.3) [-0.3,-0.3] Trivial	(-0.5) [-0.5,-0.5] Small	(-0.4) [-0.9,0.2] Small	(-1.2) [-1.6,-0.8] Moderate	(-1) [-1.5,-0.6] Moderate
+6%	(0.3) [0.3,0.3] Trivial	(0.3) [0.3,0.3] Trivial	(0.2) [0.2,0.2] Trivial	(-0.2) [-0.5,0.2] Trivial	(-0.1) [-0.5,0.3] Trivial	(0) [-0.4,0.4] Trivial

Vascular Endothelial Growth Factor (VEGF)			
-18%	(0.3) [0.2,0.3] Trivial	(0.1) [0.1,0.2] Trivial	(-0.6) [-0.6,-0.5] Small
-6%	(0.5) [0.5,0.5] Small	(0.4) [0.4,0.4] Small	(-0.3) [-0.3,-0.3] Trivial
+6%	(0.3) [0.2,0.3] Trivial	(0.4) [0.4,0.4] Small	(0.3) [0.2,0.3] Trivial

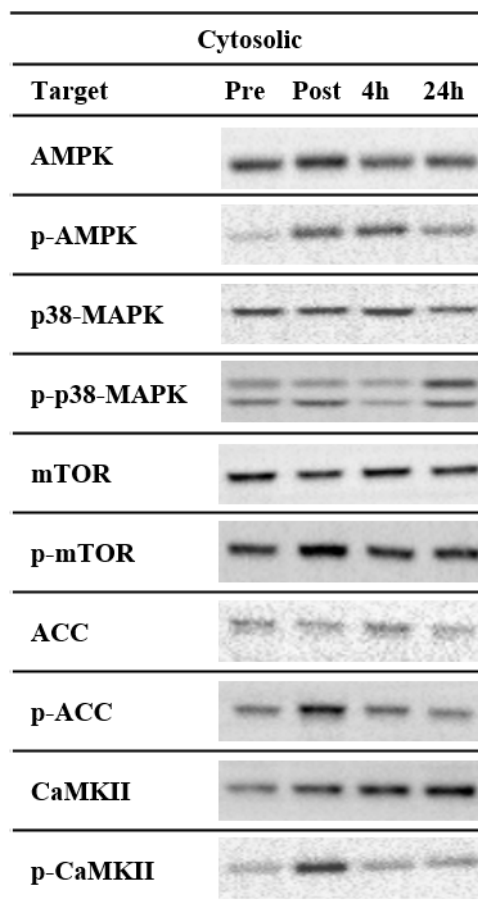


**Figure 4.16. Representative western blots for the phosphorylation and total of mammalian target of rapamycin (mTOR),  $\text{Ca}^{2+}$  calmodulindependent protein kinase II (CaMKII), acetyl-CoA carboxylase (ACC), AMP-activated protein kinase alpha (AMPK) protein, acetyl-CoA carboxylase (ACC) protein, p38 mitogen-activated protein kinase (p38 MAPK) protein.**

#### 4.5 Discussion

The main findings of the present study include a disproportionate increase in blood and intramuscular lactate concentration when exercise intensity was increased from below to above the MLSS. The greater homeostatic perturbations produced by the highest exercise intensity were associated with a larger number of differentially expressed genes at +4 h when compared

with exercise performed at intensities below the MLSS. However, when comparing -6% and +6% MLSS there was no difference in the number of differentially expressed genes at +24 h. Increasing the intensity above the MLSS led to a decrease in the number of upregulated genes and an increase in the number of downregulated genes. The results of the qPCR indicated that PGC-1 $\alpha$  and p53 mRNA were influenced by exercise intensity, with the largest fold changes observed following exercise performed at +6% MLSS at +4 h and +24 h, respectively. The lowest intensity yielded the greatest fat oxidation rate as well as the greatest changes in the expression of genes associated with fatty acid metabolism (e.g., PPAR $\delta$ ); however, with the scope of our analysis it is impossible to confirm this association as a mechanism.

The blood and muscle lactate data are consistent with previous research [13, 57, 87, 88, 90, 185, 446]. Exercise at -18% MLSS resulted in a blood lactate concentration close to resting values ( $\sim 1.6 \text{ mmol}\cdot\text{L}^{-1}$ ), and a large increase in muscle lactate ( $+6 \text{ mmol}\cdot\text{kg}^{-1} \text{ dw}$ ; ES: 1.7 [0.5, 3.0]) (**Figure 4.4, B and C**). There was a steady state above baseline for blood lactate following exercise at -6% MLSS and a very large increase in muscle lactate ( $+24 \text{ mmol}\cdot\text{kg}^{-1} \text{ dw}$ ; ES: 2.7 [-0.4, 5.9]) (**Figure 4.4, B and C**). The highest intensity (+6% MLSS) resulted in a continual increase in blood lactate without a steady state and a very very large increase in muscle lactate ( $+52 \text{ mmol}\cdot\text{kg}^{-1} \text{ dw}$ ; ES: 6.1 [2.9, 9.2]) (**Figure 4.4, B and C**). There was a larger gain in post-exercise intramuscular lactate concentration when exercise exceeded the MLSS (ES: 0.7). Thus, consistent with previous literature, increasing exercise intensity increased both blood and muscle lactate, with a disproportionate increase when exercise went from below (-6% MLSS) to above (+6%) the MLSS.

Of the signalling kinases measured in the cytosolic subcellular muscle fraction, there was no main effect for any of the targets measured (**Figure 4.5**). These findings contrast with

some previous research; for example, increases in p-AMPK have been reported in whole-muscle samples following exercise above 70%  $\dot{V}O_{2\max}$  [15, 18, 286, 443, 472, 473]. However, this was not observed in the cytosolic fraction in the present study following exercise any of the 3 exercise biopsy trials (i.e., 70-90% of  $\dot{V}O_{2\max}$  or 50 to 65% of  $\dot{W}_{\max}$ ). To my knowledge, no study has investigated the influence of exercise intensity on cytosolic signalling kinases using the present subcellular fractionation protocol. One study used a commercially-available subcellular fraction kit [69]; however, the purity of subcellular fractions using the commercially-available kit has been questioned [19]. Nonetheless, consistent with the present results they observed no significant changes in the measured signalling kinases (i.e., p-p38 MAPK and p-ACC) in the cytosolic fraction following submaximal exercise (i.e., 55%  $\dot{W}_{\max}$ ). They did observe significant increases in these kinases following sprint interval training. This, while more research is required, it appears the cytosolic content of the measured signalling kinases is not influenced by submaximal exercise. Lastly, the lack of observed change in signalling kinases in the cytosol could possibly be attributed to the translocation of these kinases to the nucleus in response to exercise [10, 15, 96].

Despite observing no main effect for the effect of exercise on the measured cytosolic signalling kinases, intensity appeared to influence the modulation of p-CaMKII<sup>Thr286</sup> with a 2.0- and a 3.4-fold change observed immediately post exercise performed at -6% and +6% of the MLSS, respectively. The lack of statistical significance could be attributed to the high variability associated with western blotting [474]. Previous research has shown that higher exercise intensities result in significantly greater increases in p-CaMKII in whole-muscle samples compared with lower exercise intensities [15, 18]. Indirect measures of Ca<sup>2+</sup> flux (e.g., glycogen phosphorylase or pyruvate dehydrogenase activity) [14] or reactive oxygen species (ROS) production [352], which both modulate p-CaMKII<sup>Thr286</sup>, were not quantified due to

insufficient muscle sample sizes. Nonetheless, previous research examining the influence of exercise intensity on glycogen phosphorylase and pyruvate dehydrogenase activity across three intensities has reported a disproportionate increase in the activity of these enzymes at the highest exercise intensity [14]. Furthermore, higher exercise intensities are associated with greater increases in ROS production [16, 352], which may be attributed, at least in part, to the greater lactate produced via glycolysis [352]. Thus, multiple lines of evidence suggest there is an intensity-dependent effect on p-CaMKII, with a disproportionate increase when intensity exceeds the maximal steady state.

The number of differentially expressed genes is similar to previous research, which has reported 1,024 and 853 differentially expressed genes +4.5 h and +7 h, respectively, from the onset of an aerobic exercise session (i.e., 2 hours at 60% of  $\dot{V}O_{2peak}$ ) - measured via DNA microarray [475]. Another study examined the differential expression of genes via microarray +5 h from the onset of an hour of cycling (i.e., ~73%  $\dot{V}O_{2max}$ ) immediately followed by an hour of running (i.e., ~87%  $\dot{V}O_{2max}$ ) and reported 102 differentially expressed genes [476]. A similar result was observed via cDNA microarrays +4.25 h from the onset of exercise (i.e., 60 to 85% of  $\dot{V}O_{2max}$ ; described in [477]), where 118 genes were differentially expressed [441]. Neither study examined the response +24 h from the onset of exercise. To my knowledge, there is no research investigating the influence of multiple exercise intensities within the same population on the number of differentially expressed genes assessed via RNA-sequencing.

The qPCR results indicate that exercise intensity also influenced the expression of some of the measured genes. For example, PGC-1 $\alpha$  total mRNA increased  $3.1 \pm 1.9$ ,  $3.6 \pm 1.6$ , and  $4.9 \pm 5.5$  fold +4 hours following the onset of exercise at -18, -6, and +6% of the MLSS, respectively – these findings are consistent with the RNA-sequencing analysis (**Figure 4.10**,

**Panel C; Figure 4.15, Panel A).** These fold changes are consistent with previous research following exercise at similar intensities [15, 282, 284, 439, 442]. A larger increase in PGC-1 $\alpha$  mRNA was observed following exercise at 80% compared with 40% of  $\dot{V}O_{2\max}$  (10.0 vs. 3.8 fold-change, respectively) [15], and PGC-1 $\alpha$  mRNA was higher following exercise at 81% compared to 65% of  $\dot{V}O_{2\max}$  (5.5 vs. 2.7 fold-change, respectively) [282]. However, these studies only compared responses between two different exercise intensities. The present study employed three intensities, which allowed the investigation of if there was a linear or non-linear relationship between exercise intensity and markers associated with exercise-induced mitochondrial biogenesis. There was a larger fold change in PGC-1 $\alpha$  total mRNA when exercise intensity was increased to above the MLSS; mRNA increased 0.5 fold-change from -18% to -6% MLSS and 1.3 fold-change from -6% to +6% MLSS – a similar change was observed via RNA-seq (**Figure 4.15; Panel A**). The present results show a greater fold-change in PGC-1 $\alpha$  total mRNA for the same absolute increases in power above the MLSS compared to below the MLSS. These results suggest that increasing exercise intensity above the MLSS yields a disproportionate increase in PGC-1 $\alpha$  total mRNA.

There also appears to be an intensity-dependent increase in p53 – another gene associated with mitochondrial biogenesis (**Figure 4.10, Panel D**) [121, 415]. There was no significant change in p53 mRNA following exercise at -18% MLSS, but there was a significant increase in p53 mRNA +24 h from the onset of exercise at -6 and +6% of the MLSS ( $2.7 \pm 1.5$  and  $4.2 \pm 3.0$  fold-change, respectively) – this result is consistent with the RNA-seq analysis (**Figure 4.10, Panel C; Figure 4.15, Panel B**). Another study also observed significant increase in p53 mRNA (2.0 to 2.7-fold-change) +22 hours from the onset of the first of two high-intensity exercise sessions (i.e., 8 x 5 min @ 85% of  $\dot{V}O_{2\text{peak}}$ ) performed in a single day [478]. There was a larger fold change in p53 mRNA when exercise intensity was increased to

above the MLSS; mRNA increased 0.9 fold from -18% to -6% MLSS and 1.5 fold from -6% to +6% MLSS. These results suggest that exercise intensity influences the expression of p53 mRNA and that the MLSS yields a disproportionate increase +24 h from the onset of exercise. The absence of significant increase in p53 at the earlier time points is consistent with previous research that has observed < 1.5 fold changes 3 to 4 hours post exercise [69, 475, 478-483]

Previous research has demonstrated there is a reciprocal regulation of p53 and SOD2 mRNA [484]. Accordingly, SOD2 mRNA was also significantly increased +24 h from the onset of exercise following exercise at +6% MLSS – this result is consistent with the RNA-seq analysis (**Figure 4.10 Panel E; Figure 4.15, Panel C**). To my knowledge, there is no research that has measured SOD2 mRNA +24 h from the onset of exercise. However, previous research has reported non-significant changes in SOD2 mRNA +4 h from the onset of exercise, which is consistent with the small changes observed in the present study (i.e., 1.2, 1.4 and 1.2 fold change, for -18, -6, and +6% MLSS, respectively) [69, 70, 475, 478-483]. Furthermore, the phosphorylation of nuclear p53 (p-p53) modulates both p53 and p21 mRNA [485]. Similar to p53, there was an increase in p21 mRNA +4 and +24 h from the onset of exercise. These results are consistent with previous research, which has observed an increase in p21 mRNA +4 to 6 hours from the onset of exercise [480, 481, 486]. There was a sustained increase in p21 mRNA following exercise at the two highest intensities +24 h from the onset of exercise and, to my knowledge, no study has measured p21 mRNA +24 h from the onset of exercise. These results demonstrate that while SOD2 mRNA may not be upregulated until +24 h from the onset of exercise, p21 mRNA upregulation is sustained from +4 h to +24 h from the onset of exercise. These results further support the reciprocal regulation of p53 and SOD2 mRNA as well as the concomitant modulation of p53 and p21 mRNA.

There was an inverse relationship between exercise intensity and PPAR $\delta$  mRNA +4h after the onset of exercise – this result was consistent with the RNA-seq. analysis. There was a significant increase +4 h from the onset of exercise following exercise at both -18% and -6% MLSS, with the largest fold-change occurring after exercise performed at -18% MLSS (i.e., 2.3 fold-change) (**Figure 4.11 Panel B**). There is no research directly investigating the influence of exercise intensity on PPAR $\delta$  mRNA; however, a significant increase in PPAR $\delta$  mRNA has been reported +5 h from the onset of high-intensity exercise (i.e., 10 x 4-min intervals at ~90%  $\dot{V}O_{2peak}$ ) [64]. Furthermore, 75 min of exercise at 60 to 85% of  $\dot{V}O_{2max}$  (described in [477]), yielded a significant increase in PPAR $\delta$  ( $1.7 \pm 0.1$  fold-change) +4.25 h from the onset of exercise [441]. The fold changes observed in these studies and the present study are consistent with previous research [475, 479-483, 486, 487]. The inverse relationship between intensity and increases in PPAR $\delta$  mRNA in the present study could be explained by the higher rate of fat oxidation during the lower exercise intensities, as fatty acid transport into the nucleus via fatty acid binding protein (FABP) has been reported to modulate peroxisome proliferator activated receptor (PPARs) gene expression [403-405]. As previously mentioned, future research should elucidate the mechanism of fat acid oxidation and the pathways associated with exercise-induced mitochondrial biogenesis.

There was a significant increase in PDK4 mRNA +4 h from the onset of exercise compared to pre following all three intensities (**Figure 4.11, Panel D**). This is consistent with previous research [282], where PDK4 mRNA expression was independent of exercise intensity. [488]. It is possible that any exercise intensity that activates the oxidative pathways will upregulate PDK4 mRNA expression.

A limitation of the present study is the absence of measures related to primary messengers; specifically, indirect measures of  $\text{Ca}^{2+}$  flux (e.g., glycogen phosphorylase  $\alpha$  and PDH  $\alpha$ ), the redox state (e.g.,  $\text{NAD}^+/\text{NADH}$ ), and the AMP/ATP ratio were not measured. Therefore, I could not adequately characterise these responses relative to the MLSS which may have helped explain some of the present findings. Another limitation of the present study was that the  $\dot{V}\text{O}_2$  observed during the +6% MLSS underestimated the  $\dot{V}\text{O}_{2\text{max}}$  observed from the GXT, suggesting that the MLSS in the present may have underestimated the maximal steady state. This has also been observed in previous research, where exercise performed above the MLSS resulted in an underestimation of  $\dot{V}\text{O}_{2\text{max}}$  despite an observed continual rise in blood lactate [489]. It is possible that  $\dot{V}\text{O}_{2\text{max}}$  could have been achieved if the constant power-exercise bouts were not stopped at the pre-determined time derived from the familiarisation exhaustive trials. A recent review highlighted the shortcomings of the 30-min MLSS as a delineator of the maximal metabolic steady state [49]. Therefore, other anchors should also be considered when investigating exercise-induced mitochondrial biogenesis. Furthermore, it is not possible to conclude that this intensity corresponded to the maximal fat oxidation rate, even though the absolute rate of fat oxidation is similar to previously reported values ( $>6 \text{ kcal}\cdot\text{min}^{-1}$ ) [303, 310, 490], and future research should examine the influence of exercise performed at the maximal fat oxidation rate on cell signalling.

#### **4.6 Conclusions**

As discussed in Chapter 1, and as highlighted in the present study, prescribing exercise relative to a submaximal anchor is an advantageous approach to prescribing exercise. Despite a heterogeneous group of participants we observed a consistent homeostatic perturbations in all participants. Moreover, there appeared to be a larger fold-change following the exercise

performed above the MLSS in most measured targets associated with exercise-induced mitochondrial biogenesis. Although a similar relationship has been observed when prescribing exercise as a percentage of  $\text{VO}_{2\text{max}}$ , these results demonstrate that the MLSS allows for a more ‘fine-tuning’ approach to prescribing intensity. Specifically, exercise prescribed in close proximity to an anchor that represents a metabolic shift in the working state of muscle yields notable changes in homeostatic perturbations as well as changes in signalling pathways associated with exercise-induced mitochondrial biogenesis. Therefore, we recommend methods to prescribe exercise intensity based on their efficacy to yield an explicit and/or homogenous homeostatic perturbation.

## **Chapter 5: Findings, Limitations, and Practical Applications**

## 5.1 Key Findings

*Review 1 (Chapter 1)* highlighted the complexity of prescribing exercise intensity. There are a number of methods currently employed to prescribe exercise intensity, which include using maximal anchors (i.e.,  $\dot{V}O_{2\max}$ ,  $\dot{W}_{\max}$ , and/or  $HR_{\max}$ ), submaximal anchors ( $LT_1$ ,  $LT_2$ , GET/VT, RCP, MLSS, CP/CS), or a combination of anchors (i.e., “ $\Delta$ ”,  $\dot{V}O_{2R}$ ,  $HR_R$ ). Maximal anchors or a combination of anchors, although commonly used in sport and exercise physiology research, fail to normalise exercise intensity so as to elicit distinct and/or homogeneous homeostatic perturbations in different individuals. In contrast, the premise of submaximal anchors is to differentiate between exercise intensities based on substrate utilisation, oxygen uptake kinetics, and or blood lactate responses. Nonetheless, the validity of many submaximal anchors commonly used to establish training zones/intensities has not been robustly examined. The main conclusion from this review was that the validity of different methods to prescribe intensity should be based on whether they can accurately and reliably identify the boundaries between the different domains of exercise. There is promising evidence suggesting the GET/VT or  $LT_1$  derived from a GXT can identify the boundary between moderate and heavy exercise; however, more research is needed to confirm the validity of these methods. There is no research supporting the validity of GXT-derived submaximal anchors to identify the boundary between the heavy and severe domains of exercise; this can be attributed to the influence of GXT protocol design, the curvilinear increase in metabolic responses to exercise performed within the heavy or severe domains of exercise, and validity based on concurrent validity with another submaximal anchor. The MLSS derived via the traditional 30-min criteria appears to underestimate the heavy and severe boundary due to its conservative criterion. The single-visit MLSS has emerged as a technique that relies on abrupt changes in blood lactate to determine the MLSS; however, this has not been confirmed via  $\dot{V}O_2$  kinetics as a valid method to establish the boundary between heavy and severe domains of exercise. Therefore, future research should investigate the validity of the single-visit MLSS. There is

strong evidence to support the validity of CP/CS to identify the boundary between the heavy and severe domains of exercise but again, more research is required to optimise the testing procedures associated with CP/CS. In summary, I recommended that the systemic responses during constant work load exercise be used to confirm the domain of exercise relative to any submaximal anchor derived.

The writing of *Chapter 1 (Review 1)* has been ongoing since the start of 2017, and has been updated/supported by recent publications and discussions of controversies pertaining to prescribing submaximal aerobic exercise intensity. In this regard, the design of *Study 1 (Chapter 2)* occurred early in 2016 and was completed in May 2017. In particular, *Study 1* was based on publications questioning the use of GXT-derived submaximal anchors and the use of the MLSS as the “gold standard” for delineating the heavy and severe domains of exercise [5, 6, 49, 166, 168, 185, 194, 206, 211, 216, 237, 381, 491, 492]. The aim of *Study 1* was therefore to assess the validity of various lactate parameters derived from a GXT to identify the 30-min MLSS, the rationale being the LT had been long accepted as a viable method to prescribe exercise intensity. However, as described above, since completing this study some researchers have questioned the validity of the 30-min MLSS; specifically, the ability to delineate the boundary between the heavy and severe domains of exercise [49].

*Study 1 (Chapter 2)* investigated the relationship between various lactate parameters derived from different GXT protocols and the 30-min MLSS, and the agreement between  $\dot{V}O_{2\text{peak}}$  values obtained from different GXT protocols [1]. Participants completed five GXTs with varying stage lengths (1, 3, 4, 7 and 10 minute stages) and total durations (~11, 27, 35, 59 and 82 minutes, respectively). Fourteen LTs were calculated from the four longer GXTs, the RCP was calculated from the 1-min GXT, and  $\dot{V}O_{2\text{peak}}$  was assessed from each GXT and each

subsequent verification exhaustive bout (VEB). Of the 56 total calculated LTs, 10 met our stringent inclusion criteria (mean difference < 7.9 W; effect size < 0.2; intraclass correlation > 0.90). Select OBLA methods had high agreement with the MLSS from the longest three GXTs, and the original modified  $D_{\max}$  methods had high agreement with the MLSS from the GXT with 4-min stages (GXT<sub>4</sub>). Newly developed variations of the modified  $D_{\max}$  method, using the log-log as the initial data point, also had high agreement with the MLSS; moreover, these newly developed methods employed both polynomial regression and exponential regressions for determination of the LT. The values for  $\dot{V}O_{2\text{peak}}$  assessed from the longer duration GXTs and their subsequent VEBs underestimated the  $\dot{V}O_{2\text{peak}}$  determined from the shortest duration GXTs. The results from this study highlight the substantial influence of GXT protocol design on both the LT and the agreement with the MLSS. Until future research establishes the reliability and reproducibility of the LT methods derived in this study, caution is advised when using the LT derived from a GXT as a surrogate for other submaximal anchors. Lastly, considering the concerns raised pertaining to the 30-min MLSS it is unlikely the LT derived from a GXT can appropriately identify the boundary between the heavy and severe domains of exercise.

These results were consistent with previous findings discussed in *Review 1 (Chapter 1)*. In particular, GXT-derived submaximal anchors should be avoided as proxies for other submaximal anchors due to the poor statistical confirmation of validity and the poor efficacy of GXT-derived LTs. An additional purpose of this study was to validate a LT method that could be used in *Study 2 (Chapter 4)* to prescribe exercise intensity. However, due to these findings I abandoned the LT as a method to prescribe exercise and opted for the 30-min MLSS in *Study 2 (Chapter 4)*.

*Review 2 (Chapter 3)* highlights the influence of exercise intensity on the primary and secondary messengers, transcription factors, and coactivators and genes associated with exercise-induced mitochondrial biogenesis. Exercise intensity dictates changes in the primary messengers via alteration in the bioenergetics or source of ATP production for the working muscle, as well as the magnitude of homeostatic perturbations. In particular, this review focused on key homeostatic perturbations such as  $\text{Ca}^{2+}$  flux, redox state, ATP turnover, lactate production, and mechanical stress. During low-intensity exercise the predominant source of ATP is derived from fatty acid oxidation in type I fibres, with little to no recruitment of more glycolytic muscle fibres (i.e., type II); this results in a low rate of calcium flux, redox state, and ATP turnover rate as measured by the AMP/ATP ratio, which is comparable to rest. The high uptake of fatty acids act as natural ligands that modulate the expression of transcription factors and coactivators of genes associated with fatty acid oxidation (e.g., PPAR $\alpha$ , PPAR $\delta$ , and PPAR $\gamma$ ). As exercise intensity increases, substrate utilisation shifts from predominately fatty acids to a greater contribution from glucose and stored glycogen and there is the added recruitment of type II muscle fibres that drives the production of ATP from cytosolic sources (i.e., lactate). This results in an increase in  $\text{Ca}^{2+}$  flux, the redox state, and the AMP/ATP ratio. The increased magnitude of homeostatic perturbations drives the greater activation of secondary messengers (i.e., signalling kinases) (e.g., p-CaMKII, p-AMPK, p-p38 MAPK, etc.) that ultimately modulate transcription factors and coactivators associated with exercise-induced mitochondrial biogenesis (e.g., PGC-1 $\alpha$ , p53, etc.). There is an apparent relationship between exercise intensity and exercise-induced mitochondrial biogenesis and there is strong research to support the use of submaximal anchors to modulate the primary messengers, which would likely have a stronger influence of mitigating the variability of homeostatic perturbations and the subsequent effect on markers of exercise-induced mitochondrial biogenesis. Despite this, the identification of exercise intensities that stimulate a disproportional increase in

markers of mitochondrial biogenesis has been limited by research that has almost exclusively prescribed exercise relative to  $\dot{V}O_{2\max}$  or  $\dot{W}_{\max}$ . As highlighted in Chapters 1 and 2, there are well-established limitations of these methods to normalise exercise intensity. To date, there is no research employing more valid methods to normalise exercise intensity (e.g., MLSS or CP/CS) to investigate the influence of exercise intensity on markers of exercise-induced mitochondrial biogenesis. Furthermore, research that has investigated the influence of exercise intensity on cell signalling associated with exercise-induced mitochondrial biogenesis have only employed two intensities. Without employing three or more intensities a potential non-linear relationship between exercise intensity and these markers cannot be quantified (e.g., a dose-response or a threshold response).

The findings from *Study 1 (Chapter 2)* and the research summarised in *Reviews 1 and 2 (Chapters 1 and 3)* were used to design *Study 2 (Chapter 4)*. The MLSS was identified as a potential critical exercise intensity that represented the boundary between steady and non-steady-state exercise, with exercise above the MLSS intensity resulting in a disproportionate increase in a range of homeostatic perturbations. Based on this, it was hypothesised exercise above the MLSS would yield a disproportionate increase in primary and secondary messengers and the differential expression of genes associated with mitochondrial biogenesis.

*Study 2 (Chapter 4)* examined the influence of exercise intensity prescribed relative to the MLSS on cell-signalling responses associated with exercise-induced mitochondrial biogenesis. Participants performed three exercise bouts, at -18%, -6%, and +6% of the MLSS, respectively, and muscle biopsies were taken at rest, immediately post exercise and +4 and +24 hours from the onset of exercise. The lowest intensity yielded the greatest fat oxidation rate, which could be a driver of the greater upregulation of genes associated with fat oxidation. Total

PGC-1 $\alpha$  and p53 mRNA was highest following exercise performed at +6% of the MLSS at +4 h and +24 h from the onset of exercise, respectively. Exercise performed at -6% of the MLSS resulted in the highest number of upregulated genes, whereas exercise at +6% of the MLSS resulted in the highest number of down regulated genes, at +4 h and +24 h from the onset of exercise. These findings demonstrate that the MLSS represents a critical exercise intensity and that when exercise is performed above the MLSS this leads to a disproportionate increase in blood and muscle lactate and the transcriptional activity of some targets.

Together, the work contained in this thesis highlights some of the complexities of prescribing exercise intensity. The premise of submaximal anchors is they represent transitions in the metabolic state of the muscle, but many of these methods lack evidence to support this premise. This work also highlights the challenge of assessing the concurrent validity of GXT-derived anchors with other methods, due to the influence of GXT protocol design as well as the statistical assessment of validity. Exercise intensities associated with the transition between steady and non-steady state exercise, such as the MLSS, appear to represent a critical intensity above which there is a disproportionate change in homeostatic perturbation and where there is some differential expression of genes associated with exercise induced mitochondrial biogenesis.

## **5.2 Limitations of the Present Work**

**According to a power analysis I should have recruited 20 participants.** Therefore, a potential limitation of *Chapter 2 (Study 1)*, is the moderate sample size (n=17) for assessing validity. Unfortunately, due to time constraints and difficulties recruiting a homogeneous population of well-trained athletes, a slightly smaller number of participants was recruited. Employing stage lengths of 3, 4, 7, and 10 min in *Study 1 (Chapter 2)* clearly demonstrated the

influence GXT protocol design on LT calculations; even manipulating stage length by 1 min had a significant effect on the LT calculations (**Table 2.1 & 2.6**). Thus, it is possible lactate parameters derived from GXTs with 5- and 6-min stages may also have had high agreement with the MLSS but these were not assessed. The Log-Exp-MD<sub>max</sub> overestimated (+7 W) and underestimated (-4 W) the MLSS when calculated from GXT<sub>4</sub> and GXT<sub>7</sub>, respectively. It is therefore possible the Log-Exp-MD<sub>max</sub> derived from a GXT with 5- or 6-min stages would have had a higher agreement with the MLSS and possibly fit an *a priori* agreement (i.e., bias ± precision vs. standard error) [184]. Lastly, after publication in *PloS ONE* (*Study 2*), a review was published discrediting the efficacy of the 30-min MLSS as means to identify the maximal metabolic steady state [49]. An original research article also presented a newly derived single visit MLSS test [5] that remains to be confirmed as a valid delineator of the boundary between the heavy and severe domains of exercise.

Based on the results described in *Study 1* (*Chapter 2*), the MLSS was chosen in lieu of the LT as the criterion measure of the boundary between heavy and severe exercise. However, after conception of the study research was published that provided empirical evidence of the limitations of the 30-min MLSS as a valid method to identify the maximal metabolic steady state [6, 46, 49, 94, 185, 211, 381, 493]. Despite this, it was highly likely that exercise performed at +6% of the MLSS in *Study 2* was above the maximal steady state - as indicated by blood and intramuscular lactate data (**Figure 4.4**). Based on the above discussion, one of the unavoidable potential limitations of *Study 2* (*Chapter 4*) was the use of the traditional, commonly-used, 30-min MLSS. Again, another potential limitation was the sample size (n=10); ideally 16-24 participants should have participated based on recommendations for an optimum repeated measure design [8]. Unfortunately, due to time constraints, difficulties recruiting a homogeneous population of well-trained athletes, and the overall cost of analysing

tissue samples, a slightly smaller study population was recruited. Nonetheless, this sample size is equal to or greater than most similar research. Lastly, it would have been better suited to prescribe the lowest intensity at the maximal fat oxidation rate this could have strengthened the possibility of fatty acid oxidation as a perturbation to drive molecular responses.

The results from *Study 1 (Chapter 2)* are specific to the study demographics as well as the testing equipment; this is consistent with most research in applied sport and exercise science. Validity is often used as a broad term and the differentiation between subtypes remains absent. For example, although certain LT methods were deemed “valid”, only the internal validity of the LT was tested and until the reliability and reproducibility is confirmed it is not possible to generalise these results to other populations (i.e., external validity). The results from *Study 2 (Chapter 4)* are also specific to the study demographics and until tested may not be applicable to other populations.

### **5.3 Recommendations for Future Research**

Future research pertaining to the validity of various submaximal anchors discussed in *Review 1 (Chapter 1)* should assess validity based on the ability to identify the boundaries between the domains of exercise. Testing the validity of these methods should rely on transient oxygen uptake kinetics during exercise [119], performed in proximity to the anchors (e.g., within the limits of agreement), as well as blood lactate responses. For example, the breath-by-breath transient oxygen uptake kinetics during at the limits of agreement for CP should be consistent with its respective domains (e.g., below = heavy and above = severe). The same testing procedures should be applied to the other submaximal anchors discussed. Moreover, larger cohorts should be recruited in sport and exercise science research when assessing the validity of different methods to prescribe exercise ( $n \geq 30$ ) [8]. If LT testing remains a staple

technique, future research should expand on the findings described in *Study 1 (Chapter 2)* and investigate the reliability and reproducibility of the various LT methods. Furthermore, the validity and reliability should be explored in other populations (e.g., females) and other modes of exercise (e.g., treadmill).

Future research pertaining to the discussion in *Reviews 1 and 2 (Chapters 1 and 3)* should avoid  $\dot{V}O_2$ ,  $\dot{W}_{\max}$ , and HR-based methods to prescribe exercise intensity. Researchers should instead opt for methods that yield a distinct and homogeneous homeostatic perturbation in a range of individuals. For example, future research should investigate the influence of prescribing exercise relative to the maximal fat oxidation rate on markers associated with exercise-induced mitochondrial biogenesis. Future research pertaining to the discussion in *Chapter 2 (Study 2)* should employ techniques such as ‘omics’ analysis of mRNA and protein, as well as subcellular fraction and single-fibre analysis to further quantify the markers associated with exercise-induced mitochondrial biogenesis. This will provide an opportunity to obtain an in-depth map of all genes and proteins associated with cell signalling and the abundance of different proteins in different subcellular compartments as well as fibre type. Lastly, the translation of exercise-induced mitochondrial biogenesis to athletic performance remains inconclusive, and future research should elucidate this relationship to affirm the findings of this research.

#### **5.4 Practical Applications**

Graded Exercise Tests are often employed as a time-effective and convenient means to obtain indices associated with athletic performance and health. The results from the present work demonstrate the shortcomings of GXT protocol design to establish these indices. Moreover, this work challenges many assumptions associated with prescribing exercise

intensity. Due to these assumptions, submaximal anchors are often used to define training intensities. Instead, the findings contained in this thesis provide an argument for domain-based exercise prescription, where the domains are independent of the submaximal anchors, and the validity of said anchor should be contingent on the homeostatic responses above and below said anchor. These results also demonstrate that prescribing exercise relative to submaximal anchors modulates markers associated with exercise-induced mitochondrial biogenesis. Specifically, the MLSS represents a critical intensity that promotes a disproportionate differential expression of genes, supporting its use as a method to prescribe exercise intensity. Sport scientists, researchers, clinicians, and coaches can employ appreciate submaximal anchors to not only characterise the metabolic state of the working muscle but to also promote skeletal muscle adaptations that may impact athletic performance.

## References

1. Jamnick NA, Botella J, Pyne DB, Bishop DJ. Manipulating graded exercise test variables affects the validity of the lactate threshold and VO<sub>2</sub>peak. *PLoS ONE*. 2018;13(7):e0199794.
2. Zoladz JA, Duda K, Majerczak J. Oxygen uptake does not increase linearly at high power outputs during incremental exercise test in humans. *European Journal of Applied Physiology and Occupational Physiology*. 1998;77(5):445-51.
3. Baldwin J, Snow RJ, Febbraio MA. Effect of training status and relative exercise intensity on physiological responses in men. *Medicine and Science in Sports and Exercise*. 2000;32(9):1648-54.
4. Adami A, Sivieri A, Moia C, Perini R, Ferretti G. Effects of step duration in incremental ramp protocols on peak power and maximal oxygen consumption. *European Journal of Applied Physiology*. 2013;113(10):2647-53.
5. Hering GO, Hennig EM, Riehle HJ, Stepan J. A Lactate Kinetics Method for Assessing the Maximal Lactate Steady State Workload. *Front Physiol*. 2018 2018-March-29;9(310):310.
6. Vanhatalo A, Black MI, DiMenna FJ, Blackwell JR, Schmidt JF, Thompson C, et al. The mechanistic bases of the power–time relationship: muscle metabolic responses and relationships to muscle fibre type. *The Journal of Physiology*. 2016;594(15):4407-23.
7. Cohen J. A power primer. *Psychological Bulletin*. 1992;112(1):155.
8. Hopkins W, Marshall S, Batterham A, Hanin J. Progressive statistics for studies in sports medicine and exercise science. *Medicine and Science in Sports and Exercise*. 2009;41(1):3.
9. Hauser T, Bartsch D, Baumgärtel L, Schulz H. Reliability of maximal lactate-steady-state. *International Journal of Sports Medicine*. 2013;34(3):196-9.
10. Egan B, Zierath JR. Exercise metabolism and the molecular regulation of skeletal muscle adaptation. *Cell Metabolism*. 2013;17(2):162-84.
11. Romijn JA, Coyle EF, Sidossis LS, Gastaldelli A, Horowitz JF, Endert E, et al. Regulation of endogenous fat and carbohydrate metabolism in relation to exercise intensity and duration. *Am J Physiol*. 1993 Sep;265(1):380-91.
12. van Loon LJ, Greenhaff PL, Constantin-Teodosiu D, Saris WH, Wagenmakers AJ. The effects of increasing exercise intensity on muscle fuel utilisation in humans. *The Journal of Physiology*. 2001;536(1):295-304.
13. Sahlin K, Katz A, Henriksson J. Redox state and lactate accumulation in human skeletal muscle during dynamic exercise. *Biochemical Journal*. 1987;245(2):551-6.
14. Howlett RA, Parolin ML, Dyck DJ, Hultman E, Jones NL, Heigenhauser GJ, et al. Regulation of skeletal muscle glycogen phosphorylase and PDH at varying exercise power

outputs. *American Journal of Physiology-Regulatory, Integrative and Comparative Physiology*. 1998;275(2):R418-R25.

15. Egan B, Carson BP, Garcia-Roves PM, Chibalin AV, Sarsfield FM, Barron N, et al. Exercise intensity-dependent regulation of peroxisome proliferator-activated receptor  $\gamma$  coactivator-1 $\alpha$  mRNA abundance is associated with differential activation of upstream signalling kinases in human skeletal muscle. *The Journal of Physiology*. 2010;588(10):1779-90.

16. Sureda A, Ferrer MD, Tauler P, Romaguera D, Drobic F, Pujol P, et al. Effects of exercise intensity on lymphocyte H<sub>2</sub>O<sub>2</sub> production and antioxidant defences in soccer players. *British Journal of Sports Medicine*. 2009;43(3):186-90.

17. Martineau LC, Gardiner PF. Insight into skeletal muscle mechanotransduction: MAPK activation is quantitatively related to tension. *Journal of Applied Physiology*. 2001;91(2):693-702.

18. Rose AJ, Kiens B, Richter EA. Ca<sup>2+</sup>-calmodulin-dependent protein kinase expression and signalling in skeletal muscle during exercise. *The Journal of Physiology*. 2006;574(3):889-903.

19. Dimauro I, Pearson T, Caporossi D, Jackson MJ. A simple protocol for the subcellular fractionation of skeletal muscle cells and tissue. *BMC Research Notes*. 2012;5(1):513.

20. Bourdon P. Blood lactate transition thresholds: concepts and controversies. *Physiological Tests for Elite Athletes*. 2000.

21. Coombes J, Skinner T. ESSA's Student Manual for Health, Exercise and Sport Assessment. 2014 14th July 2014

22. Seiler S. What is best practice for training intensity and duration distribution in endurance athletes? *International Journal of Sports Physiology and Performance*. 2010;5(3):276-91.

23. Seiler KS, Kjerland GØ. Quantifying training intensity distribution in elite endurance athletes: is there evidence for an "optimal" distribution? *Scandinavian Journal of Medicine and Science in Sports*. 2006;16(1):49-56.

24. Stoggl T, Sperlich B. Polarized training has greater impact on key endurance variables than threshold, high intensity, or high volume training. *Frontiers in Physiology*. 2014 Feb 4;5.

25. Stoggl TL, Sperlich B. The training intensity distribution among well-trained and elite endurance athletes. *Frontiers in Physiology*. 2015 Oct 27;6.

26. Burnley M, Jones AM. Oxygen uptake kinetics as a determinant of sports performance. *European Journal of Sport Science*. 2007;7(2):63-79.

27. MacInnis MJ, Gibala MJ. Physiological adaptations to interval training and the role of exercise intensity. *The Journal of Physiology*. 2017;595(9):2915-30.

28. Hofmann P, Tschakert G. Intensity-and duration-based options to regulate endurance training. *Frontiers in Physiology*. 2017;8:337.

29. Bacon AP, Carter RE, Ogle EA, Joyner MJ. VO<sub>2</sub> max trainability and high intensity interval training in humans: a meta-analysis. *PLoS one*. 2013;8(9):e73182.
30. Milanović Z, Sporiš G, Weston M. Effectiveness of high-intensity interval training (HIT) and continuous endurance training for VO<sub>2</sub>max improvements: a systematic review and meta-analysis of controlled trials. *Sports Medicine*. 2015;45(10):1469-81.
31. Wenger HA, Bell GJ. The interactions of intensity, frequency and duration of exercise training in altering cardiorespiratory fitness. *Sports Medicine*. 1986;3(5):346-56.
32. van Tol BA, Huijsmans RJ, Kroon DW, Schothorst M, Kwakkel G. Effects of exercise training on cardiac performance, exercise capacity and quality of life in patients with heart failure: a meta-analysis. *European Journal of Heart Failure*. 2006;8(8):841-50.
33. Balady GJ, Williams MA, Ades PA, Bittner V, Comoss P, Foody JM, et al. Core components of cardiac rehabilitation/secondary prevention programs: 2007 update. A scientific statement from the American Heart Association Exercise, Cardiac Rehabilitation, and Prevention Committee, the Council on Clinical Cardiology; the Councils on Cardiovascular Nursing, Epidemiology and Prevention, and Nutrition, Physical Activity, and Metabolism; and the American Association of Cardiovascular and Pulmonary Rehabilitation. *Circulation*. 2007.
34. Bherer L, Erickson KI, Liu-Ambrose T. A review of the effects of physical activity and exercise on cognitive and brain functions in older adults. *Journal of Aging Research*. 2013;2013.
35. Holloszy JO. Exercise-induced increase in muscle insulin sensitivity. *Journal of Applied Physiology*. 2005;99(1):338-43.
36. Bishop DJ, Granata C, Eynon N. Can we optimise the exercise training prescription to maximise improvements in mitochondria function and content? *Biochimica et Biophysica Acta (BBA)-General Subjects*. 2014;1840(4):1266-75.
37. Kelley GA, Kelley KS, Kohrt WM. Exercise and bone mineral density in premenopausal women: a meta-analysis of randomized controlled trials. *International Journal of Endocrinology*. 2013;2013.
38. Mann T, Lamberts RP, Lambert MI. Methods of prescribing relative exercise intensity: physiological and practical considerations. *Sports Medicine*. 2013;43(7):613-25.
39. Pettitt R, Clark I, Ebner S, Sedgeman D, Murray S. Gas exchange threshold and VO<sub>2</sub>max testing for athletes: an update. *Journal of Strength and Conditioning Research*. 2013;27(2):549-55.
40. Jones AM, Vanhatalo A, Burnley M, Morton RH, Poole DC. Critical power: implications for determination of VO<sub>2</sub>max and exercise tolerance. *Medicine and Science in Sports and Exercise*. 2010;42(10):1876-90.
41. Beneke R. Methodological aspects of maximal lactate steady state—implications for performance testing. *European Journal of Applied Physiology*. 2003;89(1):95-9.
42. Pettitt R, Jamnick N, Clark I. 3-min all-out exercise test for running. *International Journal of Sports Medicine*. 2012;33(06):426-31.

43. Vanhatalo A, Doust JH, Burnley M. Determination of critical power using a 3-min all-out cycling test. *Medicine and Science in Sports and Exercise*. 2007;39(3):548.
44. Lansley K, Dimenna F, Bailey S, Jones A. A 'new' method to normalise exercise intensity. *International Journal of Sports Medicine*. 2011;32(07):535-41.
45. Bergstrom HC, Housh TJ, Zuniga JM, Traylor DA, Camic CL, Lewis Jr RW, et al. The relationships among critical power determined from a 3-min all-out test, respiratory compensation point, gas exchange threshold, and ventilatory threshold. *Research Quarterly for Exercise and Sport*. 2013;84(2):232-8.
46. Mattioni Maturana F, Keir DA, McLay KM, Murias JM. Can measures of critical power precisely estimate the maximal metabolic steady-state? *Applied Physiology, Nutrition, and Metabolism*. 2016;41(11):1197-203.
47. Pringle JS, Jones AM. Maximal lactate steady state, critical power and EMG during cycling. *European Journal of Applied Physiology*. 2002;88(3):214-26.
48. Smith CG, Jones AM. The relationship between critical velocity, maximal lactate steady-state velocity and lactate turnpoint velocity in runners. *European Journal of Applied Physiology*. 2001;85(1):19-26.
49. Jones AM, Burnley M, Black MI, Poole DC, Vanhatalo A. The maximal metabolic steady state: redefining the 'gold standard'. *Physiological Reports*. 2019;7(10):e14098.
50. ACSM. ACSM's guidelines for exercise testing and prescription. 9th ed: Lippincott Williams & Wilkins; 2013.
51. Esteve-Lanao J, Foster C, Seiler S, Lucia A. Impact of training intensity distribution on performance in endurance athletes. *The Journal of Strength and Conditioning Research*. 2007;21(3):943-9.
52. Seiler S, Tønnessen E. *Sportscience· sportsci. org. Sportscience*. 2009;13:32-53.
53. Whipp BJ, Wasserman K. Oxygen uptake kinetics for various intensities of constant-load work. *Journal of Applied Physiology*. 1972 1972-09-01 00:00:00;33(3):351-6.
54. Xu F, Rhodes EC. Oxygen uptake kinetics during exercise. *Sports Medicine*. 1999;27(5):313-27.
55. Gaesser GA, Poole DC. The slow component of oxygen uptake kinetics in humans. *Exercise and Sport Sciences Reviews*. 1996;24(1):35-70.
56. Barstow TJ, Casaburi R, Wasserman K. O<sub>2</sub> uptake kinetics and the O<sub>2</sub> deficit as related to exercise intensity and blood lactate. *Journal of Applied Physiology*. 1993;75(2):755-62.
57. Jorfeldt L, Juhlin-Dannfelt A, Karlsson J. Lactate release in relation to tissue lactate in human skeletal muscle during exercise. *Journal of Applied Physiology*. 1978;44(3):350-2.
58. Juel C. Lactate-proton cotransport in skeletal muscle. *Physiological Reviews*. 1997;77(2):321-58.

59. Robergs RA, Ghiasvand F, Parker D. Biochemistry of exercise-induced metabolic acidosis. *American Journal of Physiology-Regulatory, Integrative and Comparative Physiology*. 2004;287(3):R502-R16.
60. Stanley WC, Gertz EW, Wisneski JA, Morris DL, Neese RA, Brooks GA. Systemic lactate kinetics during graded exercise in man. *American Journal of Physiology-Endocrinology and Metabolism*. 1985;249(6):E595-E602.
61. Nielsen HB, Febbraio MA, Ott P, Krstrup P, Secher NH. Hepatic lactate uptake versus leg lactate output during exercise in humans. *Journal of Applied Physiology*. 2007;103(4):1227-33.
62. Poole DC, Ward SA, Gardner GW, Whipp BJ. Metabolic and respiratory profile of the upper limit for prolonged exercise in man. *Ergonomics*. 1988;31(9):1265-79.
63. Jones AM, Wilkerson DP, DiMenna F, Fulford J, Poole DC. Muscle metabolic responses to exercise above and below the “critical power” assessed using 31P-MRS. *American Journal of Physiology-Regulatory, Integrative and Comparative Physiology*. 2008;294(2):R585-R93.
64. Perry CG, Lally J, Holloway GP, Heigenhauser GJ, Bonen A, Spriet LL. Repeated transient mRNA bursts precede increases in transcriptional and mitochondrial proteins during training in human skeletal muscle. *The Journal of Physiology*. 2010;588(23):4795-810.
65. Meyer T, Gabriel HH, Kindermann W. Is determination of exercise intensities as percentages of VO<sub>2</sub>max or HRmax adequate? *Medicine and Science in Sports and Exercise*. 1999;31(9):1342-5.
66. Vollaard NB, Constantin-Teodosiu D, Fredriksson K, Rooyackers O, Jansson E, Greenhaff PL, et al. Systematic analysis of adaptations in aerobic capacity and submaximal energy metabolism provides a unique insight into determinants of human aerobic performance. *Journal of Applied Physiology*. 2009;106(5):1479-86.
67. Scharhag-Rosenberger F, Meyer T, Gäßler N, Faude O, Kindermann W. Exercise at given percentages of VO<sub>2</sub>max: Heterogeneous metabolic responses between individuals. *Journal of Science and Medicine in Sport*. 2010;13(1):74-9.
68. Katch V, Weltman A, Sady S, Freedson P. Validity of the relative percent concept for equating training intensity. *European Journal of Applied Physiology and Occupational Physiology*. 1978;39(4):219-27.
69. Granata C, Oliveira RS, Little JP, Renner K, Bishop DJ. Sprint-interval but not continuous exercise increases PGC-1 $\alpha$  protein content and p53 phosphorylation in nuclear fractions of human skeletal muscle. *Scientific Reports*. 2017;7:44227.
70. Fiorenza M, Gunnarsson TP, Hostrup M, Iaia F, Schena F, Pilegaard H, et al. Metabolic stress-dependent regulation of the mitochondrial biogenic molecular response to high-intensity exercise in human skeletal muscle. *The Journal of Physiology*. 2018;596(14):2823-40.
71. Caiozzo VJ, Davis JA, Ellis JF, Azus JL, Vandagriff R, Prietto C, et al. A comparison of gas exchange indices used to detect the anaerobic threshold. *Journal of Applied Physiology*. 1982;53(5):1184-9.

72. Beaver W, Wasserman K, Whipp B. A new method for detecting anaerobic threshold by gas exchange. *Journal of Applied Physiology*. 1986;60(6):2020-7.
73. Whipp BJ, Davis JA, Wasserman K. Ventilatory control of the 'isocapnic buffering' region in rapidly-incremental exercise. *Respiration Physiology*. 1989;76(3):357-67.
74. Cheng B, Kuipers H, Snyder A, Keizer H, Jeukendrup A, Hesselink M. A new approach for the determination of ventilatory and lactate thresholds. *International Journal of Sports Medicine*. 1992;13(7):518-22.
75. Bishop D, Jenkins DG, Mackinnon LT. The relationship between plasma lactate parameters,  $W_{peak}$  and 1-h cycling performance in women. *Medicine and Science in Sports and Exercise*. 1998;30(8):1270-5.
76. Heck H, Mader A, Hess G, Mücke S, Müller R, Hollmann W. Justification of the 4-mmol/l lactate threshold. *International Journal of Sports Medicine*. 1985;03(6):117-30.
77. Machado FA, Nakamura FY, Moraes SMFD. Influence of regression model and incremental test protocol on the relationship between lactate threshold using the maximal-deviation method and performance in female runners. *Journal of Sports Sciences*. 2012;30(12):1267-74.
78. Santos-Concejero J, Tucker R, Granados C, Irazusta J, Bidaurrezaga-Letona I, Zabala-Lili J, et al. Influence of regression model and initial intensity of an incremental test on the relationship between the lactate threshold estimated by the maximal-deviation method and running performance. *Journal of Sports Sciences*. 2014;32(9):853-9.
79. Keir DA, Fontana FY, Robertson TC, Murias JM, Paterson DH, Kowalchuk JM, et al. *Exercise Intensity Thresholds: Identifying the Boundaries of Sustainable Performance*. *Medicine and Science in Sports and Exercise*. 2015.
80. Rusko H, Luhtanen P, Rahkila P, Viitasalo J, Rehunen S, Härkönen M. Muscle metabolism, blood lactate and oxygen uptake in steady state exercise at aerobic and anaerobic thresholds. *European Journal of Applied Physiology and Occupational Physiology*. 1986;55(2):181-6.
81. Skinner JS, McLellan TH. The transition from aerobic to anaerobic metabolism. *Research Quarterly for Exercise and Sport*. 1980;51(1):234-48.
82. Burnley M, Doust JH, Vanhatalo A. A 3-min all-out test to determine peak oxygen uptake and the maximal steady state. *Medicine and Science in Sports and Exercise*. 2006;38(11):1995-2003.
83. Monod H, Scherrer J. The work capacity of a synergic muscular group. *Ergonomics*. 1965;8(3):329-38.
84. Moritani T, Nagata A, Devries HA, Muro M. Critical power as a measure of physical work capacity and anaerobic threshold. *Ergonomics*. 1981;24(5):339-50.
85. Whipp B, Huntsman D, Storer T, Lamarra N, Wasserman K. A constant which determines the duration of tolerance to high-intensity work. *Federation Proceedings*; 1982: *Federation Amer Soc Exp Biol*; 1982. p. 1591-2.

86. Fukuba Y, Whipp BJ. A metabolic limit on the ability to make up for lost time in endurance events. *Journal of Applied Physiology*. 1999;87(2):853-61.
87. Hollidge-Horvat M, Parolin M, Wong D, Jones N, Heigenhauser G. Effect of induced metabolic acidosis on human skeletal muscle metabolism during exercise. *American Journal of Physiology-Endocrinology and Metabolism*. 1999;277(4):E647-E58.
88. Hollidge-Horvat M, Parolin M, Wong D, Jones N, Heigenhauser G. Effect of induced metabolic alkalosis on human skeletal muscle metabolism during exercise. *American Journal of Physiology-Endocrinology And Metabolism*. 2000;278(2):E316-E29.
89. Özyener F, Rossiter H, Ward S, Whipp B. Influence of exercise intensity on the on-and off-transient kinetics of pulmonary oxygen uptake in humans. *The Journal of Physiology*. 2001;533(3):891-902.
90. Roston WL, Whipp BJ, Davis JA, Cunningham DA, Effros RM, Wasserman K. Oxygen uptake kinetics and lactate concentration during exercise in humans. *American Review of Respiratory Disease*. 1987;135(5):1080-4.
91. Rossiter H, Ward S, Kowalchuk J, Howe F, Griffiths J, Whipp B. Dynamic asymmetry of phosphocreatine concentration and O<sub>2</sub> uptake between the on-and off-transients of moderate-and high-intensity exercise in humans. *The Journal of Physiology*. 2002;541(3):991-1002.
92. Saltin B, Karlsson J. Muscle glycogen utilization during work of different intensities. *Muscle Metabolism During Exercise*: Springer; 1971. p. 289-99.
93. Messonnier LA, Emhoff C-AW, Fattor JA, Horning MA, Carlson TJ, Brooks GA. Lactate kinetics at the lactate threshold in trained and untrained men. *Journal of Applied Physiology*. 2013;114(11):1593-602.
94. Black MI, Jones AM, Blackwell JR, Bailey SJ, Wylie LJ, McDonagh STJ, et al. Muscle metabolic and neuromuscular determinants of fatigue during cycling in different exercise intensity domains. *Journal of Applied Physiology*. 2017;122(3):446-59.
95. Granata C, Jamnick NA, Bishop DJ. Training-induced changes in mitochondrial content and respiratory function in human skeletal muscle. *Sports Medicine*. 2018 Aug;48(8):1809-28.
96. Hood DA. Mechanisms of exercise-induced mitochondrial biogenesis in skeletal muscle. *Applied Physiology, Nutrition, and Metabolism*. 2009;34(3):465-72.
97. Chwalbinska-Moneta J, Robergs RA, Costill DL, Fink WJ. Threshold for muscle lactate accumulation during progressive exercise. *Journal of Applied Physiology*. 1989;66(6):2710-6.
98. Green H, Hughson R, Orr G, Ranney D. Anaerobic threshold, blood lactate, and muscle metabolites in progressive exercise. *Journal of Applied Physiology*. 1983;54(4):1032-8.
99. Black MI, Jones AM, Blackwell JR, Bailey SJ, Wylie LJ, McDonagh ST, et al. Muscle metabolic and neuromuscular determinants of fatigue during cycling in different exercise intensity domains. *Journal of Applied Physiology*. 2016;122(3):446-59.

100. Rossiter H, Ward S, Doyle V, Howe F, Griffiths J, Whipp B. Inferences from pulmonary O<sub>2</sub> uptake with respect to intramuscular [phosphocreatine] kinetics during moderate exercise in humans. *The Journal of Physiology*. 1999;518(3):921-32.
101. Barstow TJ, Buchthal S, Zanconato S, Cooper D. Muscle energetics and pulmonary oxygen uptake kinetics during moderate exercise. *Journal of Applied Physiology*. 1994;77(4):1742-9.
102. Henneman E, Somjen G, Carpenter DO. Functional significance of cell size in spinal motoneurons. *J Neurophysiol*. 1965;28(3):560-80.
103. Gollnick P, Piehl K, Saltin B. Selective glycogen depletion pattern in human muscle fibres after exercise of varying intensity and at varying pedalling rates. *The Journal of Physiology*. 1974;241(1):45-57.
104. Jones AM, Grassi B, Christensen PM, Krstrup P, Bangsbo J, Poole DC. Slow component of VO<sub>2</sub> kinetics: mechanistic bases and practical applications. *Medicine and Science in Sports and Exercise*. 2011;43(11):2046-62.
105. Jones AM, Poole DC, Grassi B, Christensen PM. The slow component of VO<sub>2</sub> kinetics: mechanistic bases and practical applications: *Healthy Learning*; 2010.
106. Katz A, Sahlin K. Regulation of lactic acid production during exercise. *Journal of Applied Physiology*. 1988;65(2):509-18.
107. Katz A, Sahlin K. Role of oxygen in regulation of glycolysis and lactate production in human skeletal muscle. *Exercise and Sport Sciences Reviews*. 1990;18(1):1-28.
108. Billat V, Sirvent P, Lepretre P-M, Koralsztein JP. Training effect on performance, substrate balance and blood lactate concentration at maximal lactate steady state in master endurance-runners. *Pflügers Archiv*. 2004;447(6):875-83.
109. Gollnick P, Armstrong R, Sembrowich W, Shepherd R, Saltin B. Glycogen depletion pattern in human skeletal muscle fibers after heavy exercise. *Journal of Applied Physiology*. 1973;34(5):615-8.
110. Zoladz JA, Majerczak J, Grassi B, Szkutnik Z, Korostyński M, Gołda S, et al. Mechanisms of attenuation of pulmonary V'O<sub>2</sub> slow component in humans after prolonged endurance training. *PloS ONE*. 2016;11(4):e0154135.
111. Caputo F, Mello M, Denadai B. Oxygen uptake kinetics and time to exhaustion in cycling and running: a comparison between trained and untrained subjects. *Archives of Physiology and Biochemistry*. 2003;111(5):461-6.
112. Emhoff C-AW, Messonnier LA, Horning MA, Fattor JA, Carlson TJ, Brooks GA. Direct and indirect lactate oxidation in trained and untrained men. *Journal of Applied Physiology*. 2013;115(6):829-38.
113. Jones AM, Poole DC. Oxygen uptake kinetics in sport, exercise and medicine. London: Routledge; 2013.

114. Koppo K, Bouckaert J, Jones AM. Effects of training status and exercise intensity on phase II VO<sub>2</sub> kinetics. *Medicine and Science in Sports and Exercise*. 2004;36(2):225-32.
115. Carter H, Jones AM, Barstow TJ, Burnley M, Williams C, Doust JH. Effect of endurance training on oxygen uptake kinetics during treadmill running. *Journal of Applied Physiology*. 2000;89(5):1744-52.
116. Vøllestad NK, Blom PCS. Effect of varying exercise intensity on glycogen depletion in human muscle fibres. *Acta Physiologica Scandinavica*. 1985;125(3):395-405.
117. Spriet LL, Ren J, Hultman E. Epinephrine infusion enhances muscle glycogenolysis during prolonged electrical stimulation. *Journal of Applied Physiology*. 1988;64(4):1439-44.
118. Barstow TJ, Molé PA. Linear and nonlinear characteristics of oxygen uptake kinetics during heavy exercise. *Journal of Applied Physiology*. 1991;71(6):2099-106.
119. Bell C, Paterson DH, Kowalchuk JM, Padilla J, Cunningham DA. A comparison of modelling techniques used to characterise oxygen uptake kinetics during the on-transient of exercise. *Experimental Physiology*. 2001;86(05):667-76.
120. Jones AM, Wilkerson DP, Fulford J. Muscle [phosphocreatine] dynamics following the onset of exercise in humans: the influence of baseline work-rate. *The Journal of Physiology*. 2008;586(3):889-98.
121. Granata C, Jamnick NA, Bishop DJ. Principles of exercise prescription, and how they influence exercise-induced changes of transcription factors and other regulators of mitochondrial biogenesis. *Sports Medicine*. 2018;48(7):1541-59.
122. Baldwin J, Snow RJ, Carey MF, Febbraio MA. Muscle IMP accumulation during fatiguing submaximal exercise in endurance trained and untrained men. *American Journal of Physiology-Regulatory, Integrative and Comparative Physiology*. 1999;277(1):R295-R300.
123. Gass G, McLellan T, Gass E. Effects of prolonged exercise at a similar percentage of maximal oxygen consumption in trained and untrained subjects. *European Journal of Applied Physiology and Occupational Physiology*. 1991;63(6):430-5.
124. Sedgeman D, Dalleck L, Clark IE, Jamnick N, Pettitt R. Analysis of square-wave bouts to verify VO<sub>2</sub>max. *Int J Sports Med*. 2013;34(12):1058-62.
125. Pettitt RW, Jamnick NA. Commentary on “Measurement of the maximum oxygen uptake  $\dot{V}O_{2\max}$ :  $\dot{V}O_{2\text{peak}}$  is no longer acceptable”. *Journal of Applied Physiology*. 2017;123(3):696-.
126. Poole DC, Jones AM. Measurement of the maximum oxygen uptake  $\dot{V}O_{2\max}$ :  $\dot{V}O_{2\text{peak}}$  is no longer acceptable. *Journal of Applied Physiology*. 2017;122(4):997-1002.
127. Jamnick NA, By S, Pettitt CD, Pettitt RW. Comparison of the YMCA and a custom submaximal exercise test for determining VO<sub>2</sub>max. *Medicine and Science in Sports and Exercise*. 2016 Feb;48(2):254-9.
128. Kirkeberg J, Dalleck L, Kamphoff C, Pettitt R. Validity of 3 protocols for verifying VO<sub>2</sub>max. *International Journal of Sports Medicine*. 2011;32(04):266-70.

129. Pettitt RW, Placek AM, Clark IE, Jamnick NA, Murray SR. Sensitivity of prescribing high-intensity, interval training using the critical power concept. *International Journal of Exercise Science*. 2015;8(3):1.
130. Clark IE, Murray SR, Pettitt RW. Alternative procedures for the three-minute all-out exercise test. *The Journal of Strength and Conditioning Research*. 2013;27(8):2104-12.
131. Sedgeman D, Dalleck L, Clark IE, Jamnick N, Pettitt R. Analysis of square-wave bouts to verify VO<sub>2</sub>max. *International Journal of Sports Medicine*. 2013;34(12):1058-62.
132. Dicks ND, Jamnick NA, Murray SR, Pettitt RW. Load determination for the 3-minute all-out exercise test for cycle ergometry. *International Journal of Sports Physiology and Performance*. 2016;11(2):197-203.
133. Aunola S, Rusko H. Reproducibility of aerobic and anaerobic thresholds in 20–50 year old men. *European Journal of Applied Physiology and Occupational Physiology*. 1984;53(3):260-6.
134. Lourenço TF, Martins LEB, Tessutti LS, Brenzikofer R, Macedo DV. Reproducibility of an incremental treadmill VO<sub>2</sub>max test with gas exchange analysis for runners. *The Journal of Strength and Conditioning Research*. 2011;25(7):1994-9.
135. Wisén AG, Wohlfart B. A refined technique for determining the respiratory gas exchange responses to anaerobic metabolism during progressive exercise—repeatability in a group of healthy men. *Clinical Physiology and Functional Imaging*. 2004;24(1):1-9.
136. Weltman A, Snead D, Stein P, Seip R, Schurrer R, Rutt R, et al. Reliability and validity of a continuous incremental treadmill protocol for the determination of lactate threshold, fixed blood lactate concentrations, and VO<sub>2</sub>max. *International Journal of Sports Medicine*. 1990;11(01):26-32.
137. Yoon B-K, Kravitz L, Robergs R. VO<sub>2</sub>max, protocol duration, and the vo<sub>2</sub> plateau. *Medicine and Science in Sport and Exercise*. 2007;39(7):1186-92.
138. Bishop D, Jenkins DG, Mackinnon LT. The effect of stage duration on the calculation of peak VO<sub>2</sub> during cycle ergometry. *Journal of Science and Medicine in Sport*. 1998;1(3):171-8.
139. Bentley DJ, McNaughton LR. Comparison of W<sub>peak</sub>, VO<sub>2peak</sub> and the ventilation threshold from two different incremental exercise tests: relationship to endurance performance. *Journal of Science and Medicine in Sport*. 2003;6(4):422-35.
140. Bentley DJ, Newell J, Bishop D. Incremental exercise test design and analysis. *Sports Medicine*. 2007;37(7):575-86.
141. Coyle EF, Coggan AR, Hopper M, Walters TJ. Determinants of endurance in well-trained cyclists. *Journal of Applied Physiology*. 1988;64(6):2622-30.
142. Scharhag-Rosenberger F, Meyer T, Gäßler N, Faude O, Kindermann W. Exercise at given percentages of VO<sub>2</sub>max: heterogeneous metabolic responses between individuals. *Journal of Science and Medicine in Sport*. 2010;13(1):74-9.

143. Poole DC, Gaesser GA. Response of ventilatory and lactate thresholds to continuous and interval training. *Journal of Applied Physiology*. 1985;58(4):1115-21.
144. Zoladz JA, Rademaker A, Sargeant AJ. Non-linear relationship between O<sub>2</sub> uptake and power output at high intensities of exercise in humans. *Journal of Physiology*. 1995;488(Pt 1):211.
145. Boone J, Bourgois J. The oxygen uptake response to incremental ramp exercise. *Sports Medicine*. 2012;42(6):511-26.
146. Keir DA, Benson AP, Love LK, Robertson TC, Rossiter HB, Kowalchuk JM. Influence of muscle metabolic heterogeneity in determining the  $\dot{V}O_{2p}$  kinetic response to ramp-incremental exercise. *Journal of Applied Physiology*. 2016;120(5):503-13.
147. Hopkins WG, Schabort EJ, Hawley JA. Reliability of power in physical performance tests. *Sports Medicine*. 2001;31(3):211-34.
148. Morton RH. Why peak power is higher at the end of steeper ramps: An explanation based on the “critical power” concept. *Journal of Sports Sciences*. 2011;29(3):307-9.
149. Poole DC, Jones AM. Reply to Pettitt and Jamnick’s letter in reference to: Measurement of the maximum oxygen uptake  $\dot{V}O_{2max}$ :  $\dot{V}O_{2peak}$  is no longer acceptable. *Journal of Applied Physiology*. 2017;123(3):697-.
150. Bentley D, McNaughton L, Batterham A. Prolonged stage duration during incremental cycle exercise: effects on the lactate threshold and onset of blood lactate accumulation. *European Journal of Applied Physiology*. 2001;85(3-4):351-7.
151. Amann M, Subudhi A, Foster C. Influence of testing protocol on ventilatory thresholds and cycling performance. *Medicine and Science in Sports and Exercise*. 2004;36(4):613-22.
152. Bishop DJ, Botella J, Genders AJ, Lee MJ, Saner NJ, Kuang J, et al. High-intensity exercise and mitochondrial biogenesis: current controversies and future research directions. *Physiology*. 2018;34(1):56-70.
153. Jensen K, Johansen L. Reproducibility and validity of physiological parameters measured in cyclists riding on racing bikes placed on a stationary magnetic brake. *Scandinavian Journal of Medicine and Science in Sports*. 1998;8(1):1-6.
154. Weston SB, Gabbett TJ. Reproducibility of ventilation of thresholds in trained cyclists during ramp cycle exercise. *Journal of Science and Medicine in Sport*. 2001;4(3):357-66.
155. Lamberts RP, Swart J, Woolrich RW, Noakes TD, Lambert MI. Measurement error associated with performance testing in well-trained cyclists: Application to the precision of monitoring changes in training status. *International Sportmed Journal*. 2009;10(1):33-44.
156. Cunha F, Midgley A, Monteiro W, Farinatti P. Influence of cardiopulmonary exercise testing protocol and resting VO<sub>2</sub> assessment on % HR<sub>max</sub>, %HRR, %VO<sub>2max</sub> and %VO<sub>2R</sub> relationships. *International Journal of Sports Medicine*. 2010;31(5):319-26.

157. Machado FA, Kravchychyn ACP, Peserico CS, da Silva DF, Mezzaroba PV. Effect of stage duration on maximal heart rate and post-exercise blood lactate concentration during incremental treadmill tests. *Journal of Science and Medicine in Sport*. 2013;16(3):276-80.
158. Santos ALd, Silva SC, Farinatti PdTV, Monteiro WD. Peak heart rate responses in maximum laboratory and field tests. *Revista Brasileira de Medicina do Esporte*. 2005;11(3):177-80.
159. Coutinho C, Watson A, Brickson S, Sanfilippo J. Maximal heart rate differs between laboratory and field conditions among female athletes. *Journal of Human Sport and Exercise*. 2017;12(2).
160. Semin K, Stahlnecker IV AC, Heelan K, Brown GA, Shaw BS, Shaw I. Discrepancy between training, competition and laboratory measures of maximum heart rate in NCAA division 2 distance runners. *Journal of Sports Science and Medicine*. 2008;7(4):455.
161. Pettitt RW, Symons JD, Taylor JE, Eisenman PA, White AT. Adjustment for gas exchange threshold enhances precision of heart rate-derived VO<sub>2</sub> estimates during heavy exercise. *Applied Physiology, Nutrition, and Metabolism*. 2007;33(1):68-74.
162. Wasserman K, Whipp BJ, Koysl S, Beaver W. Anaerobic threshold and respiratory gas exchange during exercise. *Journal of Applied Physiology*. 1973;35(2):236-43.
163. Jones A, Burnley M, Vanhatalo A. *Aerobic Exercise Performance: Kinanthropometry and Exercise Physiology* 4th ed. London; 2018.
164. Faude O, Kindermann W, Meyer T. Lactate threshold concepts. *Sports Medicine*. 2009;39(6):469-90.
165. Billat VL, Sirvent P, Py G, Koralsztejn J-P, Mercier J. The concept of maximal lactate steady state. *Sports Medicine*. 2003;33(6):407-26.
166. Pallarés JG, Morán-Navarro R, Ortega JF, Fernández-Elías VE, Mora-Rodriguez R. Validity and reliability of ventilatory and blood lactate thresholds in well-trained cyclists. *PloS ONE*. 2016;11(9):e0163389.
167. Morton RH, Stannard SR, Kay B. Low reproducibility of many lactate markers during incremental cycle exercise. *British Journal of Sports Medicine*. 2012;46(1):64-9.
168. Cerezuela-Espejo V, Courel-Ibáñez J, Morán-Navarro R, Martínez-Cava A, Pallarés JG. The relationship between lactate and ventilatory thresholds in runners: validity and reliability of exercise test performance parameters. *Frontiers in Physiology*. 2018;9.
169. Davis J, Caiozzo V, Lamarra N, Ellis J, Vandagriff R, Prietto C, et al. Does the gas exchange anaerobic threshold occur at a fixed blood lactate concentration of 2 or 4 mM? *International Journal of Sports Medicine*. 1983;4(2):89-93.
170. Gaskill SE, Ruby BC, Walker AJ, Sanchez OA, Serfass RC, Leon AS. Validity and reliability of combining three methods to determine ventilatory threshold. *Medicine and Science in Sports and Exercise*. 2001;33(11):1841-8.

171. Simon J, Young JL, Blood DK, Segal KR, Case RB, Gutin B. Plasma lactate and ventilation thresholds in trained and untrained cyclists. *Journal of Applied Physiology*. 1986;60(3):777-81.
172. Von Duvillard S, LeMura L, Bacharach D, Di Vico P. Determination of lactate threshold by respiratory gas exchange measures and blood lactate levels during incremental load work. *Journal of Manipulative and Physiological Therapeutics*. 1993;16(5):312-8.
173. McLellan T. Ventilatory and plasma lactate response with different exercise protocols: a comparison of methods. *International Journal of Sports Medicine*. 1985;6(1):30-5.
174. Thomas V, Costes F, Chatagnon M, Pouilly J-P, Busso T. A comparison of lactate indices during ramp exercise using modelling techniques and conventional methods. *Journal of Sports Sciences*. 2008;26(13):1387-95.
175. Davis JA, Rozenek R, DeCicco DM, Carizzi MT, Pham PH. Comparison of three methods for detection of the lactate threshold. *Clinical Physiology and Functional Imaging*. 2007;27(6):381-4.
176. Denadai B, Figueira T, Favaro O, Gonçalves M. Effect of the aerobic capacity on the validity of the anaerobic threshold for determination of the maximal lactate steady state in cycling. *Brazilian Journal of Medical and Biological Research*. 2004;37(10):1551-6.
177. Czuba M, Zając A, Cholewa J, Poprzęcki S, Waśkiewicz Z, Mikołajec K. Lactate threshold (D-max method) and maximal lactate steady state in cyclists. *Journal of Human Kinetics*. 2009;21:49-56.
178. Grossl T, De Lucas RD, De Souza KM, Antonacci Guglielmo LG. Maximal lactate steady-state and anaerobic thresholds from different methods in cyclists. *European Journal of Sport Science*. 2012;12(2):161-7.
179. Bourdon PC, Woolford SM, Buckley JD. Effects of varying the step duration on the determination of lactate thresholds in elite rowers. *International Journal of Sports Physiology and Performance*. 2018;13(6):687-93.
180. Hauser T, Adam J, Schulz H. Comparison of selected lactate threshold parameters with maximal lactate steady state in cycling. *International Journal of Sports Medicine*. 2014;35(6):517-21.
181. Chalmers S, Esterman A, Eston R, Norton K. Standardization of the Dmax method for calculating the second lactate threshold. *Int J Sports Physiol Perform*. 2015 Oct;10(7):921-6.
182. Kindermann W, Simon G, Keul J. The significance of the aerobic-anaerobic transition for the determination of work load intensities during endurance training. *European Journal of Applied Physiology and Occupational Physiology*. 1979;42(1):25-34.
183. Aldrich J. Correlations genuine and spurious in Pearson and Yule. *Statistical Science*. 1995:364-76.
184. Hanneman SK. Design, analysis and interpretation of method-comparison studies. *AACN Advanced Critical Care*. 2008;19(2):223.

185. Iannetta D, Inglis EC, Fullerton C, Passfield L, Murias JM. Metabolic and performance-related consequences of exercising at and slightly above MLSS. *Scandinavian Journal of Medicine and Science in Sports*. 2018;28(12):2481-93.
186. Marwood S, Goulding RP, Roche DM. Determining the Upper Limit of the Metabolic Steady State. *Med Sci Sports Exerc*. 2019 Mar;51(3):602.
187. Baron B, Noakes TD, Deckerle J, Moullan F, Robin S, Matran R, et al. Why does exercise terminate at the maximal lactate steady state intensity? *British Journal of Sports Medicine*. 2008;42(10):828-33.
188. De Lucas R, De Souza K, Costa V, Grossl T, Guglielmo L. Time to exhaustion at and above critical power in trained cyclists: The relationship between heavy and severe intensity domains. *Science and Sports*. 2013;28(1):e9-e14.
189. Bergstrom HC, Housh TJ, Zuniga JM, Traylor DA, Lewis RW, Camic CL, et al. Responses during exhaustive exercise at critical power determined from the 3-min all-out test. *Journal of Sports Sciences*. 2013;31(5):537-45.
190. Foxdal P, Sjödin A, Sjödin B. Comparison of blood lactate concentrations obtained during incremental and constant intensity exercise. *International Journal of Sports Medicine*. 1996;17(05):360-5.
191. Stainsby WN, Brooks GA. Control of lactic acid metabolism in contracting muscles and during exercise. *Exercise and Sport Sciences Reviews*. 1990;18(1):29-64.
192. Brooks GA. Anaerobic threshold: review of the concept and directions for future research. *Medicine and Science in Sports and Exercise*. 1985;17(1):22-34.
193. Keir DA, Fontana FY, Robertson TC, Murias JM, Paterson DH, Kowalchuk JM, et al. Exercise intensity thresholds: identifying the boundaries of sustainable performance. *Med Sci Sports Exerc*. 2015 Sep;47(9):1932-40.
194. Keir D, Pogliaghi S, Murias I. The respiratory compensation point and the deoxygenation break point are valid surrogates for critical power and maximum lactate steady state. *Medicine and Science in Sports and Exercise*. 2018;50(11):2375-8.
195. Weatherwax RM, Harris NK, Kilding AE, Dalleck LC. Incidence of VO<sub>2</sub>max responders to personalized versus standardized exercise prescription. *Medicine and Science in Sports and Exercise*. 2019;51(4):681-91.
196. Wolpern AE, Burgos DJ, Janot JM, Dalleck LC. Is a threshold-based model a superior method to the relative percent concept for establishing individual exercise intensity? a randomized controlled trial. *BMC Sports Science, Medicine and Rehabilitation*. 2015;7(1):1.
197. Péronnet F, Aguilaniu B. Lactic acid buffering, nonmetabolic CO<sub>2</sub> and exercise hyperventilation: a critical reappraisal. *Respiratory Physiology and Neurobiology*. 2006;150(1):4-18.
198. Wasserman K, McIlroy MB. Detecting the threshold of anaerobic metabolism in cardiac patients during exercise. *The American Journal of Cardiology*. 1964;14(6):844-52.

199. Posner JD, Gorman KM, Klein HS, Cline CJ. Ventilatory threshold: measurement and variation with age. *Journal of Applied Physiology*. 1987;63(4):1519-25.
200. Leo JA, Sabapathy S, Simmonds MJ, Cross TJ. The respiratory compensation point is not a valid surrogate for critical power. *Medicine and Science in Sports and Exercise*. 2017;49(7):1452-60.
201. Wasserman K, Stringer W, Casaburi R, Koike A, Cooper C. Determination of the anaerobic threshold by gas exchange: biochemical considerations, methodology and physiological effects. *Zeitschrift fur Kardiologie*. 1994;83:1-12.
202. Santos EL, Giannella-Neto A. Comparison of computerized methods for detecting the ventilatory thresholds. *European Journal of Applied Physiology*. 2004;93(3):315-24.
203. Meyer T, Faude O, Scharhag J, Urhausen A, Kindermann W. Is lactic acidosis a cause of exercise induced hyperventilation at the respiratory compensation point? *British Journal of Sports Medicine*. 2004;38(5):622-5.
204. Weston S, Gray A, Schneider DA, Gass GC. Effect of ramp slope on ventilation thresholds and  $\dot{V}O_{2peak}$  in male cyclists. *International Journal of Sports Medicine*. 2002;23(01):22-7.
205. Scheuermann B, Kowalchuk J. Attenuated respiratory compensation during rapidly incremented ramp exercise. *Respiration Physiology*. 1998;114(3):227-38.
206. Broxterman R, Craig J, Richardson R. The respiratory compensation point and the deoxygenation break point are not valid surrogates for critical power and maximum lactate steady state. *Medicine and Science in Sports and Exercise*. 2018;50(11):2379-82.
207. Broxterman R, Ade C, Craig J, Wilcox S, Schlup S, Barstow T. The relationship between critical speed and the respiratory compensation point: coincidence or equivalence. *European Journal of Sport Science*. 2015;15(7):631-9.
208. Jones AM, Vanhatalo A. The 'Critical Power' Concept: Applications to sports performance with a focus on intermittent high-intensity exercise. *Sports Medicine*. 2017:1-14.
209. Bishop D, Jenkins DG, Howard A. The critical power function is dependent on the duration of the predictive exercise tests chosen. *International Journal of Sports Medicine*. 1998;19(02):125-9.
210. Busso T, Gimenez P, Chatagnon M. A comparison of modelling procedures used to estimate the power-exhaustion time relationship. *European Journal of Applied Physiology*. 2010;108(2):257.
211. Maturana FM, Fontana FY, Pogliaghi S, Passfield L, Murias JM. Critical power: How different protocols and models affect its determination. *Journal of Science and Medicine in Sport*. 2018;21(7):742-7.
212. Vandewalle H, Péérès G, Monod H. Standard anaerobic exercise tests. *Sports Medicine*. 1987;4(4):268-89.

213. Bergstrom HC, Housh TJ, Zuniga JM, Traylor DA, Lewis Jr RW, Camic CL, et al. Differences among estimates of critical power and anaerobic work capacity derived from five mathematical models and the three-minute all-out test. *The Journal of Strength and Conditioning Research*. 2014;28(3):592-600.
214. Jones AM, Wilkerson D, Vanhatalo A, Burnley M. Influence of pacing strategy on O<sub>2</sub> uptake and exercise tolerance. *Scandinavian Journal of Medicine and Science in Sports*. 2008;18(5):615-26.
215. Laursen PB, Francis GT, Abbiss CR, Newton MJ, Nosaka K. Reliability of time-to-exhaustion versus time-trial running tests in runners. *Medicine and Science in Sports and Exercise*. 2007;39(8):1374-9.
216. Muniz-Pumares D, Karsten B, Triska C, Glaister M. Methodological approaches and related challenges associated with the determination of critical power and curvature constant. *The Journal of Strength Conditioning Research*. 2019 Feb;33(2):584-96.
217. Puchowicz MJ, Mizelman E, Yogev A, Koehle MS, Townsend NE, Clarke DC. The critical power model as a potential tool for anti-doping. *Frontiers in Physiology*. 2018;9:643.
218. Vanhatalo A, Fulford J, DiMenna FJ, Jones AM. Influence of hyperoxia on muscle metabolic responses and the power–duration relationship during severe-intensity exercise in humans: a <sup>31</sup>P magnetic resonance spectroscopy study. *Experimental Physiology*. 2010;95(4):528-40.
219. Triska C, Tschan H, Tazreiter G, Nimmerichter A. Critical power in laboratory and field conditions using single-visit maximal effort trials. *International Journal of Sports Medicine*. 2015;36(13):1063-8.
220. Karsten B, Jobson SA, Hopker J, Passfield L, Beedie C. The 3-min test does not provide a valid measure of critical power using the SRM isokinetic mode. *International Journal of Sports Medicine*. 2014;35(04):304-9.
221. Housh DJ, Housh TJ, Bauge SM. A methodological consideration for the determination of critical power and anaerobic work capacity. *Research Quarterly for Exercise and Sport*. 1990;61(4):406-9.
222. Simpson LP, Kordi M. Comparison of critical power and  $W'$  derived from 2 or 3 maximal tests. *International Journal of Sports Physiology and Performance*. 2017;12(6):825-30.
223. Triska C, Karsten B, Beedie C, Koller-Zeisler B, Nimmerichter A, Tschan H. Different durations within the method of best practice affect the parameters of the speed–duration relationship. *European Journal of Sport Science*. 2018;18(3):332-40.
224. Bosquet L, Duchene A, Lecot F, Dupont G, Leger L.  $V_{max}$  estimate from three-parameter critical velocity models: validity and impact on 800 m running performance prediction. *European Journal of Applied Physiology*. 2006;97(1):34.
225. Bull AJ, Housh TJ, Johnson GO, Perry SR. Effect of mathematical modeling on the estimation of critical power. *Medicine and Science in Sports and Exercise*. 2000;32(2):526-30.

226. Bull AJ, Housh TJ, Johnson GO, Rana SR. Physiological responses at five estimates of critical velocity. *European Journal of Applied Physiology*. 2008;102(6):711-20.
227. Gaesser GA, Carnevale TJ, Garfinkel A, Walter DO, Womack CJ. Estimation of critical power with nonlinear and linear models. *Medicine and Science in Sports and Exercise*. 1995;27(10):1430-8.
228. Housh TJ, Cramer JT, Bull AJ, Johnson GO, Housh DJ. The effect of mathematical modeling on critical velocity. *European Journal of Applied Physiology*. 2001;84(5):469-75.
229. Sawyer BJ, Morton RH, Womack CJ, Gaesser GA.  $\dot{V}O_2$ max may not be reached during exercise to exhaustion above critical power. *Medicine and Science in Sports and Exercise*. 2012;44(8):1533-8.
230. Galbraith A, Hopker J, Lelliott S, Diddams L, Passfield L. A single-visit field test of critical speed. *International Journal of Sports Physiology and Performance*. 2014;9(6):931-5.
231. Black MI, Jones AM, Bailey SJ, Vanhatalo A. Self-pacing increases critical power and improves performance during severe-intensity exercise. *Applied Physiology, Nutrition, and Metabolism*. 2015;40(7):662-70.
232. Gaesser G, Wilson L. Effects of continuous and interval training on the parameters of the power-endurance time relationship for high-intensity exercise. *International Journal of Sports Medicine*. 1988;9(06):417-21.
233. Hopkins W. Measures of reliability in sports medicine and science. *Sports Medicine*. 2000;30(1):1-15.
234. Johnson TM, Sexton PJ, Placek AM, Murray SR, Pettitt RW. Reliability analysis of the 3-min all-out exercise test for cycle ergometry. *Medicine and Science in Sports and Exercise*. 2011;43(12):2375-80.
235. Wright J, Bruce-Low S, Jobson SA. The reliability and validity of the 3-min all-out cycling critical power test. *International Journal of Sports Medicine*. 2017;38(06):462-7.
236. Bergstrom HC, Housh TJ, Zuniga JM, Camic CL, Traylor DA, Schmidt RJ, et al. A new single work bout test to estimate critical power and anaerobic work capacity. *The Journal of Strength and Conditioning Research*. 2012;26(3):656-63.
237. Daniel M-P, Bettina K, Christoph T, Mark G. Authors' Response. *The Journal of Strength and Conditioning Research*. 2019;33(8):e225-e6.
238. Hartman ME, Ekkekakis P, Dicks ND, Pettitt RW. Dynamics of pleasure–displeasure at the limit of exercise tolerance: conceptualizing the sense of exertional physical fatigue as an affective response. *Journal of Experimental Biology*. 2019;222(3):jeb186585.
239. Burnley M, Vanhatalo A, Jones AM. Distinct profiles of neuromuscular fatigue during muscle contractions below and above the critical torque in humans. *Journal of Applied Physiology*. 2012;113(2):215-23.

240. Casaburi R, Storer TW, Ben-Dov I, Wasserman K. Effect of endurance training on possible determinants of VO<sub>2</sub> during heavy exercise. *Journal of Applied Physiology*. 1987;62(1):199-207.
241. Karvonen MJ. The effects of training on heart rate: a longitudinal study. *Annales Medicinæ Experimentalis Et Biologiae Fenniae*. 1957;35:307-15.
242. Davis JA, Convertino VA. A comparison of heart rate methods for predicting endurance training intensity. *Medicine and Science in Sports*. 1975;7(4):295-8.
243. Faude O, Hecksteden A, Hammes D, Schumacher F, Besenius E, Sperlich B, et al. Reliability of time-to-exhaustion and selected psycho-physiological variables during constant-load cycling at the maximal lactate steady-state. *Applied Physiology, Nutrition, and Metabolism*. 2016;42(2):142-7.
244. Saunders PU, Pyne DB, Telford RD, Hawley JA. Reliability and variability of running economy in elite distance runners. *Medicine and Science in Sports and Exercise*. 2004;36(11):1972-6.
245. Bailey SJ, Wilkerson DP, DiMenna F, Jones AM. Influence of repeated sprint training on pulmonary O<sub>2</sub> uptake and muscle deoxygenation kinetics in humans. *Journal of Applied Physiology*. 2009.
246. Burnley M, Jones AM, Carter H, Doust JH. Effects of prior heavy exercise on phase II pulmonary oxygen uptake kinetics during heavy exercise. *Journal of Applied Physiology*. 2000;89(4):1387-96.
247. Gerbino A, Ward SA, Whipp BJ. Effects of prior exercise on pulmonary gas-exchange kinetics during high-intensity exercise in humans. *Journal of Applied Physiology*. 1996;80(1):99-107.
248. Wilkerson DP, Berger NJ, Jones AM. Influence of hyperoxia on pulmonary O<sub>2</sub> uptake kinetics following the onset of exercise in humans. *Respiratory Physiology and Neurobiology*. 2006;153(1):92-106.
249. Granata C, Oliveira RS, Little JP, Renner K, Bishop DJ. Training intensity modulates changes in PGC-1 $\alpha$  and p53 protein content and mitochondrial respiration, but not markers of mitochondrial content in human skeletal muscle. *The FASEB Journal*. 2015;30(2):959-70.
250. Compher C, Frankenfield D, Keim N, Roth-Yousey L, Group EAW. Best practice methods to apply to measurement of resting metabolic rate in adults: a systematic review. *Journal of the American Dietetic Association*. 2006;106(6):881-903.
251. Stanforth PR, Gagnon J, Rice T, Bouchard C, Leon AS, Rao D, et al. Reproducibility of resting blood pressure and heart rate measurements: the HERITAGE Family Study. *Annals of Epidemiology*. 2000;10(5):271-7.
252. da Cunha FA, Farinatti PdTV, Midgley AW. Methodological and practical application issues in exercise prescription using the heart rate reserve and oxygen uptake reserve methods. *Journal of Science and Medicine in Sport*. 2011;14(1):46-57.

253. Cunha FA, Midgley AW, Monteiro WD, Campos FK, Farinatti PT. The relationship between oxygen uptake reserve and heart rate reserve is affected by intensity and duration during aerobic exercise at constant work rate. *Applied Physiology, Nutrition, and Metabolism*. 2011;36(6):839-47.
254. Weltman A, Snead D, Seip R, Schurrer R, Weltman J, Rutt R, et al. Percentages of maximal heart rate, heart rate reserve and VO<sub>2</sub>max for determining endurance training intensity in male runners. *International Journal of Sports Medicine*. 1990;11(03):218-22.
255. Londeree BR. Effect of training on lactate/ventilatory thresholds: a meta-analysis. *Medicine and Science in Sport and Exercise*. 1997;29(6):837-43.
256. Coen B, Schwarz L, Urhausen A, Kindermann W. Control of training in middle-and long-distance running by means of the individual anaerobic threshold. *International Journal of Sports Medicine*. 1991;12(06):519-24.
257. González-Haro C. Differences in Physiological Responses Between Short-vs. Long-Graded Laboratory Tests in Road Cyclists. *Journal of Strength and Conditioning Research*. 2015;29(4):1040-8.
258. McNaughton LR, Roberts S, Bentley DJ. The relationship among peak power output, lactate threshold, and short-distance cycling performance: effects of incremental exercise test design. *Journal of Strength and Conditioning Research*. 2006;20(1):157.
259. Buchfuhrer MJ, Hansen JE, Robinson TE, Sue DY, Wasserman K, Whipp BJ. Optimizing the exercise protocol for cardiopulmonary assessment. *Journal of Applied Physiology*. 1983;55(5):1558-64.
260. Van Schuylenbergh R, Vanden EB, Hespel P. Correlations between lactate and ventilatory thresholds and the maximal lactate steady state in elite cyclists. *International Journal of Sports Medicine*. 2004;25(6):403-8.
261. Ivy JL, Withers RT, Vanhandel PJ, Elger DH, Costill DL. Muscle respiratory capacity and fiber type as determinants of the lactate threshold. *Journal of Applied Physiology*. 1980;48(3):523-7.
262. Kindermann W, Simon G, Keul J. Significance of the aerobic-anaerobic transition for the determination of work load intensities during endurance training. *European Journal of Applied Physiology and Occupational Physiology*. 1979;42(1):25-34.
263. Heck H, Mader A, Hess G, Mucke S, Muller R, Hollmann W. Justification of the 4-mmol/L lactate threshold. *International Journal of Sports Medicine*. 1985;6(3):117-30.
264. Hill AV, Long C, Lupton H. Muscular exercise, lactic acid, and the supply and utilisation of oxygen. *Proceedings of the Royal Society of London Series B, Containing Papers of a Biological Character*. 1924;97(681):84-138.
265. Riebe D, Franklin BA, Thompson PD, Garber CE, Whitfield GP, Magal M, et al. Updating ACSM's recommendations for exercise preparticipation health screening. *Medicine and Science in Sport and Exercise*. 2015;47(11):2473-9.

266. Jackson AS, Blair SN, Mahar MT, Wier LT, Ross RM, Stuteville JE. Prediction of functional aerobic capacity without exercise testing. *Medicine and Science in Sports and Exercise*. 1990 Dec;22(6):863-70.
267. Medicine ACoS. ACSM's guidelines for exercise testing and prescription: Lippincott Williams & Wilkins; 2013.
268. Smekal G, von Duvillard SP, Pokan R, Hofmann P, Braun WA, Arciero PJ, et al. Blood lactate concentration at the maximal lactate steady state is not dependent on endurance capacity in healthy recreationally trained individuals. *European Journal of Applied Physiology*. 2012;112(8):3079-86.
269. Beaver W, Wasserman K, Whipp B. Improved detection of lactate threshold during exercise using a log-log transformation. *Journal of Applied Physiology*. 1985;59(6):1936-40.
270. Berg A, Jakob E, Lehmann M, Dickhuth H, Huber G, Keul J. Current aspects of modern ergometry. *Pneumologie (Stuttgart, Germany)*. 1990;44(1):2.
271. Hughson RL, Weisiger KH, Swanson GD. Blood lactate concentration increases as a continuous function in progressive exercise. *Journal of Applied Physiology*. 1987;62(5):1975-81.
272. Lamarra N, Whipp BJ, Ward SA, Wasserman K. Effect of interbreath fluctuations on characterizing exercise gas exchange kinetics. *Journal of Applied Physiology*. 1987;62(5):2003-12.
273. Keir DA, Murias JM, Paterson DH, Kowalchuk JM. Breath-by-breath pulmonary O<sub>2</sub> uptake kinetics: effect of data processing on confidence in estimating model parameters. *Experimental Physiology*. 2014;99(11):1511-22.
274. Lawrence I, Lin K. A concordance correlation coefficient to evaluate reproducibility. *Biometrics*. 1989:255-68.
275. Bland JM, Altman D. Statistical methods for assessing agreement between two methods of clinical measurement. *The Lancet*. 1986;327(8476):307-10.
276. Hopkins W. Analysis of validity by linear regression (Excel spreadsheet). 2015;19:36-44.
277. McBride HM, Neuspiel M, Wasiak S. Mitochondria: more than just a powerhouse. *Current Biology*. 2006;16(14):R551-R60.
278. Li X, Fang P, Mai J, Choi ET, Wang H, Yang X-f. Targeting mitochondrial reactive oxygen species as novel therapy for inflammatory diseases and cancers. *Journal of Hematology and Oncology*. 2013;6(1):19.
279. Green DR. Apoptotic pathways: the roads to ruin. *Cell*. 1998;94(6):695-8.
280. Klinge CM. Estrogenic control of mitochondrial function and biogenesis. *Journal of Cellular Biochemistry*. 2008;105(6):1342-51.

281. Egan B, Hawley JA, Zierath JR. SnapShot: Exercise Metabolism. *Cell Metabolism*. 2016 2016/08/09/;24(2):342-.e1.
282. Nordsborg NB, Lundby C, Leick L, Pilegaard H. Relative workload determines exercise-induced increases in PGC-1 $\alpha$  mRNA. *Medicine and Science in Sports and Exercise*. 2010;42(8):1477-84.
283. Popov D, Zinovkin R, Karger E, Tarasova O, Vinogradova O. The effect of aerobic exercise on the expression of genes in skeletal muscles of trained and untrained men. *Human Physiology*. 2013;39(2):190-5.
284. Sriwijitkamol A, Coletta DK, Wajcberg E, Balbontin GB, Reyna SM, Barrientes J, et al. Effect of acute exercise on AMPK signaling in skeletal muscle of subjects with type 2 diabetes: a time-course and dose-response study. *Diabetes*. 2007;56(3):836-48.
285. Bartlett JD, Joo CH, Jeong T-S, Louhelainen J, Cochran AJ, Gibala MJ, et al. Matched work high-intensity interval and continuous running induce similar increases in PGC-1 $\alpha$  mRNA, AMPK, p38, and p53 phosphorylation in human skeletal muscle. *Journal of Applied Physiology*. 2012;112(7):1135-43.
286. Wadley G, Lee-Young RS, Canny BJ, Wasuntarawat C, Chen Z, Hargreaves M, et al. Effect of exercise intensity and hypoxia on skeletal muscle AMPK signaling and substrate metabolism in humans. *American Journal of Physiology-Endocrinology and Metabolism*. 2006;290(4):E694-E702.
287. Purdom T, Kravitz L, Dokladny K, Mermier C. Understanding the factors that effect maximal fat oxidation. *Journal of the International Society of Sports Nutrition*. 2018;15(1):3.
288. Ogasawara J, Izawa T, Sakurai T, Sakurai T, Shirato K, Ishibashi Y, et al. The molecular mechanism underlying continuous exercise training-induced adaptive changes of lipolysis in white adipose cells. *Journal of Obesity*. 2015;2015.
289. Watt MJ, Spriet LL. Triacylglycerol lipases and metabolic control: implications for health and disease. *American Journal of Physiology-Endocrinology and Metabolism*. 2010;299(2):E162-E8.
290. William Tank A, Lee Wong D. Peripheral and central effects of circulating catecholamines. *Comprehensive Physiology*. 2011;5(1):1-15.
291. Jeppesen J, Kiens B. Regulation and limitations to fatty acid oxidation during exercise. *The Journal of Physiology*. 2012;590(5):1059-68.
292. Schenk S, Horowitz JF. Coimmunoprecipitation of FAT/CD36 and CPT I in skeletal muscle increases proportionally with fat oxidation after endurance exercise training. *American Journal of Physiology-Endocrinology and Metabolism*. 2006;291(2):E254-E60.
293. Yoshida Y, Jain SS, McFarlan JT, Snook LA, Chabowski A, Bonen A. Exercise-and training-induced upregulation of skeletal muscle fatty acid oxidation are not solely dependent on mitochondrial machinery and biogenesis. *The Journal of Physiology*. 2013;591(18):4415-26.

294. Shaw CS, Clark J, Wagenmakers AJ. The effect of exercise and nutrition on intramuscular fat metabolism and insulin sensitivity. *Annual Review of Nutrition*. 2010;30:13-34.
295. Moro C, Bajpeyi S, Smith SR. Determinants of intramyocellular triglyceride turnover: implications for insulin sensitivity. *American Journal of Physiology-Endocrinology and Metabolism*. 2008;294(2):E203-E13.
296. Yeo WK, Carey AL, Burke L, Spriet LL, Hawley JA. Fat adaptation in well-trained athletes: effects on cell metabolism. *Applied Physiology, Nutrition, and Metabolism*. 2011;36(1):12-22.
297. Stephens FB, Constantin-Teodosiu D, Greenhaff PL. New insights concerning the role of carnitine in the regulation of fuel metabolism in skeletal muscle. *The Journal of Physiology*. 2007;581(2):431-44.
298. Calvani M, Reda E, Arrigoni-Martelli E. Regulation by carnitine of myocardial fatty acid and carbohydrate metabolism under normal and pathological conditions. *Basic Research in Cardiology*. 2000;95(2):75-83.
299. DeLany JP, Windhauser MM, Champagne CM, Bray GA. Differential oxidation of individual dietary fatty acids in humans. *The American Journal of Clinical Nutrition*. 2000;72(4):905-11.
300. Jeukendrup AE, Aldred S. Fat supplementation, health, and endurance performance. *Nutrition*. 2004;20(7-8):678-88.
301. Kiens B. Skeletal muscle lipid metabolism in exercise and insulin resistance. *Physiological Reviews*. 2006;86(1):205-43.
302. Horton HR, Moran LA, Ochs RS, Rawn JD, Scrimgeour KG. *Principles of Biochemistry*: Prentice Hall Upper Saddle River, NJ; 1996.
303. Achten J, Jeukendrup AE. Optimizing fat oxidation through exercise and diet. *Nutrition*. 2004;20(7-8):716-27.
304. Venables MC, Achten J, Jeukendrup AE. Determinants of fat oxidation during exercise in healthy men and women: a cross-sectional study. *Journal of Applied Physiology*. 2005;98(1):160-7.
305. Volek JS, Noakes T, Phinney SD. Rethinking fat as a fuel for endurance exercise. *European Journal of Sport Science*. 2015;15(1):13-20.
306. Zouhal H, Jacob C, Delamarche P, Gratas-Delamarche A. Catecholamines and the effects of exercise, training and gender. *Sports Medicine*. 2008;38(5):401-23.
307. Frayn K. Fat as a fuel: emerging understanding of the adipose tissue–skeletal muscle axis. *Acta Physiologica*. 2010;199(4):509-18.
308. Amaro-Gahete FJ, Sanchez-Delgado G, Ruiz JR. Commentary: Contextualising Maximal Fat Oxidation During Exercise: Determinants and Normative Values. *Front Physiol*. 2018;9:1460.

309. Maunder E, Plews DJ, Kilding AE. Contextualising maximal fat oxidation during exercise: Determinants and normative values. *Frontiers in Physiology*. 2018;9.
310. Achten J, Gleeson M, Jeukendrup AE. Determination of the exercise intensity that elicits maximal fat oxidation. *Medicine and Science in Sports and Exercise*. 2002;34(1):92-7.
311. Valizadeh A, Khosravi A, Azmoon H. Fat oxidation rate during and after three exercise intensities in non-athlete young men. *World Appl Sci J*. 2011;15(9):1260-6.
312. Horowitz JF, Klein S. Lipid metabolism during endurance exercise. *The American Journal of Clinical Nutrition*. 2000;72(2):558S-63S.
313. Rosell S, Belfrage E. Blood circulation in adipose tissue. *Physiological Reviews*. 1979;59(4):1078-104.
314. San-Millán I, Brooks GA. Assessment of metabolic flexibility by means of measuring blood lactate, fat, and carbohydrate oxidation responses to exercise in professional endurance athletes and less-fit individuals. *Sports Medicine*. 2018;48(2):467-79.
315. Gmada N, Marzouki H, Sassi RH, Tabka Z, Shephard R, Brun J-F, et al. Relative and absolute reliability of the crossover and maximum fat oxidation points and their relationship to ventilatory threshold. *Science and Sports*. 2013;28(4):e99-e105.
316. Achten J, Jeukendrup A. Relation between plasma lactate concentration and fat oxidation rates over a wide range of exercise intensities. *International Journal of Sports Medicine*. 2004;25(01):32-7.
317. Richter EA, Hargreaves M. Exercise, GLUT4, and skeletal muscle glucose uptake. *Physiological Reviews*. 2013;93(3):993-1017.
318. Jensen TE, Richter EA. Regulation of glucose and glycogen metabolism during and after exercise. *The Journal of Physiology*. 2012;590(5):1069-76.
319. Hearn M, Hammond K, Fell J, Morton J. Regulation of muscle glycogen metabolism during exercise: implications for endurance performance and training adaptations. *Nutrients*. 2018;10(3):298.
320. Ui M. A role of phosphofructokinase in pH-dependent regulation of glycolysis. *Biochimica et Biophysica Acta (BBA)-General Subjects*. 1966;124(2):310-22.
321. Roach PJ, Depaoli-Roach AA, Hurley TD, Tagliabracci VS. Glycogen and its metabolism: some new developments and old themes. *Biochemical Journal*. 2012;441(3):763-87.
322. Winder W, Carling J, Duan C, Jones J, Palmer S, Walker M. Muscle fructose-2, 6-bisphosphate and glucose-1, 6-bisphosphate during insulin-induced hypoglycemia. *Journal of Applied Physiology*. 1994;76(2):853-8.
323. Sahlin K. Metabolic changes limiting muscle performance. *Biochemistry of Exercise*. 1986;6:323-43.

324. Karlson P. Regulation in Metabolism: By EA Newsholme and C. Start. 1973. John Wiley and Sons, New York and London. Pp. 349. Biochemical Education. 1974;2(2):33-.
325. Richter EA, Ruderman NB, Gavras H, Belur E, Galbo H. Muscle glycogenolysis during exercise: dual control by epinephrine and contractions. American Journal of Physiology-Endocrinology and Metabolism. 1982;242(1):E25-E32.
326. Li Y, Dash RK, Kim J, Saidel GM, Cabrera ME. Role of NADH/NAD<sup>+</sup> transport activity and glycogen store on skeletal muscle energy metabolism during exercise: in silico studies. American Journal of Physiology-Cell Physiology. 2009;296(1):C25-C46.
327. White AT, Schenk S. NAD<sup>+</sup>/NADH and skeletal muscle mitochondrial adaptations to exercise. American Journal of Physiology-Endocrinology and Metabolism. 2012;303(3):E308-E21.
328. Brooks GA, Mercier J. Balance of carbohydrate and lipid utilization during exercise: the "crossover" concept. Journal of Applied Physiology. 1994;76(6):2253-61.
329. Jansson E, Hjemdahl P, Kaijser L. Epinephrine-induced changes in muscle carbohydrate metabolism during exercise in male subjects. Journal of Applied Physiology. 1986 1986;60(5):1466-70.
330. Febbraio MA, Lambert DL, Starkie RL, Proietto J, Hargreaves M. Effect of epinephrine on muscle glycogenolysis during exercise in trained men. Journal of Applied Physiology. 1998 1998;84(2):465-70.
331. Greenhaff PL, Ren JM, Soderlund K, Hultman E. Energy metabolism in single human muscle fibers during contraction without and with epinephrine infusion. American Journal of Physiology - Endocrinology and Metabolism. 1991 1991;260(5):E713-E8.
332. Richter EA, Ruderman NB, Galbo H. Alpha and Beta adrenergic effects on metabolism in contracting, perfused muscle. Acta Physiologica Scandinavica. 1982;116(3):215-22.
333. Cori GT, Illingworth B. The effect of epinephrine and other glycogenolytic agents on the phosphorylase a content of muscle. Biochimica et Biophysica acta. 1956;21(1):105-10.
334. Fischer EH, Heilmeyer L, Haschke R. Phosphorylase and the control of glycogen degradation. Curr Top Cell Regul. 1971;4:211-51.
335. Chasiotis D, Sahlin K, Hultman E. Regulation of glycogenolysis in human muscle in response to epinephrine infusion. J Appl Physiol Respir Environ Exerc Physiol. 1983 Jan;54(1):45-50.
336. Tesch P, Sjodin B, Karlsson J. Relationship between lactate accumulation, LDH activity, LDH isozyme and fibre type distribution in human skeletal muscle. Acta Physiologica Scandinavica. 1978;103(1):40-6.
337. Blanchaer MC, Van Wijhe M. Isozymes of lactic dehydrogenase in skeletal muscle. Am J Physiol. 1962 May;202(5):827-9.

338. Zajac FE, Faden JS. Relationship among Recruitment Order, Axonal Conduction-Velocity, and Muscle-Unit Properties of Type-Identified Motor Units in Cat Plantaris Muscle. *J Neurophysiol.* 1985 1985-05-01 00:00:00;53(5):1303-22.
339. Yang Y, Sauve AA. NAD<sup>+</sup> metabolism: Bioenergetics, signaling and manipulation for therapy. *Biochimica et Biophysica Acta (BBA)-Proteins and Proteomics.* 2016;1864(12):1787-800.
340. Ying W, Alano CC, Garnier P, Swanson RA. NAD<sup>+</sup> as a metabolic link between DNA damage and cell death. *Journal of Neuroscience Research.* 2005;79(1-2):216-23.
341. Kahn BB, Alquier T, Carling D, Hardie DG. AMP-activated protein kinase: ancient energy gauge provides clues to modern understanding of metabolism. *Cell Metabolism.* 2005;1(1):15-25.
342. Richter EA, Ruderman NB. AMPK and the biochemistry of exercise: implications for human health and disease. *Biochemical Journal.* 2009;418(2):261-75.
343. Chen Z-P, Stephens TJ, Murthy S, Canny BJ, Hargreaves M, Witters LA, et al. Effect of exercise intensity on skeletal muscle AMPK signaling in humans. *Diabetes.* 2003;52(9):2205-12.
344. Tullson PC, Bangsbo J, Hellsten Y, Richter EA. IMP metabolism in human skeletal muscle after exhaustive exercise. *Journal of Applied Physiology.* 1995;78(1):146-52.
345. Wahr PA, Metzger JM. Role of Ca<sup>2+</sup> and cross-bridges in skeletal muscle thin filament activation probed with Ca<sup>2+</sup> sensitizers. *Biophysical Journal.* 1999;76(4):2166-76.
346. Sale DG. 5 Influence of Exercise and Training on Motor Unit Activation. *Exercise and sport sciences reviews.* 1987;15(1):95-152.
347. Ashour B, Hansford RG. Effect of fatty acids and ketones on the activity of pyruvate dehydrogenase in skeletal-muscle mitochondria. *Biochemical Journal.* 1983;214(3):725-36.
348. Derick H, Williams E, Cadenas E. Mitochondrial respiratory chain-dependent generation of superoxide anion and its release into the intermembrane space. *Biochemical Journal.* 2001;353(2):411-6.
349. Muller F. The nature and mechanism of superoxide production by the electron transport chain: its relevance to aging. *Journal of the American Aging Association.* 2000;23(4):227-53.
350. Trewin A, Berry B, Wojtovich A. Exercise and mitochondrial dynamics: keeping in shape with ROS and AMPK. *Antioxidants.* 2018;7(1):7.
351. Steinbacher P, Eckl P. Impact of oxidative stress on exercising skeletal muscle. *Biomolecules.* 2015;5(2):356-77.
352. Hashimoto T, Hussien R, Oommen S, Gohil K, Brooks GA. Lactate sensitive transcription factor network in L6 cells: activation of MCT1 and mitochondrial biogenesis. *The FASEB Journal.* 2007;21(10):2602-12.

353. Powers SK, Jackson MJ. Exercise-induced oxidative stress: cellular mechanisms and impact on muscle force production. *Physiological Reviews*. 2008;88(4):1243-76.
354. He F, Li J, Liu Z, Chuang C-C, Yang W, Zuo L. Redox mechanism of reactive oxygen species in exercise. *Frontiers in Physiology*. 2016;7:486.
355. Gomes EC, Silva AN, de Oliveira MR. Oxidants, antioxidants, and the beneficial roles of exercise-induced production of reactive species. *Oxid Med Cell Longev*. 2012;2012:756132.
356. Neubauer O, Reichhold S, Nics L, Hoelzl C, Valentini J, Stadlmayr B, et al. Antioxidant responses to an acute ultra-endurance exercise: impact on DNA stability and indications for an increased need for nutritive antioxidants in the early recovery phase. *British Journal of Nutrition*. 2010;104(8):1129-38.
357. Hanson J, Huxley HE. Structural basis of the cross-striations in muscle. *Nature*. 1953;172(4377):530.
358. Huxley HE. Fifty years of muscle and the sliding filament hypothesis. *European Journal of Biochemistry*. 2004;271(8):1403-15.
359. Maruyama K, Matsubara S, Natori R, Nonomura Y, Kimura S, Ohashi K, et al. Connectin, an elastic protein of muscle: characterization and function. *The Journal of Biochemistry*. 1977;82(2):317-37.
360. Reznick RM, Shulman GI. The role of AMP-activated protein kinase in mitochondrial biogenesis. *The Journal of Physiology*. 2006;574(1):33-9.
361. Scott JW, Hawley SA, Green KA, Anis M, Stewart G, Scullion GA, et al. CBS domains form energy-sensing modules whose binding of adenosine ligands is disrupted by disease mutations. *The Journal of Clinical Investigation*. 2004;113(2):274-84.
362. Hawley SA, Davison M, Woods A, Davies SP, Beri RK, Carling D, et al. Characterization of the AMP-activated protein kinase kinase from rat liver and identification of threonine 172 as the major site at which it phosphorylates AMP-activated protein kinase. *Journal of Biological Chemistry*. 1996;271(44):27879-87.
363. Woods A, Johnstone SR, Dickerson K, Leiper FC, Fryer LG, Neumann D, et al. LKB1 is the upstream kinase in the AMP-activated protein kinase cascade. *Current Biology*. 2003;13(22):2004-8.
364. Hawley SA, Pan DA, Mustard KJ, Ross L, Bain J, Edelman AM, et al. Calmodulin-dependent protein kinase kinase- $\beta$  is an alternative upstream kinase for AMP-activated protein kinase. *Cell Metabolism*. 2005;2(1):9-19.
365. Thomson D. The role of AMPK in the regulation of skeletal muscle size, hypertrophy, and regeneration. *International Journal of Molecular Sciences*. 2018;19(10):3125.
366. Toyoda T, Hayashi T, Miyamoto L, Yonemitsu S, Nakano M, Tanaka S, et al. Possible involvement of the  $\alpha 1$  isoform of 5' AMP-activated protein kinase in oxidative stress-stimulated glucose transport in skeletal muscle. *American Journal of Physiology-Endocrinology and Metabolism*. 2004;287(1):E166-E73.

367. Witczak C, Sharoff C, Goodyear L. AMP-activated protein kinase in skeletal muscle: from structure and localization to its role as a master regulator of cellular metabolism. *Cellular and Molecular Life Sciences*. 2008;65(23):3737-55.
368. Wojtaszewski JF, Nielsen P, Hansen BF, Richter EA, Kiens B. Isoform-specific and exercise intensity-dependent activation of 5'-AMP-activated protein kinase in human skeletal muscle. *The Journal of Physiology*. 2000;528(1):221-6.
369. Schwalm C, Jamart C, Benoit N, Naslain D, Prémont C, Prévet J, et al. Activation of autophagy in human skeletal muscle is dependent on exercise intensity and AMPK activation. *The FASEB Journal*. 2015;29(8):3515-26.
370. Merrill G, Kurth E, Hardie D, Winder W. AICA riboside increases AMP-activated protein kinase, fatty acid oxidation, and glucose uptake in rat muscle. *American Journal of Physiology-Endocrinology and Metabolism*. 1997;273(6):E1107-E12.
371. Winder W, Holmes B, Rubink D, Jensen E, Chen M, Holloszy J. Activation of AMP-activated protein kinase increases mitochondrial enzymes in skeletal muscle. *Journal of Applied Physiology*. 2000;88(6):2219-26.
372. Cantó C, Gerhart-Hines Z, Feige JN, Lagouge M, Noriega L, Milne JC, et al. AMPK regulates energy expenditure by modulating NAD<sup>+</sup> metabolism and SIRT1 activity. *Nature*. 2009;458(7241):1056.
373. Czubryt MP, McAnally J, Fishman GI, Olson EN. Regulation of peroxisome proliferator-activated receptor  $\gamma$  coactivator 1 $\alpha$  (PGC-1 $\alpha$ ) and mitochondrial function by MEF2 and HDAC5. *Proceedings of the National Academy of Sciences*. 2003;100(4):1711-6.
374. Jones RG, Plas DR, Kubek S, Buzzai M, Mu J, Xu Y, et al. AMP-activated protein kinase induces a p53-dependent metabolic checkpoint. *Molecular Cell*. 2005;18(3):283-93.
375. Saleem A, Adhietty PJ, Hood DA. Role of p53 in mitochondrial biogenesis and apoptosis in skeletal muscle. *Physiological Genomics*. 2009;37(1):58-66.
376. Lee C, Kim KH, Cohen P. MOTS-c: a novel mitochondrial-derived peptide regulating muscle and fat metabolism. *Free Radical Biology and Medicine*. 2016;100:182-7.
377. Kim KH, Son JM, Benayoun BA, Lee C. The mitochondrial-encoded peptide MOTS-c translocates to the nucleus to regulate nuclear gene expression in response to metabolic stress. *Cell Metabolism*. 2018;28(3):516-24. e7.
378. Son JM, Lee C. Mitochondria: multifaceted regulators of aging. *BMB Reports*. 2019;52(1):13.
379. Chin ER. Intracellular Ca<sup>2+</sup> signaling in skeletal muscle: decoding a complex message. *Exercise and Sport Sciences Reviews*. 2010;38(2):76-85.
380. Hashimoto T, Brooks GA. Mitochondrial lactate oxidation complex and an adaptive role for lactate production. *Medicine and Science in Sports and Exercise*. 2008;40(3):486.
381. Brooks GA. The science and translation of lactate shuttle theory. *Cell Metabolism*. 2018;27(4):757-85.

382. Ojuka EO, Jones TE, Han D-H, Chen M, Wamhoff BR, Sturek M, et al. Intermittent increases in cytosolic Ca<sup>2+</sup> stimulate mitochondrial bioenergetics in muscle cells. *American Journal of Physiology-Endocrinology and Metabolism*. 2002.
383. Chen G, Carroll S, Racay P, Dick J, Pette D, Traub I, et al. Deficiency in parvalbumin increases fatigue resistance in fast-twitch muscle and upregulates mitochondria. *American Journal of Physiology-Cell Physiology*. 2001;281(1):C114-C22.
384. Braun AP, Schulman H. The multifunctional calcium/calmodulin-dependent protein kinase: from form to function. *Annual Review of Physiology*. 1995;57(1):417-45.
385. Aronson D, Boppart MD, Dufresne SD, Fielding RA, Goodyear LJ. Exercise stimulates c-Jun NH<sub>2</sub>Kinase activity and c-Jun transcriptional activity in human skeletal muscle. *Biochemical and Biophysical Research Communications*. 1998;251(1):106-10.
386. Goodyear L, Chang P, Sherwood D, Dufresne S, Moller D. Effects of exercise and insulin on mitogen-activated protein kinase signaling pathways in rat skeletal muscle. *American Journal of Physiology-Endocrinology and Metabolism*. 1996;271(2):E403-E8.
387. Hayashi T, Hirshman MF, Dufresne SD, Goodyear LJ. Skeletal muscle contractile activity in vitro stimulates mitogen-activated protein kinase signaling. *American Journal of Physiology-Cell Physiology*. 1999;277(4):C701-C7.
388. Long YC, Widegren U, Zierath JR. Exercise-induced mitogen-activated protein kinase signalling in skeletal muscle. *Proceedings of the Nutrition Society*. 2004;63(2):227-32.
389. Chen Z, Gibson TB, Robinson F, Silvestro L, Pearson G, Xu B-e, et al. MAP kinases. *Chemical Reviews*. 2001;101(8):2449-76.
390. Schwer B, Verdin E. Conserved metabolic regulatory functions of sirtuins. *Cell Metabolism*. 2008;7(2):104-12.
391. Cantó C, Auwerx J. Targeting sirtuin 1 to improve metabolism: all you need is NAD<sup>+</sup>? *Pharmacological Reviews*. 2012;64(1):166-87.
392. Michishita E, Park JY, Burneskis JM, Barrett JC, Horikawa I. Evolutionarily conserved and nonconserved cellular localizations and functions of human SIRT proteins. *Molecular Biology of the Cell*. 2005;16(10):4623-35.
393. Vaziri H, Dessain SK, Eaton EN, Imai S-I, Frye RA, Pandita TK, et al. hSIRT2/SIRT1 functions as an NAD-dependent p53 deacetylase. *Cell*. 2001;107(2):149-59.
394. Gurd BJ, Yoshida Y, McFarlan JT, Holloway GP, Moyes CD, Heigenhauser GJ, et al. Nuclear SIRT1 activity, but not protein content, regulates mitochondrial biogenesis in rat and human skeletal muscle. *American Journal of Physiology-Regulatory, Integrative and Comparative Physiology*. 2011;301(1):R67-R75.
395. Gurd BJ, Little JP, Perry CG. Last Word on Viewpoint: Does SIRT1 determine exercise-induced skeletal muscle mitochondrial biogenesis: differences between in vitro and in vivo experiments? *Journal of Applied Physiology*. 2012;112(5):931-.

396. Gurd BJ, Perry CG, Heigenhauser GJ, Spriet LL, Bonen A. High-intensity interval training increases SIRT1 activity in human skeletal muscle. *Applied Physiology, Nutrition, and Metabolism*. 2010;35(3):350-7.
397. Dumke CL, Davis JM, Murphy EA, Nieman DC, Carmichael MD, Quindry JC, et al. Successive bouts of cycling stimulates genes associated with mitochondrial biogenesis. *European Journal of Applied Physiology*. 2009;107(4):419.
398. Civitarese AE, Carling S, Heilbronn LK, Hulver MH, Ukropcova B, Deutsch WA, et al. Calorie restriction increases muscle mitochondrial biogenesis in healthy humans. *PLoS Medicine*. 2007;4(3):e76.
399. Guerra B, Guadalupe-Grau A, Fuentes T, Ponce-González JG, Morales-Alamo D, Olmedillas H, et al. SIRT1, AMP-activated protein kinase phosphorylation and downstream kinases in response to a single bout of sprint exercise: influence of glucose ingestion. *European Journal of Applied Physiology*. 2010;109(4):731-43.
400. Lagouge M, Argmann C, Gerhart-Hines Z, Meziane H, Lerin C, Daussin F, et al. Resveratrol improves mitochondrial function and protects against metabolic disease by activating SIRT1 and PGC-1 $\alpha$ . *Cell*. 2006;127(6):1109-22.
401. Gerhart-Hines Z, Rodgers JT, Bare O, Lerin C, Kim SH, Mostoslavsky R, et al. Metabolic control of muscle mitochondrial function and fatty acid oxidation through SIRT1/PGC-1 $\alpha$ . *The EMBO Journal*. 2007;26(7):1913-23.
402. Rodgers JT, Lerin C, Haas W, Gygi SP, Spiegelman BM, Puigserver P. Nutrient control of glucose homeostasis through a complex of PGC-1 $\alpha$  and SIRT1. *Nature*. 2005;434(7029):113.
403. Wolfrum C, Borrmann CM, Borchers T, Spener F. Fatty acids and hypolipidemic drugs regulate peroxisome proliferator-activated receptors  $\alpha$ - and  $\gamma$ -mediated gene expression via liver fatty acid binding protein: a signaling path to the nucleus. *Proceedings of the National Academy of Sciences*. 2001;98(5):2323-8.
404. Rigano D, Sirignano C, Tagliatela-Scafati O. The potential of natural products for targeting PPAR $\alpha$ . *Acta Pharmaceutica Sinica B*. 2017;7(4):427-38.
405. Marion-Letellier R, Savoye G, Ghosh S. Fatty acids, eicosanoids and PPAR gamma. *European Journal of Pharmacology*. 2016;785:44-9.
406. Ehrenborg E, Krook A. Regulation of skeletal muscle physiology and metabolism by peroxisome proliferator-activated receptor  $\delta$ . *Pharmacological Reviews*. 2009;61(3):373-93.
407. Burns KA, Heuvel JPV. Modulation of PPAR activity via phosphorylation. *Biochimica et Biophysica Acta (BBA)-Molecular and Cell Biology of Lipids*. 2007;1771(8):952-60.
408. Puigserver P, Spiegelman BM. Peroxisome proliferator-activated receptor- $\gamma$  coactivator 1 $\alpha$  (PGC-1 $\alpha$ ): transcriptional coactivator and metabolic regulator. *Endocrine Reviews*. 2003;24(1):78-90.

409. Vainshtein A, Tryon LD, Pauly M, Hood DA. Role of PGC-1 $\alpha$  during acute exercise-induced autophagy and mitophagy in skeletal muscle. *American Journal of Physiology-Cell Physiology*. 2015;308(9):C710-C9.
410. Little JP, Safdar A, Bishop D, Tarnopolsky MA, Gibala MJ. An acute bout of high-intensity interval training increases the nuclear abundance of PGC-1 $\alpha$  and activates mitochondrial biogenesis in human skeletal muscle. *American Journal of Physiology-Regulatory, Integrative and Comparative Physiology*. 2011;300(6):R1303-R10.
411. Wright DC, Han D-H, Garcia-Roves PM, Geiger PC, Jones TE, Holloszy JO. Exercise-induced mitochondrial biogenesis begins before the increase in muscle PGC-1 $\alpha$  expression. *Journal of Biological Chemistry*. 2007;282(1):194-9.
412. Safdar A, Little JP, Stokl AJ, Hettinga BP, Akhtar M, Tarnopolsky MA. Exercise increases mitochondrial PGC-1 $\alpha$  content and promotes nuclear-mitochondrial cross-talk to coordinate mitochondrial biogenesis. *Journal of Biological Chemistry*. 2011;286(12):10605-17.
413. Puigserver P, Rhee J, Lin J, Wu Z, Yoon JC, Zhang C-Y, et al. Cytokine stimulation of energy expenditure through p38 MAP kinase activation of PPAR $\gamma$  coactivator-1. *Molecular Cell*. 2001;8(5):971-82.
414. Andrade-Souza VA, Ghiarone T, Sansonio A, Silva KAS, Tomazini F, Arcoverde L, et al. Exercise twice-a-day potentiates skeletal muscle signalling responses associated with mitochondrial biogenesis in humans, which are independent of lowered muscle glycogen content. *bioRxiv*. 2019:547489.
415. Bartlett JD, Close GL, Drust B, Morton JP. The emerging role of p53 in exercise metabolism. *Sports Medicine*. 2014;44(3):303-9.
416. Levine A, Hu W, Feng Z. The P53 pathway: what questions remain to be explored? *Cell Death and Differentiation*. 2006;13(6):1027.
417. Vousden KH, Ryan KM. p53 and metabolism. *Nature Reviews Cancer*. 2009;9(10):691.
418. Matoba S, Kang J-G, Patino WD, Wragg A, Boehm M, Gavrilova O, et al. p53 regulates mitochondrial respiration. *Science*. 2006;312(5780):1650-3.
419. Irrcher I, Ljubcic V, Kirwan AF, Hood DA. AMP-activated protein kinase-regulated activation of the PGC-1 $\alpha$  promoter in skeletal muscle cells. *PloS ONE*. 2008;3(10):e3614.
420. Park J-Y, Wang P-y, Matsumoto T, Sung HJ, Ma W, Choi JW, et al. p53 improves aerobic exercise capacity and augments skeletal muscle mitochondrial DNA content. *Circulation Research*. 2009;105(7):705-12.
421. Tachtsis B, Smiles WJ, Lane SC, Hawley JA, Camera DM. Acute endurance exercise induces nuclear p53 abundance in human skeletal muscle. *Frontiers in Physiology*. 2016;7:144.
422. Backs J, Backs T, Bezprozvannaya S, McKinsey TA, Olson EN. Histone deacetylase 5 acquires calcium/calmodulin-dependent kinase II responsiveness by oligomerization with histone deacetylase 4. *Molecular and Cellular Biology*. 2008;28(10):3437-45.

423. McGee SL, Van Denderen BJ, Howlett KF, Mollica J, Schertzer JD, Kemp BE, et al. AMP-activated protein kinase regulates GLUT4 transcription by phosphorylating histone deacetylase 5. *Diabetes*. 2008;57(4):860-7.
424. McKinsey TA, Zhang CL, Olson EN. Activation of the myocyte enhancer factor-2 transcription factor by calcium/calmodulin-dependent protein kinase-stimulated binding of 14-3-3 to histone deacetylase 5. *Proceedings of the National Academy of Sciences*. 2000;97(26):14400-5.
425. De Ruijter AJ, Van Gennip AH, Caron HN, Stephan K, Van Kuilenburg AB. Histone deacetylases (HDACs): characterization of the classical HDAC family. *Biochemical Journal*. 2003;370(3):737-49.
426. Lu J, McKinsey TA, Nicol RL, Olson EN. Signal-dependent activation of the MEF2 transcription factor by dissociation from histone deacetylases. *Proceedings of the National Academy of Sciences*. 2000;97(8):4070-5.
427. Mayr B, Montminy M. Transcriptional regulation by the phosphorylation-dependent factor CREB. *Nature Reviews Molecular Cell Biology*. 2001;2(8):599.
428. Shaywitz AJ, Greenberg ME. CREB: a stimulus-induced transcription factor activated by a diverse array of extracellular signals. *Annual Review of Biochemistry*. 1999;68(1):821-61.
429. Bensinger SJ, Tontonoz P. Integration of metabolism and inflammation by lipid-activated nuclear receptors. *Nature*. 2008;454(7203):470.
430. Tyagi S, Gupta P, Saini AS, Kaushal C, Sharma S. The peroxisome proliferator-activated receptor: A family of nuclear receptors role in various diseases. *Journal of Advanced Pharmaceutical Technology and Research*. 2011;2(4):236.
431. Morino K, Petersen KF, Sono S, Choi CS, Samuel VT, Lin A, et al. Regulation of mitochondrial biogenesis by lipoprotein lipase in muscle of insulin-resistant offspring of parents with type 2 diabetes. *Diabetes*. 2012;61(4):877-87.
432. Barres R, Yan J, Egan B, Treebak JT, Rasmussen M, Fritz T, et al. Acute exercise remodels promoter methylation in human skeletal muscle. *Cell metabolism*. 2012;15(3):405-11.
433. Fritz T, Krämer DK, Karlsson HK, Galuska D, Engfeldt P, Zierath JR, et al. Low-intensity exercise increases skeletal muscle protein expression of PPAR $\delta$  and UCP3 in type 2 diabetic patients. *Diabetes/metabolism research and reviews*. 2006;22(6):492-8.
434. Edgett BA, Foster WS, Hankinson PB, Simpson CA, Little JP, Graham RB, et al. Dissociation of increases in PGC-1 $\alpha$  and its regulators from exercise intensity and muscle activation following acute exercise. *PLoS ONE*. 2013;8(8):e71623.
435. Cochran AJ, Little JP, Tarnopolsky MA, Gibala MJ. Carbohydrate feeding during recovery alters the skeletal muscle metabolic response to repeated sessions of high-intensity interval exercise in humans. *Journal of Applied Physiology*. 2010;108(3):628-36.

436. Pilegaard H, Osada T, Andersen LT, Helge JW, Saltin B, Neufer PD. Substrate availability and transcriptional regulation of metabolic genes in human skeletal muscle during recovery from exercise. *Metabolism*. 2005;54(8):1048-55.
437. Cluberton LJ, McGee SL, Murphy RM, Hargreaves M. Effect of carbohydrate ingestion on exercise-induced alterations in metabolic gene expression. *Journal of Applied Physiology*. 2005;99(4):1359-63.
438. Stepto NK, Benziene B, Wadley GD, Chibalin AV, Canny BJ, Eynon N, et al. Short-term intensified cycle training alters acute and chronic responses of PGC1 $\alpha$  and Cytochrome C oxidase IV to exercise in human skeletal muscle. *PLoS One*. 2012;7(12):e53080.
439. Popov DV, Bachinin AV, Lysenko EA, Miller TF, Vinogradova OL. Exercise-induced expression of peroxisome proliferator-activated receptor  $\gamma$  coactivator-1 $\alpha$  isoforms in skeletal muscle of endurance-trained males. *The Journal of Physiological Sciences*. 2014;64(5):317-23.
440. Slivka D, Dumke C, Tucker T, Cuddy J, Ruby B. Human mRNA response to exercise and temperature. *International Journal of Sports Medicine*. 2012;33(02):94-100.
441. Mahoney D, Parise G, Melov S, Safdar A, Tarnopolsky M. Analysis of global mRNA expression in human skeletal muscle during recovery from endurance exercise. *The FASEB Journal*. 2005;19(11):1498-500.
442. Wang L, Psilander N, Tonkonogi M, Ding S, Sahlin K. Similar expression of oxidative genes after interval and continuous exercise. *Medicine and Science in Sports and Exercise*. 2009;41(12):2136-44.
443. Coffey VG, Zhong Z, Shield A, Canny BJ, Chibalin AV, Zierath JR, et al. Early signaling responses to divergent exercise stimuli in skeletal muscle from well-trained humans. *The FASEB Journal*. 2006;20(1):190-2.
444. Psilander N, Frank P, Flockhart M, Sahlin K. Exercise with low glycogen increases PGC-1 $\alpha$  gene expression in human skeletal muscle. *European Journal of Applied Physiology*. 2013;113(4):951-63.
445. Niklas P, Li W, Jens W, Michail T, Kent S. Mitochondrial gene expression in elite cyclists: effects of high-intensity interval exercise. *European Journal of Applied Physiology*. 2010;110(3):597-606.
446. Watt MJ, Southgate R, Holmes AG, Febbraio M. Suppression of plasma free fatty acids upregulates peroxisome proliferator-activated receptor (PPAR)  $\alpha$  and  $\delta$  and PPAR coactivator 1 $\alpha$  in human skeletal muscle, but not lipid regulatory genes. *Journal of Molecular Endocrinology*. 2004;33(2):533-44.
447. Brandt N, Gunnarsson TP, Hostrup M, Tybirk J, Nybo L, Pilegaard H, et al. Impact of adrenaline and metabolic stress on exercise-induced intracellular signaling and PGC-1 $\alpha$  mRNA response in human skeletal muscle. *Physiological Reports*. 2016;4(14):e12844.
448. Slivka DR, Heesch MW, Dumke CL, Cuddy JS, Hailes WS, Ruby BC. Human skeletal muscle mRNA response to a single hypoxic exercise bout. *Wilderness & Environmental Medicine*. 2014;25(4):462-5.

449. Slivka D, Heesch M, Dumke C, Cuddy J, Hailes W, Ruby B. Effects of post-exercise recovery in a cold environment on muscle glycogen, PGC-1 $\alpha$ , and downstream transcription factors. *Cryobiology*. 2013;66(3):250-5.
450. Heesch MW, Shute RJ, Kreiling JL, Slivka DR. Transcriptional control, but not subcellular location, of PGC-1 $\alpha$  is altered following exercise in a hot environment. *Journal of Applied Physiology*. 2016;121(3):741-9.
451. Russell AP, Hesselink MK, Lo SK, Schrauwen P. Regulation of metabolic transcriptional co-activators and transcription factors with acute exercise. *The FASEB Journal*. 2005;19(8):986-8.
452. Cochran AJ, Percival ME, Tricarico S, Little JP, Cermak N, Gillen JB, et al. Intermittent and continuous high-intensity exercise training induce similar acute but different chronic muscle adaptations. *Experimental Physiology*. 2014;99(5):782-91.
453. Little JP, Safdar A, Cermak N, Tarnopolsky MA, Gibala MJ. Acute endurance exercise increases the nuclear abundance of PGC-1 $\alpha$  in trained human skeletal muscle. *American Journal of Physiology-Regulatory, Integrative and Comparative Physiology*. 2010;298(4):R912-R7.
454. Gibala MJ, McGee SL, Garnham AP, Howlett KF, Snow RJ, Hargreaves M. Brief intense interval exercise activates AMPK and p38 MAPK signaling and increases the expression of PGC-1 $\alpha$  in human skeletal muscle. *Journal of Applied Physiology*. 2009;106(3):929-34.
455. Scarpulla RC. Nuclear activators and coactivators in mammalian mitochondrial biogenesis. *Biochimica et Biophysica Acta (BBA)-Gene Structure and Expression*. 2002;1576(1-2):1-14.
456. Scarpulla RC, Vega RB, Kelly DP. Transcriptional integration of mitochondrial biogenesis. *Trends in Endocrinology and Metabolism*. 2012;23(9):459-66.
457. Wu Z, Puigserver P, Andersson U, Zhang C, Adelmant G, Mootha V, et al. Mechanisms controlling mitochondrial biogenesis and respiration through the thermogenic coactivator PGC-1. *Cell*. 1999;98(1):115-24.
458. De Filippis E, Alvarez G, Berria R, Cusi K, Everman S, Meyer C, et al. Insulin-resistant muscle is exercise resistant: evidence for reduced response of nuclear-encoded mitochondrial genes to exercise. *American Journal of Physiology-Endocrinology and Metabolism*. 2008;294(3):E607-E14.
459. Egan B, O'connor PL, Zierath JR, O'gorman DJ. Time course analysis reveals gene-specific transcript and protein kinetics of adaptation to short-term aerobic exercise training in human skeletal muscle. *PloS ONE*. 2013;8(9):e74098.
460. Cartoni R, Léger B, Hock MB, Praz M, Crettenand A, Pich S, et al. Mitofusins 1/2 and ERR $\alpha$  expression are increased in human skeletal muscle after physical exercise. *The Journal of Physiology*. 2005;567(1):349-58.

461. Granata C, Oliveira RS, Little JP, Renner K, Bishop DJ. Mitochondrial adaptations to high-volume exercise training are rapidly reversed after a reduction in training volume in human skeletal muscle. *The FASEB Journal*. 2016;30(10):3413-23.
462. Gordon JW, Rungi AA, Inagaki H, Hood DA. Selected contribution: effects of contractile activity on mitochondrial transcription factor A expression in skeletal muscle. *Journal of Applied Physiology*. 2001;90(1):389-96.
463. Pettitt R. Applying the Critical Speed Concept to Racing Strategy and Interval Training Prescription. *International Journal of Sports Physiology and Performance*. 2016.
464. Bishop DJ, Botella J, Granata C. CrossTalk opposing view: Exercise training volume is more important than training intensity to promote increases in mitochondrial content. *J Physiol-London*. 2019 Aug;597(16):4115-8.
465. Tobina T, Yoshioka K, Hirata A, Mori S, Kiyonaga A, Tanaka H. Peroxisomal proliferator-activated receptor gamma co-activator-1 alpha gene expression increases above the lactate threshold in human skeletal muscle. *The Journal of Sports Medicine and Physical Fitness*. 2011;51(4):683-8.
466. Frayn K. Calculation of substrate oxidation rates in vivo from gaseous exchange. *Journal of Applied Physiology*. 1983;55(2):628-34.
467. Bergstrom J. Muscle electrolytes in man determined by neutron activation analysis on needle biopsy specimens. *Scandinavian Journal of Clinical and Laboratory Investigation*. 1962;14(Suppl 68).
468. Evans W, Phinney S, Young V. Suction applied to a muscle biopsy maximizes sample size. *Medicine and Science in Sports and Exercise*. 1982;14(1):101-2.
469. Passonneau JV, Lowry OH. *Enzymatic analysis: a practical guide*: Springer Science & Business Media; 1993.
470. Kuang J, Yan X, Genders AJ, Granata C, Bishop DJ. An overview of technical considerations when using quantitative real-time PCR analysis of gene expression in human exercise research. *PloS ONE*. 2018;13(5):e0196438.
471. Ye J, Coulouris G, Zaretskaya I, Cutcutache I, Rozen S, Madden TL. Primer-BLAST: a tool to design target-specific primers for polymerase chain reaction. *BMC Bioinformatics*. 2012;13(1):134.
472. McGee SL, Howlett KF, Starkie RL, Cameron-Smith D, Kemp BE, Hargreaves M. Exercise increases nuclear AMPK  $\alpha$ 2 in human skeletal muscle. *Diabetes*. 2003;52(4):926-8.
473. Watt MJ, Steinberg GR, Chan S, Garnham A, Kemp BE, Febbraio MA.  $\beta$ -Adrenergic stimulation of skeletal muscle HSL can be overridden by AMPK signaling. *The FASEB Journal*. 2004;18(12):1445-6.
474. Taylor SC, Berkelman T, Yadav G, Hammond M. A defined methodology for reliable quantification of Western blot data. *Molecular Biotechnology*. 2013;55(3):217-26.

475. Vissing K, Schjerling P. Simplified data access on human skeletal muscle transcriptome responses to differentiated exercise. *Scientific Data*. 2014;1:140041.
476. Neubauer O, Sabapathy S, Ashton KJ, Desbrow B, Peake JM, Lazarus R, et al. Time course-dependent changes in the transcriptome of human skeletal muscle during recovery from endurance exercise: from inflammation to adaptive remodeling. *Journal of Applied Physiology*. 2013;116(3):274-87.
477. Mahoney DJ, Carey K, Fu M-H, Snow R, Cameron-Smith D, Parise G, et al. Real-time RT-PCR analysis of housekeeping genes in human skeletal muscle following acute exercise. *Physiological Genomics*. 2004;18(2):226-31.
478. Hammond KM, Sale C, Fraser W, Tang J, Shepherd SO, Strauss JA, et al. Post-exercise carbohydrate and energy availability induce independent effects on skeletal muscle cell signalling and bone turnover: implications for training adaptation. *J Physiol*. 2019 Sep;597(18):4779-96.
479. Rowlands DS, Nelson AR, Raymond F, Metairon S, Mansourian R, Clarke J, et al. Protein-leucine ingestion activates a regenerative inflammo-myogenic transcriptome in skeletal muscle following intense endurance exercise. *Physiological Genomics*. 2015;48(1):21-32.
480. Popov DV, Makhnovskii PA, Kurochkina NS, Lysenko EA, Vepkhvadze TF, Vinogradova OL. Intensity-dependent gene expression after aerobic exercise in endurance-trained skeletal muscle. *Biology of Sport*. 2018;35(3):277.
481. Romero SA, Hocker AD, Mangum JE, Luttrell MJ, Turnbull DW, Struck AJ, et al. Evidence of a broad histamine footprint on the human exercise transcriptome. *The Journal of Physiology*. 2016;594(17):5009-23.
482. Rowlands DS, Thomson JS, Timmons BW, Raymond F, Fuerholz A, Mansourian R, et al. Transcriptome and translational signaling following endurance exercise in trained skeletal muscle: impact of dietary protein. *Physiological Genomics*. 2011;43(17):1004-20.
483. Neubauer O, Sabapathy S, Lazarus R, Jowett JB, Desbrow B, Peake JM, et al. Transcriptome analysis of neutrophils after endurance exercise reveals novel signaling mechanisms in the immune response to physiological stress. *Journal of Applied Physiology*. 2013;114(12):1677-88.
484. Drane P, Bravard A, Bouvard V, May E. Reciprocal down-regulation of p53 and SOD2 gene expression—implication in p53 mediated apoptosis. *Oncogene*. 2001;20(4):430.
485. Gartel AL, Tyner AL. The role of the cyclin-dependent kinase inhibitor p21 in apoptosis 1 supported in part by NIH grant R01 DK56283 (to ALT) for the p21 research and Campus Research Board and Illinois Department of Public Health Penny Severns Breast and Cervical Cancer grants (to ALG). 1. *Molecular Cancer Therapeutics*. 2002;1(8):639-49.
486. Pattamaprapanont P, Garde C, Fabre O, Barrès R. Muscle contraction induces acute hydroxymethylation of the exercise-responsive gene Nr4a3. *Frontiers in Endocrinology*. 2016;7:165.

487. Crane JD, Ogborn DI, Cupido C, Melov S, Hubbard A, Bourgeois JM, et al. Massage therapy attenuates inflammatory signaling after exercise-induced muscle damage. *Sci Transl Med*. 2012 Feb 1;4(119):119ra13.
488. Howald H, Poortmans JR. *Metabolic adaptation to prolonged physical exercise*. Birkhäuser, Basel. 1975;45:24-31.
489. Scheen A, Juchmes J, Cession-Fossion A. Critical analysis of the “anaerobic threshold” during exercise at constant workloads. *European Journal of Applied Physiology and Occupational Physiology*. 1981;46(4):367-77.
490. Achten J, Jeukendrup A. Maximal fat oxidation during exercise in trained men. *International Journal of Sports Medicine*. 2003;24(08):603-8.
491. Boone J, Bourgeois JG. Are RCP and Critical Power Equivalent? The Issue of Mean Response Time. *Med Sci Sports Exerc*. 2017 Dec;49(12):2608.
492. Pettitt RW, Jannick NA, Kramer M, Dicks ND. A Different Perspective of the 3-Minute All-Out Exercise Test. *The Journal of Strength and Conditioning Research*. 2019;33(8):e223-e4.
493. Maturana FM, Keir DA, Mclay KM, Murias JM. Critical power testing or self-selected cycling: Which one is the best predictor of maximal metabolic steady-state? *Journal of Science and Medicine in Sport*. 2017 Aug;20(8):795-9.

## Appendices